INVESTIGATING THE CHEMICAL SPACE AND METABOLIC BIOACTIVATION OF NATURAL PRODUCTS AND CROSS-REACTIVITY OF CHEMICAL INHIBITORS IN CYP450 PHENOTYPING

Nicholas M. Njuguna

Supervisor:
Prof. Kelly Chibale
Department of Chemistry, University of Cape Town

Co-supervisor:
Dr. Collen Masimirembwa
African Institute of Biomedical Science and Technology, Harare, Zimbabwe

Thesis presented for the Degree of

Doctor of Philosophy

In the Department of Chemistry

UNIVERSITY OF CAPE TOWN

November 2014

DECLARATION

I, **Nicholas Mwaura Njuguna**, hereby declare that:

(i) This thesis is my own unaided work, both in conception and execution, and that apart from the normal guidance of my supervisors; I have received no assistance apart from that acknowledged;

(ii) Neither the substance nor any part of the thesis has been submitted in the past, or is to be submitted for a Degree in the University of Cape Town or any other University.

Signed: ..... Date:

DEDICATION

To my family:

Dad, Mum, Kim, Maureen, Joe and Shi

For your enduring love, steadfast support and unshakeable belief that have made my journey into the unknown so much more bearable.

ACKNOWLEDGEMENTS

I wish to convey my heartfelt gratitude to all the people that contributed in every way, great or small, in the conceptualisation, execution and conclusion of this work.

To my supervisor, Prof. Kelly Chibale: no words in the English language (or any other) can truly express the eternal gratitude and boundless appreciation I have for granting me the opportunity to work under your guidance. Your exceptional scientific mentorship, great vision, unrelenting work ethic, generosity, and humility are a true inspiration. *Ahsante sana!*

To my co-supervisor, the indefatigable Dr. Collen Masimirembwa, who taught me everything I know about drug metabolism, a bit about *tae kwondo* and lots more besides, I extend my heartfelt thanks and utmost admiration. I shall always cherish the unforgettable time I spent working on my project at AiBST and the unbelievable warmth of our hosts in Zimbabwe. *Shukran sensei* Collen!

Past and present members of the Medicinal Chemistry and H3-D Research Groups, too numerous to mention here, from whom I received invaluable advice, assistance, support and genuine friendship throughout my time in Cape Town.

Special thanks go to Ms. Elaine Rutherfoord-Jones, for her amazing organizational skills, warm spirit and generous heart - truly the 'glue' that binds our research group so covalently together.

I also wish to wholeheartedly acknowledge Novartis Pharma AG for their sponsorship to participate in the once-in-a-lifetime experience 2013 Novartis Next Generation Scientist Program in Basel, Switzerland. Particular thanks go to our mentors from the Novartis D&I Team: Drs. Colin Pillay, Fareed Mirza, Marcello Gutierrez, Henri-Michelle Yere, Rita Michelle and Isabella Alberini. Special thanks also go to my scientific mentors at the Novartis DMPK Department: Dr. Gian Camenisch, Dr. Kenichi Umehara, Marc Witschi and Claire Juif.

I also wish to gratefully acknowledge Prof. Peter J. Smith and Dr. Lubbe Weisner at the UCT Department of Pharmacology for unfettered access to their laboratory facilities and especially their expert advice on LC-MS instrumentation and experimentation.

To Pete Roberts and Gianpiero Benincasa, many thanks for your technical assistance in the characterisation of compounds using NMR and MS.

To the South African Medical Research Council, National Research Foundation and the Novartis Research Foundation, I convey my heartfelt appreciation for generously funding my studies.

Finally and most important, my eternal gratitude goes to our Heavenly Father God, for mercifully granting me the health, strength and perseverance to see this through.

ABSTRACT

Natural products have been exploited by humans as the most consistently reliable source of medicines for hundreds of years. Owing to the great diversity in chemical scaffolds they encompass, these compounds provide an almost limitless starting point for the discovery and development of novel semi-synthetic or wholly synthetic drugs. In Africa, and many other parts of the world, natural products in the form of herbal remedies are still used as primary therapeutic interventions by populations far removed from conventional healthcare facilities. However, unlike conventional drugs that typically undergo extensive safety studies during development, traditional remedies are often not subjected to similar evaluation and could therefore harbour unforeseen risks alongside their established efficacy.

A comparison of the 'drug-like properties' of 335 natural products from medicinal plants reported in the *African Herbal Pharmacopoeia* with those of 608 compounds from the *British Pharmacopoeia 2009* was performed using *in silico* tools. The data obtained showed that the natural products differed significantly from conventional drugs with regard to molecular weight, rotatable bonds and H-bond donor distributions but not with regard to lipophilicity (cLogP) and H-bond acceptor distributions. In general, the natural products were found to exhibit a higher degree of deviation from Lipinski's 'Rule-of-Five'. Additionally, these compounds possessed a slightly greater number of structural alerts per molecule compared to conventional drugs, suggesting a higher likelihood of undergoing metabolic bioactivation.

A combination of CYP450 enzyme inactivation assays and reactive metabolite trapping experiments was used to evaluate *in vitro* bioactivation of 15 natural product and natural product-derived compounds. **Gedunin, Justicidin A** and **Jamaicin** were found to be potent inhibitors of the main drug metabolizing isoform CYP3A4. **Gedunin** also exhibited potent inhibition of CYP2C19. The inhibition of CYP3A4 was, however, not time-dependent and therefore unlikely to be due to reactive metabolite-mediated inactivation of the enzyme. Inhibition of the other

main drug metabolizing isoforms, CYP1A2, CYP2C9 and CYP2C19 was markedly less pronounced.

Direct assessment of the formation of electrophilic reactive metabolites was carried out by incubating 11 of the 15 compounds in hepatic microsomal preparations fortified with nucleophilic trapping agents. Using methoxylamine as a trapping agent, incubations of the monosubstituted furan ring-containing compounds **Gedunin** and the tetraol **DC3** were found to contain components strongly suspected to be trapped reactive metabolites. None of the compounds tested formed detectable adducts when incubated in the presence of either reduced glutathione or potassium cyanide.

The cross-reactivity of eight chemical inhibitors commonly used in early CYP450 phenotyping assays revealed the relatively low selectivity of ticlopidine and diethyldithiocarbamate. These assays also highlighted the particularly low potency of diethylthiocarbamate as the routinely preferred inhibitor for determining the contribution of hepatic CYP2E1 to xenobiotic metabolism. The data obtained provided ample evidence for the need to identify and characterise a superior replacement inhibitor for CYP2E1 phenotyping.

The determined cross-reactivity values of different inhibitors were used to formulate a mathematical strategy to compensate for cross-inhibition in CYP450 enzyme phenotyping calculations. Recalculation of previously obtained CYP3A4 phenotyping data using the new strategy appeared to improve the correlation between *fm,*CYP3A4 values determined using different phenotyping approaches. A similar effect on phenotyping data from other CYP450 enzymes could not be established owing to a limitation in the size of the pre-existing dataset.

LIST OF ABBREVIATIONS AND SYMBOLS

°C	Degrees Celsius
µg	Microgram
µM	Micromolar
Å	Angström
ACE	Angiotensin converting enzyme
ADMET	Absorption, distribution, metabolism, excretion and toxicology
AHP	African Herbal Pharmacopoeia
AKR	Aldo-keto reductase enzyme
AO	Aldehyde oxidase
APCI	Atmospheric pressure chemical ionization
BFC	7-Benzyloxy-4-(trifluoromethyl)coumarin
BP	British Pharmacopoeia
$CDCl_3$	Deuterated chloroform
cDNA	Complementary DNA
CEC	3-Cyano-7-ethoxycoumarin
cLogP	Calculated water-octanol partition coefficient
CLPG	Calopogonium isoflavone A
CNL	Constant neutral loss
CNS	Central Nervous System
COMT	Catechol-*O*-methyl transferase enzyme
COX	Cyclooxygenase enzyme
CQ-R	Chloroquine resistant
CQ-S	Chloroquine sensitive
CSIR	Council for Scientific and Industrial Research (South Africa)
CUC-A	Cucurbitacin A
CUC-B	Cucurbitacin B
CUC-C	Cucurbitacin C
CYP450	Cytochrome P450 Enzyme
Da	Daltons
DC14	Leoleorin A

DETC	Diethyldithiocarbamate
DMF	Dimethylformamide
DMPK	Drug metabolism and pharmacokinetics
DMSO	Dimethylsulfoxide
DNA	Deoxyribonucleic acid
EMA	European Medicines Agency
EMS	Enhanced mass spectrum
EPI	Enhanced product ion
ESI	Electro-spray ionisation
FDA	(United States) Food and Drug Administration
fm,CYP	Fraction of substrate metabolized by CYP450 enzyme
FMO	Flavin-containing monoxygenase
FMTN	Formononetin
FSDA	Fusidic acid
GB	Gigabytes
GEDN	Gedunin
GHz	Gigahertz
GIT	Gastro-intestinal tract
GSH	Reduced glutathione
GST	Glutathione transferase enzyme
HCOOH	Formic acid
$HCOONH_4$	Ammonium formate
HLM	Human liver microsomes
HPLC	High performance liquid chromatography
HTS	High throughput screening
IADR	Idiosyncratic adverse drug reaction
ICIPE	International Centre of Insect Physiology and Ecology
InChI	International chemical identifier
INN	International non-proprietary name
ISEF	Intersystem extrapolation factors
JMCN	Jamaicin

JSTN	Justicidin A
KCN	Potassium cyanide
KTZ	Ketoconazole
LC-MS	Tandem liquid chromatography - mass spectrometry
m/z	Mass-to-charge ratio
MAO	Monoamine oxidase enzyme
MFC	7-Methoxy-4-(trifluoromethyl)coumarin
mg	Milligram
MHz	Megahertz
min	Minutes
mL	Milliliter
mM	Millimolar
mm	Millimetre
MRM	Multiple reaction monitoring
MTGN	Metergoline
mwt	Molecular weight
MZG	Muzigadial
NADPH	Nicotinamide adenine dinucleotide phosphate (reduced form)
NAT	*N*-acetyl transferase enzyme
NH_4OAc	Ammonium acetate
nm	Nanometer
NMR	Nuclear magnetic resonance
OLE	Object Linking and Embedding
PBS	Phosphate buffered saline
PCA	Principle component analysis
PI	Precursor ion
pKa	Acid dissociation constant
pmol	Picomole
ppm	Parts per million
PTFE	Polytetrafluoroethylene
QSAR	Quantitative Structure Activity Relationship

RAM	Random access memory
rCYP	Recombinant Cytochrome P450 Enzyme
R_f	Retention factor
rhCYP450	Recombinant human Cytochrome P450 enzyme
RLM	Rat liver microsomes
RNA	Ribonucleic acid
rpm	Revolutions per minute
Rt	Retention time
SAM	*S*-adenosyl methionine
SLN	SYBYL line notation
SMILES	Simplified molecular input line entry system
sp.	Species
SQTL	Sesquiterpene lactone (Dehydrobrachylaenolide)
TAO	Troleandomycin
TDI	Time dependent (enzyme) inhibition
THF	Tetrahydrofuran
TIC	Total ion current (chromatogram)
UDPGA	Uridine 5’-diphosphoglucuronic acid
UGT	Uridine glucuronosyl transferase
V	Volts
WHO	World Health Organization
XIC	Extracted ion chromatogram

TABLE OF CONTENTS

LIST OF FIGURES

LIST OF TABLES

PUBLICATIONS AND CONFERENCES

Publications arising from this Thesis

Nicholas M. Njuguna, Collen Masimirembwa and Kelly Chibale. Identification and characterization of reactive metabolites in natural products-driven drug discovery. *Journal of Natural Products.* **2012**, 75(3): 507-513.

Marlene Espinoza-Moraga, **Nicholas M. Njuguna**, Grace Mugumbate, Julio Caballero and Kelly Chibale. *In silico* comparison of antimycobacterial natural products with known antituberculosis drugs. *Journal of Chemical Information and Modeling.* **2013**, 53(3): 649-660.

Reviews and related peer reviewed journal articles

Nicholas M. Njuguna, Dennis S. B. Ongarora and Kelly Chibale. Artemisinin derivatives: a patent review (2006 - present). *Expert Opinion on Therapeutic Patents.* **2012**, 22(10): 1179-1203.

Dyanne L. Cruickshank, Yassir Younis, **Nicholas M. Njuguna**, Dennis S. B. Ongarora, Kelly Chibale and Mino R. Caira. Alternative solid-state forms of a potent antimalarial aminopyridine: X-ray crystallographic, thermal and solubility aspects. *CrystEngComm.* **2014**, 16: 5781-5792.

Mathew Njoroge, **Nicholas M. Njuguna**, Peggoty Mutai, Dennis S. B. Ongarora, Paul W. Smith, and Kelly Chibale. Recent Approaches to Chemical Discovery and Development against Malaria and the Neglected Tropical Diseases Human African Trypanosomiasis and Schistosomiasis. *Chemical Reviews.* **2014** (*Article in Press:* dx.doi.org/10.1021/cr500098f).

Conferences and Training Courses

Inaugural H3-D Symposium (15 - 18 October 2012). Cape Town, South Africa. Poster Presentation: *In silico* comparison of antimycobacterial natural products with conventional antituberculosis drugs and compounds in preclinical/clinical development.

Novartis Next Generation Scientist Program (June - August 2013). Novartis Pharma AG, Basel, Switzerland. Novartis Research Day, 27th August 2013. Poster Presentation: Estimation of relative contribution of CYP enzymes to hepatic metabolism by a modified chemical inhibition approach evaluating cross-inhibition potential of selective inhibitors.

17th World Congress on Basic and Clinical Pharmacology (13 - 18 July 2014). Cape Town, South Africa. Poster Presentation: Investigating *in vitro* metabolic bioactivation of the natural product Gedunin.

248th American Chemical Society National Meeting and Exposition (10 - 14 August 2014). San Francisco, USA. Poster Presentation: *In vitro* metabolic enzyme inhibition and reactive metabolite trapping studies on natural and semi-synthetic furanoid labdane terpenoids.

CHAPTER ONE:

INTRODUCTION AND LITERATURE REVIEW

1.1 Summary

In this Chapter, the role played by natural products as a well established resource from which drugs have been discovered is discussed. Metabolism of xenobiotic compounds through different enzymatic systems in man is highlighted as a primer to more detailed discussions on metabolism-mediated adverse reactions to xenobiotics. The potential for natural products to cause adverse reactions in humans resulting from their metabolic bioactivation is discussed with reference to specific examples cited in the literature. The different approaches used to predict, detect and mitigate against undesirable toxicity arising from metabolism of xenobiotics in the early stages of the drug development process are covered. The research question to be answered, study justification and specific objectives of this work are highlighted at the conclusion of the Chapter.

1.2 Natural Products

In medicinal chemistry, the term 'natural product' is used to describe a low molecular weight chemical compound, usually excluding proteins and nucleic acids, produced or extracted from living organisms. Natural products are therefore obtained from terrestrial plants, microbes, marine organisms and animals.[1,2] In many instances, natural products are sometimes referred to as secondary metabolites, usually because the exact physiological or biochemical role(s) they play in the source organism is often unknown. In plants, however, some natural products are known to play a variety of functions, including providing defence mechanisms against predators or pathogens, or acting as chemo-attractants of pollinators and seed dispersers.[3,4] Microbes on the other hand are known to synthesize natural products that kill or inhibit the growth of sensitive strains of the same or related microbial species in their immediate environment.[5]

Although not usually essential for the survival of the host organisms, natural products confer an evolutionary advantage that boosts chances of survival in adverse environmental conditions.

1.3 Natural Products as Sources of Drugs

1.3.1 Historical Perspective

Since antiquity, natural products have been used, usually in crude form, as a key component of ancient yet sophisticated traditional medicine systems to combat disease.[6] Paleoanthropological field studies have uncovered evidence suggesting that prehistoric Neanderthal man may have been aware of the medicinal properties of some plants more than 60,000 years ago. Records from ancient civilisations in Mesopotamia, Egypt and Greece provide documented proof of the systematic use of natural products in medicine in meticulously detailed pharmacopoeia dating back many centuries before the current era. Traditional Chinese Medicine (TCM) and Indian Ayurvedic therapies still in widespread use today both rely heavily on natural product-derived remedies, which have been in use for hundreds of years.[7]

For centuries, natural products were used for therapeutic purposes in their crude forms, usually as combinations of both pharmacologically active and inactive compounds. In the early 1800s, however, the laboratory isolation of morphine as the first pure natural compound by the German pharmacist Friedrich Wilhelm Adam Sertürner opened a new age of medicinal natural product chemistry.[8,9] Following this discovery and subsequent commercialization of morphine by the pharmaceutical company E. Merck, focus on natural products gradually shifted towards the identification of active compounds, their isolation, purification and characterization from crude preparations. By 1820, for example, isolation of the antimalarial drug quinine from the bark of *Cinchona* species had been reported by Pierre Joseph Pelletier and Joseph Bienamié Caventou.[10] Yet another shift in the paradigm to natural products chemistry was realized in the mid-nineteenth century. Although the bark of the willow tree (*Cortex salicis*) had been used as early as 400 B.C. by the Greeks and Romans to alleviate pain, its natural product active ingredient, salicin, was only identified in the 1800s. Degradation of salicin yields salicylic acid, which has superior analgesic and antipyretic properties. The German chemist, Hermann Kolbe,

reported the successful total synthesis of salicylic acid in 1859, the earliest recorded instance of a natural product-derived medicinal compound being prepared in the laboratory. Chemical modification of salicylic acid to the better tolerated acetyl salicylic acid by Felix Hoffmann led to large scale manufacture and commercialization of the drug Aspirin® by Bayer in 1899.[11] Thus, the age of commercial drug discovery based on chemical synthesis of natural product-inspired analogues was born.

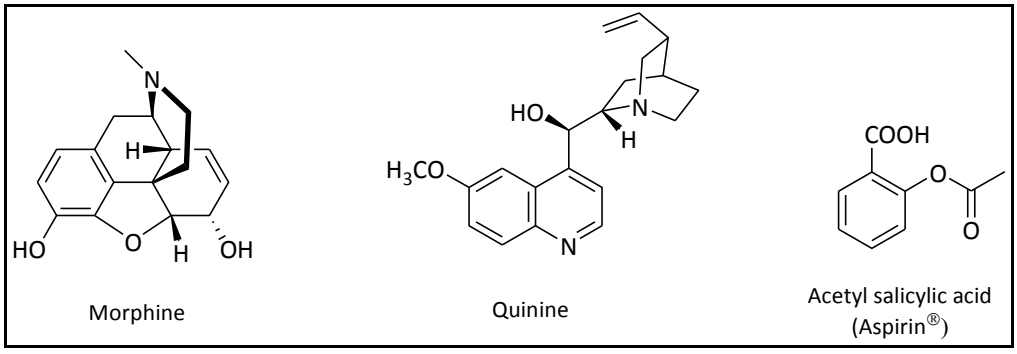

Figure 1.1 Earliest examples of drugs isolated from or inspired by natural products

Natural products have contributed to the development of new drugs in mainly three ways: (1) By serving as active medicinal compounds in their free unmodified state, as illustrated by both morphine and quinine; (2) acting as chemical starting points or building blocks for the synthesis of more complex molecules. For example, diosgenin is used as the starting material for the synthesis of steroidal contraceptive drugs; (3) providing insights into new modes of pharmacological action and paving way for the preparation of novel or wholly synthetic analogues.[2]

Due to technical improvements in screening programs as well as in separation, purification and characterization techniques, more than 1,000,000 natural compounds have been discovered since the early efforts of Sertürner. An estimated 50 - 60% of these compounds are produced by plants while about 5% are of microbial origin. Of all reported natural products, approximately 20 - 25% exhibit some kind of biological activity.[12]

1.3.2 Drugs from Plant Natural Products

Plants are the oldest sources from which natural product-based remedies have been obtained. It is, therefore, unsurprising that more than half of the natural products successfully developed into medicines are derived from plants. Although

approximately 250,000 unique higher plant species have been identified to-date, only about 5 - 15% of these have been investigated chemically and pharmacologically. Considering the known potential for plants to produce hundreds of secondary metabolites unique to certain species or genera, the possibilities of sourcing still more novel medicinal compounds from such an array would appear almost unlimited. The chemical diversity of plant-derived natural products is well illustrated by the sheer volume of chemical scaffolds they encompass, including but not limited to alkaloids, terpenoids, lignans, flavanoids, tannins and phytosteroids.[13] This diversity in chemotypes has resulted in the isolation and development of compounds that are used to treat a wide spectrum of medical conditions as briefly summarized in **Table 1.1**.[14,15]

Table 1.1: Examples of drugs obtained from plant derived natural products

Drug	Chemical Class	Plant source	Therapeutic use
Artemisinin	Sesquiterpene	*Artemisia sp.*	Antimalarial
Atropine	Alkaloid	*Atropa belladonna*	Anticholinergic
Digitalin, Digitoxin	Cardiac glycosides	*Digitalis purpurea*	Cardiotonic
Ephedrine	Phenylpropanolamine	*Ephedra sinica*	Sympathomimetic
Galanthamine	Alkaloid	*Galanthus sp.*	Anti-Alzheimer
Paclitaxel	Taxane diterpene	*Taxus brevifolia*	Antineoplastic
Podophyllotoxin	Lignan	*Podophyllum peltatum*	Antiviral
Quinidine	Alkaloid	*Cinchona ledgeriana*	Antiarrhythmic
Vincristine, Vinblastine	Vinca alkaloids	*Catharanthus roseus*	Antineoplastic

Plant-derived natural products have been particularly successful as sources of antitumour and anti-infective agents. Of all drugs approved for the treatment of cancer between 1940 and 2002, 40% were derived directly from or inspired by plant-based natural products.[16] This relatively high proportion may be partly explained by the concerted efforts of the US National Cancer Institute to screen large numbers of plant-based natural products for anti-tumour activity over the last 60 years. Between 1960 and 1982, over 35,000 plant samples mostly from temperate regions of the

world were collected randomly, from which more than 114,000 plant extracts were screened for anti-tumour activity. It is from these efforts that anticancer drugs such as paclitaxel and camptothecin were ultimately developed.[17,18]

In the treatment of malaria too, plant natural products play a central role in chemotherapy. Quinine is still used as the drug of choice in the management of severe complicated *P. falciparum* malaria while artemisinin derivatives are currently recommended as first line treatments for uncomplicated *P. falciparum* malaria in the form of artemisinin-based combination therapies.[19]

1.3.3 Drug Discovery from Microbial Natural Products

The discovery of the prototype antibiotic penicillin by Alexander Fleming from a mould in 1929 and its subsequent commercialisation in the 1940s revolutionalized the practice of medicine and ushered in the age of antibiotic drug discovery.[20–22] Due to the astounding impact of penicillin, pharmaceutical companies embarked on concerted efforts to discover new antibiotics from microbial sources over the following decade. This resulted in the discovery of such compounds as streptomycin in 1943,[23] chlortetracycline in 1945,[24] chloramphenicol in 1947,[25] cephalosporins such as cephalosporin C in 1949, erythromycin in 1952[26] and vancomycin in 1953.[27] Most of these compounds are still used clinically as drugs today.

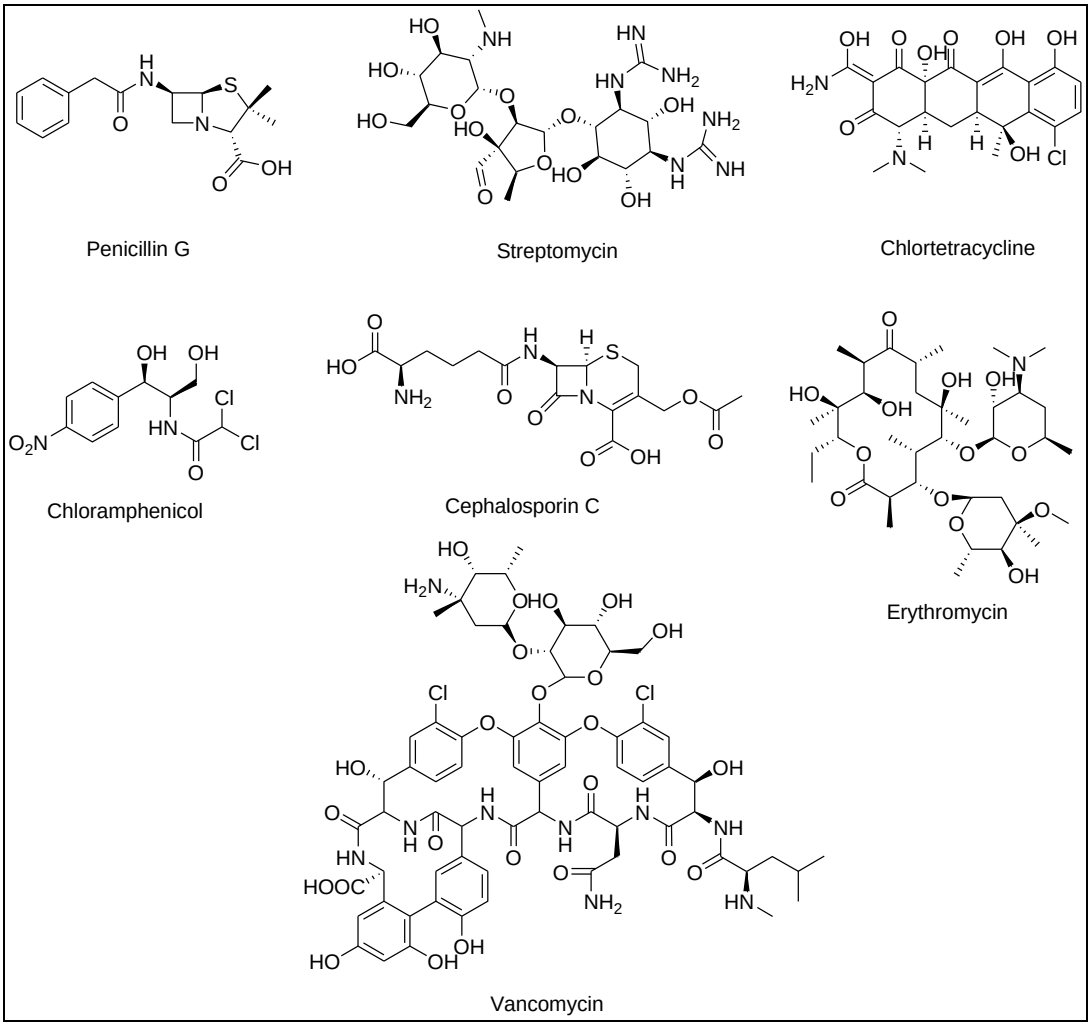

Figure 1.2: Prototype antibiotics of different classes isolated from microbial sources

Microbes, especially fungi and actinobacteria, are perhaps the richest source of drugs currently used as antibiotics in the treatment of infectious diseases as briefly summarized in **Table 1.2.**

Table 1.2: Examples of natural product antibiotics from microbial sources in current clinical use

Compound	Chemical Class	Microbial source	Species
Benzylpenicillin	Penicillin	Fungi	*Penicillium spp e.g. P. chrysogenum*
Griseofulvin	Antifungal	Fungus	*Penicillium griseofulvum*
Rifampicin	Rifamycin	Actinobacteria	*Amycolatopsis mediterranei*
Gentamycin	Aminoglycoside	Actinobacteria	*Micromonospora purpurea*
Oxytetracycline	Tetracycline	Actinomycete	*Streptomyces rimosus*
Vancomycin	Glycopeptide	Actinobacteria	*Amycolatopsis orientalis*
Daptomycin	Lipopeptide	Actinobacteria	*Streptomyces roseosporus*

Compound	Chemical Class	Microbial source	Species
Erythromycin	Macrolide	Actinomycete	*Saccharopolyspora erythraea*
Lincomycin	Lincosamide	Actinobacteria	*Streptomyces lincolnensis*
Bacitracin	Polypeptide	Bacteria (Gram+)	*Bacillus subtilis*
Mupirocin	Carboxylic acid	Bacteria (Gram-)	*Pseudomonas fluorescens*

Microbial natural product-derived drugs have also been licensed for use in the treatment of non-infectious diseases. For example, the fungal metabolite mevastatin is the natural-product inspiration behind the development of cholesterol lowering statin drugs such as lovastatin, atorvastatin and rosuvastatin.[28,29] Anthracycline antibiotics such as the natural product daunorubicin and its semi-synthetic derivative doxorubicin are clinically used as antineoplastic agents for the treatment of cancer while the macrolide rapamycin (sirolimus) is used as an immunosuppressant to prevent organ rejection following transplant surgery.[30,31]

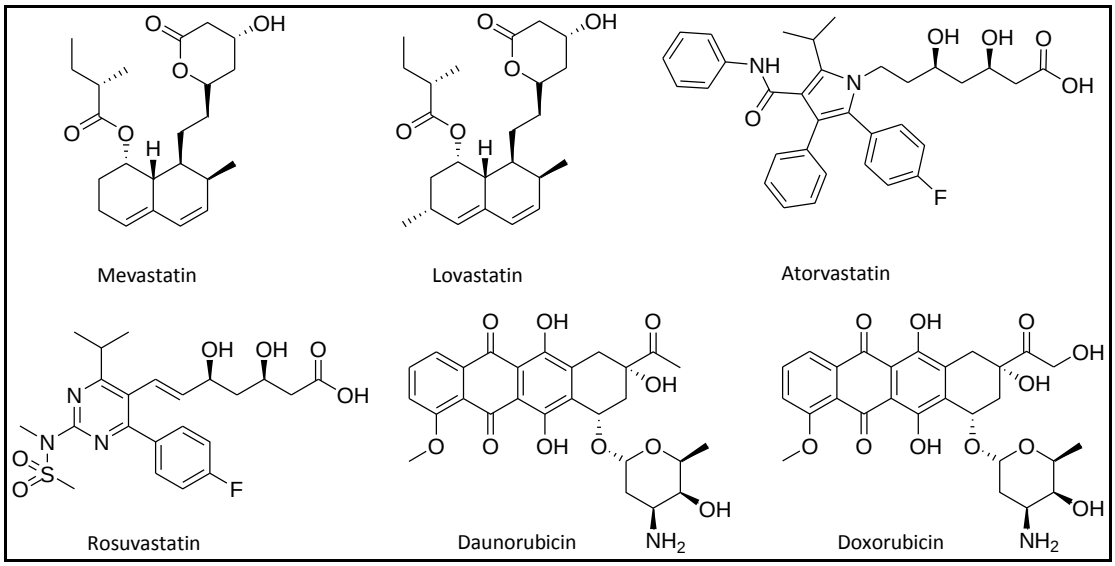

Figure 1.3: Drugs derived from microbial sources used for treatment of non-infectious diseases

1.3.4 Drug Discovery from Animal-Derived Natural Products

Compared to plants and microbes, the animal kingdom has been relatively neglected as a source of natural product-derived drugs.[32] Nevertheless, some notable examples of clinically used compounds from different animal species exist, mostly having been developed from animal toxins, venoms or hormones. For instance, the discovery and development of angiotensin converting enzyme (ACE) inhibitors such as captopril

and later analogues such as enalapril, ramipril and lisinopril was inspired from a nonapeptide found in venom obtained from the Brazilian pit viper (*Bothrops jararaca*).[33] Since their launch in the early 1980s, ACE inhibitors have become some of the most widely used drugs in the management of cardiovascular diseases including hypertension and some types of congestive cardiac failure.[34]

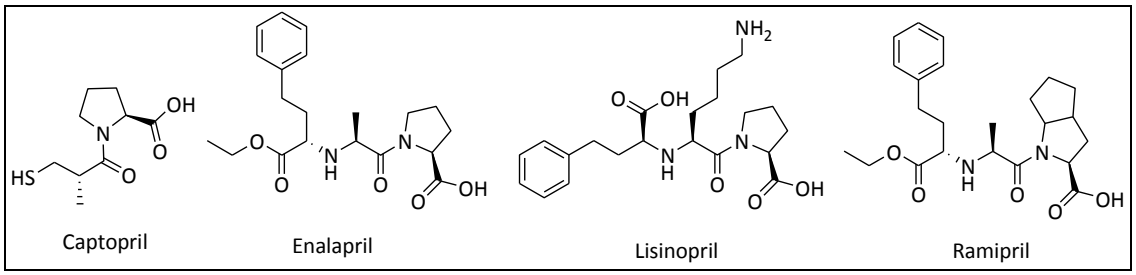

Figure 1.4: ACE inhibitors developed from an animal derived natural product

The antidiabetic drug exenatide obtained from the hormone exendin-4 found in saliva of the Gila monster (*Heloderma suspectum*) is another drug from an animal derived natural product currently in clinical use. Other examples of drugs developed from animal-derived natural products include the antiplatelet compounds eptifibatide, derived from the peptide barbourin found in the venom of the south-eastern pygmy rattlesnake (*Sistrurus barbouri*) and bivalirudin, engineered from hirudin present in the saliva of leeches (*Haementeria officinalis)*.[35,36]

Figure 1.5: Gila monster. Source of exendin-4, precursor of antidiabetic drug exenatide

1.3.5 Marine Invertebrates

Considering that oceans and seas make up almost 70% of the earth's surface and are home to an enormously rich biodiversity, the marine environment has been comparatively frugal in yielding natural products that have been successfully developed into drugs.[37] Among the factors that have contributed to the relatively

low return in marine drug discovery may be the fact that a vast expanse of the world's oceans and seas still remains unexplored. Another challenge lies in the reality that many of the rich sources of marine natural products, such as sponges and their fauna, survive exclusively in marine environments and are virtually uncultureable.[38] Nevertheless, advances in marine research technology and exploration have gradually made this environment more accessible and resulted in a steady increase in the number of novel marine natural products isolated and reported in the literature over the past 30 years as periodically reviewed by Faulkner and Blunt *et al*. [39–45] A common feature that has raised interest in marine natural products as potential sources of drugs is the extremely high potency exhibited by many of the bioactive marine compounds thus far isolated. This characteristic is thought to be most likely a means of circumventing the inevitable dilution of secondary metabolites produced by marine organisms necessitating such high potency for efficacy.[46]

The first drugs to be developed and licensed from marine natural products were the anti-leukaemic compound cytarabine and the antiviral vidarabine in 1969 and 1976, respectively. These drugs were developed from the nucleosides spongouridine and spongothymidine isolated from the demosponge *Techtitethya crypta* found in the Caribbean sea.[47,48]

Thereafter, the next marine-derived compound to receive marketing approval in the USA was the potent non-opioid analgesic ziconotide isolated from a cone snail species and which was only licensed as recently as 2004. Ziconotide is used for the management of severe chronic pain and was developed as a synthetic form of the hydrophilic conopeptide ω-MVIIA obtained from the venom of the Pacific fish-hunting snail, *Conus magus*. This drug is the prototype in a new class of selective N-type voltage sensitive calcium channel blockers.[49]

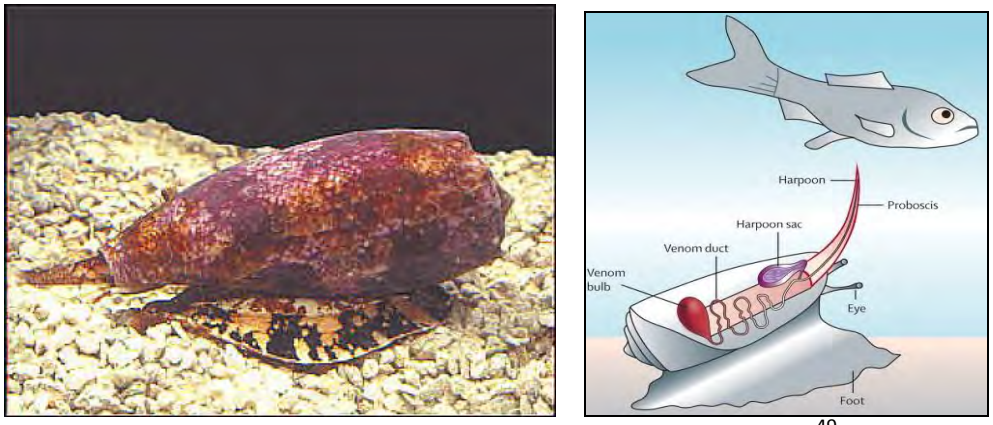

Figure 1.6: Fish-hunting cone snail (*Conus magus*)[49]

The drug trabectedin (ET-743) is another marine natural product that has been successfully developed into a clinical anticancer agent for treatment of soft tissue sarcomas and ovarian cancer. This compound was initially isolated from aqueous extracts obtained from the sea squirt *Ecteinascidia turbinata* in the Caribbean, and found to be a potent cytotoxic agent having good stability and relatively high natural abundance.[50] Trabectedin was licensed for clinical use by the EMA in 2007.

Another marine-derived anti-cancer agent, eribulin, was approved by the US FDA for clinical use in the treatment of intractable metastatic breast cancer in 2010. Although eribulin is a fully synthetic compound, its development was inspired from the polyether macrolide natural product halichondrin B, originally isolated from the marine sponge *Halichondria okadai*. Halichondrin B has extremely potent anticancer activity, and acts through tubulin binding similar to that exhibited by the vinca alkaloid antineoplastic agents vinblastine and vincristine. Eribulin was developed from halichondrin B as a structurally simplified and pharmaceutically optimized form of this compound for clinical use.[51]

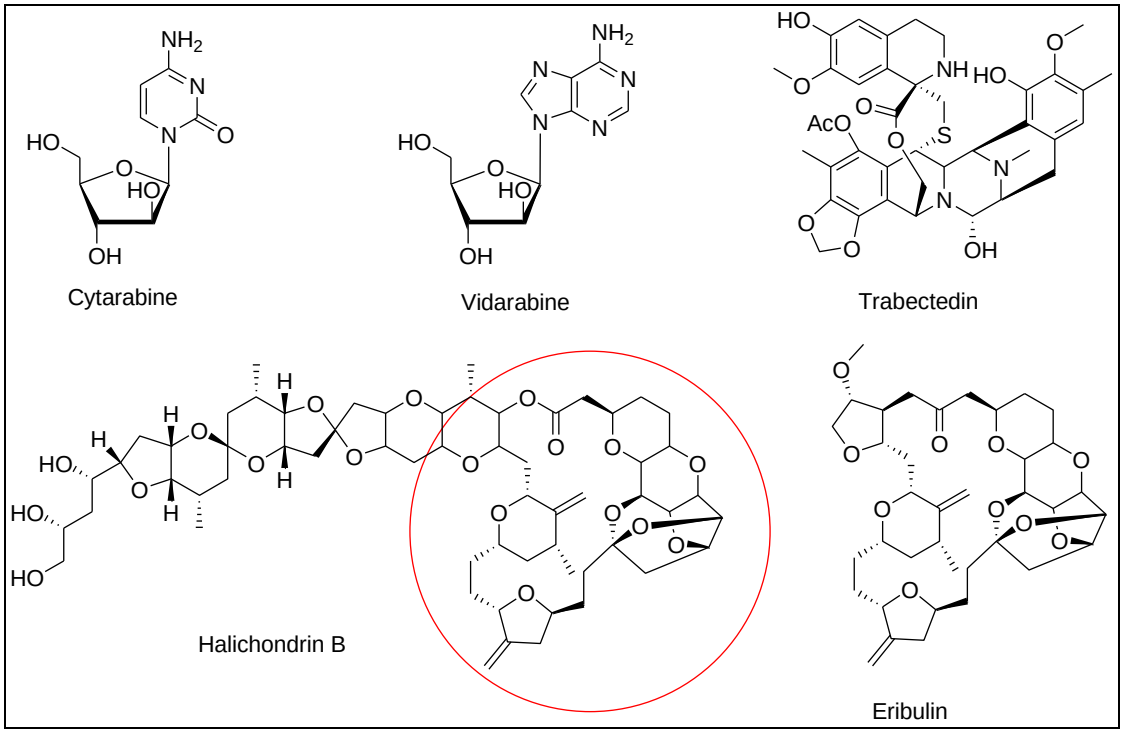

Figure 1.7: Examples of marine natural product derived drugs. The portion of Halichondrin B from which the drug eribulin was developed is circled for ease of reference.

Marine-derived natural products that have been advanced to various stages of clinical trials for different applications in recent years are summarized in **Table 1.3.**[52,53]

Table 1.3: Examples of drugs obtained from marine-derived natural products currently in clinical trials

Clinical Phase	Compound	Natural product lead	Marine source	Therapeutic indication
III	Tetrodotoxin	Tetrodotoxin	Tetraondontiformes	Analgesic
II-III	Plitidepsin	Plitidepsin	*Aplidium albicans*	Anticancer
II	XEN-2174	χ-conotoxin MrIA	*Conus marmoreus*	Analgesic
II	Kahalalide F	Kahalalide F	*Elysia rufescens*	Anticancer
II	Plinabulin	Halimide	*Aspergillus spp.*	Anticancer
II	DMXBA	Anabaseine	Marine worms	Schizophrenia
II	PM1004	Jorumycin	*Joruna funebris*	Anticancer
I-II	PM-10450	Jorumycin	*Joruna funebris*	Anticancer
I	Leconotide	ω-conotoxin CVID	*Conus catus*	Analgesic
I	Marizomib®	Salinosporamide A	*Salinispora tropica*	Anticancer

1.3.6 Other Potential Sources of Natural Product-Derived Drugs

It has been estimated that the chemical space occupied by organic compounds, including natural products, having a molecular weight of less than 500 extends to approximately 10^{60} compounds.[54] It is therefore, perhaps not an understatement to claim that despite a significant number of drugs in clinical use having been derived from natural products, these represent only a small fraction of the vast drug discovery opportunities yet to be exploited.

Based on the success of drugs from animal natural products, one area that has been proposed for potential exploitation is the field of venomics, involving drug discovery from building and screening venom libraries obtained from both terrestrial and marine organisms.[55]

Natural products obtained from organisms that inhabit and thrive in extreme environments have also attracted growing interest in recent years. Extremophilic microbes such as acidophiles, alkaliphiles, halophiles, piezothermophiles, hyperthermophiles or psychrophiles[56] are increasingly being evaluated as sources of novel secondary metabolites and possible drug leads.[57] For example, the extremolyte ectoine found in many halophilic microbes that survive in high salt concentration environments has been investigated as a cytoprotectant and protein stabiliser with potential application in treatment of conditions such as Alzheimer's disease.[58,59]

Organisms that inhabit the deep sea environment are highly adapted to survive in a habitat characterized by intensely high pressures, low temperature, oxygen and light concentrations as well as scarce nutrients. Under such conditions, these organisms have evolved unique primary metabolic pathways resulting in the production of entirely novel secondary metabolites. With advances in marine exploration equipment enabling greater access to this largely unexplored habitat, deep sea marine organisms continue to attract greater study and have yielded a growing number of unique bioactive natural products.[60] Deep-sea hydrothermal vents have been identified as habitats occupied by invertebrates capable of surviving and thriving under possibly the harshest conditions on earth. Though such organisms are not known to produce natural products, most survive through symbiotic associations with micro-organisms that do produce secondary metabolites. The first true new

natural products isolated from deep-sea hydrothermal vents were the ammonificins and loichichelins reported in 2009. These may represent the first in a possibly rich resource that provides compounds of medicinal interest in future.[61]

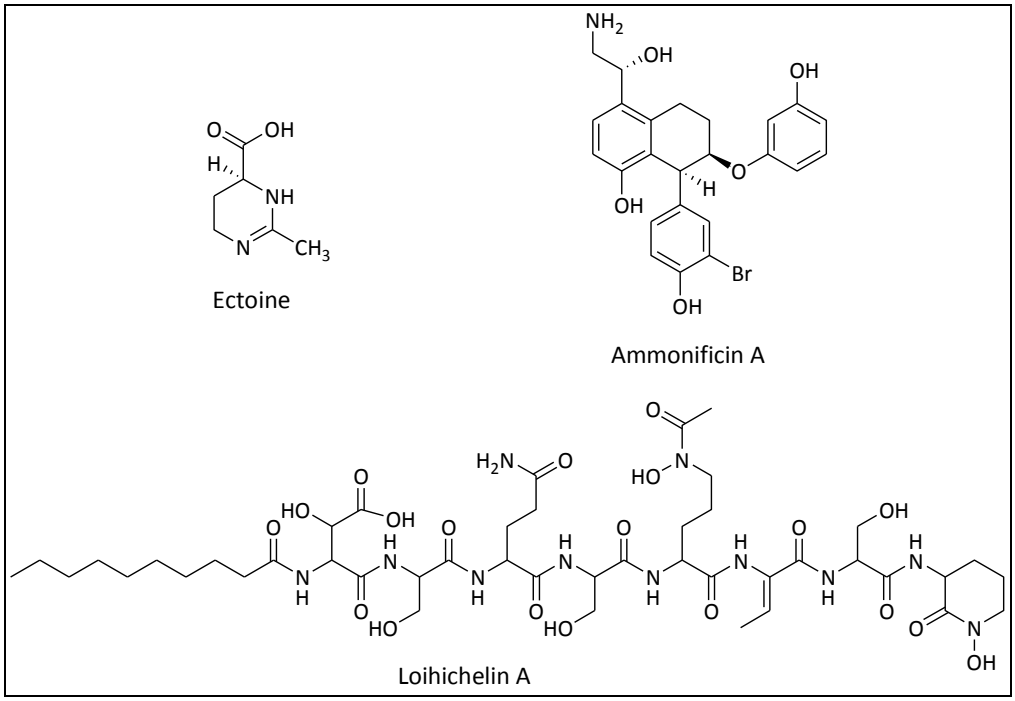

Figure 1.8: Natural products isolated from organisms that inhabit extreme environments

1.4 Past Decline, Current Status and Future Prospects of Natural Product-Based Drug Discovery

Despite the numerous successes in obtaining drugs from natural products, there has been a gradual de-emphasis in natural product drug discovery by most of the major pharmaceutical companies over the last 20 years. Several factors have led to this shift, including a greater investment in newer drug discovery approaches based on synthesis and high throughput screening of large libraries of synthetic compounds created using combinatorial chemistry. Although the success-rate of drug discovery using such methodology is lower than that based on natural products, it possesses the key advantage of speed. Since the compounds screened are already known, the time and effort needed to characterise and identify them is eliminated, whereas in natural product-based drug discovery, such technical aspects take up considerable time and effort. Furthermore, synthetic compounds are much more easily packaged

into physical libraries for large-scale high throughput screening for biological activity compared to natural products.[62]

The reviews published by Newman and Cragg, however, provide compelling evidence that natural products have been the single-most successful source of approved drugs over the last 30 years.[63–66] Thus, despite the challenges often encountered in obtaining drugs from nature, the advantages they possess have been successfully circumvented in those compounds advanced to clinical use. Factors that might explain these successes include increased access to natural products through (1) Exploration and research into new environments; (2) advances in compound separation, isolation and characterization techniques often employing coupled technologies such as liquid chromatography coupled to solid-phase extraction and nuclear magnetic resonance[67–69] (3) more sensitive and accurate analytical equipment allowing ease of characterization using non-destructive techniques and minute quantities of material, for example, multidimensional NMR spectroscopy using cryoprobes and advances in high resolution mass spectroscopy instrumentation.[70]

Additionally, in many cases, natural products possess certain advantages over synthetic compounds that have distinguished them as more reliable sources of drugs:[71]

1. Unmatched diversity and chemical complexity. Chemical scaffolds that would be virtually impossible or extremely difficult to replicate in the laboratory even using modern chemical synthetic techniques (e.g. due to presence of numerous chiral centres, and unusual bond patterns are often commonly encountered in nature. Even where such synthesis is possible, it may not be amenable to large scale application necessary for commercial drug manufacture.
2. Natural products tend to occupy a complementary chemical space to that of conventional drugs, and many quite often violate what are considered to be the rules of 'drug-likeness' yet still possess desirable chemotherapeutic profiles.[72]
3. Most natural products are the result of thousands of years of evolutionary development representing optimized output that has been perfected over countless generations. Thus, unlike synthetic drugs that usually need to undergo numerous iterative improvements to enhance their pharmacological profiles

prior to attaining the desired properties, many natural products, such as antibiotics from microbes, are often produced in a form ready for direct exploitation.

The paradigm shift of drug discovery driven through wholly synthetic combinatorial chemistry has not had the anticipated returns in terms of yielding large numbers of block-buster drugs despite enabling the screening of vast libraries of compounds in short time-frames. Considering the successes of natural-product driven drug discovery on the other hand, it appears that an approach that embraces a combination of both aspects offers the best option for future drug-discovery programs.[73] For example, it has been proposed that natural products could be used as a basis for creating combinatorial libraries of synthetic compounds, either as a source of chemical scaffolds or as an inspiration towards natural-product-like synthetics.[74,75] Alternatively, generation of natural product analogues using biosynthetic enzymes or genetically altered microorganisms may provide an avenue for accessing unique derivatives of natural product hits, circumventing the challenges associated with synthetic chemical modification.[76] To counter the problem of limited quantities of rare natural products, bioengineering easily cultured heterologous microbial vectors to produce the desired compound or its synthetic intermediate(s) could become commonplace. This approach has been successfully demonstrated in the production of artemisinic acid, a precursor of the plant derived sesquiterpene antimalarial artemisinin, using yeast cells.[77] Related to this is the application of metagenomic techniques involving the isolation and identification of genes present in the environment directly without the need to identify their source organisms beforehand and producing secondary metabolite natural products by expressing such genes using heterologous vectors.[78,79]

1.5 Metabolism of Xenobiotics

To maintain chemical and functional homeostasis in all body tissues upon exposure to chemical challenges, most organisms have evolved elaborate metabolic systems. In man, metabolic transformation of xenobiotics is performed by a diverse array of proteins, collectively referred to as drug metabolizing enzymes. These convert chemicals present in food, the environment, pollutants, toxins, cosmetics and drugs into compounds that can be more readily eliminated from the body. The enzymes also often catalyse the transformation of endogenous substrates such as steroids, hormones, and neurotransmitters into active or inactive forms for elimination.[80]

Metabolism of xenobiotics has traditionally been classified as occurring in phases. Phase I metabolism involves functionalization reactions on substrates resulting in the introduction or unmasking of chemical functional groups such as hydroxyls, amines, carboxylic acids or thiols. Phase II metabolism involves synthetic conjugation reactions in which the functionalized xenobiotic metabolite is chemically bound to a polar endogenous substrate. Although phase II metabolism often involves the product formed from phase I reactions, it can also take place directly on the parent substrate.The overall goal of xenobiotic metabolism is to transform foreign compounds into more polar, water soluble forms that can be more readily eliminated from the body**.**

Phase I metabolic reactions introduce or unmask a functional group in the xenobiotic substrate to provide a chemical site for subsequent conjugation reactions. Several enzymes are involved in these reactions which chemically broadly encompass aliphatic and aromatic hydroxylations usually through monooxygenation reactions, reductions and hydrolysis of esters and amides. In most cases, phase I metabolism results in only a slight increase in substrate hydrophilicity.

The cytochrome P450 (CYP450) superfamily of enzymes is a class of oxidoreductases coded for by 57 genes and 58 pseudogenes in humans which are the most important group of drug metabolising enzymes in man.[81] These enzymes are monooxygenases that catalyse the chemical addition of a single oxygen atom to a vast array of both endogenous and xenobiotic substrates in a general reaction simplified thus:

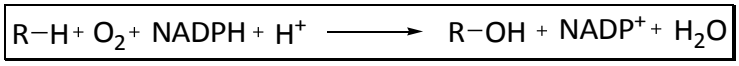

Structurally, CYP450 enzymes are haemoproteins with an average molecular weight of approximately 50,000 Da.[82] At their active sites, they contain a prosthetic ferroprotophyrin IX ring at the centre of which a reduced iron (Fe) atom is bound to four nitrogen atoms and has two free coordination sites for bonding to a conserved cysteine residue from the surrounding protein chain and to substrate atoms.[83]

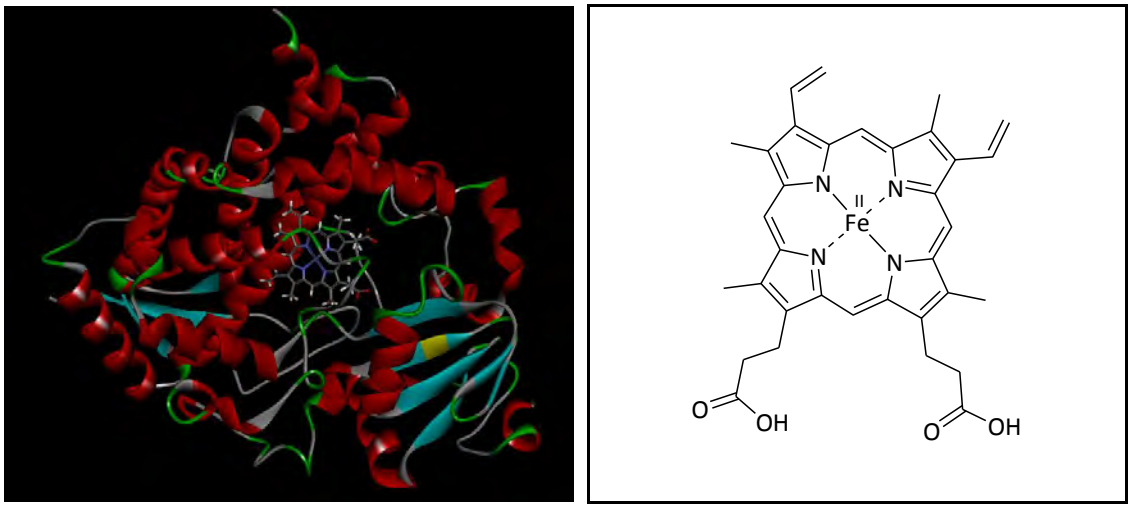

Figure 1.9: Structure of chain A of human CYP3A4 enzyme. (The prosthetic iron protoporphyrin IX ring system is clearly visible at the active site of the enzyme).

Intracellularly, CYP450s are bound to the membrane of the smooth endoplasmic reticulum in close proximity to cytochrome P450 reductase and cytochrome b_5 which are both important components in the CYP450 oxidation cycle. CYP450s are also found in mitochondrial membranes but in this case having their globular domain oriented towards the lumen.[84]

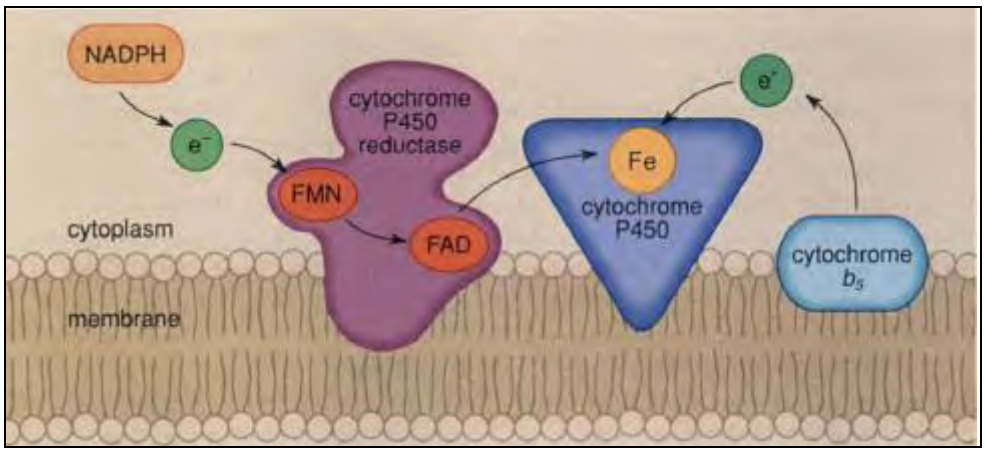

Figure 1.10: Location of CYP450 and related proteins in the endoplasmic reticulum membrane[85]

CYP450s are distributed in virtually all body tissues but occur at their highest concentrations in the liver. Other organs in which the enzymes are present in significant concentrations include the respiratory tract, kidneys, gastro-intestinal tract, brain, heart and skin.[86] Some isoforms are present in varying concentrations in all these different sites, while others are known to be preferentially expressed only in certain tissues or stages of embryonic development. For example, CYP3A7 is expressed abundantly in the endometrium and fetal liver during pregnancy but its concentration and activity rapidly decline after birth and the isoform is virtually absent in adult tissue. On the other hand, all other CYP isoforms are only present at extremely low concentrations in fetal liver but gradually increase after birth.[87]

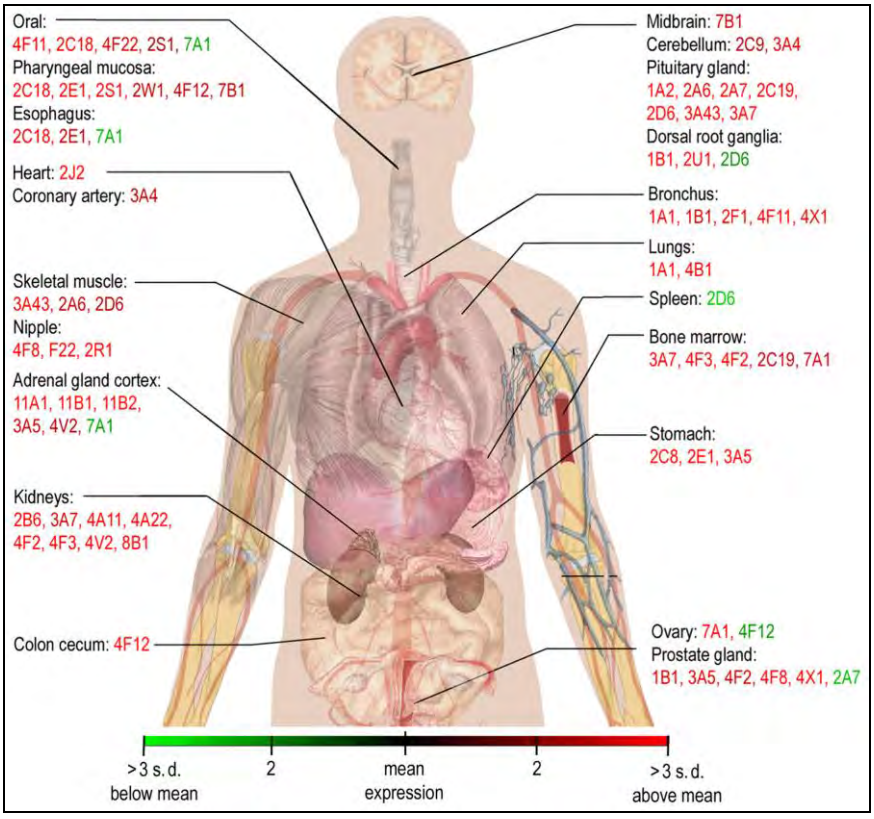

Figure 1.11: Body map illustrating distribution of CYP isoforms in extra-hepatic tissues[88]

A few CYP450 enzymes belonging to the families CYP1, CYP2 and CYP3 have been identified as being involved in the metabolism of xenobiotics. Of these, five specific isoforms (CYP1A2, 2C9, 2C19, 2D6 and 3A4) contribute to the metabolism of approximately 95% of drugs that are metabolized by the CYP enzyme system, representing approximately 75% of all clinically used drugs.[89]

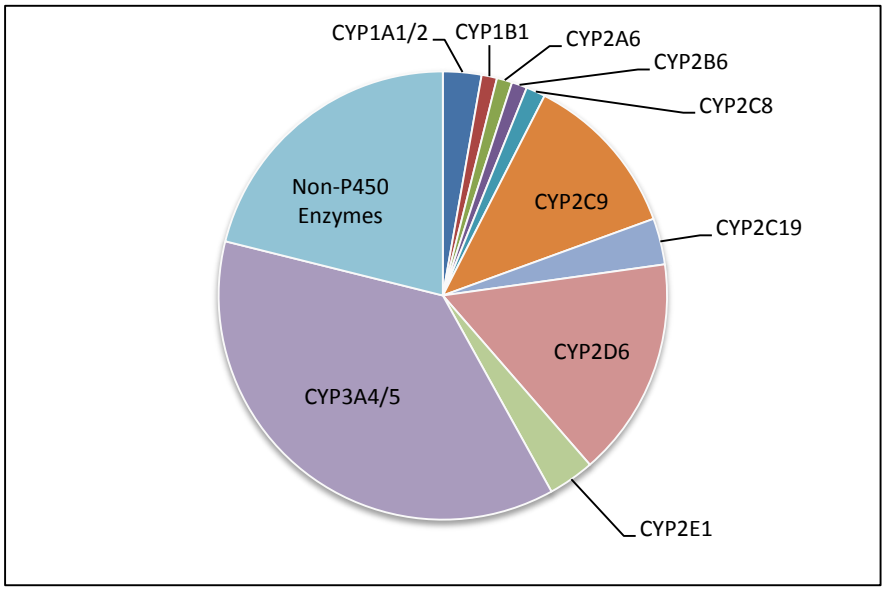

Figure 1.12: Relative contribution of CYP450 isoforms to phase I drug metabolism[90]

Oxidation of substrates by CYP450s is a complex multistep process involving the enzyme, reduced nicotinamide adenine dinucleotide phosphate (NADPH) as the electron donor and flavin adenine dinucleotide (FAD)-containing P450 reductase serving as the electron transfer bridge as illustrated in **Figure 1.13**.[85]

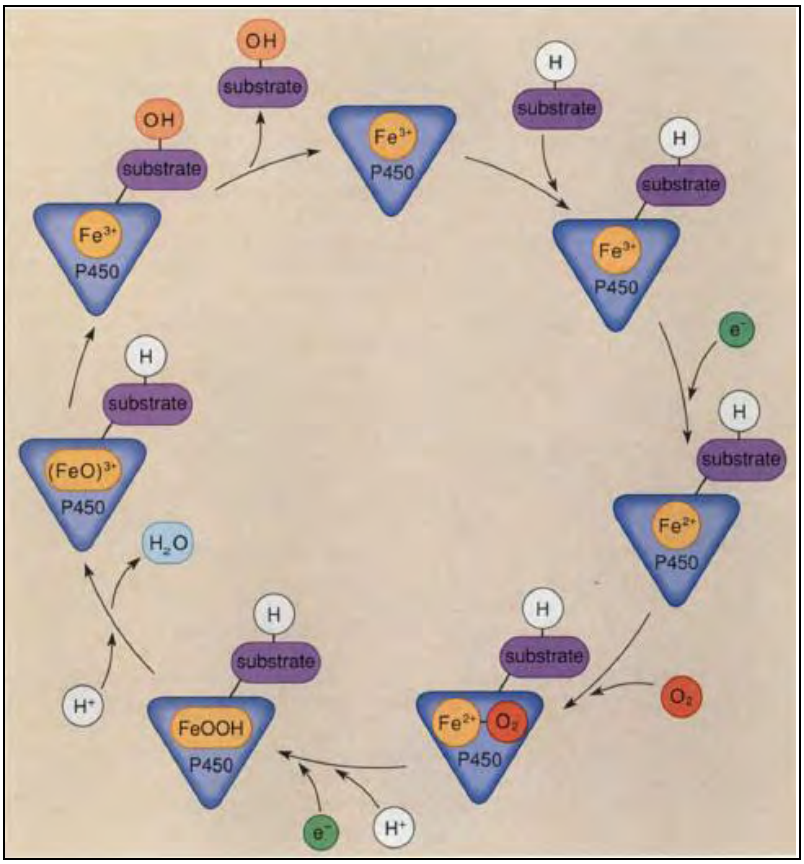

Figure 1.13: Simplified catalytic cycle illustrating substrate oxygenation by CYP enzymes[85]

In addition to catalyzing classical and relatively direct monooxygenation reactions, CYP450s have been found to mediate more complex transformations such as chlorine oxygenation, aromatic dehalogenation, ring expansion and ring formation, as well as cleavage of amino oxazoles and the 1,2,4-oxadiazole ring.[91,92]

Genes encoding for CYP450s belonging to the families CYP1, CYP2 and CYP3 are polymorphic. However, the phenotypic importance of the variant alleles in terms of catalytic activity and protein expression differs. Of the major drug metabolising isoforms, CYP2C9, CYP2C19 and CYP2D6 in particular are well known to exhibit pronounced polymorphism, which often translates to significant inter-individual or inter-population variations in how these enzymes metabolize xenobiotics.[93] Such variation can have a major impact on the therapeutic efficacy of drugs metabolised predominantly by these isoforms as well as on their potential toxicity due to phenotypic variability in metabolism-mediated detoxification and elimination.[94]

Table 1.4: Summary of other non-CYP450 enzymes involved in metabolism of xenobiotics

	Enzyme class	**Characteristics**
Phase I	Flavin-containing monoxygenases (FMOs)	Complementary redox system to CYP450s in drug metabolism but thermally labile, less prone to inhibition and/or induction[95–97]
	Aldehyde oxidase and xanthine oxidoreductases	Molybdenum hydroxylases involved in oxidation of aromatic azaheterocyclic xenobiotics and activation of prodrugs such as allopurinol and pyrazinamide[98]
	Monoamine oxidases	Key in metabolism of endogenous catecholamine neurotransmitters; inhibitors used clinically as antidepressants and in Parkinson's disease[99–102]
	Alcohol and aldehyde dehydrogenases	Extensively diverse superfamilies of polymorphic enzymes critical in the oxidative metabolism of alcohols and aldehydes[103]
	Esterases	Important for activation of ester, thioester and amide prodrugs[104]
	Aldo-keto reductases	Involved in detoxification of reactive aldehydes and α,β-unsaturated carbonyl xenobiotics[105–107]
Phase II	Uridine glucuronosyl transferases Sulfotransferases *N*-acetyl transferases Glutathione-*S*-transferases Methyl transferases	Principally conjugative enzymes that couple xenobiotics or their Phase I metabolites to an endogenous substrate donated by cofactors such as uridine 5'-diphosphoglucuronic acid (UDPGA), 3'-phosphoadenosine-5'-phosphosulfate (PAPS), acetyl-coenzyme A, glutathione and *S*-adenosyl methionine (SAM).[108–121]

1.6 Classification of Metabolites

Regardless of the route through which xenobiotic substrates are metabolized, the net result is the formation of metabolic species that may be broadly classified based upon chemical reactivity as stable or reactive.

1.6.1 Stable Metabolites

1.6.1.1 Biologically inactive stable metabolites

In many instances, the chemical modification of xenobiotics by metabolic enzymes results in a total or significant loss of pharmacological activity due to changes in their chemical properties and ability to interact with therapeutic targets *in vivo*. When designing drugs, emphasis is often placed on developing compounds that possess optimal metabolic stability to allow for convenient dosing. In some cases, however, drugs may be intentionally designed to be readily metabolised to inactive species in a predictable and controllable manner after exerting their therapeutic activity by incorporating metabolic hotspots in the molecule. This 'soft drug' design is particularly useful in developing medicines that have minimal adverse effects arising from their interaction with off-target receptors or due to biotransformation to multiple metabolic products.[122]

1.6.1.2 Biologically active metabolites

Conversely, metabolism of the xenobiotic substance may result in products that possess pharmacological activity of equal, lesser or greater magnitude than the parent. Active metabolites are thus be defined as metabolic products of biotransformation that have pharmacological activity against the same pharmacological target as the parent drug molecule.[123] The phenomenon of active metabolite formation is sometimes utilized in the formulation of medicines as prodrugs which are inherently inactive but designed to undergo metabolic biotransformation to yield therapeutically active metabolites. The prodrug approach is useful in allowing for the design of compounds that possess optimized physicochemical properties such as membrane permeability, aqueous solubility or chemical stability and enhanced pharmacokinetic profiles.[124,125]

Most active drug metabolites arise from phase I metabolism, but some medicines are known to yield both active and inactive phase II metabolites. For example,

morphine-6-glucuronide is known to possess even greater analgesic activity than its parent morphine, whereas morphine-3-glucuronide has been shown to be a potent opioid antagonist in animal models and somewhat paradoxically, also appears to enhance pain through unknown mechanisms.[126,127]

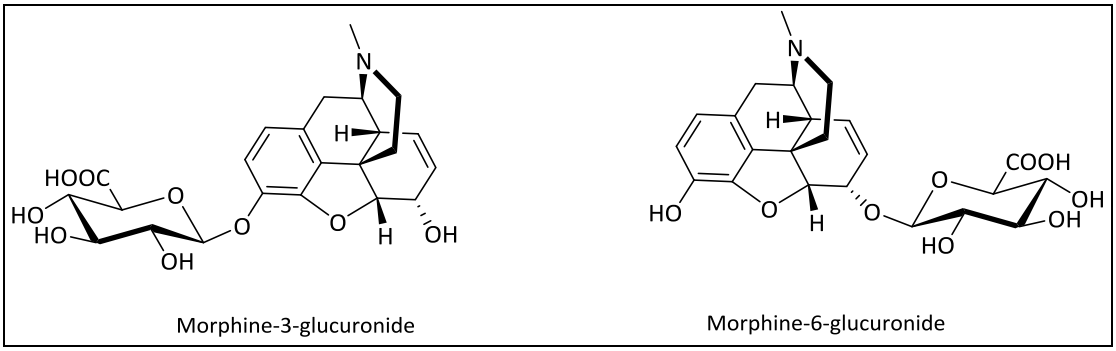

Figure 1.14: Glucuronide metabolites of morphine having different pharmacological activities

1.6.2 Reactive Metabolites

Reactive metabolites were first recognized in work reported in the 1940s when James and Elizabeth Miller investigated the metabolism in rats of the carcinogenic dye 4-dimethylaminoazobenzene (DAB) formerly used as a food coloring agent. They observed that liver proteins of animals treated with DAB became permanently yellow colored. Upon treatment with alkali, these proteins released 3-methylthio-*N*-methyl-4-aminoazobenzene, suggesting that covalent binding involved modification of protein methionine residues by an "active form" of a mono-demethylated metabolite of the dye.[128] Reactive metabolites are unstable and chemically reactive products of metabolism capable of reacting with endogenous macromolecules in their immediate environment, including the enzymes responsible for their formation. These metabolites may be classified into two broad categories: electrophiles - which may be further classified as being either alkylating or acylating agents and free radicals. Alternatively, electrophiles may also be classified as being soft or hard species. The classic soft electrophiles include epoxides, α,β-unsaturated carbonyls, quinones, quinone imines, quinone methides, imine methides, isocyanate, isothiocyanates, aziridinium and episulfonium ions. Aldehydes and iminium ions are regarded as being hard electrophiles.[129] Electrophiles vary in their selectivity for biological nucleophiles but in general, mainly target cysteine, methionine, lysine,

histidine and to a lesser extent glutamate and aspartate amino acid residues on proteins.

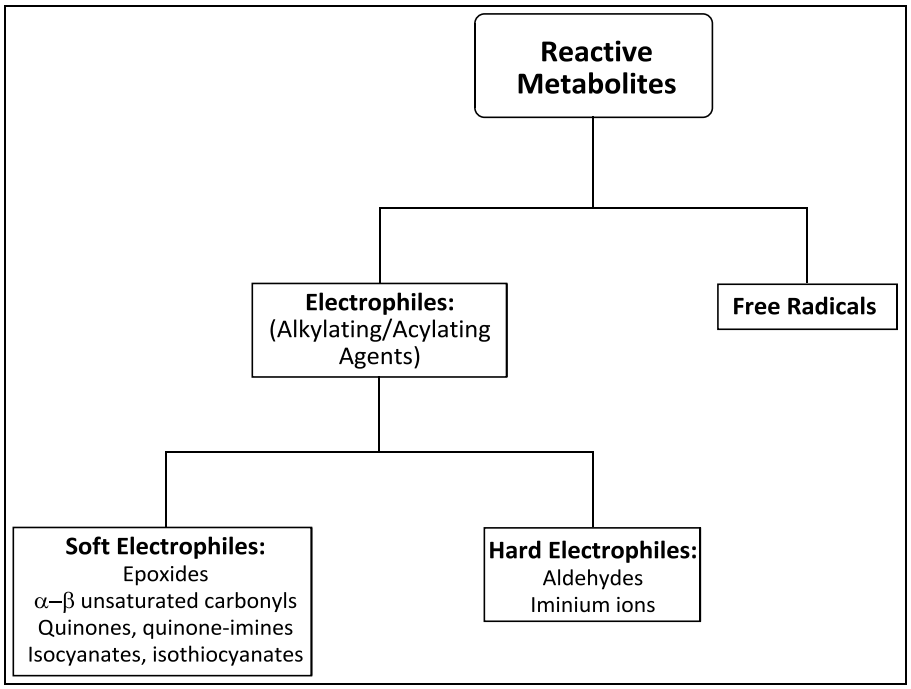

Figure 1.15: Generalised classification of reactive metabolites

Reactive metabolites are difficult to isolate or characterize and their chemical structures can only be inferred from trapped products. Even in the cases where they can be synthesized, these compounds are stable only in aprotic solvents and cannot be administered to animals to study their *in vivo* effects directly.[130]

1.7 Metabolism-Mediated Xenobiotic Toxicity

Metabolism of xenobiotics is usually a detoxification process. In some instances, however, metabolism may lead to formation of the reactive metabolites alluded to previously causing deleterious effects due to their interaction with endogenous macromolecules. The mechanisms through which reactive metabolites cause toxicity are complex but generally involve covalent binding of such metabolites to enzymes, membrane proteins or nucleic acid bases in DNA or RNA.[131–133] Covalent binding may result in sufficient structural modification of the endogenous target causing it to lose its primary biological function. In the case of enzymes, inhibition of catalytic activity may occur, while for DNA and RNA, disruption of genetic material may result in mutations and possibly carcinogenesis. In addition to binding directly to cellular

targets, reactive metabolites may undergo chemical transformation to yield highly reactive oxygen species or radicals that trigger damaging oxidative stress in target tissues.[134]

It is now almost universally accepted that idiosyncratic adverse reactions (IADRs) to xenobiotics are mediated through reactive metabolites interacting with macromolecular targets *in vivo.*[135] Among the mechanisms proposed that lead to such idiosyncratic reactions is an immune response triggered by covalent binding of the reactive metabolite changing the 3-dimensional structure of the target macromolecule.

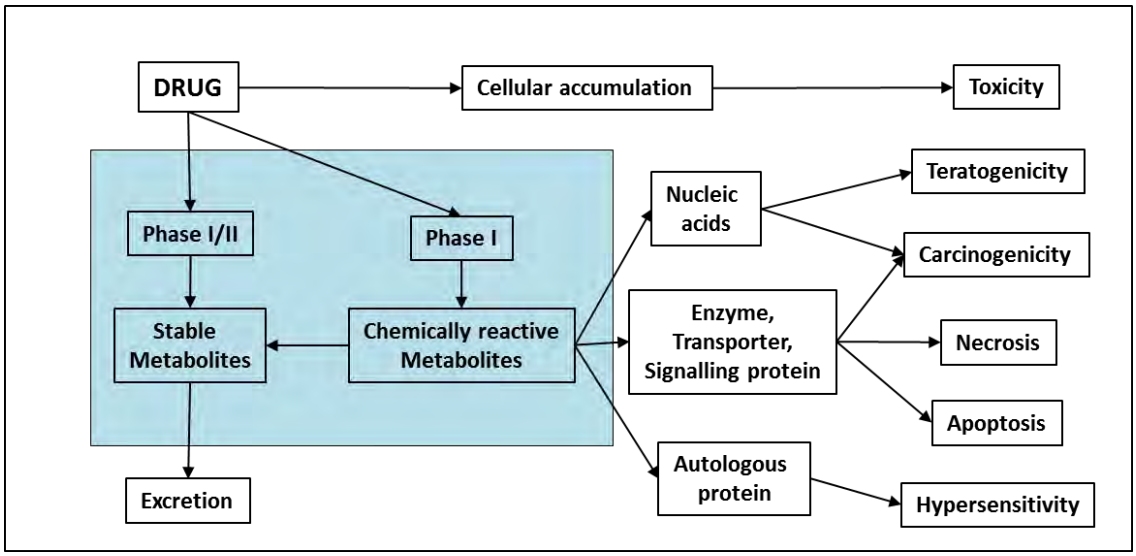

Figure 1.16: Relationship between metabolism and toxicity [136]

Idiosyncratic adverse reactions are particularly difficult to predict during drug development because they are unrelated to the known pharmacology of the compound, are usually not dose-dependent and since they only occur only rarely, might not be observed in the relatively small number of patients monitored during clinical trials. Additionally, these reactions cannot easily be studied using animal models during preclinical development since their occurrence in such models is often idiosyncratic as well.[137]

1.7.1 Metabolism-Mediated Toxicity of Conventional Drugs

Numerous examples of drugs withdrawn from the market or whose clinical use is restricted due to toxicity arising from metabolic biotransformation exist. Paracetamol is one of the most widely used over-the-counter analgesic-antipyretic

medications worldwide with a good safety profile when administered at therapeutic doses. However, in overdose, paracetamol is a potent hepatotoxin due to its metabolism to a reactive quinone-imine intermediate that covalently binds to hepatocellular proteins resulting in necrosis and acute liver failure.[138,139] At normal doses, CYP450-mediated quinone-imine biotransformation is a minor metabolic pathway with most of the drug undergoing glucuronidation and sulfonation as the preferred routes of metabolism. At high drug concentrations, however, quinone-imine formation may occur at a rate that exceeds the capacity of normal glutathione-mediated detoxification leading to the toxic effects observed clinically.[140]

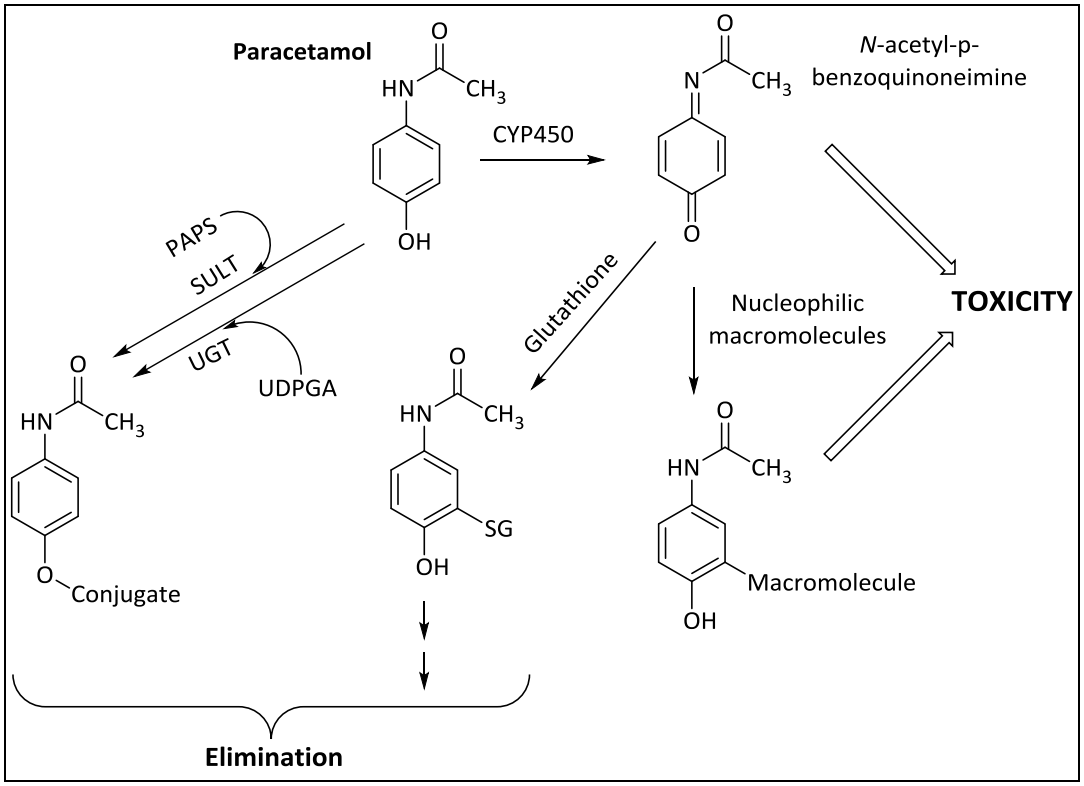

Figure 1.17: Metabolism and bioactivation of paracetamol

The antipsychotic drug clozapine is another example known to exhibit reactive metabolite-mediated drug toxicity. Clinically, clozapine is associated with adverse incidences of agranulocytosis in about 0.8% of patients characterised by depletion of neutrophil counts triggered by the formation of a reactive nitrenium or iminium ion metabolic intermediate.[141] Clozapine toxicity appears to affect neutrophils most because they express high levels of myeloperoxidases, which are the enzymes thought to be responsible for the formation of the reactive metabolic intermediates.

Further evidence that clozapine toxicity is mediated via iminium intermediates is provided by the fact that the structurally analogous drugs quetiapine and loxapine in which the diazepine ring is replaced by thiazepine and oxazepine rings respectively, are devoid of similar adverse effects.[142] Absence of the bridging N atom required to form an iminium ion in both cases supports the proposed bioactivation theory.

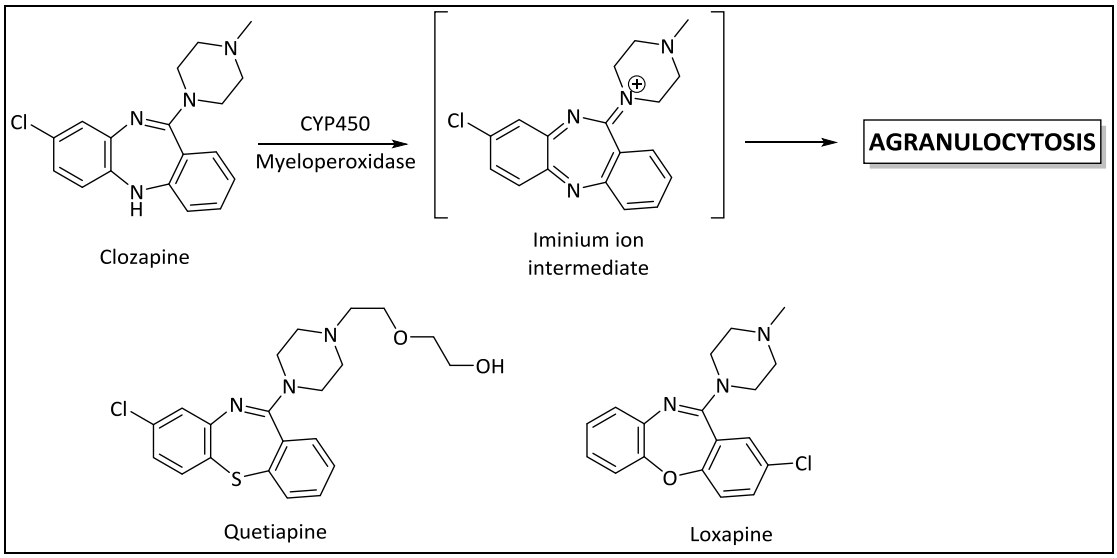

Figure 1.18: Bioactivation of clozapine. (The non-reactive intermediate forming analogues quetiapine and loxapine are illustrated for structural comparison).

As illustrated with paracetamol, for many compounds, toxicity due to reactive metabolite formation is partly influenced by the dose of the drug administered. A survey published in 2011 by Stepan *et al.* found that 84% of drugs withdrawn from the market due to IADRs associated with reactive metabolites had daily doses greater than 100 mg compared to none administered at doses less than 10 mg and only 6% administered at 10 – 50 mg daily. Similar trends were observed for marketed drugs whose use is restricted by so-called "black-box" warnings. In this case, 81% have typical daily doses greater than 100 mg, 11% are administered at 50 – 100 mg while none administered at less than 10 mg fall under such restrictions.[143]

1.7.2 Metabolism-Mediated Toxicity of Natural Products

Natural products that cause toxic effects in humans mediated through metabolic biotransformation have been widely reported. Aflatoxin B1 is a long established thermo-labile hepatotoxin produced by the fungal species *Aspergillus flavus* and *A.*

parasiticus commonly found as contaminants in poorly stored mouldy grains such as maize or wheat.[144] The mechanism by which aflatoxin B1 causes toxicity involves initial formation of a highly reactive exo-epoxide resulting from oxidative metabolism of the parent. The epoxide intermediate reacts with DNA, specifically binding to the N7 atom of guanine residues, thereby causing defects in the DNA sequence. Although the epoxide can also bind directly to amino acid residues in proteins, this process usually involves initial acid-catalysed hydrolysis of the epoxide to aflatoxin B1 dihydrodiol followed by base-catalysed conversion to aflatoxin B1 dialdehyde. The dialdehyde form then attacks lysine residues present in hepatocyte proteins, disrupting their 3D structure and functionality and resulting in toxicity.[145]

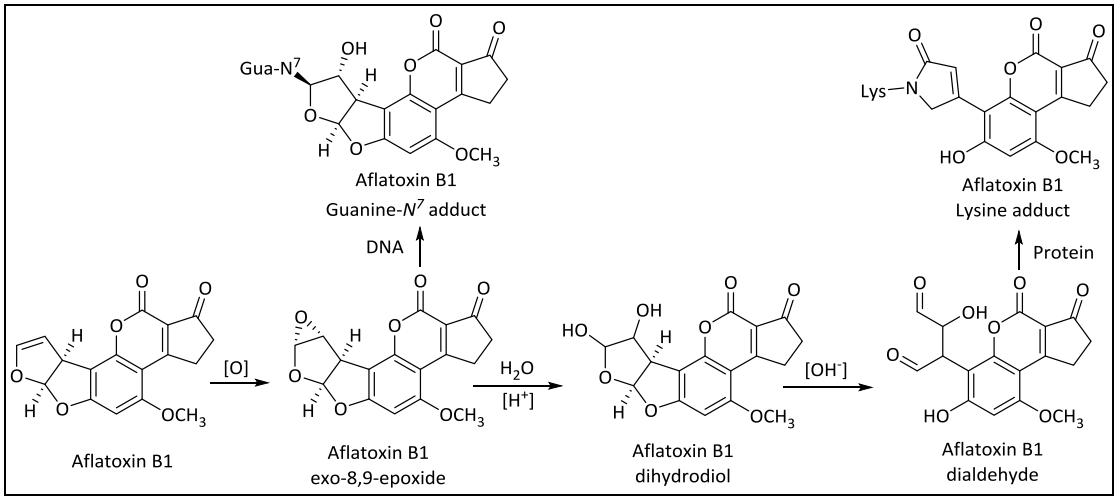

Figure 1.19: Metabolic bioactivation of aflatoxin B1 and formation of DNA and protein adducts

Aristolochic acids are nitrophenanthrene carboxylic acid natural products present in plants of the genus *Aristolochia*. In incidences first reported in 1993, when components of these plant species were inadvertently included in herbal preparations used as weight loss agents in Belgium, cases of terminal renal failure resulted in patients.[146] It has since been established that aristolochic acids are metabolized to reactive intermediates implicated in causing nephropathies characterised by renal fibrosis and development of urothelial cancer.[147,148] Metabolic bioactivation of aristolochic acids involves the initial reduction of the nitro group catalysed by CYP1A1, CYP1A2 or COX-I followed by condensation resulting in formation of a lactam ring. Oxidation of the lactam at the N atom forms the *N*-hydroxide which is transformed to a reactive cyclic nitrenium ion in a reaction

possibly mediated by sulphotransferases.[149–151] The nitrenium ion intermediate covalently binds with adenosine and guanine residues in DNA leading to mutations that trigger carcinogenesis in renal tissue where the enzymes responsible for reactive intermediate formation appear to have high activity.[152]

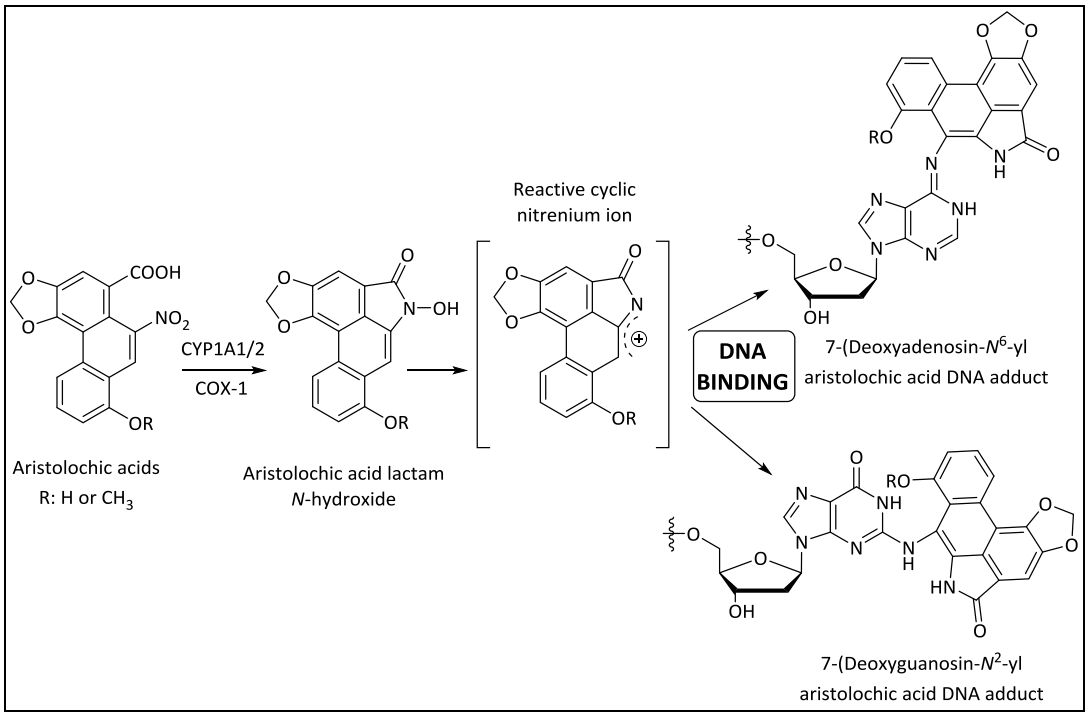

Figure 1.20: Bioactivation of aristolochic acids and binding to DNA residues

The botanical dietary supplement kava derived from *Piper methysticum* contains the natural products kawain and methysticin as the main active ingredients thought to be responsible for its sedative, anxiolytic, muscle relaxant, anaesthetic and anticonvulsant properties.[153] Reports of hepatotoxicity associated with kava use have been linked to the bioactivation of methysticin *in vivo*. The proposed mechanism for bioactivation involves initial CYP450-catalysed conversion of the benzodioxole ring in methysticin to a catechol metabolite that undergoes further oxidation to form the electrophilic *ortho*-quinone which may react with glutathione or covalently bind and modify hepatic proteins.[154]

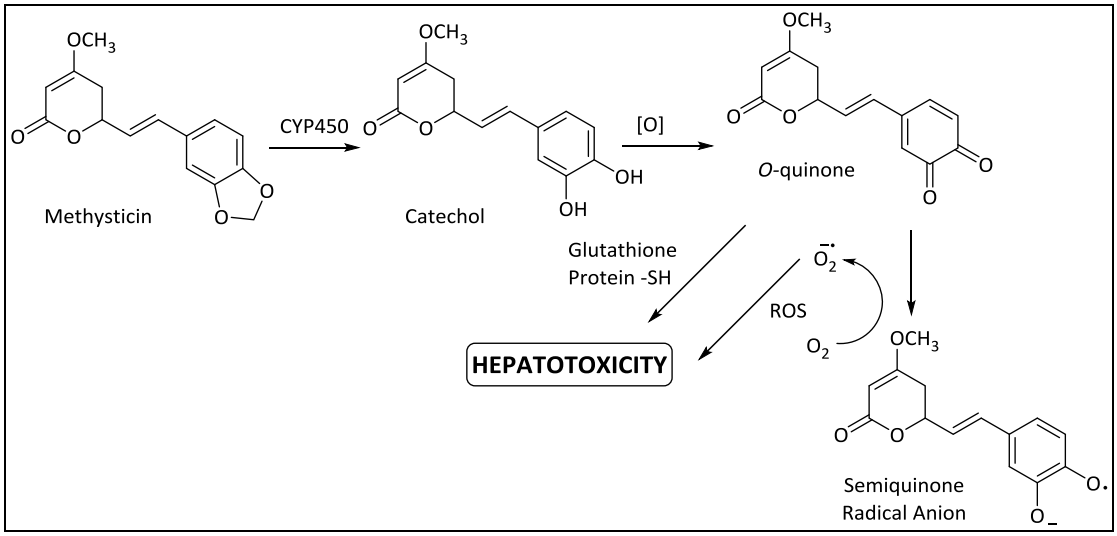

Figure 1.21: Proposed bioactivation of methysticin in kava preparations

Other natural product metabolites exert their toxic effects indirectly through drug interactions with conventional medicines. A well documented example of this is the interaction of grapefruit juice and numerous drugs, first reported with the antihypertensive calcium channel blocker felodipine.[155] Components in grapefruit juice have been shown to be potent inhibitors of enterocyte CYP3A4, which is responsible for presystemic metabolism of many orally administered drugs in the GIT.[156] The enzyme inhibition is mechanism-based and for drugs such as felodipine, may result in a clinically significant increase in the amount of drug absorbed from the GIT and its subsequent plasma concentrations. Enzyme inhibition and reactive metabolite studies have shown that the main component in grapefruit juice responsible for CYP3A4 inhibition is the furanocoumarin bergamottin acting via bioactivation to a reactive epoxide intermediate.[157,158]

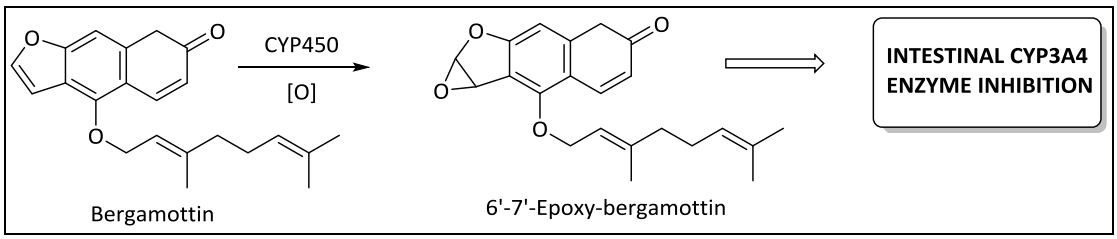

Figure 1.22: Proposed bioactivation of bergamottin by intestinal CYPs and resultant CYP3A4 inhibition

1.8 Profiling ADME Properties in Early Drug Discovery

Prior to 2000, the majority of drug candidates progressing through to clinical trials but which failed to receive marketing approval were mainly unsuccessful due to poor absorption, distribution, metabolism, excretion (ADME) and toxicology properties or drug metabolism and pharmacokinetic (DMPK) profiles.[159,160] To avert such high attrition rates, pharmaceutical companies began to increasingly conduct ADME studies much earlier in the drug discovery process as part of rational drug design.[161–163] This shift has had a dramatic effect in reducing the percentage of drug candidates that fail to meet regulatory requirements due to ADMET/DMPK liabilities over the last decade. Despite these changes in emphasis, however, drug toxicity and lack of efficacy are still the leading causes of attrition during late stage drug development or withdrawal of marketing approval for already licensed drugs.[164]

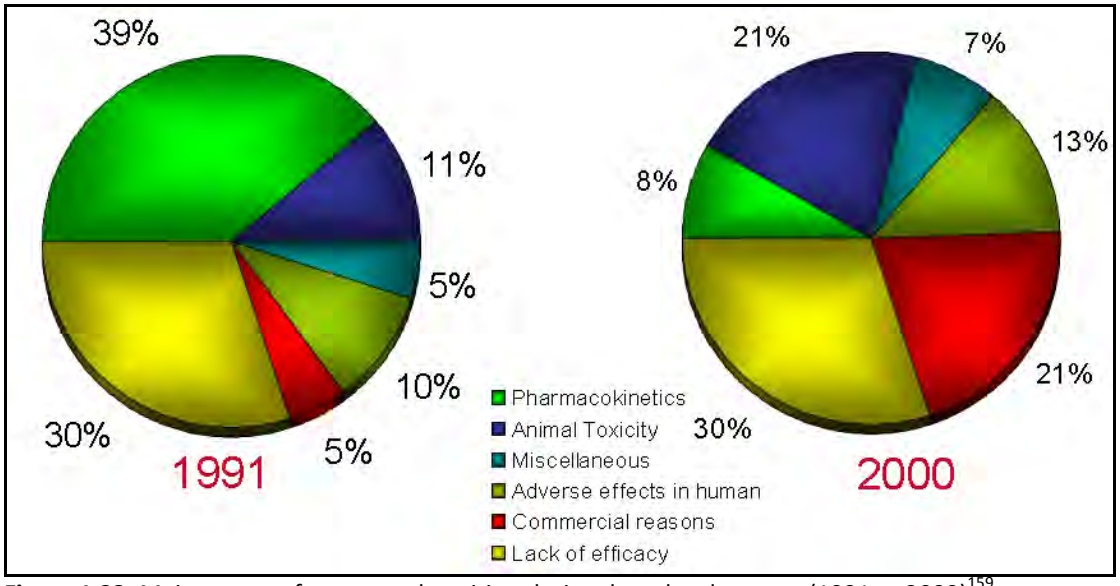

Figure 1.23: Main causes of compound attrition during drug development (1991 vs 2000)[159]

1.8.1 Computational Tools in ADMET Profiling

Computational tools are an integral part of modern drug discovery and are employed in virtually all aspects of development from initial hit identification to marketing authorisation.[165] They are used to help predict ADMET properties of drug candidates early in the development cycle to minimise the costs and time taken to determine such profiles experimentally. *In silico* tools are used to calculate or predict structure-based physicochemical parameters such as acid dissociation constants (pKa), lipophilicity, aqueous solubility, H-bonding, polar surface area and other so-called

"Lipinski Rule of Five" descriptors for drug-likeness on which ADMET properties largely depend.[166,167] Additionally, actual ADMET properties may be predicted based on combinations of the physicochemical data generated and simulated models using mathematical algorithms based on experimental data from real drugs. Predicting ADMET properties such as absorption, which are dependent on both known characteristics such as compound solubility, lipophilicity, and polar surface area but also on unknown parameters such as active transport is challenging even using computational tools. Consequently, many software applications differ in the algorithms and statistical approaches they use to predict these properties, usually incorporating numerous property descriptors and assigning different weights to them in overall property calculations.[168–170] Despite this, however, predictive computational tools for ADMET profiling are never 100% accurate with models and simulations being highly dependent upon the quality of the real-world experimental data used to build them.[171,172]

Prediction of compound metabolism using *in silico* tools uses several approaches, usually combinations of rule-based and structure-based QSAR models often relying on known 3D structures or protein homology models of enzymes to calculate the probability and magnitude of interactions between compounds and enzymes using ligand docking simulations.[173,174] These tools are typically designed to predict the most likely site(s) of metabolism on test molecules and the chemical species likely to arise from transformation at the identified sites by specific xenobiotic metabolizing enzymes.[175–177]

Apart from the prediction of metabolism and toxicity, computational tools are also used to profile other ADMET properties such as compound absorption, oral bioavailability and distribution *in vivo*, particularly for drugs intended to exert their effects in specific target organs such as the CNS.[178,179] At present, however, success in accurate prediction of metabolism using current *in silico* tools remains still somewhat limited.

1.8.2 Metabolic Stability and Enzyme Phenotyping

A key determinant of the rate at which drugs are cleared from the body and therefore their therapeutic effectiveness is the ability to resist metabolic

transformation. For compounds that are metabolised to toxic species, ease of biotransformation may be an important factor in determining the magnitude or risk of toxicity *in vivo*. *In vitro* metabolic stability assays are therefore conducted in early ADME profiling to provide data for use in predicting or extrapolating *in vivo* intrinsic clearance rates and possibly to identify the relative contribution of different organs or tissues to compound clearance.[180]

Experimental *in vitro* metabolic stability data is obtained by incubating compounds in a variety of metabolism systems most commonly, microsomal fractions from liver, kidney, lung or intestines, fresh or cryopreserved hepatocytes, liver slices, as well as plasma and S9 fractions.[181,182] In addition to using human tissue, metabolic systems from animal models such as mice, rats, dogs and primates are also used to conduct these assays. Data from *in vitro* metabolic stability experiments is used to extrapolate the *in vivo* metabolic disposition of compounds in both humans and animals and provides information for prioritising compounds to be advanced to more capital intensive and technically involving preclinical *in vivo* pharmacokinetic assays. Identification of the metabolites formed from such stability assays also provides information on the metabolic hotspots in the substrates and insights on how such can be modified through medicinal chemistry efforts if necessary.[183]

Enzyme phenotyping assays are performed to identify the specific enzymes involved in any transformation observed from metabolic stability assays and the individual contribution of these enzymes to overall compound disposition. Phenotyping assays provide an early indication of compounds whose disposition in different patient populations may vary significantly because their main route of metabolism is mediated by genetically polymorphic enzyme isoforms. Since CYP450s are the enzymes known to metabolize the vast majority of drugs in clinical use, *in vitro* CYP450 phenotyping assays are by far the most commonly performed in early ADMET profiling. Enzyme phenotyping may be carried out by incubating test substrates in different individual isolated purified recombinant enzymes and subsequently determining the relative contribution of each to metabolism. Alternatively, compounds may be incubated in microsomes which typically contain a mixture of enzyme isoforms and the individual contribution of each to metabolism determined by adding specific inhibitors of the different isoforms then calculating

the difference in metabolism observed in either case.[184] Enzyme inhibitors used in the latter approach are usually specific chemicals and drug compounds, or alternatively, poly- or monoclonal antibodies that bind and inhibit specific enzyme isoforms.[185]

These techniques have inherent shortcomings that often lead to poor correlation between enzyme phenotyping data generated using the two methods for the same compound. For instance, CYP450 phenotyping using liver microsomes and specific chemical inhibitors is often confounded by the fact that the inhibitors used exhibit some degree of cross-reactivity with different isoforms. Use of specific antibodies in place of chemical inhibitors may minimize unwanted cross-reactivity effects but introduces higher costs and experimental complexity. On the other hand, CYP450 phenotyping using recombinant enzymes expressed from heterologous systems such as *E. coli* or yeast is often affected by the fact that activity of the enzymes may vary widely owing to differences in CYP450 protein:NADPH reductase: cytochrome *b5* co-expression ratios.[186]

1.8.3 Predicting Formation of Reactive Metabolites from Structural Alerts

Structural alerts are chemical functional groups in xenobiotics that may undergo metabolic bioactivation to reactive intermediates that result in toxicity. These groups are sometimes referred to as toxicophores. The presence of structural alerts is, however, not always definitive proof of bioactivation to form reactive metabolites. Many drugs that possess structural alerts are devoid of reactive metabolite formation liabilities and exhibit good safety profiles. Nevertheless, in early drug discovery ADME profiling, structural alerts are often flagged and used as a basis for 'go-no go' decisions (**Figure 1.24**) based on the existing body of evidence supporting their involvement in formation of toxic reactive metabolites and covalent protein binding.[187]

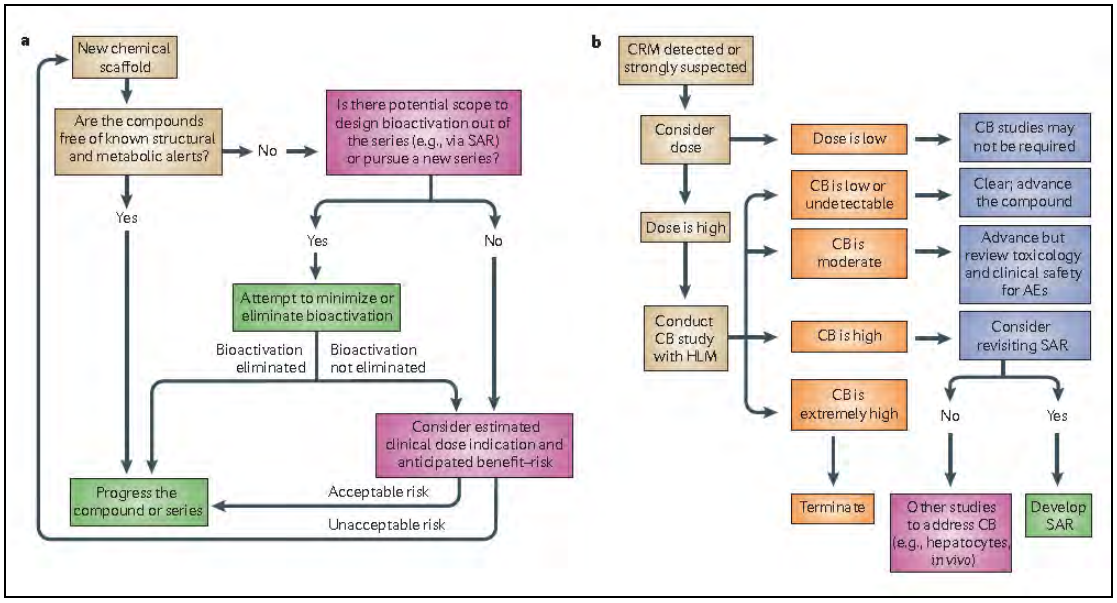

Figure 1.24: Example of possible decision scheme for handling bioactivation data at different stages of drug development. **Scheme (a):** Reactive metabolite data from early drug design and optimization; **Scheme (b):** Covalent binding data in late preclinical or early clinical research (CRM: Chemically reactive metabolites; CB: Covalent binding)[187]

Established toxicophores whose presence in drug design is avoided as much as possible include anilines, quinones, quinone methides, monosubstituted furan and thiophene rings, benzodioxoles, α,β-unsaturated carbonyls, terminal alkenes, terminal and ω-1 alkynes, cyclic tertiary amines, aldehydes and epoxides, among others.[188]

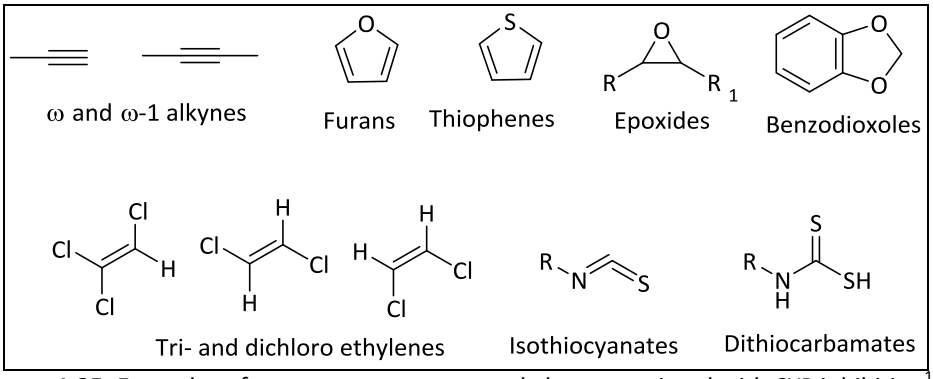

Figure 1.25: Examples of some common structural alerts associated with CYP inhibition[189]

Detection of structural alerts when conducting early ADME profiling on potential drug compounds may involve simple unaided visual inspection of molecular structures when working with small compound libraries or, more commonly, the use of software to screen large compound sets.[190] Apart from allowing faster screening of compounds, computational tools have the advantage of being programmable for

detection of structural alerts that might be 'masked' within complex chemical structures and thus not immediately obvious to the inexperienced eye.

1.9 *In vitro* Determination of Reactive Metabolite Formation

1.9.1 Enzyme Inhibition Assays

Enzyme inhibition assays using substrates that generate metabolites which can be monitored through relatively simple detection techniques such as fluorospectrometry are routinely used for high throughput compound screening for assessing potential drug-drug interaction. In these screens, the test compounds are incubated in purified recombinant enzymes or microsomal proteins in the presence of probe substrates of the drug metabolizing enzyme(s) to be monitored for inhibition.[191] Comparison of the rate or extent of probe substrate metabolism in incubations containing the test compound against those without the test compound provides an indication of how strongly enzyme activity is inhibited. Detection techniques such as fluorimetry may be used to quantify enzyme inhibition if the metabolites generated are fluorescent compounds.[192]

A modification of the enzyme inhibition assay that determines if inhibition of enzyme activity is time-dependent involves first incubating the test compound with the enzyme in the presence and absence of co-factors before adding the probe substrate. If enzyme inhibition is observed to be significantly higher following pre-incubation with the test compound compared to no pre-incubation, this is strongly indicative that the formation of reactive metabolites may be responsible for the observed inhibition.[193,194]

Enzyme inhibition assays in early drug discovery are typically aimed at screening a large number of compounds in a short time and are usually carried out in 96-well microplates to increase throughput. At this stage, emphasis is placed more on approximating the relative enzyme inhibition potential of different compounds for purposes of ranking. Detailed inhibition assays are only being carried out later to determine parameters such as the mode of inhibition and enzyme inhibition constants.

1.9.2 Reactive Metabolite Trapping Assays

In vitro reactive metabolite trapping experiments are perhaps the most common technique for detecting electrophilic reactive metabolic intermediates in early drug discovery. While time dependent enzyme inhibition assays are typically used to screen large volumes of compounds in a short time, in most cases they do not provide data related to the actual intermediate or species responsible for any observed inhibition, thus the need to carry out trapping experiments.

The general procedure in these assays involves the incubation of test substrates in a suitable metabolic system, most commonly human hepatic microsomes with the necessary cofactors included and in the presence of a nucleophilic trapping agent capable of forming stable covalent adducts with any reactive metabolites formed. In the case of reactive metabolites arising from oxidative bioactivation reactions, *in vitro* assay systems that make use of electrochemical oxidation cells in place of biological systems such as microsomes have been reported.[195,196] The ideal choice of trapping agent used to capture reactive metabolites depends on the reactivity of the metabolites formed. Soft electrophilic reactive metabolites are most commonly trapped using reduced glutathione (GSH) or glutathione analogues such as glutathione ethyl ester. Hard electrophiles such as iminium ions may be too reactive to be effectively trapped using GSH but ideal for trapping using cyanide ions. Reactive aldehyde metabolites are similarly best trapped using amines such as methoxylamine and semicarbazide.[197] Stable isotope radiolabelled analogues and fluorescent dansylated derivatives of glutathione have also been reported to improve sensitivity in detecting trapped reactive metabolites.[198–200]

Highly sensitive analytical techniques are required to detect trapped intermediates from these *in vitro* assays due to the typically low concentrations of the metabolites formed and also the need to have structural data that can be used in adduct identification. At present, liquid chromatography coupled to tandem mass spectrometry (LC-MS/MS) offers the best analytical option by allowing for the separation of analytes from the often complex biological sample incubation matrix and subsequent identification of trapped metabolites based on their mass/charge (*m/z*) ratios and fragmentation patterns.[201,202]

1.9.3 Covalent Binding Studies

Covalent binding studies are usually only conducted in the later stages of reactive metabolite profiling of drug leads because they require the use of radiolabelled test compounds. Due to the relatively high costs, hazards and technical expertise involved in synthesizing radiolabelled substrates, these studies are only performed on compounds already in fairly advanced phases of preclinical drug development.[203] In these assays, the general procedure involves incubation of the radiolabelled drug in a metabolising system, usually microsomal proteins, in the presence of the necessary cofactors. At the end of the incubation, microsomal proteins are precipitated, centrifuged and washed to remove any unbound drug or metabolites. The washed proteins are then digested and residual radioactivity measured as an indicator of the radiolabelled drug or metabolite covalently bound to the proteins. Nucleophilic trapping agents such as reduced glutathione may also be incorporated in the incubation to determine their influence on the extent of any covalent binding observed.[204]

1.10 Research Program

1.10.1 Study Justification

Toxicity of drug candidates is a major cause of attrition of promising compounds in drug discovery. Only about 11% of compounds entering clinical development ever reach the market - more than a third are withdrawn due to reasons related to toxicology and clinical safety.[205] Although overt toxicity studies are often conducted *in vitro* alongside assays to determine pharmacological activity on drug candidates from synthetic or natural product origin, these studies are often not equipped to predict toxicity arising from *in vivo* metabolism of the test compounds. Numerous drugs have been developed, licensed and marketed but subsequently discovered to cause IADRs mediated through metabolic intermediates that have significant toxicity profiles leading to their withdrawal from the market. Even in situations where the drug is not withdrawn, severe limitations in its therapeutic application may have to be implemented in the form of "black box" warning labels that restrict its use.

From a drug development perspective, such scenarios greatly undermine the time, effort and cost involved in developing a compound for therapeutic use in patients. To minimize these situations, ADME profiling studies are increasingly being incorporated early in the drug discovery process.

Drugs from natural sources are often considered to be safer and less likely to cause toxicity compared to synthetic compounds. While this assumption may be true for many natural products, it does not apply universally. In many third world countries, access to medicine and healthcare services is an unmet need to the majority of the population. Consequently, natural product-based alternative and traditional herbal medicines play an important role in providing remedies to ailments and are often used by patients alongside conventional medicines.[206] The WHO estimates that in Africa alone, 80% of the population relies on traditional medicines for their healthcare needs, while in China, these remedies account for about 40% of all healthcare delivered.[207]

As observed with some synthetic drugs, components of natural product remedies may interact unfavourably with conventional medicines or other natural products if co-administered. Additionally, like conventional medicines, some natural products

may undergo metabolic transformation to form reactive metabolites that trigger toxic outcomes or IADRs.

Because traditional natural product medicines are not subjected to the same rigorous studies and safety profiling assessments typically accorded to conventional drugs, they may pose a potentially greater risk of causing adverse reactions. Therefore, investigating the potential of natural products used as remedies for treatment of disease to undergo undesirable metabolic bioactivation would allow early discovery of toxic liabilities prior to the exploitation of these compounds as possible leads in drug discovery programs.

1.10.2 Aims and Objectives

The main objective of this study was to determine the physico-chemical and metabolic properties of natural products with respect to druggability, potential to form reactive metabolites and inhibit major drug metabolising CYP450 enzymes.

A secondary objective was to identify the cross-inhibitory effects of chemical inhibitors routinely employed in early CYP450 pehnotyping assays using human liver microsomes.

1.10.3 Specific Aims

The specific aims of this research project are:

1. To create a software database containing data on pure African natural products isolated from multiple sources.
2. Use commercially available *in silico* tools to mine the database created and map the chemical space of the natural products in comparison with that of clinically used conventional medicines.
3. Conduct *in vitro* studies on selected natural products to determine the formation of reactive metabolites through enzyme inhibition and reactive metabolite trapping assays.
4. Determine the cross-reactivity of chemical inhibitors commonly used in performing early CYP450 phenotyping assays in the pharmaceutical industry.

REFERENCES:

(1) Brahmachari, G. Natural Products in Drug Discovery: Impacts and Opportunities - An Assessment. In *Bioactive Natural Products*; Brahmachari, G., Ed.; World Scientific Publishing Company: Singapore, 2011; pp. 1–199.

(2) Sarker, S. D.; Latif, Z.; Gray, A. I. Natural Product Isolation - An Overview. In *Natural Product Isolation*; Sarker, S. D.; Latif, Z.; Gray, A. I., Eds.; Humana Press: Totowa, New Jersey, 2006; Vol. 20, pp. 1–25.

(3) Croteau, R.; Kutchan, T. M.; Lewis, N. G. Natural Products (Secondary Metabolites). In *Biochemistry & Molecular Biology of Plants*; Sons, J. W. &, Ed.; Somerset, New Jersey, 2000; pp. 1250–1318.

(4) Dixon, R. A. Natural Products and Plant Disease Resistance. *Nature* **2001**, *411*, 843–847.

(5) Czárán, T. L.; Hoekstra, R. F.; Pagie, L. Chemical Warfare between Microbes Promotes Biodiversity. *Proceedings of the National Academy of Sciences of the United States of America* **2002**, *99*, 786–790.

(6) Newman, D. J.; Cragg, G. M.; Snader, K. M. The Influence of Natural Products upon Drug Discovery. *Natural Product Reports* **2000**, *17*, 215–234.

(7) Ji, H.-F.; Li, X.-J.; Zhang, H.-Y. Natural Products and Drug Discovery. Can Thousands of Years of Ancient Medical Knowledge Lead Us to New and Powerful Drug Combinations in the Fight against Cancer and Dementia? *EMBO Reports* **2009**, *10*, 194–200.

(8) Schmitz, R. Friedrich Wilhelm Sertürner and the Discovery of Morphine. *Pharmacy in History* **1985**, *27*, 61–74.

(9) Hamilton, G. R.; Baskett, T. F. In the Arms of Morpheus: The Development of Morphine for Postoperative Pain Relief. *Canadian Journal of Anesthesia* **2000**, *47*, 367–374.

(10) Meshnik, S. R.; Dobson, M. J. The History of Antimalarial Drugs. In *Antimalarial Chemotherapy Mechanisms of Action, Resistance, and New Directions in Drug*

Discovery; Rosenthal, P. J., Ed.; Humana Press: Totowa, New Jersey, 2001; pp. 15–25.

(11) Grabley, S.; Thiericke, R. The Impact of Natural Products on Drug Discovery. In *Drug Discovery from Nature*; Grabley, S.; Thiericke, R., Eds.; Springer-Verlag: Berlin, Heilderberg, 1999; pp. 3–37.

(12) Demain, A. L.; Sanchez, S. Microbial Drug Discovery: 80 Years of Progress. *The Journal of Antibiotics* **2009**, *62*, 5–16.

(13) Kaufman, P. B.; Cseke, L. J.; Warber, S.; Duke, J. A.; Brielmann, H. L. *Natural Products From Plants*; Kane, H.; Mogck, M., Eds.; CRC Press LLC: Boca Raton, Florida, 1999; pp. 3–35.

(14) Fabricant, D. S.; Farnsworth, N. R. The Value of Plants Used in Traditional Medicine for Drug Discovery. *Environmental Health Perspectives* **2001**, *109*, 69–75.

(15) Balunas, M. J.; Kinghorn, A. D. Drug Discovery from Medicinal Plants. *Life Sciences* **2005**, *78*, 431–441.

(16) Cragg, G. M.; Newman, D. J. Plants as a Source of Anti-Cancer Agents. *Journal of Ethnopharmacology* **2005**, *100*, 72–79.

(17) Cragg, G. M.; Newman, D. J. Nature: A Vital Source of Leads for Anticancer Drug Development. *Phytochemistry Reviews* **2009**, *8*, 313–331.

(18) Beutler, J. A.; Cragg, G. M.; Newman, D. J. Drug Discovery in Africa. In *Drug Discovery in Africa - Impacts of Genomics, Natural Products, Traditional Medicines, Insights into medicinal chemistry and technology platforms in pursuit of new drugs*; Chibale, K.; Davies-Coleman, M.; Masimirembwa, C., Eds.; Springer Berlin Heidelberg: Berlin, Heidelberg, Heidelberg, 2012; pp. 29–52.

(19) World Health Organization. *Guidelines For The Treatment of Malaria - Second Edition*; World Health Organization: Geneva, 2010.

(20) Bennett, J. W.; Chung, K.-T. Alexander Fleming and the Discovery of Penicillin. *Advances in Applied Microbiology* **2001**, *49*, 163–184.

(21) Butler, M. S. The Role of Natural Product Chemistry in Drug Discovery. *Journal of Natural Products* **2004**, *67*, 2141–2153.

(22) Drews, J. Drug Discovery: A Historical Perspective. *Science* **2000**, *287*, 1960–1964.

(23) Waksman, S. A. Streptomycin: Background, Isolation, Properties, and Utilization. *Science* **1953**, *118*, 259–266.

(24) Jukes, T. H. Some Historical Notes on Chlortetracycline. *Reviews of Infectious Diseases* **1985**, *7*, 702–707.

(25) Gottlieb, D.; Bhattacharya, P. K.; Anderson, H. W.; Carter, H. E. Some Properties of an Antibiotic Obtained from a Species of Streptomyces. *Journal of Bacteriology* **1948**, *55*, 409–417.

(26) Garrod, L. P. The Erythromycin Group of Antibiotics. *British Medical Journal* **1957**, *2*, 57–63.

(27) Levine, D. P. Vancomycin: A History. *Clinical Infectious Diseases* **2006**, *42*, S5–12.

(28) Endo, A. The Origin of the Statins. *International Congress Series* **2004**, *1262*, 3–8.

(29) Stossel, T. P. The Discovery of Statins. *Cell* **2008**, *134*, 903–905.

(30) Gewirtz, D. A. A Critical Evaluation of the Mechanisms of Action Proposed for the Antitumor Effects of the Anthracycline Antibiotics Adriamycin and Daunorubicin. *Biochemical Pharmacology* **1999**, *57*, 727–741.

(31) Saunders, R. N.; Metcalfe, M. S.; Nicholson, M. L. Rapamycin in Transplantation: A Review of the Evidence. *Kidney International* **2001**, *59*, 3–16.

(32) Alves, R. R. N.; Rosa, I. L. Why Study the Use of Animal Products in Traditional Medicines? *Journal of Ethnobiology and Ethnomedicine* **2005**, *1*.

(33) Cushman, D. W.; Ondetti, M. A. History of the Design of Captopril and Related Inhibitors of Angiotensin Converting Enzyme. *Hypertension* **1991**, *17*, 589–592.

(34) Brown, N. J.; Vaughan, D. E. Angiotensin-Converting Enzyme Inhibitors. *Circulation* **1998**, *97*, 1411–1420.

(35) Scarborough, R. M. Development of Eptifibatide. *American Heart Journal* **1999**, *138*, 1093–1104.

(36) Chin, Y.-W.; Balunas, M. J.; Chai, H. B.; Kinghorn, A. D. Drug Discovery from Natural Sources. *The AAPS Journal* **2006**, *8*, E239–53.

(37) Gullo, V. P.; McAlpine, J.; Lam, K. S.; Baker, D.; Petersen, F. Drug Discovery from Natural Products. *Journal of Industrial Microbiology & Biotechnology* **2006**, *33*, 523–531.

(38) Molinski, T. F.; Dalisay, D. S.; Lievens, S. L.; Saludes, J. P. Drug Development from Marine Natural Products. *Nature Reviews: Drug Discovery* **2009**, *8*, 69–85.

(39) Faulkner, D. J. Highlights of Marine Natural Products Chemistry (1972 – 1999). *Natural Product Reports* **2000**, *17*, 1–6.

(40) Faulkner, D. J. Marine Natural Products. *Natural Product Reports* **2001**, *18*, 1–49.

(41) Blunt, J. W.; Copp, B. R.; Hu, W.-P.; Munro, M. H. G.; Northcote, P. T.; Prinsep, M. R. Marine Natural Products. *Natural Product Reports* **2009**, *26*, 170–244.

(42) Blunt, J. W.; Copp, B. R.; Munro, M. H. G.; Northcote, P. T.; Prinsep, M. R. Marine Natural Products. *Natural Product Reports* **2010**, *27*, 165–237.

(43) Blunt, J. W.; Copp, B. R.; Munro, M. H. G.; Northcote, P. T.; Prinsep, M. R. Marine Natural Products. *Natural Product Reports* **2011**, *28*, 196–268.

(44) Blunt, J. W.; Copp, B. R.; Keyzers, R. A.; Munro, M. H. G.; Prinsep, M. R. Marine Natural Products. *Natural Product Reports* **2012**, *29*, 144–222.

(45) Blunt, J. W.; Copp, B. R.; Keyzers, R. A.; Munro, M. H. G.; Prinsep, M. R. Marine Natural Products. *Natural Product Reports* **2013**, *30*, 237–323.

(46) Penesyan, A.; Kjelleberg, S.; Egan, S. Development of Novel Drugs from Marine Surface Associated Microorganisms. *Marine Drugs* **2010**, *8*, 438–459.

(47) Proksch, P.; Edrada, R. A.; Ebel, R. Drugs from the Seas - Current Status and Microbiological Implications. *Applied Microbiology and Biotechnology* **2002**, *59*, 125–134.

(48) Glaser, K. B.; Mayer, A. M. S. A Renaissance in Marine Pharmacology: From Preclinical Curiosity to Clinical Reality. *Biochemical Pharmacology* **2009**, *78*, 440–448.

(49) Schmidtko, A.; Lötsch, J.; Freynhagen, R.; Geisslinger, G. Ziconotide for Treatment of Severe Chronic Pain. *The Lancet* **2010**, *375*, 1569–1577.

(50) Simmons, T. L.; Andrianasolo, E.; McPhail, K. L.; Flatt, P.; Gerwick, W. H. Marine Natural Products as Anticancer Drugs. *Molecular Cancer Therapeutics* **2005**, *4*, 333–342.

(51) Towle, M. J.; Salvato, K. A.; Budrow, J.; Wels, B. F.; Kuznetsov, G.; Aalfs, K. K.; Welsh, S.; Zheng, W.; Seletsky, B. M.; Palme, M. H.; Habgood, G. J.; Singer, L. A.; DiPietro, L. V; Wang, Y.; Chen, J. J.; Quincy, D. A.; Davis, A.; Yoshimatsu, K.; Kishi, Y.; Yu, M. J.; Littlefield, B. A. In Vitro and In Vivo Anticancer Activities of Synthetic Macrocyclic Ketone Analogues of Halichondrin B. *Cancer Research* **2001**, *61*, 1013–1021.

(52) Newman, D. J.; Cragg, G. M. Marine-Sourced Anti-Cancer and Cancer Pain Control Agents in Clinical and Late Preclinical Development. *Marine Drugs* **2014**, *12*, 255–278.

(53) Mayer, A. M. S.; Glaser, K. B.; Cuevas, C.; Jacobs, R. S.; Kem, W.; Little, R. D.; McIntosh, J. M.; Newman, D. J.; Potts, B. C.; Shuster, D. E. The Odyssey of Marine Pharmaceuticals: A Current Pipeline Perspective. *Trends in Pharmacological Sciences* **2010**, *31*, 255–265.

(54) Ganesan, A. The Impact of Natural Products upon Modern Drug Discovery. *Current Opinion in Chemical Biology* **2008**, *12*, 306–317.

(55) Escoubas, P.; King, G. F. Venomics as a Drug Discovery Platform. *Expert Review of Proteomics* **2009**, *6*, 221–224.

(56) Wilson, Z. E.; Brimble, M. A. Molecules Derived from the Extremes of Life. *Natural Product Reports* **2009**, *26*, 44–71.

(57) Cragg, G. M.; Grothaus, P. G.; Newman, D. J. Impact of Natural Products on Developing New Anti-Cancer Agents. *Chemical Reviews* **2009**, *109*, 3012–3043.

(58) Kanapathipillai, M.; Lentzen, G.; Sierks, M.; Park, C. B. Ectoine and Hydroxyectoine Inhibit Aggregation and Neurotoxicity of Alzheimer's Beta-Amyloid. *FEBS Letters* **2005**, *579*, 4775–4780.

(59) Lentzen, G.; Schwarz, T. Extremolytes: Natural Compounds from Extremophiles for Versatile Applications. *Applied Microbiology and Biotechnology* **2006**, *72*, 623–634.

(60) Skropeta, D. Deep-Sea Natural Products. *Natural Product Reports* **2008**, *25*, 1131–1166.

(61) Thornburg, C. C.; Zabriskie, T. M.; McPhail, K. L. Deep-Sea Hydrothermal Vents: Potential Hot Spots for Natural Products Discovery? *Journal of Natural Products* **2010**, *73*, 489–499.

(62) Li, J. W.-H.; Vederas, J. C. Drug Discovery and Natural Products: End of an Era or an Endless Frontier? *Science* **2009**, *325*, 161–165.

(63) Cragg, G. M.; Newman, D. J.; Snader, K. M. Natural Products in Drug Discovery and Development. *Journal of Natural Products* **1997**, *60*, 52–60.

(64) Newman, D. J.; Cragg, G. M.; Snader, K. M. Natural Products as Sources of New Drugs over the Period 1981-2002. *Journal of Natural Products* **2003**, *66*, 1022–1037.

(65) Newman, D. J.; Cragg, G. M. Natural Products as Sources of New Drugs over the Last 25 Years. *Journal of Natural Products* **2007**, *70*, 461–477.

(66) Newman, D. J.; Cragg, G. M. Natural Products as Sources of New Drugs over the 30 Years from 1981 to 2010. *Journal of Natural Products* **2012**, *75*, 311–335.

(67) Jaroszewski, J. W. Hyphenated NMR Methods in Natural Products Research, Part 1: Direct Hyphenation. *Planta Medica* **2005**, *71*, 691–700.

(68) Jaroszewski, J. W. Hyphenated NMR Methods in Natural Products Research, Part 2: HPLC-SPE-NMR and Other New Trends in NMR Hyphenation. *Planta Medica* **2005**, *71*, 795–802.

(69) Seger, C.; Godejohann, M.; Tseng, L.-H.; Spraul, M.; Girtler, A.; Sturm, S.; Stuppner, H. LC-DAD-MS/SPE-NMR Hyphenation. A Tool for the Analysis of Pharmaceutically Used Plant Extracts: Identification of Isobaric Iridoid Glycoside Regioisomers from Harpagophytum Procumbens. *Analytical Chemistry* **2005**, *77*, 878–885.

(70) Molinski, T. F. NMR of Natural Products at the "Nanomole-Scale". *Natural Product Reports* **2010**, *27*, 321–329.

(71) Lam, K. S. New Aspects of Natural Products in Drug Discovery. *TRENDS in Microbiology* **2007**, *15*, 279–289.

(72) Feher, M.; Schmidt, J. M. Property Distributions: Differences between Drugs , Natural Products, and Molecules from Combinatorial Chemistry. *Journal of Chemical Information and Computer Sciences* **2003**, *43*, 218–227.

(73) Nielsen, J. Combinatorial Synthesis of Natural Products. *Current Opinion in Chemical Biology* **2002**, *6*, 297–305.

(74) Ortholand, J.-Y.; Ganesan, A. Natural Products and Combinatorial Chemistry: Back to the Future. *Current Opinion in Chemical Biology* **2004**, *8*, 271–280.

(75) Ganesan, A. Natural Products as a Hunting Ground for Combinatorial Chemistry. *Current Opinion in Biotechnology* **2004**, *15*, 584–590.

(76) Zhang, M.-Q.; Wilkinson, B. Drug Discovery beyond the "Rule-of-Five". *Current Opinion in Biotechnology* **2007**, *18*, 478–488.

(77) Ro, D.-K.; Paradise, E. M.; Ouellet, M.; Fisher, K. J.; Newman, K. L.; Ndungu, J. M.; Ho, K. A.; Eachus, R. A.; Ham, T. S.; Kirby, J.; Chang, M. C. Y.; Withers, S. T.; Shiba, Y.; Sarpong, R.; Keasling, J. D. Production of the Antimalarial Drug Precursor Artemisinic Acid in Engineered Yeast. *Nature* **2006**, *440*, 940–943.

(78) Lefevre, F.; Robe, P.; Jarrin, C.; Ginolhac, A.; Zago, C.; Auriol, D.; Vogel, T. M.; Simonet, P.; Nalin, R. Drugs from Hidden Bugs: Their Discovery via Untapped Resources. *Research in Microbiology* **2008**, *159*, 153–161.

(79) Harvey, A. Strategies for Discovering Drugs from Previously Unexplored Natural Products. *Drug Discovery Today* **2000**, *5*, 294–300.

(80) Penner, N.; Woodward, C.; Prakash, C. Drug Metabolizing Enzymes and Biotransformation Reactions. In *ADME-Enabling Technologies in Drug Design and Development*; Zhang, D.; Surapaneni, S., Eds.; John Wiley & Sons, Inc.: Hoboken, NJ, USA, 2012; pp. 545–565.

(81) Nebert, D. W.; Russell, D. W. Clinical Importance of the Cytochromes P450. *The Lancet* **2002**, *360*, 1155–1162.

(82) Sligar, S. G. Nature's Universal Oxygenases: The Cytochromes P450. *Essays in Biochemistry* **1999**, *34*, 71–83.

(83) Hasler, J. A.; Estabrook, R.; Murray, M.; Pikuleva, I.; Waterman, M.; Capdevila, J.; Holla, V.; Helvig, C.; Falck, J. R.; Farrell, G.; Kaminsky, L. S.; Spivack, S. D.; Boitier, E.; Beaune, P. Human Cytochromes P450. *Molecular Aspects of Medicine* **1999**, *20*, 1–137.

(84) Seliskar, M.; Rozman, D. Mammalian Cytochromes P450 - Importance of Tissue Specificity. *Biochimica et Biophysica Acta* **2007**, *1770*, 458–466.

(85) Guengerich, F. P. Cytochrome P450 Enzymes. *American Scientist* **1993**, *81*, 440–447.

(86) Ding, X.; Kaminsky, L. S. Human Extrahepatic Cytochromes P450: Function in Xenobiotic Metabolism and Tissue-Selective Chemical Toxicity in the Respiratory and Gastrointestinal Tracts. *Annual Review of Pharmacology and Toxicology* **2003**, *43*, 149–173.

(87) Lacroix, D.; Sonnier, M.; Moncion, A.; Cheron, G.; Cresteil, T. Expression of CYP3A in the Human Liver-Evidence That the Shift between CYP3A7 and CYP3A4 Occurs Immediately after Birth. *European Journal of Biochemistry* **1997**, *247*, 625–634.

(88) Preissner, S. C.; Hoffmann, M. F.; Preissner, R.; Dunkel, M.; Gewiess, A.; Preissner, S. Polymorphic Cytochrome P450 Enzymes (CYPs) and Their Role in Personalized Therapy. *PLoS ONE* **2013**, *8*, e82562.

(89) Lamb, D. C.; Waterman, M. R.; Kelly, S. L.; Guengerich, F. P. Cytochromes P450 and Drug Discovery. *Current Opinion in Biotechnology* **2007**, *18*, 504–512.

(90) Guengerich, F. P. Cytochromes P450, Drugs and Diseases. *Molecular Interventions* **2003**, *3*, 194–204.

(91) Isin, E. M.; Guengerich, F. P. Complex Reactions Catalyzed by Cytochrome P450 Enzymes. *Biochimica et Biophysica Acta* **2007**, *1770*, 314–329.

(92) Guengerich, F. P. Common and Uncommon Cytochrome P450 Reactions Related to Metabolism and Chemical Toxicity. *Chemical Research in Toxicology* **2001**, *14*, 611–650.

(93) Ingelman-Sundberg, M.; Oscarson, M.; McLellan, R. A. Polymorphic Human Cytochrome P450 Enzymes: An Opportunity for Individualized Drug Treatment. *Trends in Pharmacological Sciences* **1999**, *20*, 342–349.

(94) Ingelman-Sundberg, M. Pharmacogenetics of Cytochrome P450 and Its Applications in Drug Therapy: The Past, Present and Future. *Trends in Pharmacological Sciences* **2004**, *25*, 193–200.

(95) Cashman, J. R. Some Distinctions between Flavin-Containing and Cytochrome P450 Monooxygenases. *Biochemical and Biophysical Research Communications* **2005**, *338*, 599–604.

(96) Cashman, J. R.; Zhang, J. Human Flavin-Containing Monooxygenases. *Annual Review of Pharmacology and Toxicology* **2006**, *46*, 65–100.

(97) Cashman, J. R. Structural and Catalytic Properties of the Mammalian Flavin-Containing Monooxygenase. *Chemical Research in Toxicology* **1995**, *8*, 165–181.

(98) Kitamura, S.; Sugihara, K.; Ohta, S. Drug-Metabolizing Ability of Molybdenum Hydroxylases. *Drug Metabolism and Pharmacokinetics* **2006**, *21*, 83–98.

(99) Strolin Benedetti, M.; Tipton, K. F.; Whomsley, R. Amine Oxidases and Monooxygenases in the in Vivo Metabolism of Xenobiotic Amines in Humans: Has the Involvement of Amine Oxidases Been Neglected? *Fundamental & Clinical Pharmacology* **2007**, *21*, 467–480.

(100) Youdim, M. B. H.; Edmondson, D.; Tipton, K. F. The Therapeutic Potential of Monoamine Oxidase Inhibitors. *Nature Reviews: Neuroscience* **2006**, *7*, 295–309.

(101) Culpepper, L. The Use of Monoamine Oxidase Inhibitors in Primary Care. *The Journal of Clinical Psychiatry* **2012**, *73*, 37–41.

(102) Jenner, P. Mitochondria, Monoamine Oxidase B and Parkinson's Disease. *Basal Ganglia* **2012**, *2*, S3–S7.

(103) Vasiliou, V.; Pappa, A.; Petersen, D. R. Role of Aldehyde Dehydrogenases in Endogenous and Xenobiotic Metabolism. *Chemico-Biological Interactions* **2000**, *129*, 1–19.

(104) Fukami, T.; Yokoi, T. The Emerging Role of Human Esterases. *Drug Metabolism and Pharmacokinetics* **2012**, *27*, 466–477.

(105) Jin, Y.; Penning, T. M. Aldo-Keto Reductases and Bioactivation/detoxication. *Annual Review of Pharmacology and Toxicology* **2007**, *47*, 263–292.

(106) Oppermann, U. Carbonyl Reductases: The Complex Relationships of Mammalian Carbonyl- and Quinone-Reducing Enzymes and Their Role in Physiology. *Annual Review of Pharmacology and Toxicology* **2007**, *47*, 293–322.

(107) Barski, O. A.; Tipparaju, S. M.; Bhatnagar, A. The Aldo-Keto Reductase Superfamily and Its Role in Drug Metabolism and Detoxification. *Drug Metabolism Reviews* **2008**, *40*, 553–624.

(108) Jancova, P.; Šiller, M. Phase II Drug Metabolism. In *Topics on Drug Metabolism*; Paxton, J., Ed.; InTech: Rijeka, 2012; pp. 35–60.

(109) De Wildt, S. N.; Kearns, G. L.; Leeder, J. S.; van den Anker, J. N. Glucuronidation in Humans. Pharmacogenetic and Developmental Aspects. *Clinical Pharmacokinetics* **1999**, *36*, 439–452.

(110) Tukey, R. H.; Strassburg, C. P. Human UDP-Glucuronosyltransferases: Metabolism, Expression, and Disease. *Annual Review of Pharmacology and Toxicology* **2000**, *40*, 581–616.

(111) Bailey, M. J.; Dickinson, R. G. Acyl Glucuronide Reactivity in Perspective: Biological Consequences. *Chemico-Biological Interactions* **2003**, *145*, 117–137.

(112) Coughtrie, M. W. H. Sulfation through the Looking Glass-Recent Advances in Sulfotransferase Research for the Curious. *The Pharmacogenomics Journal* **2002**, *2*, 297–308.

(113) Gamage, N.; Barnett, A.; Hempel, N.; Duggleby, R. G.; Windmill, K. F.; Martin, J. L.; McManus, M. E. Human Sulfotransferases and Their Role in Chemical Metabolism. *Toxicological Sciences* **2006**, *90*, 5–22.

(114) Glatt, H. Sulfotransferases in the Bioactivation of Xenobiotics. *Chemico-Biological Interactions* **2000**, *129*, 141–170.

(115) Hearse, D. J.; Weber, W. W. Multiple N-Acetyltransferases and Drug Metabolism. *Biochemistry Journal* **1973**, *132*, 519–526.

(116) Sim, E.; Pinter, K.; Mushtaq, A.; Upton, A.; Sandy, J.; Bhakta, S.; Noble, M. Arylamine N-Acetyltransferases: A Pharmacogenomic Approach to Drug Metabolism and Endogenous Function. *Biochemical Society Transactions* **2003**, *31*, 615–619.

(117) Forman, H. J.; Zhang, H.; Rinna, A. Glutathione: Overview of Its Protective Roles, Measurement, and Biosynthesis. *Molecular Aspects of Medicine* **2009**, *30*, 1–12.

(118) Hayes, J. D.; Flanagan, J. U.; Jowsey, I. R. Glutathione Transferases. *Annual Review of Pharmacology and Toxicology* **2005**, *45*, 51–88.

(119) Männistö, P. T.; Kaakkola, S. Catechol-O-Methyltransferase (COMT): Biochemistry, Molecular Biology, Pharmacology, and Clinical Efficacy of the New Selective COMT Inhibitors. *Pharmacological Reviews* **1999**, *51*, 593–628.

(120) Fontecave, M.; Atta, M.; Mulliez, E. S-Adenosylmethionine: Nothing Goes to Waste. *TRENDS in Biochemical Sciences* **2004**, *29*, 243–249.

(121) Creveling, C. R. Methyltransferases. In *Enzyme Systems that Metabolise Drugs and Other Xenobiotics*; Ioannides, C., Ed.; John Wiley & Sons, Ltd: Chichester, UK, 2001; Vol. 4, pp. 484–499.

(122) Bodor, N.; Buchwald, P. Soft Drug Design: General Principles and Recent Applications. *Medicinal Research Reviews* **2000**, *20*, 58–101.

(123) Fura, A.; Shu, Y.-Z.; Zhu, M.; Hanson, R. L.; Roongta, V.; Humphreys, W. G. Discovering Drugs through Biological Transformation: Role of Pharmacologically Active Metabolites in Drug Discovery. *Journal of Medicinal Chemistry* **2004**, *47*, 4339–4351.

(124) Rautio, J.; Kumpulainen, H.; Heimbach, T.; Oliyai, R.; Oh, D.; Järvinen, T.; Savolainen, J. Prodrugs: Design and Clinical Applications. *Nature Reviews: Drug Discovery* **2008**, *7*, 255–270.

(125) Huttunen, K. M.; Raunio, H.; Rautio, J. Prodrugs - from Serendipity to Rational Design. *Pharmacological Reviews* **2011**, *63*, 750–771.

(126) Osborne, R.; Thompson, P.; Joel, S.; Trew, D.; Patel, N.; Slevin, M. The Analgesic Activity of Morphine-6-Glucuronide. *British Journal of Clinical Pharmacology* **1992**, *34*, 130–138.

(127) Lewis, S. S.; Hutchinson, M. R.; Rezvani, N.; Loram, L. C.; Zhang, Y.; Maier, S. F.; Rice, K. C.; Watkins, L. R. Evidence That Intrathecal Morphine-3-Glucuronide May Cause Pain Enhancement via Toll-like Receptor 4/MD-2 and Interleukin-1beta. *Neuroscience* **2010**, *165*, 569–583.

(128) Miller, E. C.; Miller, J. A. The Presence and Significance of Bound Aminoazo Dyes in the Livers of Rats Fed P-Dimethylaminoazobenzene. *Cancer Research* **1947**, *7*, 468–480.

(129) Li, F.; Lu, J.; Ma, X. Profiling the Reactive Metabolites of Xenobiotics Using Metabolomic Technologies. *Chemical Research in Toxicology* **2011**, *24*, 744–751.

(130) Guengerich, F. P. Cytochrome P450s and Other Enzymes in Drug Metabolism and Toxicity. *The AAPS Journal* **2006**, *8*, E101–11.

(131) Ju, C.; Uetrecht, J. Mechanism of Idiosyncratic Drug Reactions: Reactive Metabolites Formation, Protein Binding and the Regulation of the Immune System. *Current Drug Metabolism* **2002**, *3*, 367–377.

(132) Nelson, S. D. Molecular Mechanisms of Adverse Drug Reactions. *Current Therapeutic Research* **2001**, *62*, 885–899.

(133) Guengerich, F. P. Principles of Covalent Binding of Reactive Metabolites and Examples of Activation of Bis-Electrophiles by Conjugation. *Archives of Biochemistry and Biophysics* **2005**, *433*, 369–378.

(134) Attia, S. M. Deleterious Effects of Reactive Metabolites. *Oxidative Medicine and Cellular Longevity* **2010**, *3*, 238–253.

(135) Uetrecht, J. Idiosyncratic Drug Reactions: Current Understanding. *Annual Review of Pharmacology and Toxicology* **2007**, *47*, 513–539.

(136) Park, B. K.; Naisbitt, D. J.; Gordon, S. F.; Kitteringham, N. R.; Pirmohamed, M. Metabolic Activation in Drug Allergies. *Toxicology* **2001**, *158*, 11–23.

(137) Shenton, J. M.; Chen, J.; Uetrecht, J. P. Animal Models of Idiosyncratic Drug Reactions. *Chemico-Biological Interactions* **2004**, *150*, 53–70.

(138) Dahlin, D. C.; Miwa, G. T.; Lu, A. Y.; Nelson, S. D. N-Acetyl-P-Benzoquinone Imine: A Cytochrome P-450-Mediated Oxidation Product of Acetaminophen. *Proceedings of the National Academy of Sciences of the United States of America* **1984**, *81*, 1327–1331.

(139) Williams, D. P. Toxicophores: Investigations in Drug Safety. *Toxicology* **2006**, *226*, 1–11.

(140) James, L. P.; Mayeux, P. R.; Hinson, J. A. Acetaminophen-Induced Hepatotoxicity. *Drug Metabolism and Disposition* **2003**, *31*, 1499–1506.

(141) Pirmohamed, M.; Park, B. K. Mechanism of Clozapine-Induced Agranulocytosis: Current Status of Research and Implications for Drug Development. *CNS Drugs* **1997**, *7*, 139–158.

(142) Uetrecht, J.; Zahid, N.; Tehim, A.; Fu, J. M.; Rakhit, S. Structural Features Associated with Reactive Metabolite Formation in Clozapine Analogues. *Chemico-Biological Interactions* **1997**, *104*, 117–129.

(143) Stepan, A. F.; Walker, D. P.; Bauman, J. N.; Price, D. A.; Baillie, T. A.; Kalgutkar, A. S.; Aleo, M. D. Structural Alert/reactive Metabolite Concept as Applied in Medicinal Chemistry to Mitigate the Risk of Idiosyncratic Drug Toxicity: A Perspective Based on the Critical Examination of Trends in the Top 200 Drugs Marketed in the United States. *Chemical Research in Toxicology* **2011**, *24*, 1345–1410.

(144) Peraica, M.; Radić, B.; Lucić, A.; Pavlović, M. Toxic Effects of Mycotoxins in Humans. *Bulletin of the World Health Organization* **1999**, *77*, 754–766.

(145) Guengerich, F. P. Cytochrome P450 and Chemical Toxicology. *Chemical Research in Toxicology* **2008**, *21*, 70–83.

(146) Vanherweghem, J.-L. Misuse of Herbal Remedies: The Case of an Outbreak of Terminal Renal Failure in Belgium (Chinese Herbs Nephropathy). *The Journal of Alternative and Complementary Medicine* **1998**, *4*, 9–13.

(147) Zhou, S.; Koh, H.-L.; Gao, Y.; Gong, Z.-Y.; Lee, E. J. D. Herbal Bioactivation: The Good, the Bad and the Ugly. *Life Sciences* **2004**, *74*, 935–968.

(148) Dietz, B. M.; Bolton, J. L. Biological Reactive Intermediates (BRIs) Formed from Botanical Dietary Supplements. *Chemico-Biological Interactions* **2011**, *192*, 72–80.

(149) Chen, X.-W.; Serag, E. S.; Sneed, K. B.; Zhou, S.-F. Herbal Bioactivation, Molecular Targets and the Toxicity Relevance. *Chemico-Biological Interactions* **2011**, *192*, 161–176.

(150) Stiborová, M.; Frei, E.; Arlt, V. M.; Schmeiser, H. H. Metabolic Activation of Carcinogenic Aristolochic Acid, a Risk Factor for Balkan Endemic Nephropathy. *Mutation Research* **2008**, *658*, 55–67.

(151) Meinl, W.; Pabel, U.; Osterloh-Quiroz, M.; Hengstler, J. G.; Glatt, H. Human Sulphotransferases Are Involved in the Activation of Aristolochic Acids and Are Expressed in Renal Target Tissue. *International Journal of Cancer* **2006**, *118*, 1090–1097.

(152) Stiborová, M.; Frei, E.; Hodek, P.; Wiessler, M.; Schmeiser, H. H. Human Hepatic and Renal Microsomes, Cytochromes P450 1A1/2, NADPH:cytochrome P450 Reductase and Prostaglandin H Synthase Mediate the Formation of Aristolochic Acid-DNA Adducts Found in Patients with Urothelial Cancer. *International Journal of Cancer* **2005**, *113*, 189–197.

(153) Singh, Y. N.; Singh, N. N. Therapeutic Potential of Kava in the Treatment of Anxiety Disorders. *CNS Drugs* **2002**, *16*, 731–743.

(154) Dietz, B.; Bolton, J. L. Botanical Dietary Supplements Gone Bad. *Chemical Research in Toxicology* **2007**, *20*, 586–590.

(155) Bailey, D. G.; Malcolm, J.; Arnold, O.; Spence, J. D. Grapefruit Juice-Drug Interactions. *British Journal of Clinical Pharmacology* **1998**, *46*, 101–110.

(156) Bailey, D. G.; Dresser, G.; Arnold, J. M. O. Grapefruit-Medication Interactions: Forbidden Fruit or Avoidable Consequences? *Canadian Medical Association Journal* **2013**, *185*, 309–316.

(157) He, K.; Iyer, K. R.; Hayes, R. N.; Sinz, M. W.; Woolf, T. F.; Hollenberg, P. F. Inactivation of Cytochrome P450 3A4 by Bergamottin, a Component of Grapefruit Juice. *Chemical Research in Toxicology* **1998**, *11*, 252–259.

(158) Kent, U. M.; Lin, H.; Noon, K. R.; Harris, D. L.; Hollenberg, P. F. Metabolism of Bergamottin by Cytochromes P450 2B6 and 3A5. *The Journal of Pharmacology and Experimental Therapeutics* **2006**, *318*, 992–1005.

(159) Kola, I.; Landis, J. Can the Pharmaceutical Industry Reduce Attrition Rates? *Nature Reviews: Drug Discovery* **2004**, *3*, 711–715.

(160) Kola, I. The State of Innovation in Drug Development. *Clinical Pharmacology and Therapeutics* **2008**, *83*, 227–230.

(161) Summerfield, S.; Jeffrey, P. Discovery DMPK: Changing Paradigms in the Eighties, Nineties and Noughties. *Expert Opinion on Drug Discovery* **2009**, *4*, 207–218.

(162) Eddershaw, P. J.; Beresford, A. P.; Bayliss, M. K. ADME/PK as Part of a Rational Approach to Drug Discovery. *Drug Discovery Today* **2000**, *5*, 409–414.

(163) Lin, J.; Sahakian, D. C.; de Morais, S. M. F.; Xu, J. J.; Polzer, R. J.; Winter, S. M. The Role of Absorption, Distribution, Metabolism, Excretion and Toxicity in Drug Discovery. *Current Topics in Medicinal Chemistry* **2003**, *3*, 1125–1154.

(164) Schuster, D.; Laggner, C.; Langer, T. Why Drugs Fail - A Study on Side Effects in New Chemical Entities. *Current Pharmaceutical Design* **2005**, *11*, 3545–3559.

(165) Jorgensen, W. L. The Many Roles of Computation in Drug Discovery. *Science* **2004**, *303*, 1813–1818.

(166) Van de Waterbeemd, H.; Gifford, E. ADMET in Silico Modelling: Towards Prediction Paradise? *Nature Reviews: Drug Discovery* **2003**, *2*, 192–204.

(167) Lipinski, C. A.; Lombardo, F.; Dominy, B. W.; Feeney, P. J. Experimental and Computational Approaches to Estimate Solubility and Permeability in Drug Discovery and Development Settings. *Advanced Drug Delivery Reviews* **2001**, *46*, 3–26.

(168) Ekins, S. In Silico Approaches to Predicting Drug Metabolism, Toxicology and Beyond. *Biochemical Society Transactions* **2003**, *31*, 611–614.

(169) Yu, H.; Adedoyin, A. ADME–Tox in Drug Discovery: Integration of Experimental and Computational Technologies. *Drug Discovery Today* **2003**, *8*, 852–861.

(170) Norinder, U.; Bergström, C. A. S. Prediction of ADMET Properties. *ChemMedChem* **2006**, *1*, 920–937.

(171) Stouch, T. R.; Kenyon, J. R.; Johnson, S. R.; Chen, X.-Q.; Doweyko, A.; Li, Y. In Silico ADME/Tox: Why Models Fail. *Journal of Computer-aided Molecular Design* **2003**, *17*, 83–92.

(172) Roncaglioni, A.; Toropov, A. A.; Toropova, A. P.; Benfenati, E. In Silico Methods to Predict Drug Toxicity. *Current Opinion in Pharmacology* **2013**, *13*, 802–806.

(173) Bugrim, A.; Nikolskaya, T.; Nikolsky, Y. Early Prediction of Drug Metabolism and Toxicity: Systems Biology Approach and Modeling. *Drug Discovery Today* **2004**, *9*, 127–135.

(174) Crivori, P.; Poggesi, I. Computational Approaches for Predicting CYP-Related Metabolism Properties in the Screening of New Drugs. *European Journal of Medicinal Chemistry* **2006**, *41*, 795–808.

(175) Cruciani, G.; Carosati, E.; De Boeck, B.; Ethirajulu, K.; Mackie, C.; Howe, T.; Vianello, R. MetaSite: Understanding Metabolism in Human Cytochromes from the Perspective of the Chemist. *Journal of Medicinal Chemistry* **2005**, *48*, 6970–6979.

(176) Rydberg, P.; Gloriam, D. E.; Zaretzki, J.; Breneman, C.; Olsen, L. SMARTCyp: A 2D Method for Prediction of Cytochrome P450-Mediated Drug Metabolism. *ACS Medicinal Chemistry Letters* **2010**, *1*, 96–100.

(177) Kirchmair, J.; Williamson, M. J.; Tyzack, J. D.; Tan, L.; Bond, P. J.; Bender, A.; Glen, R. C. Computational Prediction of Metabolism: Sites, Products, SAR, P450 Enzyme Dynamics, and Mechanisms. *Journal of Chemical Information and Modeling* **2012**, *52*, 617–648.

(178) Clark, D. E. In Silico Prediction of Blood-Brain Barrier Permeation. *Drug Discovery Today* **2003**, *8*, 927–933.

(179) Hou, T.; Wang, J.; Zhang, W.; Wang, W.; Xu, X. Recent Advances in Computational Prediction of Drug Absorption and Permeability in Drug Discovery. *Current Medicinal Chemistry* **2006**, *13*, 2653–2667.

(180) Masimirembwa, C. M.; Bredberg, U.; Andersson, T. B. Metabolic Stability for Drug Discovery and Development: Pharmacokinetic and Biochemical Challenges. *Clinical Pharmacokinetics* **2003**, *42*, 515–528.

(181) Baranczewski, P.; Stańczak, A.; Sundberg, K.; Svensson, R.; Wallin, A.; Jansson, J.; Garberg, P.; Postlind, H. Introduction to in Vitro Estimation of Metabolic

Stability and Drug Interactions of New Chemical Entities in Drug Discovery and Development. *Pharmacological Reports* **2006**, *58*, 453–472.

(182) Li, A. P. Screening for Human ADME/Tox Drug Properties in Drug Discovery. *Drug Discovery Today* **2001**, *6*, 357–366.

(183) Nassar, A.-E. F.; Kamel, A. M.; Clarimont, C. Improving the Decision-Making Process in Structural Modification of Drug Candidates: Reducing Toxicity. *Drug Discovery Today* **2004**, *9*, 1055–1064.

(184) Yan, Z.; Caldwell, G. W. In Vitro Identification of Cytochrome P450 Enzymes Responsible for Drug Metabolism. In *Pharmacogenomics: Methods and Protocols*; Innocenti, F.; Schaik, R. H. N., Eds.; Methods in Molecular Biology; Humana Press: Totowa, NJ, 2013; Vol. 1015, pp. 251–261.

(185) Harper, T. W.; Brassil, P. J. Reaction Phenotyping: Current Industry Efforts to Identify Enzymes Responsible for Metabolizing Drug Candidates. *The AAPS Journal* **2008**, *10*, 200–207.

(186) Zhang, H.; Davis, C. D.; Sinz, M. W.; Rodrigues, A. D. Cytochrome P450 Reaction-Phenotyping: An Industrial Perspective. *Expert Opinion on Drug Metabolism & Toxicology* **2007**, *3*, 667–687.

(187) Park, B. K.; Boobis, A.; Clarke, S.; Goldring, C. E. P.; Jones, D.; Kenna, J. G.; Lambert, C.; Laverty, H. G.; Naisbitt, D. J.; Nelson, S.; Nicoll-Griffith, D. A.; Obach, R. S.; Routledge, P.; Smith, D. A.; Tweedie, D. J.; Vermeulen, N.; Williams, D. P.; Wilson, I. D.; Baillie, T. A. Managing the Challenge of Chemically Reactive Metabolites in Drug Development. *Nature Reviews: Drug Discovery* **2011**, *10*, 292–306.

(188) Kalgutkar, A. S.; Gardner, I.; Obach, R. S.; Shaffer, C. L.; Callegari, E.; Henne, K. R.; Mutlib, A. E.; Dalvie, D. K.; Lee, J. S.; Nakai, Y.; O'Donnell, J. P.; Boer, J.; Harriman, S. P. A Comprehensive Listing of Bioactivation Pathways of Organic Functional Groups. *Current Drug Metabolism* **2005**, *6*, 161–225.

(189) Fontana, E.; Dansette, P. M.; Poli, S. M. Cytochrome P450 Enzymes Mechanism Based Inhibitors: Common Sub-Structures and Reactivity. *Current Drug Metabolism* **2005**, *6*, 413–454.

(190) Valerio, L. G. In Silico Toxicology for the Pharmaceutical Sciences. *Toxicology and Applied Pharmacology* **2009**, *241*, 356–370.

(191) Zlokarnik, G.; Grootenhuis, P. D. J.; Watson, J. B. High Throughput P450 Inhibition Screens in Early Drug Discovery. *Drug Discovery Today* **2005**, *10*, 1443–1450.

(192) Riley, R. J.; Grime, K. Metabolic Screening in Vitro: Metabolic Stability, CYP Inhibition and Induction. *Drug Discovery Today: Technologies* **2004**, *1*, 365–372.

(193) Polasek, T. M.; Miners, J. O. In Vitro Approaches to Investigate Mechanism-Based Inactivation of CYP Enzymes. *Expert Opinion on Drug Metabolism & Toxicology* **2007**, *3*, 321–329.

(194) Grime, K. H.; Bird, J.; Ferguson, D.; Riley, R. J. Mechanism-Based Inhibition of Cytochrome P450 Enzymes: An Evaluation of Early Decision Making in Vitro Approaches and Drug-Drug Interaction Prediction Methods. *European Journal of Pharmaceutical Sciences* **2009**, *36*, 175–191.

(195) Lohmann, W.; Karst, U. Generation and Identification of Reactive Metabolites by Electrochemistry and Immobilized Enzymes Coupled on-Line to Liquid Chromatography/mass Spectrometry. *Analytical Chemistry* **2007**, *79*, 6831–6839.

(196) Madsen, K. G.; Olsen, J.; Skonberg, C.; Hansen, S. H.; Jurva, U. Development and Evaluation of an Electrochemical Method for Studying Reactive Phase-I Metabolites: Correlation to in Vitro Drug Metabolism. *Chemical Research in Toxicology* **2007**, *20*, 821–831.

(197) Ma, S.; Subramanian, R. Detecting and Characterizing Reactive Metabolites by Liquid Chromatography/tandem Mass Spectrometry. *Journal of Mass Spectrometry* **2006**, *41*, 1121–1139.

(198) Yan, Z.; Caldwell, G. W. Stable-Isotope Trapping and High-Throughput Screenings of Reactive Metabolites Using the Isotope MS Signature. *Analytical Chemistry* **2004**, *76*, 6835–6847.

(199) Mutlib, A.; Lam, W.; Atherton, J.; Chen, H.; Galatsis, P.; Stolle, W. Application of Stable Isotope Labeled Glutathione and Rapid Scanning Mass Spectrometers in Detecting and Characterizing Reactive Metabolites. *Rapid Communications in Mass Spectrometry* **2005**, *19*, 3482–3492.

(200) Gan, J.; Harper, T. W.; Hsueh, M.-M.; Qu, Q.; Humphreys, W. G. Dansyl Glutathione as a Trapping Agent for the Quantitative Estimation and Identification of Reactive Metabolites. *Chemical Research in Toxicology* **2005**, *18*, 896–903.

(201) Chen, Y.; Monshouwer, M.; Fitch, W. L. Analytical Tools and Approaches for Metabolite Identification in Early Drug Discovery. *Pharmaceutical Research* **2007**, *24*, 248–257.

(202) Ma, S.; Zhu, M. Recent Advances in Applications of Liquid Chromatography-Tandem Mass Spectrometry to the Analysis of Reactive Drug Metabolites. *Chemico-Biological Interactions* **2009**, *179*, 25–37.

(203) Evans, D. C.; Watt, A. P.; Nicoll-Griffith, D. A.; Baillie, T. A. Drug-Protein Adducts: An Industry Perspective on Minimizing the Potential for Drug Bioactivation in Drug Discovery and Development. *Chemical Research in Toxicology* **2004**, *17*, 3–16.

(204) Masubuchi, N.; Makino, C.; Murayama, N. Prediction of in Vivo Potential for Metabolic Activation of Drugs into Chemically Reactive Intermediate: Correlation of in Vitro and in Vivo Generation of Reactive Intermediates and in Vitro Glutathione Conjugate Formation in Rats and Humans. *Chemical Research in Toxicology* **2007**, *20*, 455–464.

(205) Leeson, P. D.; Davis, A. M. Time-Related Differences in the Physical Property Profiles of Oral Drugs. *Journal of Medicinal Chemistry* **2004**, *47*, 6338–6348.

(206) World Health Organization. *Legal Status of Traditional Medicine and Complementary/Alternative Medicine: A Worldwide Review*; Geneva, 2001.

(207) World Health Organization. *WHO Traditional Medicine Strategy 2002-2005*; Geneva, 2002.

CHAPTER TWO:

IN SILICO PROFILING OF NATURAL PRODUCT CHEMICAL SPACE

2.1 Summary

In this Chapter, the use of computational tools to design, create and populate a database of natural products is described. The chemical space occupied by the natural products with specific regard to their predicted physico-chemical properties for 'drug-likeness' is determined using software. Statistical analysis of the chemical space data of the natural products compared to that of conventional drugs is performed to determine the significance of any similarities or differences in the properties of both data sets. An analysis of structural alerts present in the natural products compared to those present in conventional drugs is carried out to predict the relative predilection of these compounds to undergo metabolic bioactivation.

2.2 General Introduction

Computational tools are now considered virtually indispensible integral components of the drug discovery process. They are used for virtual screening of large compound libraries to identify potential drug hits either through structure-based or ligand-based screens typically at the very onset of drug discovery programs.[1–3] Their use has become more common-place following the realization that traditional high-throughput screening (HTS) assays on combinatorial chemistry compound libraries often yielded large proportions of false positive 'non-drug-like' hits that could be easily identified and excluded computationally by applying property filters.[4] Computational tools are used to predict the 'drug-likeness' of compounds in chemical libraries based on calculation of both simple 1D, 2D and more complex 3D property descriptors.

Virtual compound libraries in the form of *in silico* databases containing large volumes of information on thousands and sometimes millions of both real and hypothesized combinatorial compounds are now freely or commercially available for high-throughput drug discovery screening. At present, many of these depositories can be accessed through the world-wide-web as online databases in which data is continuously updated and new compounds uploaded. An example of such online

databases is ZINC,[5–7] which at present contains freely accessible records of more than 35 million compounds. Although ZINC is mainly populated with synthetic compounds, it also contains a sizeable collection of natural products and provides links to other online databases which specifically contain only natural product collections. For example, a library of more than 1000 natural products from African Medicinal Plants christened AfroDb is entirely housed within the ZINC database.[8] In general, however, discovery of bioactive natural products using computational tools has been hampered by a relative dearth in the availability of good quality publicly accessible natural product databases.[9]

2.3 Natural Product Database

2.3.1 Database Design

A compound database containing data on natural products was designed and created using commercially available off-the-shelf software (Microsoft® Office Access 2003 Service Pack 3, Microsoft Corporation, WA, USA). The database was created on a HP Pavilion® dv9925nr stand-alone notebook PC running on a dual-core 2.0 GHz AMD Turion® T60 microprocessor, equipped with 4.0 GB RAM and a 250 GB (5400 rpm) primary storage hard-disk. The operating system platform was a 64-bit version of Windows Vista® Home Premium.

The relational database comprised the following tables:

1. African Herbal Pharmacopoeia: Containing data on herbal products from monographs published in the *African Herbal Pharmacopoeia* (AHP)[10] including: the herbal product name, natural botanical source, reported ethno-botanical uses, experimentally determined pharmacological activities and chemical constituents isolated from the product.
2. AHP Chemical Constituents: This table contained data on the chemical compounds from the AHP monographs, specifically: their common chemical name, chemical structure appended both as OLE (Object Linking and Embedding) objects created using a different software application as well as conventional molecular text notation.

3. ICIPE Compounds: Containing similar information as the AHP Chemical Constituents table but only for natural products available from the International Centre of Insect Physiology and Ecology (ICIPE) based in Nairobi, Kenya.
4. Conventional BP 2009 Drugs: This table contained the international non-proprietary names (INN) and chemical structures of conventional drugs in current clinical use published in the British Pharmacopoeia 2009[11] for comparison against the natural product sets. This dataset contained only small molecule drug compounds and not components of biological formulations such as immunoglobulins, anti-toxins, plasma proteins or vaccines whose monographs were also present in BP 2009.

The design structure of the Natural Product database is summarised in **Table 2.1**.

Different text notations for compound structures were included to provide an option for importing and/or exporting chemical structures to other software platforms easily without having to redraw them. In this case, the notations used were SMILES (Simplified Molecular Input Line Entry System),[12] SLN (SYBYL Line Notation)[13] and the IUPAC InChI (International Chemical Identifier)[14]. These three were selected because they are currently the most widely used molecular text notation systems capable of interpretation by the vast majority of molecule manipulation software. Text notation of the molecular structures of the chemical constituents also reduced the amount of physical digital storage space taken up by such data for purposes of transfer when copying or moving between different software applications. Another advantage of incorporating the text notations was that they provided the possibility for indexing of the database, thereby allowing compound searches to be performed faster while at the same time avoiding redundancy through inadvertent capture of the same compound details more than once especially in cases of compounds having more than one common name.

Table 2.1: Natural Product Database Structure

Data Table	Data Fields	Data Field Type (Size)
African Herbal Pharmacopoeia	Monograph number	Numeric Integer
	Herbal Product	Text (50 characters)
	Natural source	Text (50 characters)

Data Table	Data Fields	Data Field Type (Size)
	Ethnobotanical use (x3)	Text (50 characters)
	Pharmacological properties (x3)	Text (50 characters)
	Chemical constituents (x10)	Text (50 characters)
African Herbal Pharmacopoeia Chemical Constituents	Common chemical name	Text (50 characters)
	Chemical structure	OLE Embedded Object
	SMILES notation	Text (255 characters)
	SLN notation	Text (255 characters)
	InCHI notation	Text (255 characters)
ICIPE Compounds	Common chemical name	Text (50 characters)
	Chemical structure	OLE Embedded Object
	SMILES notation	Text (255 characters)
	SLN notation	Text (255 characters)
	InCHI notation	Text (255 characters)
British Pharmacopoeia 2009 Drugs	Common drug name	Text (50 characters)
	SMILES notation	Text (255 characters)

The possibility of data redundancies through accidental entry of the same chemical compound more than once into any of the three compound tables was avoided by indexing the SMILES notation field and forbidding entry of replicate data.

2.3.2 Data Entry

To ease capture of data into the tables described above and ensure consistency by minimizing errors, computerized data entry forms were designed. For entering data into the AHP Chemical Constituents and ICIPE Compounds tables, an identical form was created as illustrated in **Figure 2.1**.

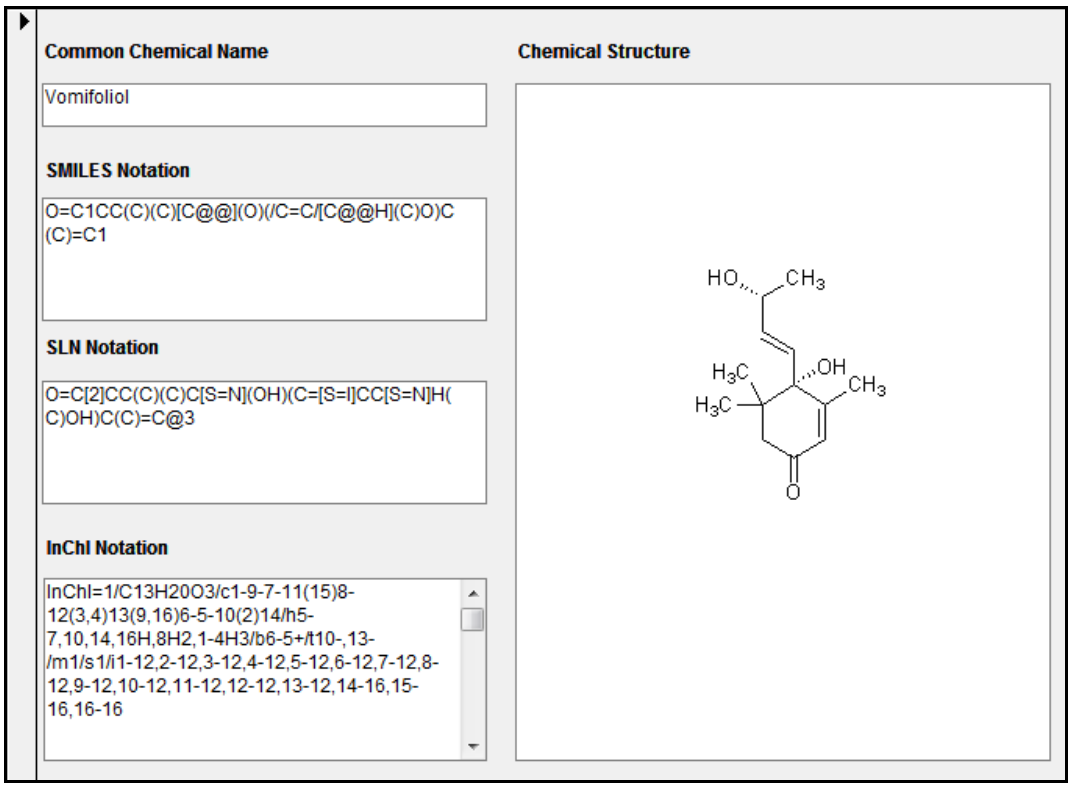

Figure 2.1: Screenshot of AHP Chemical Constituents and ICIPE Compounds Data Entry Form

To capture molecular structures of each new compound into the database, the form was designed to link with ChemDraw Ultra software ver. 11.0 (ChembridgeSoft, MA, USA). This link also allowed for the editing of already captured chemical structures using the ChemDraw molecule editor. ChemDraw was also used to generate the SMILES, SLN and InChI notations for each compound for entry into their corresponding data fields.

The information entered into the African Herbal Pharmacopoiea Table was a composite of data already captured in the Chemical Constituents Table (i.e. chemical constitutents' common names) and other data to be extracted from each product monograph (e.g. ethnobotanical use and pharmacological activity). To input this information, a separate data entry form (**Figure 2.2**) incorporating drop-down lists that allowed for entry of the chemical constituents from the pre-existing table was designed. This helped to minimize errors and avoid repetition through entry of data that had already been captured previously.

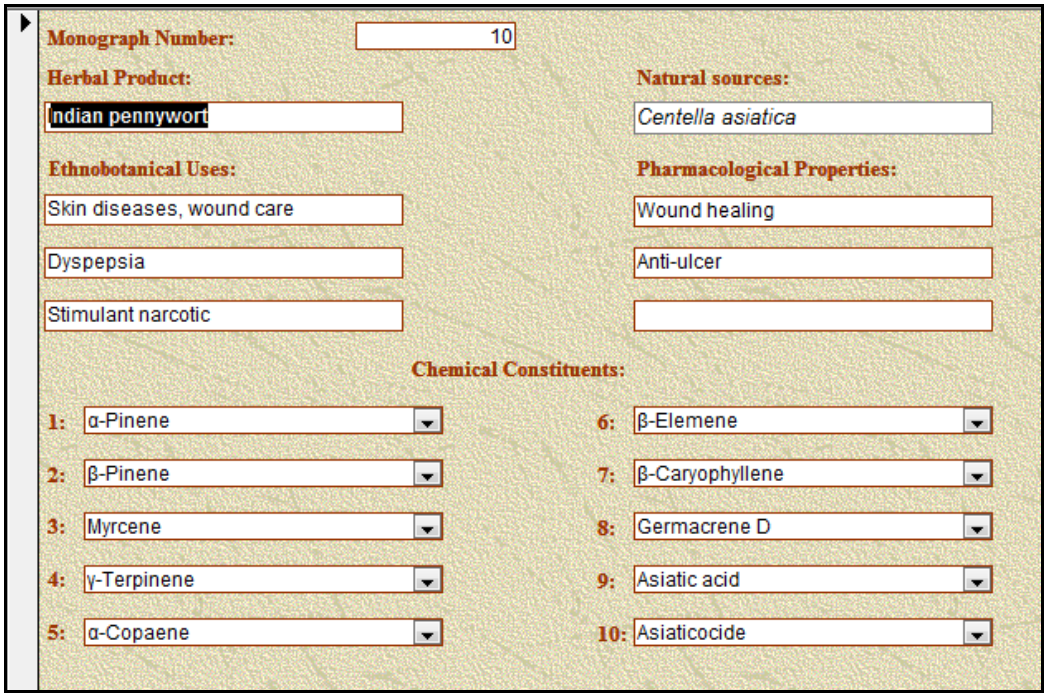

Figure 2.2: Screenshot of African Herbal Pharmacopoeia Table Data Entry Form

2.3.3 Summary Statistics

The complete database comprising the tables, data entry forms and records described above occupied 105 megabytes of hard-disk space. The data captured was fully transferable and could be freely copied and accessed using any Windows-based PC in which Microsoft Access® 2003 or newer versions was installed.

In total, data from all 51 monographs in the African Herbal Pharmacopoeia were captured into the database. 335 Unique compounds identified as components of the natural products in the AHP were input into the Chemical Constituents Table, representing an average of 6.6 compounds per monograph. By comparison, the ICIPE list of chemical compounds comprised a total of 297 natural products isolated from an undisclosed number or variety of sources while the BP 2009 table contained a total of 608 unique drug entities.

2.4 *In silico* Chemical Space Property Calculations and Predictions

It is generally accepted that natural products occupy a different chemical space to that of conventional drugs with regard to the physicochemical properties considered most critical in conferring drug-likeness. For example, natural products tend to have more oxygen and fewer nitrogen atoms per molecule compared to synthetic organic

compounds and drugs. They also tend to possess a greater number of stereogenic centres.[15]

The chemical constituents captured from the African Herbal Pharmacopoeia were evaluated using MarvinSketch software ver. 5.5.1.1 (ChemAxon Kft, Budapest, Hungary) to predict values for the four 'Rule-of-Five' parameters described by Lipinski as significantly influencing the absorption and permeability properties of orally administered drugs. According to the 'Rule-of-Five', the majority of orally active drugs tend to have molecular weights less than 500, LogP values not greater than 5.0 in addition to having no more than 5 H-bond donors or 10 H-bond acceptors.[16] In addition to these, the number of rotatable bonds in the molecules was also calculated as another critical determinant for oral bioavailability in drug-like compounds as proposed by Veber *et al*.[17] Most oral drugs have less than 10 rotatable bonds and besides contributing to bioavailability, their presence also influences ligand affinity to drug targets.[18]

Frequency distribution histograms and pie charts of the values predicted or calculated for these five parameters are illustrated in **Figures 2.3 – 2.7**. For comparison of the natural product values against conventional medicines in current clinical use, the same parameters were determined for the drug molecules captured from the British Pharmacopoeia 2009.

2.4.1 Molecular Weight

79.1% of the AHP compounds had molecular weight (mwt) < 500 with most (60.3%) ranging from 200 to 450. Only slightly more than 1% had mwt greater than 750 and none had a value below 100. The mean molecular weight for all 335 compounds was 376.6 (sd 162.3) with a median of 338.3.

In contrast, 95.4% of the B.P. compounds had molecular weights below 500 (78.5% ranging from 200 to 450). No compound had molecular weight less than 100 and only 0.8% had molecular weights in excess of 700. The mean value for B.P. drugs was 316.9 (sd 106.5) with a median of 307.4.

For the ICIPE compounds, 94.3% had mwt less than 500, with those ranging from 51 to 250 accounting for the majority (67.3%). This relatively high proportion of low molecular weight compounds was due to the fact that many of the ICIPE compounds

were small mono- and sesquiterpene components of essential oils extracted from plants. This fact was further reflected in the average molecular weight for the data set which was significantly lower than that for the AHP and BP drugs at 245.0 (sd 129.1) with a median value of 204.0. Five compounds (1.7%) had mwt less than 100 and three (1%) exceeded 650.

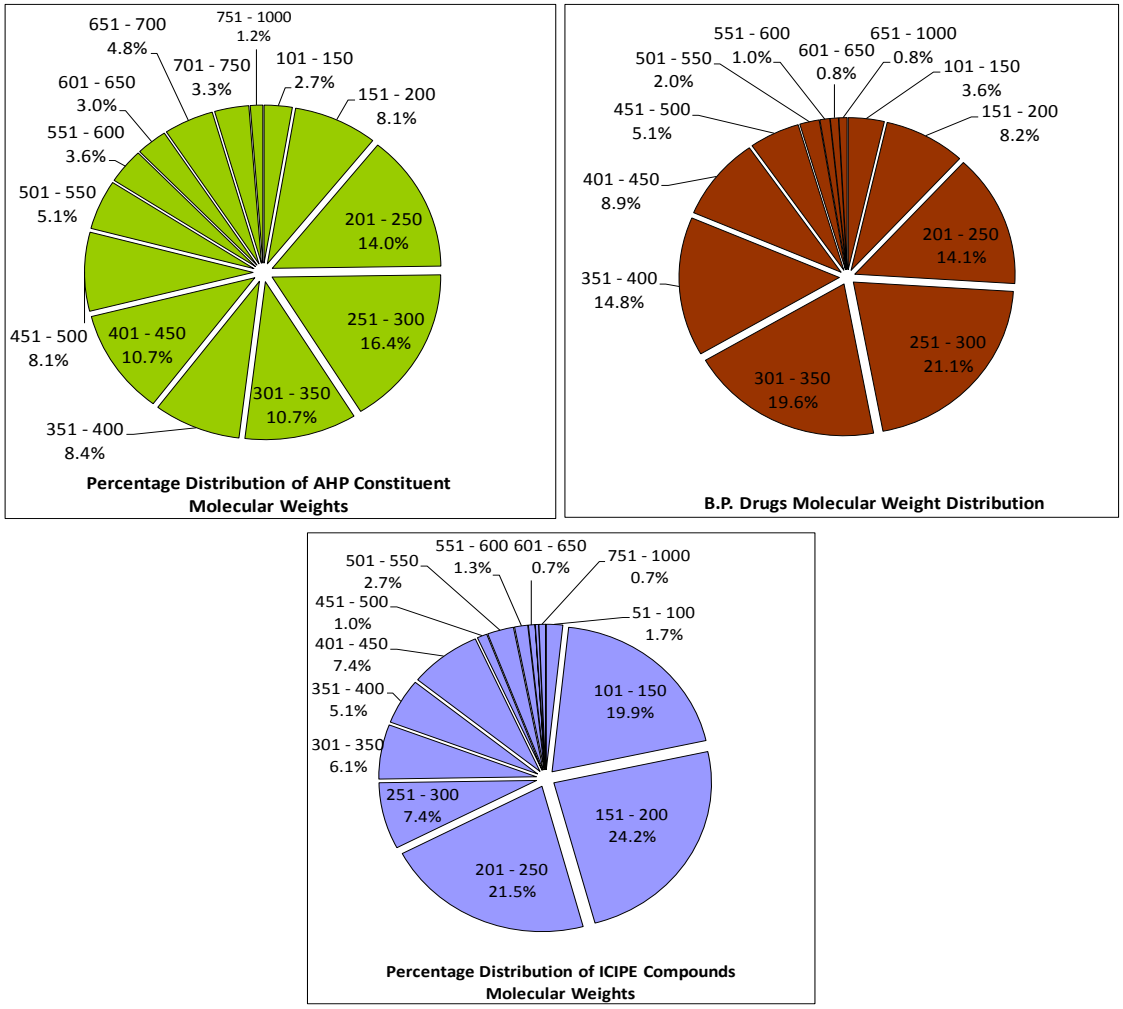

Figure 2.3: Pie charts of molecular weight distributions for the three compound datasets

2.4.2 Predicted cLogP

Estimated octanol/water partition coefficient values for the AHP compounds ranged from -5.02 to +10.0 with a mean of 2.70 and median value of 2.60. BP drugs had cLogP values ranging from -3.5 to +11.2 with a mean of 2.33 and median of 2.41. In both cases, compounds mostly clustered within the -1.0 to 5.0 cLog P range with approximately 60% having values lying between 0 and 5.0.

By contrast, the ICIPE compounds exhibited a bi-modal distribution with cLogP values clustering around the 2.01-3.00 and 5.01-6.00 ranges. The mean cLogP was

notably higher than that for the AHP and BP compounds at 3.49 indicating a higher proportion of more lipophilic compounds in this collection. This could be attributed to the fact that the terpenes mentioned previously as comprising a significant portion of this dataset are largely simple hydrocarbons devoid of heteroatoms or functional groups that might confer reduced lipophilicity.

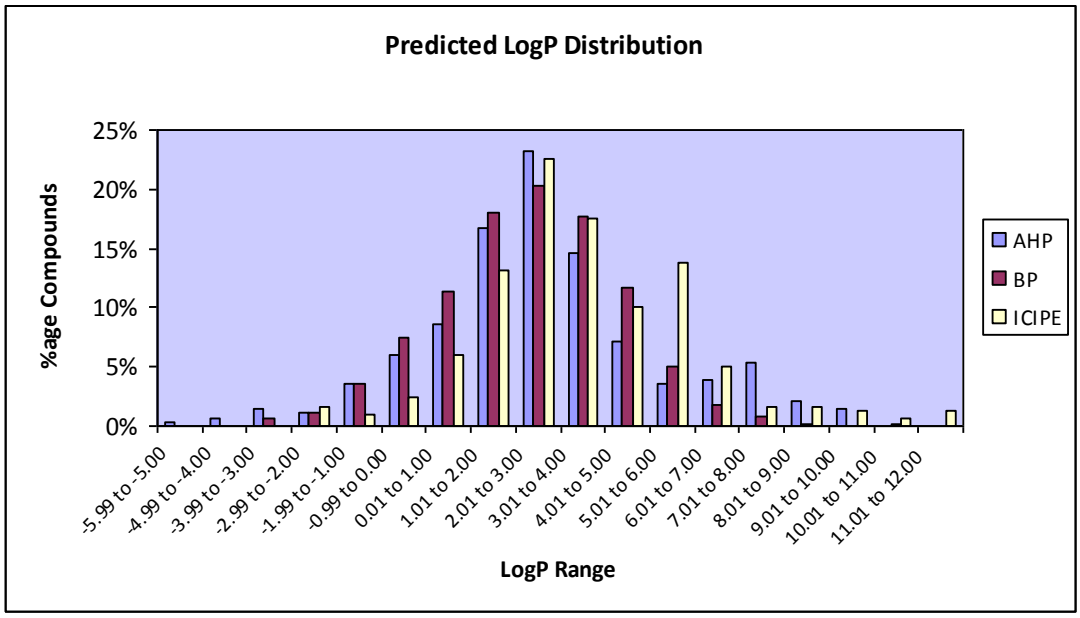

Figure 2.4: Frequency distribution histograms of predicted cLogP values for compounds in the three datasets

2.4.3 Rotatable Bonds

Veber *et al* proposed that in addition to the four physicochemical parameters highlighted in Lipinski's 'Rule-of-Five' for good bioavailability, most orally-active drug compounds appear to possess 10 or fewer rotatable bonds. The natural products from the AHP and B.P. 2009 drug molecules both exhibited similar distributions in this property with 94.9% and 93.6% of AHP and BP compounds respectively having 10 or less rotatable bonds. Notably, more than 11% of the AHP compounds but only about 4% of the BP drugs were totally devoid of rotatable bonds.

The ICIPE compounds presented a similar profile with 93.3% falling within the 10-bond limit. Two thirds of these compounds had 3 or fewer rotatable bonds with 12.1% lacking any at all.

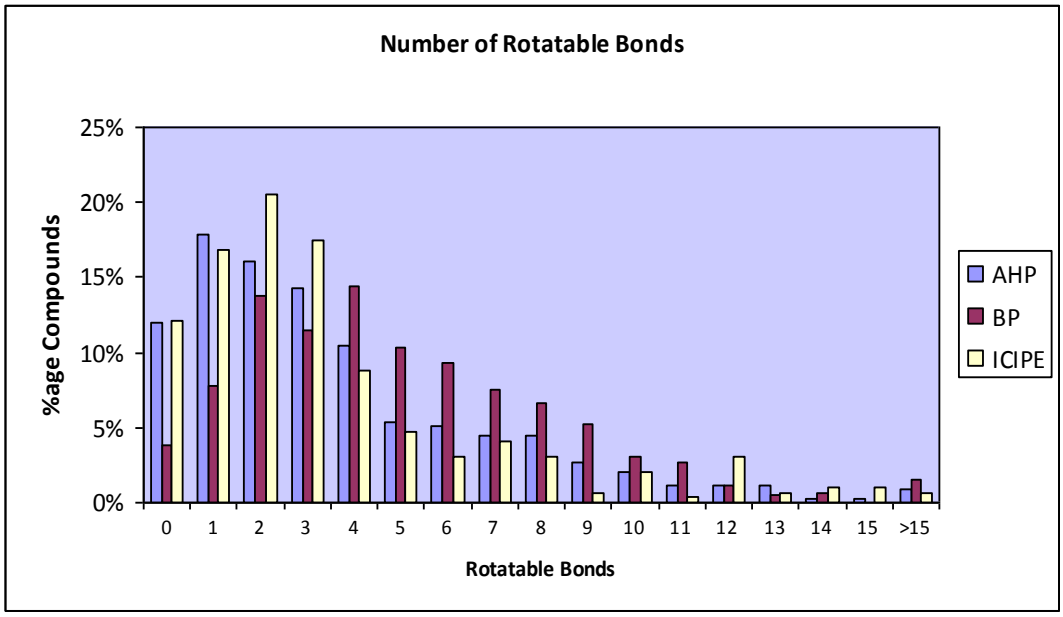

Figure 2.5: Frequency distribution histograms for number of rotatable bonds in the database compounds

2.4.4 Hydrogen Bond Donors and Acceptors

The ability to form hydrogen bonds is a key requirement for drug-like compounds to be orally active, since such bonds enhance aqueous solubility and also partly because they facilitate substrate-target interactions at the sub-cellular active sites of most drugs. However, the ideal H-bond number in a drug-like molecule must strike an optimal balance since too high a value might inadvertently limit compound permeability. The 'Rule-of-Five' specifies that the ideal number of H-bond donors in a drug-like molecule should be less than or equal to 5, while H-bond acceptors must not ideally exceed 10. In general, the majority of AHP, ICIPE and BP chemical constituents complied with this rule (82.4%, 97.0% and 97.9% respectively). The ICIPE compounds were particularly unique in having a very high proportion of molecules lacking H-bond donors (49.2%) which indicated a high incidence of molecules devoid of hydroxyl, amine or carboxylic acid functional groups in this data set. The average number of H-bond donors for the AHP, ICIPE and BP compounds was 2.69, 1.04 and 1.73 and corresponding median values of 2, 1 and 1 respectively.

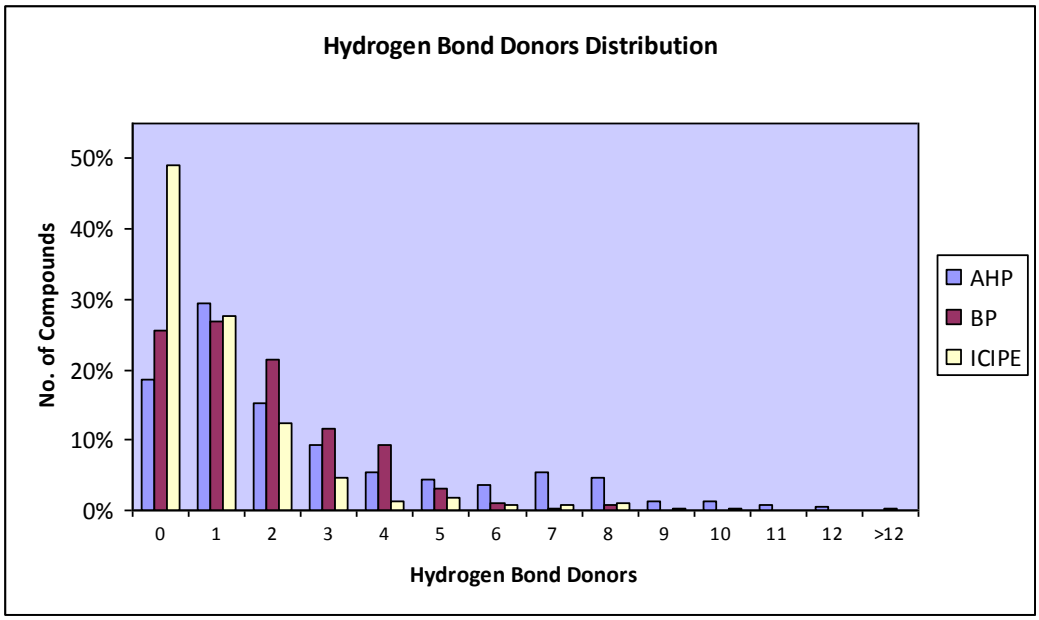

Figure 2.6: Frequency distribution histograms of H-bond donors in the database compounds

The average number of H-bond acceptors was 5.25, 2.38 and 4.86 for AHP, ICIPE and BP compounds respectively. While only 75.2% of the AHP compounds had 10 or fewer H-bond acceptors, the ICIPE and BP compounds had 98.3% and 96.9% respectively. All three compound groups presented a distribution skewed to the right (**Figure 2.7**) indicating higher incidence of fewer H-bond acceptors in general, with this characteristic being markedly pronounced with the ICIPE molecules in which more than 75% had three or less acceptors.

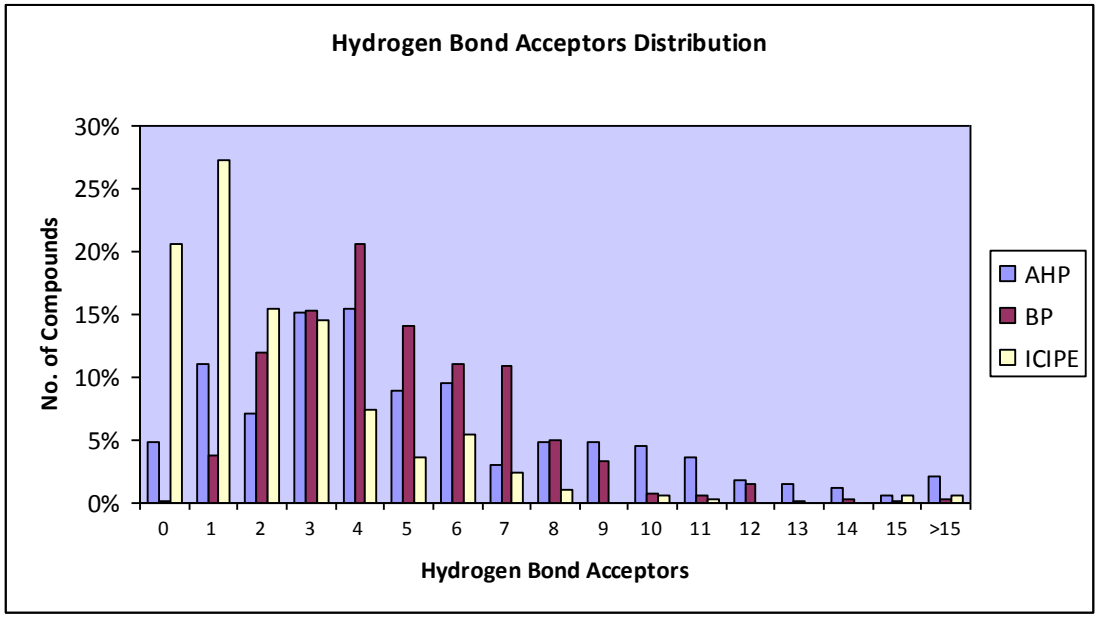

Figure 2.7: Frequency distribution histograms of H-bond acceptors in the database compounds

Table 2.2: Mean values of 'Rule-of-Five' properties

	Mean calculated values		
	AHP Natural Products (*n* = 335)	**ICIPE Compounds (*n* = 297)**	**BP 2009 Drugs (*n* = 608)**
Molecular weight	376.6	245.0	316.9
cLogP	2.7	3.5	2.3
Rotatable bonds	3.7	3.5	5.1
H-bond donors	2.7	1.0	1.7
H-bond acceptors	5.2	2.4	4.9

2.5 Statistical Evaluation and Comparison of Compound Datasets

Using SPSS[19] statistics software, the Kolmogorov-Smirnov and Shapiro-Wilk tests were applied across the three compound datasets to determine if the predicted and calculated values for the 'Rule-of-Five' and rotatable bond parameters exhibited normal frequency distributions. In all cases, the calculated *p*-values (0.000) were less than 0.05 at the 95% confidence level (**Table 2.3**), indicating that the data did not exhibit a normal distribution and could not therefore be reliably compared using standard parametric tests such as the Student's t-test.

Table 2.3: Results for statistical tests for normal distribution of data

	Kolmogorov-Smirnov Test			Shapiro-Wilk		
	Statistic	df	*p*-value	Statistic	df	*p*-value
Mwt	.080	1240	.000	.934	1240	.000
cLogP	.049	1240	.000	.988	1240	.000
Rotatable Bonds	.163	1240	.000	.884	1240	.000
H_Donors	.224	1240	.000	.793	1240	.000
H_Acceptors	.150	1240	.000	.910	1240	.000

The Mann-Whitney-Wilcoxon non-parametric statistical comparison test was therefore used to determine if there were significant differences in the respective chemical space profiles of the AHP, BP and ICIPE compounds. In this case, the variance in median values of the parameter distributions (**Table 2.4**) were used as a more robust variable for comparison of the different compound sets.

Table 2.4: Median values of 'Rule-of-Five' properties

	Median values		
	AHP Natural Products (*n* = 335)	**ICIPE Compounds (*n* = 297)**	**BP 2009 Drugs (*n* = 608)**
Molecular weight	338.3	204.0	307.4
cLogP	2.60	3.21	2.41
Rotatable bonds	3	3	4
H-bond donors	2	1	1
H-bond acceptors	4	2	4

The null hypothesis (H_o) for the Mann-Whitney-Wilcoxon statistical comparison of the similarity in the values of the datasets was that no significant difference exists in the chemical space parameters of the AHP, ICIPE and BP compounds. The test was carried out by comparing two of the datasets against each other in turns as independent sample sets for each of the 5 parameters and determining the *p-value* at the 95% confidence level (**Table 2.5**). The significance value of the calculated statistic was 0.05, therefore, for all comparisons in which the determined *p-value* was less than this cut-off, the null hypothesis was rejected. Conversely, *p-values* greater than 0.05 meant that the null hypothesis could not be rejected and that consequently, the differences between the datasets were not statistically significant.

Table 2.5: Mann-Whitney-Wilcoxon independent samples comparison test results

	Mwt		**cLogP**		**Rot. Bonds**		**HBD**		**HBA**	
	p	H_o	*p*	H_o	*p*	H_o	*p*	H_o	*p*	H_o
AHP vs BP	0.000	✕	0.114	✓	0.000	✕	0.000	✕	0.709	✓
ICIPE vs BP	0.000	✕	0.000	✕	0.000	✕	0.000	✕	0.000	✕
AHP vs ICIPE	0.000	✕	0.000	✕	0.389	✓	0.000	✕	0.000	✕

Note: *✓ indicates failure to reject the null hypothesis; ✕indicates rejection of the null hypothesis*

AHP compounds were found to share strong similarities with conventional BP 2009 drugs in the distribution of cLogP and H-bond acceptors. On the other hand, molecular weights, number of rotatable bonds and H-bond donors were significantly different between the two datasets.

In contrast, the ICIPE compounds were found to be significantly different from the BP 2009 drugs in each of the 5 parameters evaluated, strongly suggesting that this dataset appeared to consist largely of compounds devoid of drug-like characteristics. Comparison between the ICIPE and AHP compound sets also revealed that these two groups were largely dissimilar, with only the number of rotatable bonds in the molecules of either set not being significantly different from each other.

2.6 C-Lab Chemical Space Prediction and Principal Component Data Analysis

In addition to predicting the five chemical space parameters described above using MarvinSketch, the 3 data-sets were analyzed using the AstraZeneca in-house C-Lab ADMET property prediction service designed to calculate, using models, a much larger array of physicochemical and ADMET properties.[20] Using this package, it was possible to compute values for 196 related compound parameters broadly falling into the six categories summarized in **Table 2.6** below.

Table 2.6: Categorization of physico-chemical descriptors predicted using C-Lab Platform

Category	Parameters predicted
Lipophilicity	6
Hydrogen Bonding	29
Molecular Size and Shape	22
Molecular Charge/Polarity	75
Atom Counts	37
Molecular Topology	27
TOTAL	**196**

This multiplicity in prediction was due to the fact that many physicochemical properties are typically estimated *in silico* using mathematical formulas or models of which there might be several variations. For example, to estimate cLogP for each compound, the C-Lab platform calculated values using 3 different and widely recognized approaches, each yielding, in most cases, a different albeit closely approximating result. In this case, cLogP values were variously predicted based on calculations using Ghose/Crippen atom types;[21] a neural network approach on Ghose/Crippen atom types and prediction using the Daylight/Biobyte approach.

Using C-Lab, the 196 descriptors generated for each compound in all three datasets rendered simple analysis of the data to determine chemical space trends extremely challenging. To simplify this task, a different statistical application software was used to carry out multivariate component analysis aimed at reducing the complex data into a format that could be more easily interpreted. For this, SIMCA-P+ ver. 12.0.1 (Umetrics AB, Umeå, Sweden) was used. Data analysis using SIMCA again involved comparing the descriptors predicted for the conventional BP 2009 drugs as the reference against those for compounds from the AHP and ICIPE datasets. The results were plotted on 2-D principal component analysis (PCA) scatter plots (**Figure 2.8**)

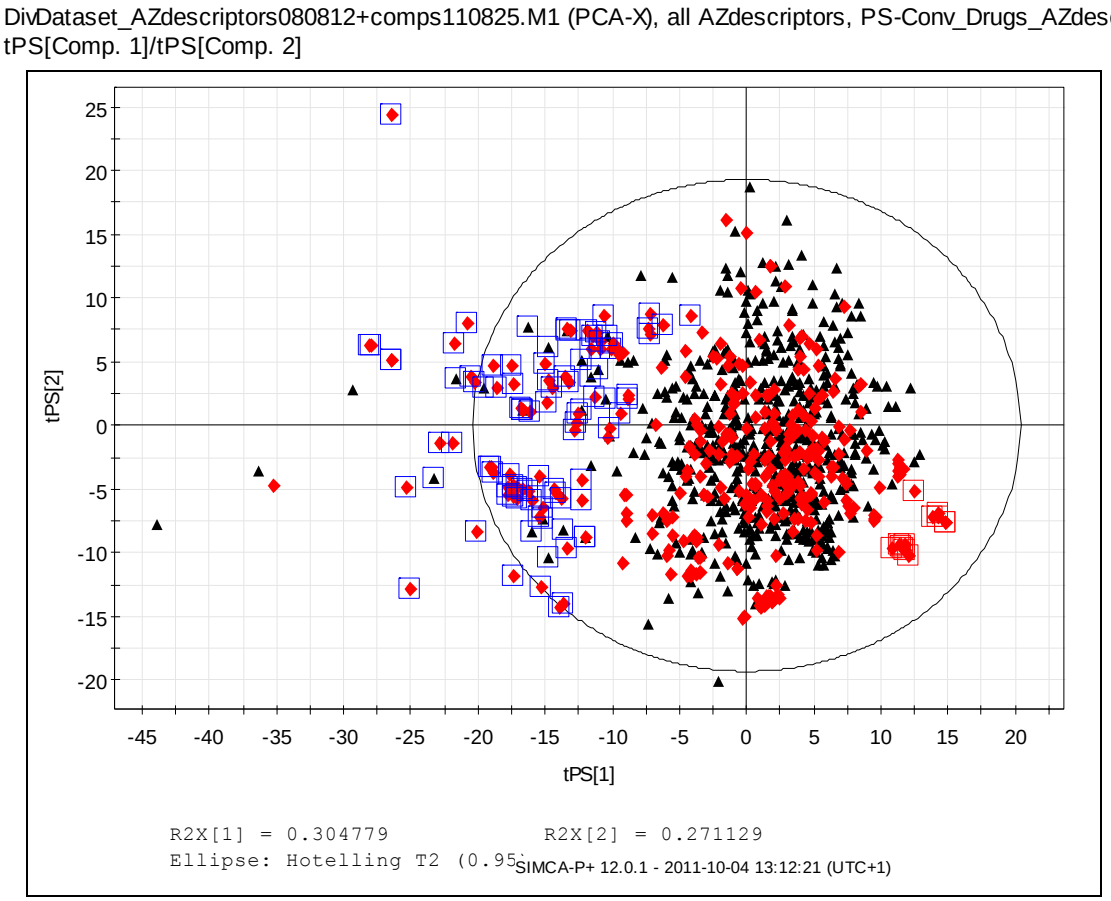

Figure 2.8: 2-D PCA scatter plot of predicted chemical space parameters of BP 2009 drugs (black triangles) and AHP chemical constituents (red diamonds, outliers highlighted in blue and red boxes).

PCA plots of the physicochemical descriptors of AHP compounds against BP 2009 drugs revealed a significant degree of overlap in compound properties but with two distinct groups of non-overlapping compounds as illustrated. The first and larger group comprising 79 compounds was clustered to the left of the main BP 2009 drugs body of plots (2nd and 3rd quadrants of the 2-D scatter plot) while the second smaller

cluster to the lower right (4th quadrant) of the BP 2009 drugs plots and comprised 12 compounds. Based on the predictions from MarvinSketch for these 91 outlying compounds, 75 (82.4%) were later found to violate one or more of the Lipinski rules while the remaining 16 were fully compliant. Of note, however, was the fact that these latter 16 compounds consisted almost entirely of the molecules in the 4th quadrant outlier zone for which the data collated indicated they were the lowest molecular weight compounds of the entire data set with values less than 250.

A similar comparison of the ICIPE compounds C-Lab predicted properties against those of BP 2009 drugs using SIMCA-P+ yielded the results illustrated in **Figure 2.9**. In this case, a much larger proportion of compounds did not overlap with the BP drugs with the most prominent cluster located to the lower right hand side of the reference plots (4th quadrant).

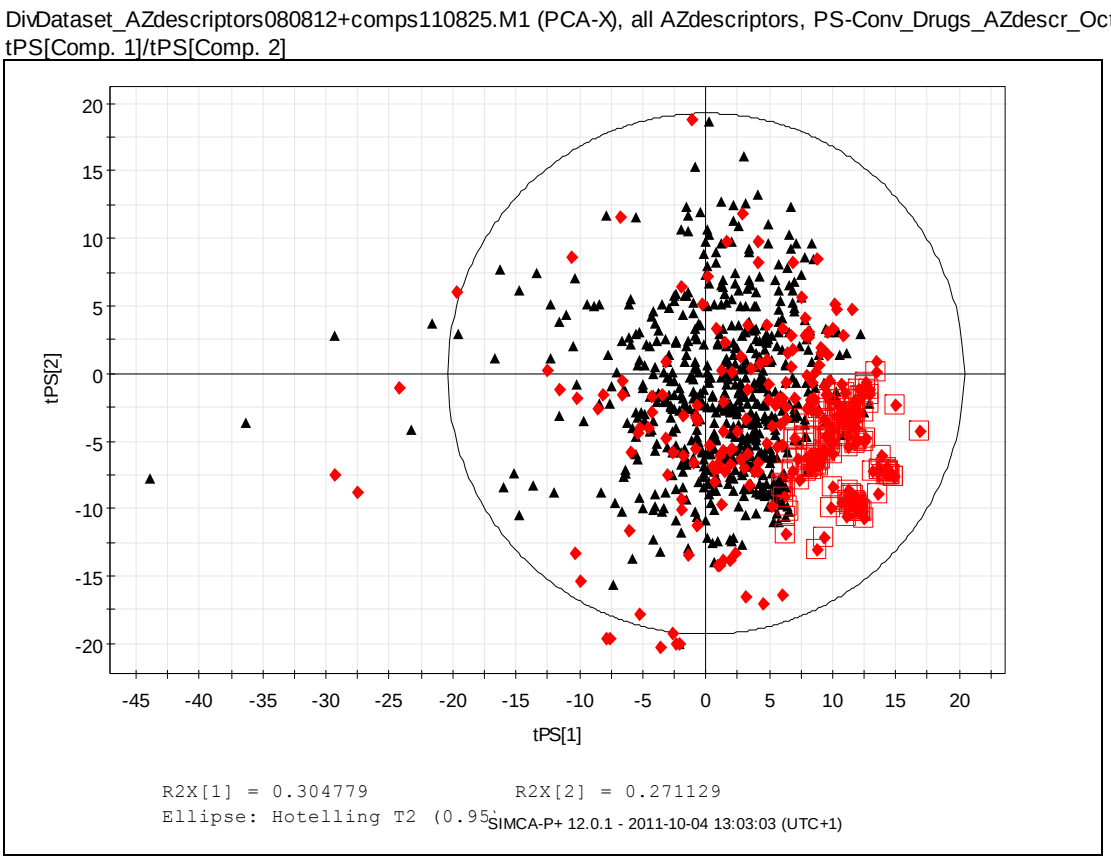

Figure 2.9: 2-D PCA scatter plot of predicted chemical space parameters of BP drugs (black triangles) and ICIPE compounds (red diamonds). Outliers are highlighted in red boxes.

A total of 145 compounds could be distinctly identified in the outlier group with a few other compounds noted in different non-overlapping areas of the scatter plot. A review of the predicted physico-chemical properties of the main group of outliers revealed that these compounds when compared to the original entire ICIPE dataset:

a) Had a markedly lower mean molecular weight (175.8 vs 245.0);
b) Had slightly higher mean cLogP values (3.95 vs 3.49);
c) On average, had significantly fewer rotatable bonds, H-bond donors and acceptors (i.e. 2.59 vs 3.55, 0.23 vs 1.04 and 0.78 vs 2.38 respectively).

Unlike the case with the AHP compounds where there appeared to be a good correlation between outliers and deviation from the 'Rule-of-Five', with the ICIPE dataset, only 44 of the 145 outliers (i.e. 30.3%) were found to deviate from the rules.

From these observations, it appeared that principal component analysis using SIMCA-P+ could be used as an easy and fairly accurate method for screening large datasets of compounds likely to vary significantly in physico-chemical properties from those of conventional drugs. On the basis of the SIMCA-P+ projections, the ICIPE compounds could be considered to be not particularly promising as potential drugs - a conclusion that was supported by the fact that the vast majority of these compounds were simple hydrocarbon components of essential oils and other secondary metabolites of plant origin.

2.7 Overall Compliance with 'Rule-of-Five'

Compliance of compounds in the three datasets with the 'Rule-of-Five' is summarized in **Table 2.7**. A total of 104 out of the 608 BP 2009 drugs (17.1%) failed to comply with at least one of the 'Rule-of-Five' parameters. 76 of these (i.e. 73.1% of non-compliant compounds) did not comply with 1 rule while 15 (14.4%), 10 (9.6%) and 3 (2.9%) failed to adhere to 2, 3 and 4 rules respectively. The most frequently violated rule was that for cLogP where 49 (47.1%) of the 104 drugs exceeded the +5.0 limit followed by rotatable bonds where 39 (37.5%) drugs fell outside the prescribed limit.

For the AHP constituents, 135 of the 335 compounds in the dataset (40.3%) violated one or more of the Lipinski rules. Among these, the proportion of multiple deviations was as follows: 1 rule - 72 compounds (53.3%), 2 rules - 33 compounds (24.4%), 3 rules - 21 compounds (15.5%) and 4 rules - 9 compounds (6.7%). Most frequent deviation occurred in the limit for molecular weight where 70 compounds (51.8%) exceeded 500. H-bond donors and cLogP were violated by an almost identical

proportion of the compounds (43.7% and 40.7% respectively) while only 17 compounds (12.6%) flouted the rule on number of rotatable bonds.

In contrast, only 85 of the 297 ICIPE compounds (28.6%) violated any of the rules with cLogP being the most prone to deviation (89.4% of the failures). 23.5% and 20.0% of the deviating compounds exceeded the limits for rotatable bonds and molecular weight while 10.6% and 5.9% of the deviants exceeded the requirements for H-bond donors and H-bond acceptors respectively. 60 of the 85 compounds failed in only one parameter while 11 deviated in both two and three of the rules. Only three compounds failed to adhere to four of the rules. In none of the three data sets was any compound found to flout all five of the Lipinski rules.

Table 2.7: Summary of compound deviations from 'Rule-of-Five'

	Compound Dataset		
	AHP (%) *n* = 335	**ICIPE (%)** *n* = 297	**BP Drugs (%)** *n* = 608
1 Parameter	72 (21.5)	60 (20.2)	76 (12.5)
2 Parameters	33 (9.8)	11 (3.7)	15 (2.5)
3 Parameters	21 (6.3)	11 (3.7)	10 (1.6)
4 Parameters	9 (2.7)	3 (1.0)	3 (0.5)
TOTAL	**135 (40.3)**	**85 (28.6)**	**104 (17.1)**

2.8 *In silico* Screening for Time Dependent Enzyme Inhibition Structural Alerts

A software script designed to detect functional groups associated with Time Dependent Inhibition (TDI) of CYP450 enzymes was used to screen the compounds in the data set. The script worked by identifying text fragments within the SMILES notations for each compound indicating the presence of structural alert groups and was designed to pick out any of 25 possible alerts, including, but not limited to:

1. 5 membered heterocyclic aromatic rings;
2. Conjugated unsaturated alkyl chains and carbonyl groups;
3. Terminal (ω) and penultimate carbon (ω-1) acetylenes;
4. Exocyclic and multi-halogenated alkenes, epoxides and thioethers;
5. Isothiocyanates, thioamides and dithiocarbamates;
6. Phenols, acetates and peroxides.

Table 2.8: Summary of number of TDI structural alerts detected per dataset

	Compound Dataset		
	AHP	**ICIPE Cmpds**	**BP Drugs**
None Detected	88	135	183
1 Detected	127	121	279
2 Detected	92	37	123
3 Detected	28	3	19
4 Detected	0	1	3
5 Detected	0	0	1
Average structural alerts per compound	**1.18**	**0.70**	**0.99**

The AHP natural products were noted to possess the greatest number of potential toxicophores per compound (1.18) compared to the ICIPE and BP drugs. The ICIPE compounds had the fewest number of potential time dependent enzyme inhibitors while the BP drugs averaged almost 1 structural alert per compound. In the three data sets, only one compound was found to contain as many as five (5) different structural alerts (**Figure 2.10** - Cefixime from BP 2009 drugs). Ironically, however, this highlighted the fact that presence of structural alerts alone is not necessarily always definitive indication of compound toxicity since cefixime, an orally active third generation cephalosporin, belongs to a class of antibiotic compounds with a generally low toxicity index in humans. The major side effect associated with cephalosporins in general is the possibility of hypersensitivity reactions in individuals allergic to this class of β-lactam antibiotics. Inhibition of CYP450 enzymes by cephalosporins has rarely been reported in the literature with cefixime in particular reported as being non-inhibitory against the major drug metabolizing hepatic CYP450 isoforms *in vitro*.[22]

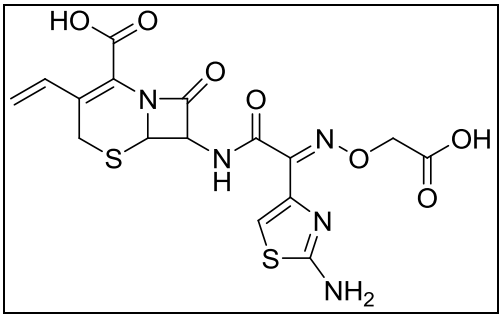

Figure 2.10: Cefixime - Five structural alerts but low toxicity in vivo

2.9 Conclusions

A virtual database of natural products and conventional clinically used drugs was successfully designed, populated and mined for data that allowed statistical comparison across different data sets. Evaluation of the *in silico* predicted physico-chemical properties in particular with regard to the Lipinski 'Rule-of-Five' parameters highlighted broad differences between natural products and the mainly synthetic conventional BP 2009 drug compounds.

As expected, a greater proportion of the natural products in the database did not comply with one or more of the Lipinski parameters compared to the BP2009 dataset. In the case of the latter group, the non-compliance rate of approximately 17.1% was thought to have been largely due to the fact that this dataset had not been filtered beforehand to remove drugs administered through non-oral routes, or whose oral absorption was largely dependent on active transporters *in vivo*.

Although the database created as described in this Chapter is relatively modest in terms of the number of compounds contained, particularly when compared to commercially available or online databases, it possesses the advantage of containing a large proportion of natural products from medicinal plants unique to the African continent. As such, it may conceivably be populated with compounds possessing unique chemical scaffolds that may lend themselves to useful ligand-based or target structure-based *in silico* virtual screening.

REFERENCES:

(1) Shoichet, B. K. Virtual Screening of Chemical Libraries. *Nature* **2004**, *432*, 862–865.

(2) Cavasotto, C. N.; Orry, A. J. W. Ligand Docking and Structure-Based Virtual Screening in Drug Discovery. *Current Topics in Medicinal Chemistry* **2007**, *7*, 1006–1014.

(3) Ghosh, S.; Nie, A.; An, J.; Huang, Z. Structure-Based Virtual Screening of Chemical Libraries for Drug Discovery. *Current Opinion in Chemical Biology* **2006**, *10*, 194–202.

(4) Clark, D. E.; Pickett, S. D. Computational Methods for the Prediction of "drug-likeness."*Drug Discovery Today* **2000**, *5*, 49–58.

(5) Irwin, J. J.; Shoichet, B. K. ZINC - A Free Database of Commercially Available Compounds for Virtual Screening. *Journal of Chemical Information and Modeling* **2005**, *45*, 177–182.

(6) Irwin, J. J.; Sterling, T.; Mysinger, M. M.; Bolstad, E. S.; Coleman, R. G. ZINC: A Free Tool to Discover Chemistry for Biology. *Journal of Chemical Information and Modeling* **2012**, *52*, 1757–1768.

(7) ZINC Database http://zinc.docking.org/ (accessed May 8, 2014).

(8) Ntie-Kang, F.; Zofou, D.; Babiaka, S. B.; Meudom, R.; Scharfe, M.; Lifongo, L. L.; Mbah, J. A.; Mbaze, L. M.; Sippl, W.; Efange, S. M. N. AfroDb: A Select Highly Potent and Diverse Natural Product Library from African Medicinal Plants. *PLoS ONE* **2013**, *8*, e78085.

(9) Rollinger, J. M.; Stuppner, H.; Langer, T. Virtual Screening for the Discovery of Bioactive Natural Products. In *Progress in Drug Research: Natural Compounds as Drugs, Volume 1*; Petersen, F.; Arnstutz, R., Eds.; Birkhauser Verlag: Basel, Switzerland, 2008; pp. 211–249.

(10) *African Herbal Pharmacopoeia*; Brendler, T.; Eloff, K.; Gurib-Fakim, A.; Phillips, D., Eds.; Graphic Press Ltd: Baie du Tombeau, Mauritius, 2010.

(11) *British Pharmacopoeia 2009*; Her Majesty's Stationery Office: London, UK, 2009.

(12) Weininger, D. SMILES, a Chemical Language and Information System. 1. Introduction to Methodology and Encoding Rules. *Journal of Chemical Information and Modeling* **1988**, *28*, 31–36.

(13) Ash, S.; Cline, M. A.; Homer, R. W.; Hurst, T.; Smith, G. B. SYBYL Line Notation (SLN): A Versatile Language for Chemical Structure Representation. *Journal of Chemical Information and Modeling* **1997**, *37*, 71–79.

(14) Heller, S.; McNaught, A.; Stein, S.; Tchekhovskoi, D.; Pletnev, I. InChI - the Worldwide Chemical Structure Identifier Standard. *Journal of Cheminformatics* **2013**, *5*, 7.

(15) Lachance, H.; Wetzel, S.; Kumar, K.; Waldmann, H. Charting, Navigating, and Populating Natural Product Chemical Space for Drug Discovery. *Journal of Medicinal Chemistry* **2012**, *55*, 5989–6001.

(16) Lipinski, C. A.; Lombardo, F.; Dominy, B. W.; Feeney, P. J. Experimental and Computational Approaches to Estimate Solubility and Permeability in Drug Discovery and Development Settings. *Advanced Drug Delivery Reviews* **2001**, *46*, 3–26.

(17) Veber, D. F.; Johnson, S. R.; Cheng, H.-Y.; Smith, B. R.; Ward, K. W.; Kopple, K. D. Molecular Properties That Influence the Oral Bioavailability of Drug Candidates. *Journal of Medicinal Chemistry* **2002**, *45*, 2615–2623.

(18) Lipinski, C. A. Lead- and Drug-like Compounds: The Rule-of-Five Revolution. *Drug Discovery Today: Technologies* **2004**, *1*, 337–341.

(19) IBM Corp. IBM SPSS Statistics for Windows, Version 22.0, 2013.

(20) Cumming, J. G.; Winter, J.; Poirrette, A. Better Compounds Faster: The Development and Exploitation of a Desktop Predictive Chemistry Toolkit. *Drug Discovery Today* **2012**, *17*, 923–927.

(21) Ghose, A. K.; Pritchett, A.; Crippen, G. M. Atomic Physicochemical Parameters for Three Dimensional Structure Directed Quantitative Structure-Activity

Relationships III: Modeling Hydrophobic Interactions. *Journal of Computational Chemistry* **1988**, *9*, 80–90.

(22) Niwa, T.; Shiraga, T.; Hashimoto, T.; Kagayama, A. Effect of Cefixime and Cefdinir, Oral Cephalosporins, on Cytochrome P450 Activities in Human Hepatic Microsomes. *Biological & Pharmaceutical Bulletin* **2004**, *27*, 97–99.

CHAPTER THREE:

IN VITRO EVALUATION OF NATURAL PRODUCT BIOACTIVATION

3.1 Summary

In this Chapter, a panel of *in vitro* experimental techniques employed to investigate the possible bioactivation of a selection of natural products is described in detail. The natural products selected for *in vitro* studies are described with particular emphasis on their potential or reported biological or medicinal properties. The evaluation strategy employed to systematically investigate the potential bioactivation of these selected natural products is highlighted. Results from both the preliminary screening as well as details of how *in vitro* trapping experiments were conducted on the selected natural products possessing different structural alerts using different trapping agents are presented. An overview of the rationale for using different LC-MS detection modes to aid in data analysis as well as interpretation of data collected from analysis of the test samples to determine which compounds appeared to form reactive metabolic intermediates is included.

3.2 General Introduction

As previously highlighted in **Chapter 1**, toxicity of drugs and natural products may arise from their inadvertent metabolic bioactivation into reactive metabolites, which are suspected to disrupt normal biochemical processes through irreversible covalent binding to sub-cellular components.[1]

The ability to predict which compounds have the potential to undergo undesirable bioactivation during early drug discovery is hampered by many factors, including the fact that animal studies cannot be used to determine this and that idiosyncratic adverse reactions only occur in a small percentage of the population. In some cases, however, the potential for reactive metabolite formation may be highlighted by the presence of functional groups, or structural alerts, known to undergo metabolic bioactivation to reactive electrophilic intermediates.[2,3] However, the presence of structural alerts is rarely conclusive evidence that a drug candidate will have a definite liability through formation of reactive metabolites. Many drugs in clinical use that have excellent safety profiles are known to

possess structural alerts that do not appear to result in the formation of toxic reactive metabolites.[4]

At present, the most reliable *in vitro* experimental technique for detecting the formation of reactive metabolites involves determination of covalent binding of test compounds to microsomal or hepatocellular proteins after co-incubation. This requires the use of radio-labelled test compounds and is based on determination of the residual radioactivity after incubation of compounds with microsomes and subsequent 'wash-out' of the test substrates. Radiation readings from the components left behind after removal of the substrate are considered evidence of covalent binding of the radiolabelled drug or its metabolites to proteins in the incubation matrix. The extent of covalent binding can be quantified from the magnitude of radiation detected in the sample. Thus, this technique allows for comparison of the relative risk of covalent binding by different compounds or their metabolites and may be used to rank them for purposes of lead optimization. The main drawback to this methodology is the need to incorporate radioisotopes into the test compounds, which may not be practically feasible in the early stages of drug discovery particularly when dealing with natural products. Consequently, such assays are only performed on a routine basis at later stages of the drug discovery cycle.[5]

An alternative, cheaper, and more universally applicable *in vitro* method to investigate covalent binding of compounds resulting from their metabolic bioactivation involves trapping of reactive metabolic intermediates using nucleophilic trapping agents. Successful application of such methods is, however, dependent on the availability of highly sensitive analytical and detection techniques since due to their reactive nature, the reactive intermediates are very short-lived and typically only generated in minute quantities. LC-MS detection is the most widely applied technique for analysing *in vitro* metabolite trapping incubation samples, providing high sensitivity and the ability to yield information that is useful in elucidating the structures of the reactive intermediate.[6–8]

3.3 Bioactivation Evaluation Strategy

To investigate the possible bioactivation of natural product constituents present in plant- or microbe-derived preparations used in both conventional and traditional medicine, the evaluation strategy, illustrated below was employed.

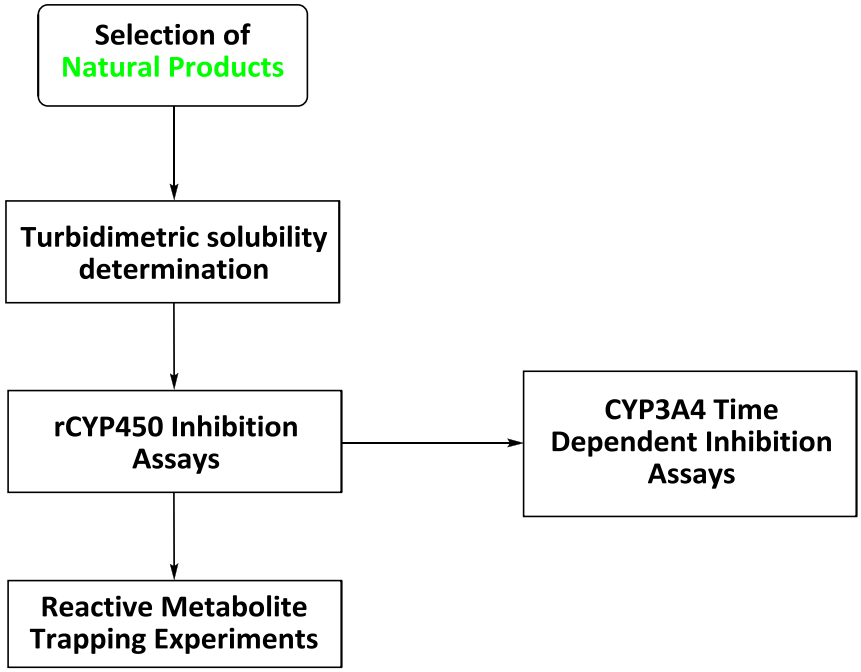

3.4 Selection of Natural Products

A total of twelve purely natural product compounds and three semi-synthetic natural product derivatives were sourced for experimental evaluation of metabolic bioactivation leading to formation of reactive intermediates. The following key considerations were made in selecting specific compounds to study:

i. The compounds are known or reported to possess biological activity of potential medicinal benefit. Alternatively, the compounds are known chemical constituents of ethnobotanical preparations reported to possess such biological activity;

ii. The compounds all contained an overt structural alert in their molecular structures that might potentially undergo metabolic bioactivation;

iii. The compounds were readily available in sufficient quantities to facilitate comprehensive *in vitro* testing;

iv. Chemical structural diversity i.e. efforts were made to ensure that the compounds chosen belonged to different chemical scaffolds. In some cases, however, semi-synthetic analogues were also selected for testing to investigate the effect of minor changes in parent natural chemical structure on possible bioactivation.

3.4.1 Gedunin

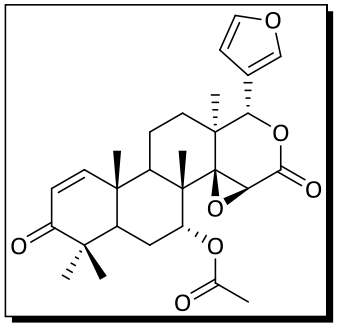

Gedunin (**GEDN**) is a triterpenoid limonoid isolated from plants of the family *Meliaceae*.[9] It is present in extracts prepared from the leaves and seeds of the Neem tree (*Azadirachta indica*), a well-known and widely used medicinal plant native to India and Burma but also common in tropical parts of West and East Africa. The medicinal properties of the Neem tree have been exploited for many years along the East African coast, where the plant is considered to be a virtual cure-all for treating diverse medical conditions – hence its Swahili name "*Mwarubaini*" (meaning reliever of forty disorders). **GEDN** has also been reported to be a constituent in preparations from other plant species including *Melia azedarach, Xylocarpus granatum, X. obovatus, Cedrela odorata, C. sinensis, Entandrophragna angolense, E. delevoyi, Khaya grandifolia* and *Carapa guainensis*.

GEDN is the most potent naturally occuring antiplasmodial limonoid identified to-date. MacKinnon *et al.* reported its *in vitro* antiplasmodial IC_{50} values as 39 ng/mL and 20 ng/mL against the chloroquine sensitive (CQ-S) *P. falciparum* D6 and resistant (CQ-R) W2 clones, respectively, comparable to those of quinine (14.8 ng/mL and 34.9 ng/mL).[10] Similar results had earlier been reported by Khalid *et al* but in this case, the strain of *P. falciparum* used in the study was not indicated.[11] An even more recent study by Chianese *et al*. reported the antiplasmodial activity of **GEDN** and other limonoids isolated from fruits of the neem tree, in which the potency of the compound against the CQ-R *P. falciparum* W2 strain was again noted to be greater than against the CQ-S D10 strain.[12]

Apart from its antiplasmodial activity, **GEDN** has also been reported to possess antitumor activity *in vitro*. For example, it was found to be a moderately potent

growth inhibitor of CaCo-2 colon cancer cells at IC_{50} 16.83 µM.[13] **GEDN** and some of its semi-synthetic derivatives have also been reported to exhibit antiproliferative activity against MCF-7 and SkBr3 breast cancer cell lines *in vitro*, acting via inhibition of 90kDa heat shock protein (Hsp90), a validated target for new anticancer drugs.[14]

In addition to its antiplasmodial and cytotoxic activities, **GEDN** has also been reported to possess inhibitory activity against H^+ K^+ - ATPase (gastric proton pump) in rats and guinea pig models comparable to the anti-ulcer drug omeprazole.[15]

The sample of **GEDN** used for all *in vitro* experiments in this work was purchased from Tocris Biosciences (Ellisville, MO, USA).

3.4.2 Justicidin A

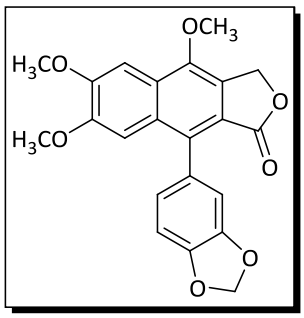

Justicidin A (**JSTN**) is an aryl naphtholignan first isolated from the plant *Justicia procumbens*. In Traditional Chinese Medicine, *J. procumbens* is used as a folk remedy in the treatment of fever, pain due to pharyngolaryngeal swelling and cancer.[16] **JSTN** is also present in other plant species, and has been isolated from members of the Geraniaceae family, in particular, *Monsonia angustifolia.*

JSTN has been reported to possess *in vitro* antiviral, antiplatelet and particularly cytotoxic activity against different human cancer cell lines.[16–19] For instance, the compound has been found to cause apoptosis in HT-29 and HCT116 human colorectal cancer cells and markedly suppressed the growth of HT-29 cells transplanted into an immunodeficient (NOD-SCID) mouse model upon oral administration.[20] **JSTN** has similarly been reported to inhibit the growth of hepatocellular carcinoma cells *in vitro* and also in mice via a mechanism thought to involve activation of caspase-8 leading to apoptosis in addition to disruption of mitochondrial function in the cancer cells.[21] Very recently, **JSTN** and other aryl naphtholignans from *M. angustifolia* have been patented for potential application in the treatment of erectile dysfunction and libido enhancement.[22]

The sample of **JSTN** used for all *in vitro* experiments in this work was obtained from the Council for Scientific and Industrial Research (CSIR), Pretoria, South Africa.

3.4.3 Dehydrobrachylaenolide

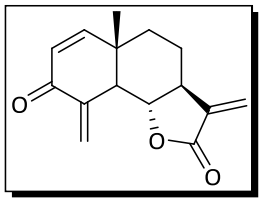

Dehydrobracylaenolide is a eudesmane-type sesquiterpene lactone (**SQTL**) originally isolated from the plant *Brachylaena transvaalensis* from which its name is derived.[23] The structure of SQTL was elucidated from NMR data reported by Bohlmann & Zdero and the absolute stereochemistry confirmed by chemical synthesis of the natural product by Higuchi *et al.*[24] More recently, the X-ray crystal structure of this compound has been reported by Rademeyer *et al.*[25]

SQTL has also been isolated from roots of the plant *Dicoma anomala*, a grassland herb species that is widely distributed in sub-Saharan Africa. This plant is reported to have numerous ethnomedicinal applications including the treatment of coughs and colds, fevers, ulcers, diarrhoea, intestinal parasites, in wound healing and also as an analgesic anti-inflammatory agent.[26–28]

The *in vitro* antiplasmodial activity of **SQTL** reported by Becker *et al* indicated IC_{50} values of approximately 1.9 µM and 4.1 µM against CQ-S D10 and CQ-R K1 *P. falciparum* strains, respectively (CQ IC_{50} 0.038 and 0.2 µM, respectively). Gene expression studies on the **SQTL**-treated parasites revealed that the compound appeared to alter the expression of 572 unique genes, many of which were different from those affected by the antimalarial drug artesunate, suggesting that **SQTL** may have a novel mechanism of antiplasmodial activity.[29]

The sample of **SQTL** used for all *in vitro* experiments in this work was obtained from the Council for Scientific and Industrial Research (CSIR), Pretoria, South Africa.

3.4.4 Metergoline

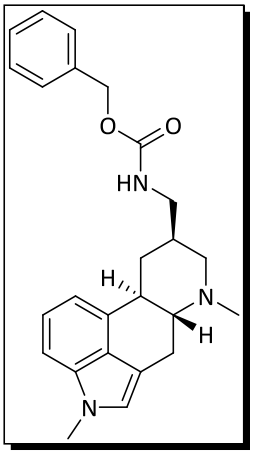

Metergoline (**MTGN**) is a semi-synthetic drug structurally related to the naturally occurring ergotamine, an ergot alkaloid first isolated from the fungus *Claviseps purpurea*.[30] The synthesis and subsequent discovery of the serotonin antagonist effects of **MTGN** was first reported by Bernardi *et al* and Beretta *et al* in the 1960s.[31] In addition, **MTGN** also acts as a dopamine agonist and is used clinically for the management of

migraine headaches and to suppress lactation via its bromocriptine-like pharmacological effects. **MTGN** has been reported to exhibit anti-fungal activity *in vitro*, inhibiting the growth of *Candida krusei* by triggering intracellular increase in reactive oxygen species and disrupting mitochondrial homeostasis.[32] Very recently, **MTGN** has been identified as a moderately potent chemosensitizer with potential use in treatment of malaria by its enhancement of the sensitivity of resistant *P. falciparum* strains to chloroquine.[33]

The sample of **MTGN** used for the *in vitro* assays in this work was purchased from Sigma Aldrich.

3.4.5 Fusidic acid

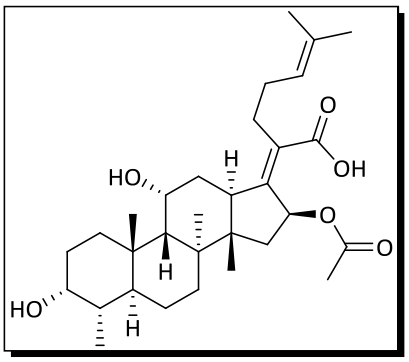

Fusidic acid (**FSDA**) is a naturally occurring steroidal antibiotic originally isolated from the fungus *Fucidium coccineum* and which has been in clinical use since the 1960s.[34] **FSDA** is used for the treatment of infections caused by gram-positive bacteria and is formulated as tablets, oral suspensions, intravenous infusions and topical preparations. **FSDA** has been reported to exhibit high oral biovailability (91%) and long plasma half-life.[35] As an antibiotic, **FSDA** has a relatively narrow spectrum of activity and is mainly active against staphylococci strains resistant to other classes of antibiotics such as the penicillins. However, the drug is reported to be generally well tolerated with a good safety profile and can be administered in large doses for prolonged periods of time.[36,37]

The sample of **FSDA** used for *in vitro* assays in this work was purchased from Sigma Aldrich.

3.4.6 Muzigadial

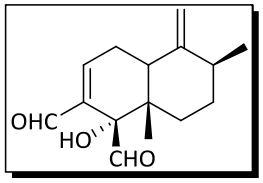

Muzigadial (**MZG**), also known as canellal, is a sesquiterpene drimane dialdehyde present in plants of the genus *Warburgia* (family Canellaceae) that was first isolated from the bark of the

plant *Warburgia ugandensis.*[38] **MZG** is also present in *W. salutaris*, the only species of the genus that extends into Southern Africa.[39] Traditionally, *W. salutaris* has been used extensively for the ethnobotanical treatment of ailments such as headaches, gum inflammation, venereal diseases, abdominal pains, malarial fevers, skin complaints and stomach ulcers.[40,41]

MZG and related drimane sesquiterpenoids have been reported to possess potent molluscidal, antifungal and broad spectrum antibacterial activity in addition to having anti-feedant effects against African army worms.[42,43] **MZG** and other drimane sesquiterpenes isolated from *Canella winterana* have also been reported to possess phytotoxic activity.[44] **MZG** has also been reported to have potent *in vitro* antiplasmodial activity against the chloroquine sensitive D10 *P. falciparum* strain. However, its utility as an anti-malarial agent appeared to be limited by the fact that it showed poor selectivity when tested for cytotoxicity against Chinese Hamster Ovarian cells.[45]

The sample of **MZG** used for *in vitro* experiments in this work was obtained from the Plants for Human Health Institute, North Carolina State University, USA.

3.4.7 Muzi-04

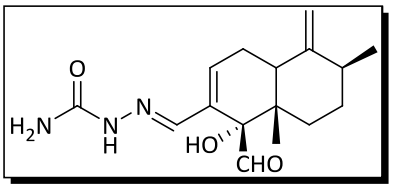

Muzi-04 is a semi-synthetic semicarbazone derivative of muzigadial prepared from the reaction of the parent compound with semicarbazide (**Scheme 3.1**) to investigate the effect of substituting one of the aldehyde groups on the biological activity of the parent natural product.

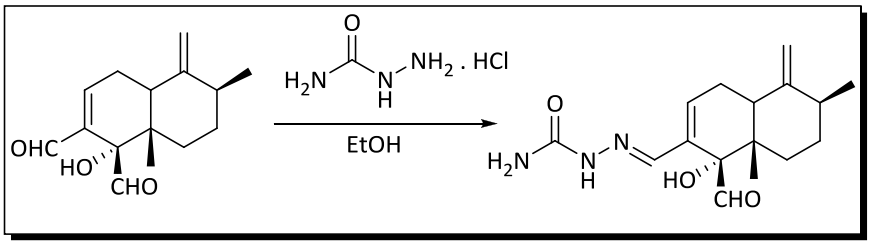

Scheme 3.1: Synthesis of **Muzi-04** from muzigadial

The sample of **MUZI-04** used in this work was synthesized by Dr. Tzu-Shean Feng at the Department of Chemistry, University of Cape Town.

3.4.8 Cucurbitacin A, B and C

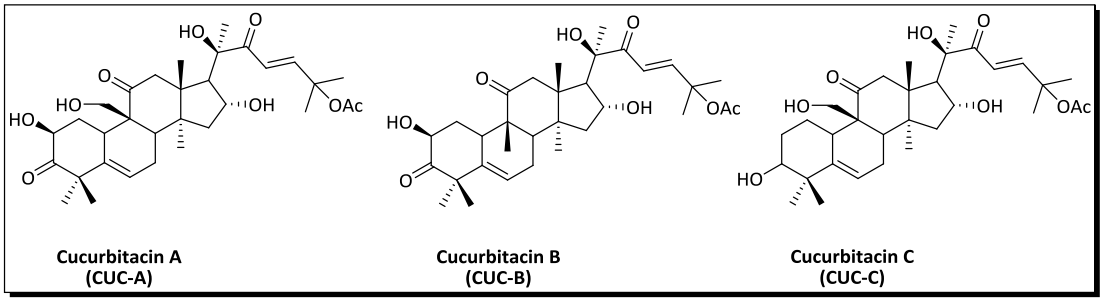

The cucurbitacins are a group of highly oxygenated, tetracyclic triterpene phytosterols characterized by the presence of the cucurbitane skeleton, 19-(10→9β) abeo-10α-lanost-5-ene, and which were first identified in plants of the family Cucurbitaceae. To date, no fewer than twenty distinct cucurbitacins have been reported in the literature, each being assigned a different letter of the alphabet to distinguish between these structurally closely related compounds (i.e. Cucurbitacin A, B, C…etc.)[46] Cucurbitacins have been reported to possess a wide range of pharmacological activities *in vitro*, with cucurbitacin B, D, E, I and Q being particularly notable for their cytotoxic activity against a variety of solid cancer cell types. The anticancer activity of this class of compounds is largely due to their potent inhibition of multiple cell signalling pathways crucial for cell proliferation and growth, resulting in fatal morphological and physiological changes in cancer cells.[47] For example, cucurbitacin B (**CUC-B**) has been reported to inhibit the growth of Hep-2 human laryngeal cancer cells and K562 leukaemia cells through inhibition of STAT3 activation leading to apoptosis and cell cycle arrest.[48,49] **CUC-B** has also been reported to inhibit the proliferation of BEL-7402 hepatocellular carcinoma cells both *in vitro* and when administered orally to BEL-7402 xenografted nude mice. In this case, the mechanism of action appears to involve inhibition of a different signalling pathway, the activation of c-Raf and not STAT3.[50] Against different leukaemia and lymphoma cell lines, **CUC-B** has been reported to exhibit dose-dependent growth inhibition arising from cell cycle arrest, increased cellular multi-nucleation and abnormal enlargement of cancer cells but not apoptosis.[51] In yet another study, **CUC-B** has been found to inhibit growth of glioma cancer cells in culture, again by causing cell-cycle arrest, apoptosis, disruption of F-actin and the microtubule cytoskeleton,

thereby disabling the ability of cells to migrate. In these cells, **CUC-B** appeared to act, at least partly, through the activation of JNK signalling pathways.[52]

The samples of cucurbitacin A, B and C used in this work were generously provided by Emeritus Prof. James Bull (Department of Chemistry, University of Cape Town).

3.4.9 DC3

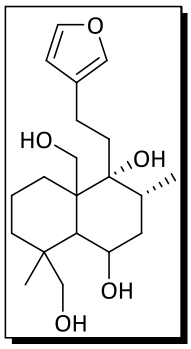

The furanoterpernoid labdane compound designated **DC3** is a semi-synthetic tetraol derived from the natural product dubiin, first reported by Eagle and Rivett in the 1970s and originally isolated from the acetone extracts of the leaves of the southern African plant *Leonotis dubia.*[53] **DC3** was prepared through the synthetic reduction of the parent compound using lithium aluminium hydride (**Scheme 3.2**).

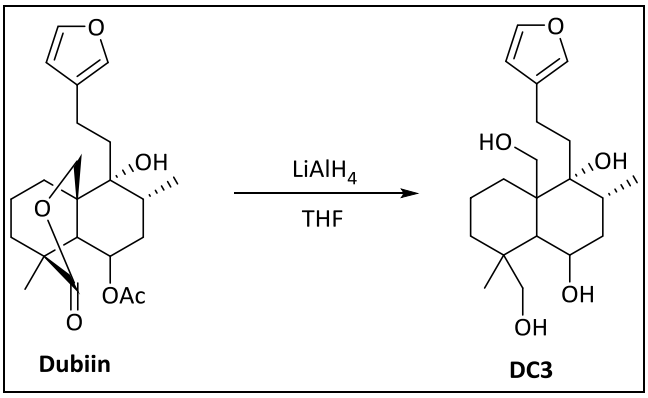

Scheme 3.2: Synthesis of DC3 from dubiin

3.4.10 Leoleorin A

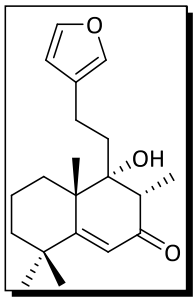

Plants of the genus *Leonorus* from which dubiin and leoleorin A (**DC14**) are obtained are indigenous to tropical parts of the world and particularly common in southern parts of Africa where they have been used as components of traditional herbal remedies. *L. leonurus* commonly known as Lion's Tail or Wild Dagga, is used as a herbal remedy for the treatment of fevers, headaches, dysentery, epilepsy, hypertension and snake bites. The plant is known to have mild psychoactive properties and its dried leaves and flowers have a calming effect when smoked. The

plant has subsequently been shown to be of potential benefit as an anxiolytic or antidepressant, possibly through modulation of the dopaminergic system.[54]

The samples of **DC3** and Leoleorin A (designated **DC14**) used for the *in vitro* assays reported in this work were a generous donation from Prof. Mike-Davies Coleman (formerly of Rhodes University, Grahamstown, South Africa and currently at the University of the Western Cape, South Africa).

3.4.11 Jamaicin and Calopogonium isoflavone A

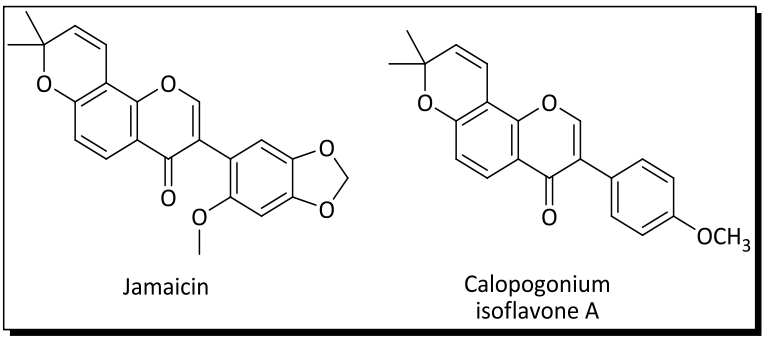

Jamaicin (**JMCN)** is an isoflavone that was first isolated from root bark extracts of the plant *Piscidia erythrina*, commonly known as Jamaica Dogwood and from which the compound's name is derived.[55] Calopogonium isoflavone A (**CLPG)** is a closely related compound isolated from plants of the genus *Millettia.*

In general, isoflavanoids have very limited distribution in the plant kingdom and are mostly found only in plants of the family Leguminoseae. **JMCN**, **CLPG** and other isoflavones are known constituents of herbal preparations that possess medicinal properties. Both compounds have, for example, been reported to exhibit moderate antiplasmodial activity *in vitro* against CQ-R Indochina 1 (W2) and CQ-S Sierra Leone 1 (D6) strains of *Plasmodium falciparum.*[56]

The samples of **JMCN** and **CLPG** used in this work were a generous donation from Prof. Abiy Yenesew (Department of Chemistry, University of Nairobi, Kenya).

3.4.12 Formononetin

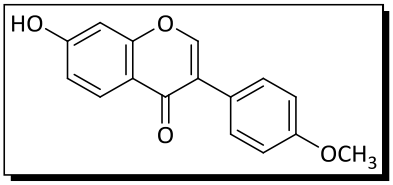

Formononetin (**FMTN)** is an isoflavone also isolated from plants of the family Leguminosae used as herbal medications. In Traditional Chinese Medicine preparations of the remedy *Danggui Buxue Tang* which comprises a mixture of *Radix astragali* and *Radix angelicae*, the content of **FMTN** and other isoflavanoids has been found to correlate with the biological activity of the preparation. **FMTN** content is therefore used as a quality control marker for *Radix astragali* preparations.[57] **FMTN** from other plant species has similarly been reported to possess varying biological activities. For example, this compound from the bark of *Dalbergia frutescens* was found to exhibit significant *in vitro* antigiardial activity against the protozoan parasite *Giardia intestinalis* with IC_{50} values superior to those of metronidazole, the current drug of choice (0.03 µg/mL vs. 0.1 µg/mL). However, although **FMTN** was also found to be active against a murine model of giardiasis *in vivo,* only high doses were effective, suggesting possible ADME liabilities when the compound is administered orally.[58] Isoflavones in general are well documented to possess phytoestrogenic biological properties, arising from their structural similarity to the hormone estrogen. **FMTN** has therefore been extensively studied to determine its effect on biological processes mediated in part by estrogens *in vivo*. For example it has been found to promote early healing of fractures in rats by activating angiogenesis and also been reported to promote endothelial repair and accelerate wound healing *ex vivo* and in a mouse model.[59,60] In a study carried out in rats, **FMTN** was reported to cause aortic vascular relaxation via both nitric oxide dependent and endothelium-independent mechanisms involving activation of BK_{Ca} and K_{ATP} channels.[61] Very recently, it has also been reported that **FMTN** may play a neuroprotective role in rats subjected to traumatic brain injury through inhibition of intracephalic inflammatory response and oxidative stress.[62]

The sample of **FMTN** used in this work was purchased from Sigma Aldrich.

Prior to carrying out *in vitro* experiments, the identity and purity of the test compounds was confirmed using a combination of NMR spectroscopy, LC coupled

mass spectrometry (LC-MS) and melting point determination. Spectral data was compared to values reported in the literature. Semi-quantitative determination of the solubility of the test compounds in aqueous buffer was measured using turbidimetric analysis as a means of identifying potential challenges in conducting subsequent *in vitro* assays in aqueous buffer solutions. The experimental procedures used for these characterizations are described in detail in **Chapter 6** and the results for each compound summarized in **Appendix 1**.

3.5 CYP450 Enzyme Inhibition Assays

Inhibition of the enzymes involved in drug metabolism often presents as one of the mechanisms by which xenobiotics lead to toxicity either directly or more commonly, through adverse drug-drug interactions. As previously highlighted in **Chapter 1**, natural products present in foods or non-conventional herbal remedies can similarly inhibit the same drug metabolizing enzymes, resulting in clinically significant adverse food-drug or herb-drug interactions. Enzyme inhibition assays are therefore routinely conducted early in the drug discovery process to identify lead compounds that might interfere with the catalytic activity of the main drug metabolizing enzymes, particularly the CYP450 isoforms.

For rapid high-throughput screening of large compound sets for CYP450 inhibition, assays based on the use of fluorogenic substrates and purified recombinant enzymes in microtitre 96-well plates are routinely used. These assays are based on the metabolism of the probe substrates to fluorescent metabolites when incubated in the presence of the drug metabolizing enzymes. Enzyme activity is proportional to the intensity of the measured fluorescence. If a compound that inhibits the activity of the enzyme is co-incubated with the probe substrate, there is a resultant decline in formation of the fluorescent metabolite, which can be determined through a measurable decrease in the fluorescence determined spectrophotometrically.

Advantages of this assay set-up include its high speed, ease of application and low set-up cost without the need for elaborate compound separation or capital-intensive equipment since it is based on the measurement of fluorescence of known metabolites whose spectral properties are well established with regard to excitation and emission wavelengths. Furthermore, fluorescence readings are taken directly from the test preparation without the need for sample work-up or separation to isolate the fluorescent metabolites. Because of the very simple setup of this type of assay, testing of compounds can be readily automated to facilitate high throughput screening.

Although ideal for rapid early screening of potential enzyme inhibitors, this method suffers from the drawback of not being suitable for testing inhibition caused by compounds that fluoresce at the same wavelengths as the probe substrate metabolites detected or which quench the fluorescence of these metabolites.

3.5.1 CYP450 Inhibition Assay Procedure and Results

In vitro CYP450 inhibition assays were carried out in 96-well microtitre plates based on the methods described by Crespi whereby test compounds were co-incubated in duplicate with purified recombinant enzymes in aqueous buffer to which the fluorogenic probe substrates was also included.[63,64] The test compounds were incubated at both 3 µM and 20 µM for 15 minutes at 37 °C at the end of which incubations were terminated by addition of an ice-cold solution of 20% 5 mM Tris in 80% acetonitrile. Inhibition of enzyme activity in incubations containing test compounds was subsequently determined based on calculations of the fluorescence intensity measurements compared to control incubations in which no compound was present. Positive control incubations in which known specific inhibitors of the individual rCYP450 enzymes screened were also included in every assay. The general set-up conditions for the enzyme inhibition assays are summarized in **Table 3.1** and described in detail in the **Experimental** Chapter.

Table 3.1: CYP450 isoforms, probe substrates, fluorescent metabolites and spectrofluorometric conditions used for CYP inhibition assays

rCYP450 Isoform	Fluorogenic Substrate	Fluorescent Metabolite	Excitation λ (nm)	Emission λ (nm)
CYP1A2	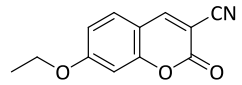 3-cyano-7-ethoxycoumarin (CEC)	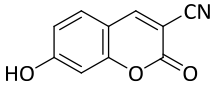 3-cyano-7-hydroxycoumarin (CHC)	405	460
CYP2C9 and CYP2C19	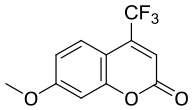 7-methoxy-4-trifluoromethyl coumarin (MFC)	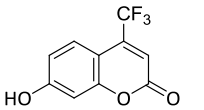 7-hydroxy-4-trifluoromethyl coumarin (HFC)	405	535
CYP2D6	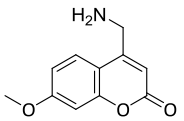 7-methoxy-4-aminomethyl coumarin (MAMC)	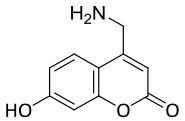 7-hydroxy-4-aminomethyl coumarin (HAMC)	390	460
CYP3A4	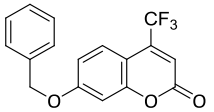 7-benzyloxy-4-trifluoromethyl coumarin (BFC)	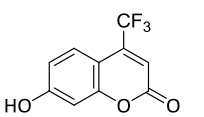 7-hydroxy-4-trifluoromethyl coumarin (HFC)	405	535

The fluorogenic probe substrates illustrated in **Table 3.1** used to evaluate CYP450 enzyme inhibition by the different compounds were synthesized, purified and characterised in-house as part of this work. However, evaluation of CYP2D6 inhibition using MAMC as probe substrate was hampered by the unusually high flourimeter readings obtained from the inhibition assay samples. Although successful use of this probe substrate and structurally related analogues has been reported in the literature, [65] the readings observed in our case were thought to be due to spectral interference by other components present in the incubation matrix. The interference was most likely largely due to NADPH, which has almost identical maximum emission wavelength (λ_{emm} 460 nm) as that of the monitored metabolite (7-hydroxy-4-methylamino coumarin, λ_{emm} 470 nm).[66] Consequently, determination of CYP2D6 inhibition by the test compounds using the methods successfully employed for other isoforms as described in this Chapter was not possible, despite minimizing NADPH concentration.

3.5.1.1 Inhibition of CYP1A2

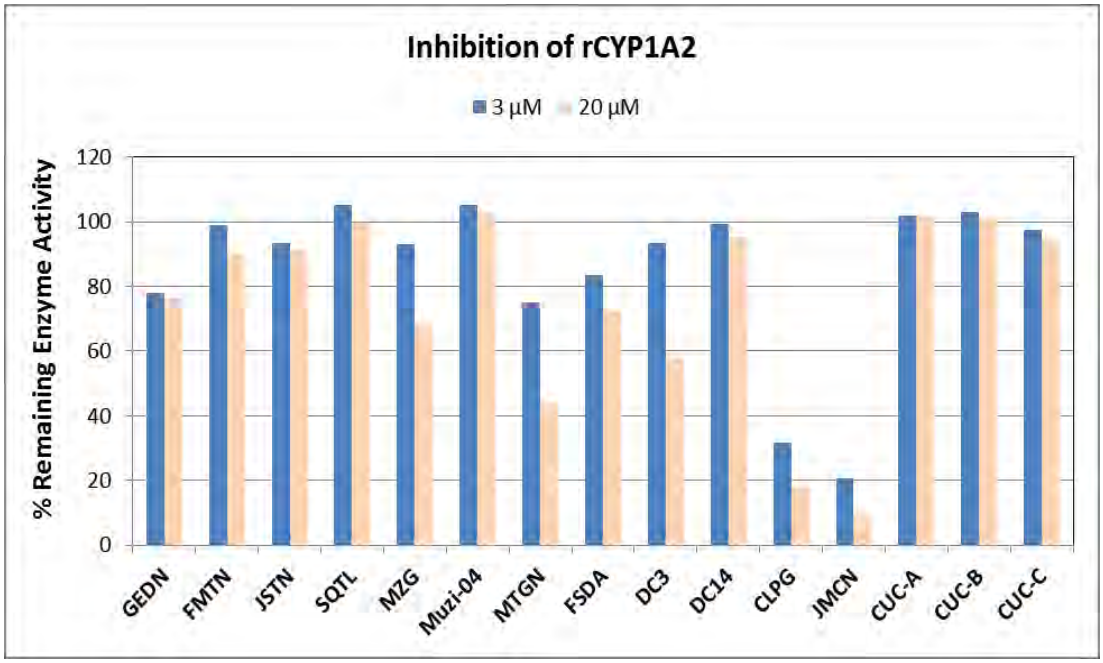

Figure 3.1: rCYP1A2 inhibition assay results (Substrate: CEC 3 µM)

rCYP1A2 appeared to be inhibited most significantly by the isoflavanoids **CLPG** and **JMCN**, both of which reduced enzyme activity to far less than 40% even at the lower assay concentration (3 µM). All other test compounds seemed to have little, if any, inhibitory effect on the activity of this isoform, with only metergoline and gedunin being noted to reduce activity to slightly less than 80% at 3 µM. This inhibition, was not, however, considered to be significant.

The isoflavone formononetin (**FMTN**), though closely structurally related to both **CLPG** and **JMCN** did not appear to inhibit enzyme activity even at the higher assay concentration (20 µM), suggesting that inhibition of the enzyme might be, in some way, dependent on the presence of the unique dimethyl pyran ring substitution on the chromone nucleus in **JMCN** and **CLPG**.

The three cucurbitacin compounds appeared to have no inhibitory effect on the enzyme.

3.5.1.2 Inhibition of CYP2C9

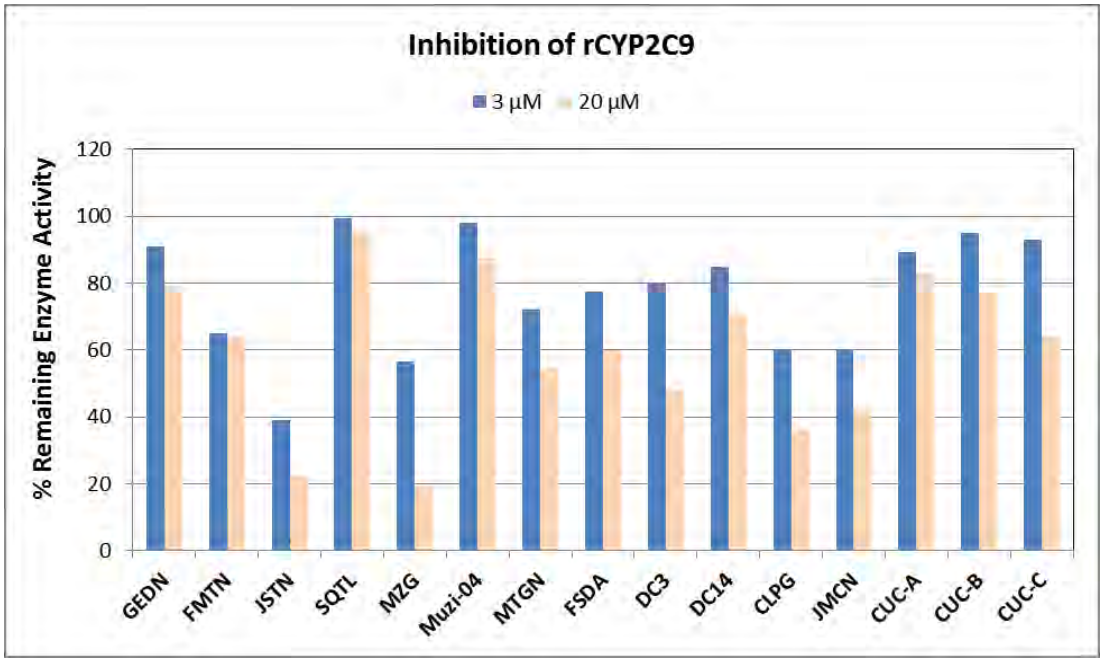

Figure 3.2: rCYP2C9 inhibition assay results (Substrate: MFC 85 µM)

rCYP2C9 appeared to be substantially more prone to inhibition by the test compounds compared to rCYP1A2 with 7 of the test substances (**FMTN**, **JSTN**, **MZG**, **MTGN**, **FSDA**, **CLPG** and **JMCN**) being found to reduce enzyme activity by more than 20% at 3 µM**.** The most potent inhibitors of this isoform were **JSTN** and **MZG** although neither seemed to reduce enzyme activity to as great an extent as observed with the most potent inhibitors of rCYP1A2 (i.e. **JMCN** and **CLPG**). Again, as also noted with rCYP1A2, none of the three cucurbitacins seemed to have any significant inhibition of rCYP2C9 enzyme at both assay concentrations, with only **CUC-C** exhibiting moderate inhibition at 20 µM.

3.5.1.3 Inhibition of CYP2C19

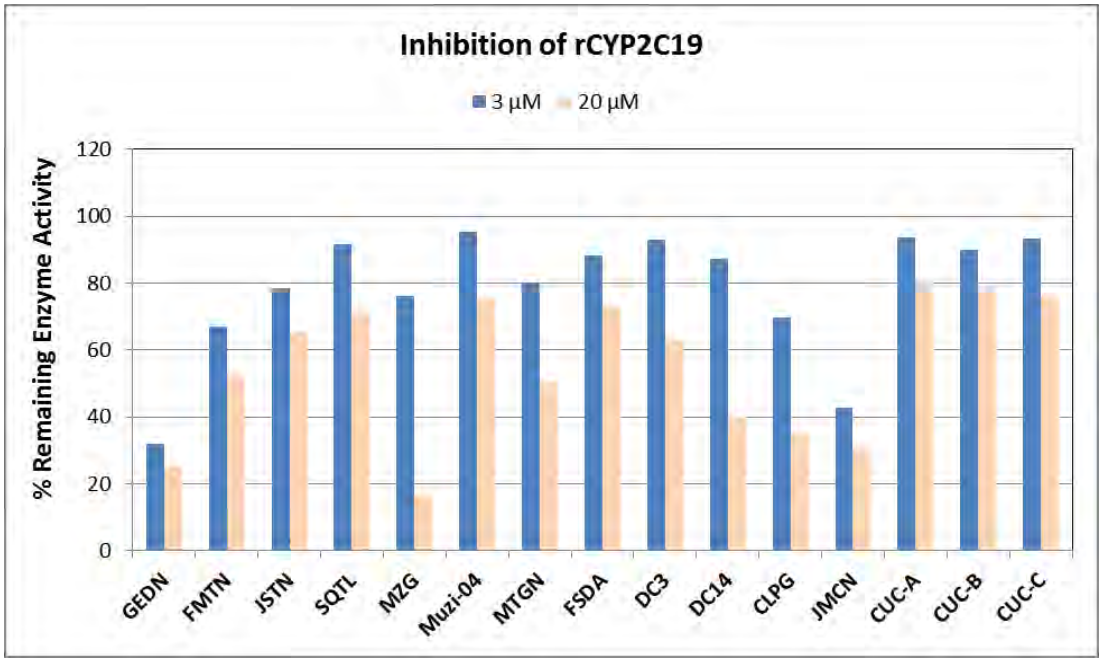

Figure 3.3: rCYP2C19 inhibition assay results (Substrate: MFC 35 µM)

GEDN and **JMCN** were the only compounds observed to inhibit rCYP2C19 to a significant degree at the lower assay concentration. Both reduced enzyme activity to less than 50% at 3 µM with **GEDN** being the more potent inhibitor. None of the remaining compounds reduced enzyme activity to below 50% although all fifteen appeared to exert greater inhibition at 20 µM in a manner largely proportional to activity at the lower concentration. The most notable exception to this behaviour was **MZG** - which at 3 µM only appeared to cause less than 25% inhibition of enzymatic activity, but was the most potent inhibitor at the higher assay concentration, reducing activity to less than 20%. As observed with rCYP2C19, such inhibitory activity was markedly absent in the semi-synthetic derivative **Muzi-04**.

The cucurbitacin compounds were, as seen with rCYP1A2 and rCYP2C9, noted to possess very little, if any, inhibitory activity against this isoform, even when assayed at 20 µM.

3.5.1.4 Inhibition of CYP3A4

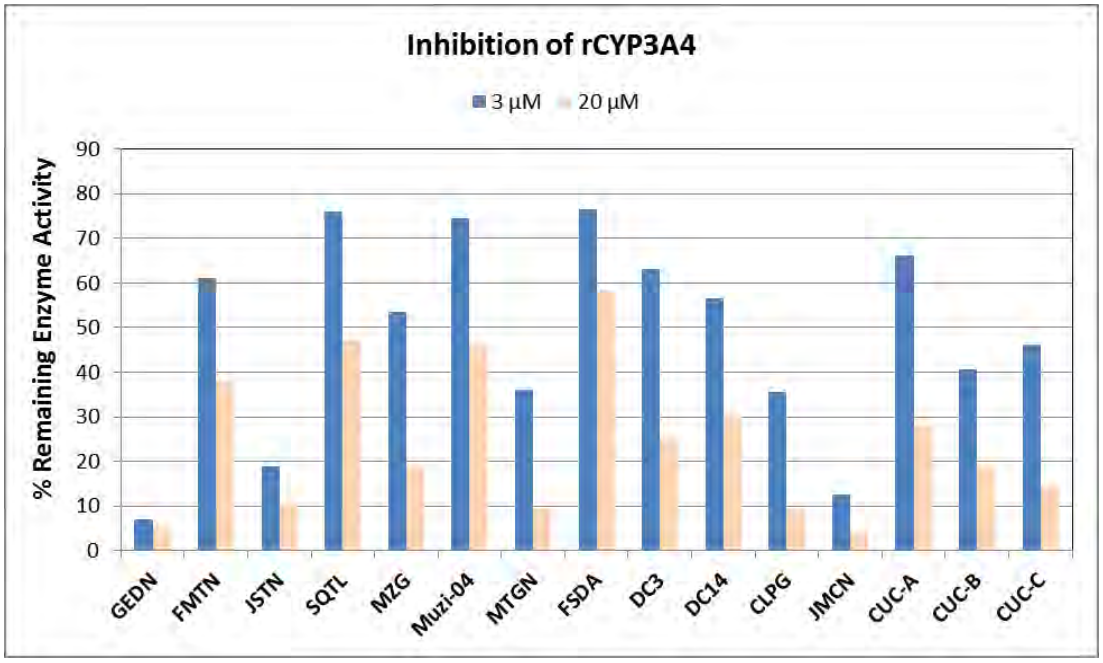

Figure 3.4: rCYP3A4 Inhibition Assay Results (Substrate: BFC 400 µM)

Of the CYP450 isoforms tested, rCYP3A4 appeared to be the most susceptible to inhibition by the test compounds. All fifteen compounds exhibited concentration dependent inhibition of this isoform, with greater inhibition of the enzyme at 20 µM compared to 3 µM. Seven (7) of the compounds reduced enzyme activity by more than 50% even at the lower assay concentration of 3 µM while only in the presence of **FSDA** at 20 µM was rCYP3A4 activity above 50% retained. **GEDN**, **JSTN**, **MTGN**, **CLPG** and **JMCN** were the most potent inhibitors, each being noted to inhibit enzyme activity by more than 60% at 3 µM.

Although the cucurbitacins were very closely related structurally, and appeared to be uniformly devoid of inhibition against the other CYP450 isoforms tested, they were noted to possess different inhibitory profiles against rCYP3A4. Against this enzyme, **CUC-B** and **CUC-C** were appreciably more potent inhibitors compared to **CUC-A**, which was the only cucurbitacin that did not cause more than 50% enzyme inhibition at 3 µM. **MZG** was a moderate inhibitor of rCYP3A4 compared to its semi-synthetic derivative **Muzi-04** which was only weakly inhibitory at 3 µM. Overall, **GEDN**, **JMCN** and **JSTN**, in that order, appeared to be the most potent enzyme inhibitors.

3.5.2 Time Dependent CYP3A4 Inhibition

Time dependent inhibition (TDI) assays were performed to determine whether inhibition of rCYP3A4 was due to reactive metabolic intermediates of the test compounds resulting in mechanism based inhibition of this isoform. This enzyme was selected for TDI assays because it is the single most abundant and important CYP450 isoform involved in drug metabolism *in vivo* and also due to the fact that it appeared to be the most susceptible to inhibition by the test compounds.

The TDI assay was performed by incubating test compounds in recombinant enzyme, in both the absence and presence of co-factor (NADPH) for a defined duration before re-incubating the test preparation in the presence of the fluorogenic substrate of the enzyme to determine the latter's subsequent metabolism. If the test compound is a TDI, the pre-incubation is necessary to provide the enzyme adequate time to metabolize the compound. Presence of NADPH is a mandatory prerequisite for enzymatic metabolism. If the test compound is metabolized into chemically reactive species that in turn inactivate the metabolizing enzyme, this is detectable as a measurable decline in the fluorescence from metabolism of the fluorogenic marker substrate in the second incubation. If the test compound is not a TDI, the difference in the metabolism of the marker substrate in the test and control incubations is negligible and can be quantified by calculating normalized inhibition ratios.

In running the TDI assays, 2 known inhibitors of CYP3A4 were used as controls. Ketoconazole (KTZ) is a non-TDI compound (i.e. inhibits the activity of CYP3A4 but not irreversibly) and was therefore used as the negative control. Troleandomycin (TAO) is an irreversible inhibitor of the enzyme and acted as the positive control.

Test compounds were incubated in duplicate at concentrations of 1 µM and 5 µM.

From the measured fluorescence values, the normalized enzyme inhibition ratios of the test compounds were calculated using the equation shown below and results interpreted according to the criteria outlined by Thelingwani *et al.* [67]

$$\text{Normalized Ratio} = \frac{(R+I^{+NADPH})/(R-I^{+NADPH})}{(R+I^{-NADPH})/(R-I^{-NADPH})}$$

where $R + I^{+NADPH}$ is the rate of reaction in the presence of both inhibitor and NADPH,
$R - I^{+NADPH}$ is the rate of reaction in the presence of NADPH but in the absence of inhibitor,
$R+ I^{-NADPH}$ is the rate of reaction in the presence of inhibitor but in the absence of NADPH,
$R - I^{-NADPH}$ is the rate of reaction in the absence of both inhibitor and NADPH

Compounds that gave normalized ratios greater than 0.9 were considered non-TDI, those between 0.7 and 0.9 were border-line while values less than 0.7 were considered to be a good indication of TDI activity.

The results of the rCYP3A4 TDI assay using the three most potent inhibitors of the enzyme isoform (**GEDN, JSTN, JMCN**), **CUC-B** as representative of the cucurbitacins, and the control drugs ketoconazole (KTZ) and troleandomycin (TAO) are illustrated in **Figure 3.5** below.

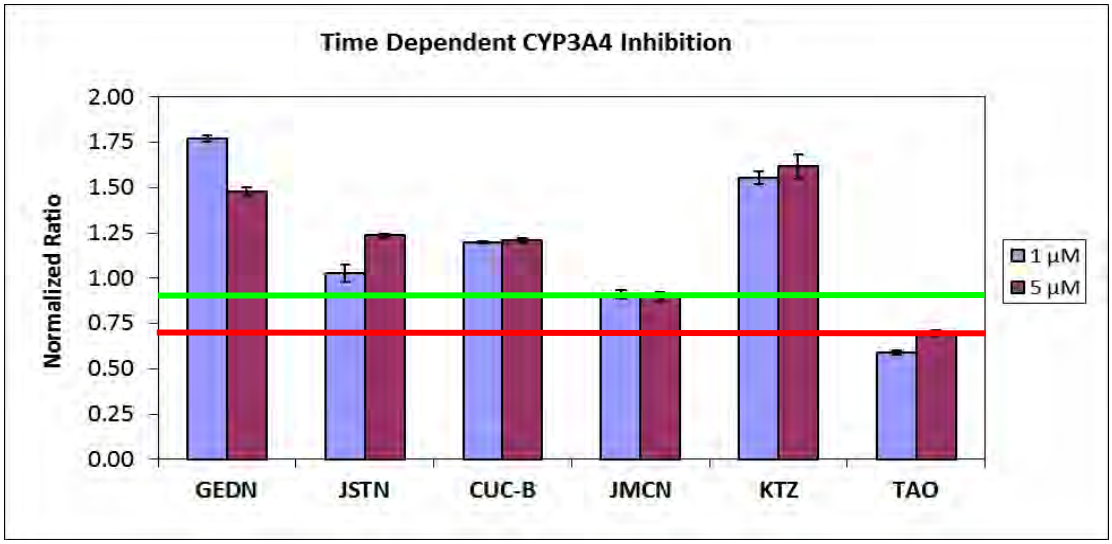

Figure 3.5: Normalized ratios of rCYP3A4 inhibitors for determination of TDI

Although all four test compounds had been observed to strongly inhibit rCYP3A4, their calculated normalized inhibition ratios at both assay concentrations were greater than 0.7, suggesting that enzyme inhibition activity was not mechanism based. For **JMCN**, the normalized ratios were calculated to be 0.91 and 0.90 at 1 µM and 5 µM, respectively. These values, by virtue of falling within the borderline region indicated that the possibility of **JMCN** being a mechanism-based rCYP3A4 inhibitor could not be entirely ruled out.

3.5.3 Glutathione-Fortified rCYP3A4 Inhibition Assay

The effect of incorporating reduced glutathione to the rCYP3A4 enzyme inhibition incubations was investigated by modifying the experimental protocol to include the endogenous redox scavenger. The four compounds tested for time dependent

inhibition of the enzyme were evaluated once more using this strategy in the presence of 1 mM reduced L-glutathione (**Figure 3.6**).

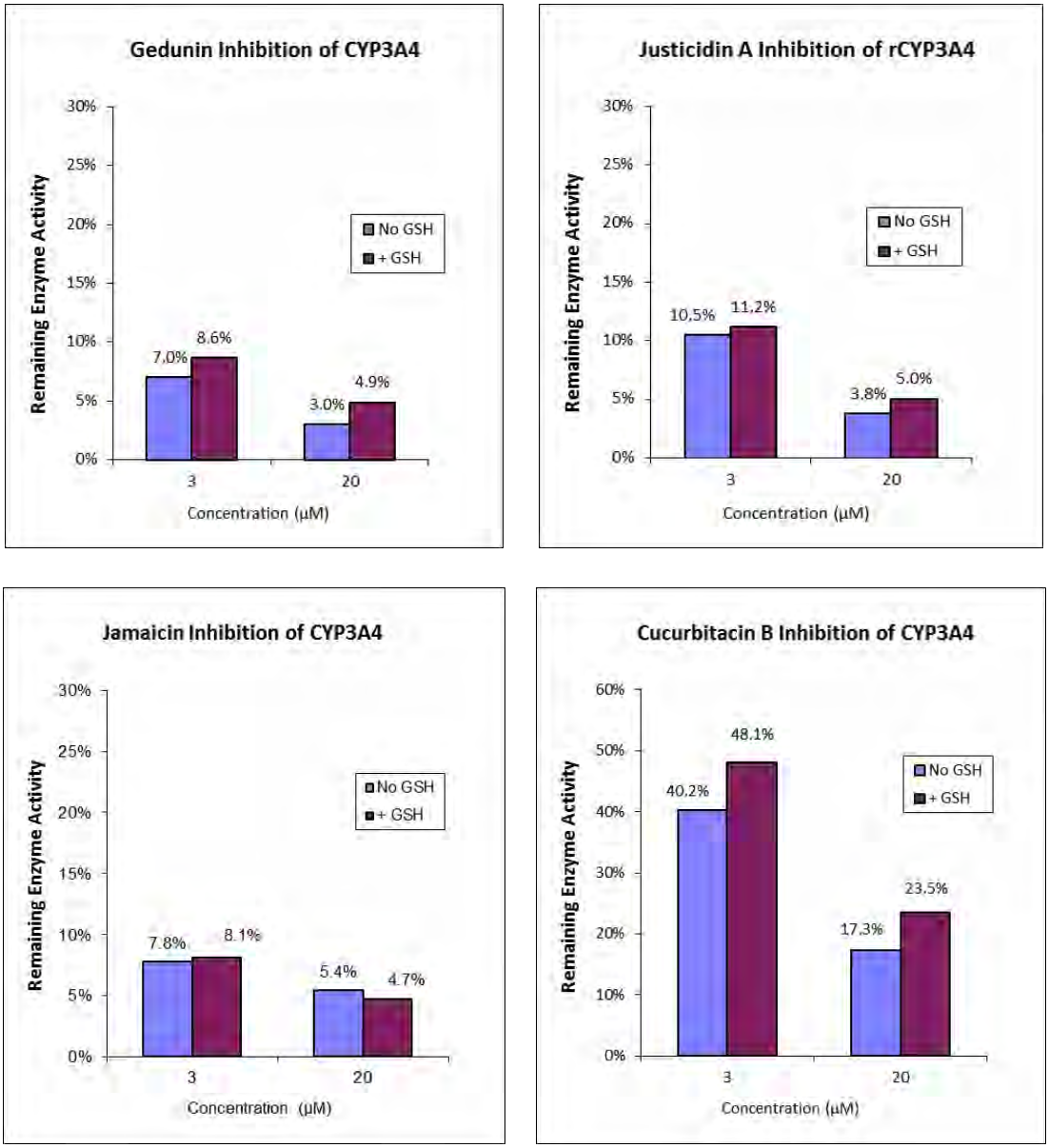

Figure 3.6: Effect of glutathione on inhibition of rCYP3A4 by selected natural products

Glutathione appeared to have little influence on the inhibition of rCYP3A4 by **GEDN**, **JSTN** and **JMCN** in which incubations the remaining enzyme activity only increased by less than 2%, which was not considered to be significantly higher than the experimental error. In the case of **CUC-B**, however, the presence of glutathione appeared to have a more noticeable effect in reducing enzyme inhibition, increasing residual enzyme activity by approximately 8% and 6% at 3 μM and 20 μM inhibitor concentrations respectively.

This observation seemed to contradict the conclusion based on TDI data that showed **CUC-B** not to be an irreversible, time dependent inhibitor of rCYP3A4. On the other hand, the data from this assay for the other compounds supported the observations made from the TDI experiment that neither **GEDN**, **JSTN** nor **JMCN** seemed to form reactive metabolites that inhibited rCYP3A4.

In order to establish more conclusively which of the test compounds screened for enzyme inhibition might act via formation of reactive metabolic intermediates, more comprehensive reactive metabolite trapping experiments were performed next.

3.6 Reactive Metabolite Trapping Experiments

In vitro reactive metabolite trapping experiments were conducted based on adopted assay protocols reported in the literature.[68,69] The general procedure involved incubating test compounds at concentrations of 10 µM in aqueous phosphate buffer (pH 7.4) in the presence of hepatic microsomes and nucleophilic trapping agents. Metabolic reactions were initiated by the addition of NADPH and maintained at 37°C for 60 minutes then terminated by adding ice-cold acetonitrile. Sample preparation involved centrifugation of the quenched reaction mixture to separate precipitated microsomal proteins, followed by filtration of the resultant supernatant solution and analysis by LC-MS. For every trapping experiment, various controls in which either the test compound, trapping agent, NADPH or microsomes was excluded from the reaction were also incubated to aid in data interpretation.

Prepared samples were analysed using reversed-phase HPLC coupled to mass spectrometry. Mass spectrometer ionisation and detection parameters for each test compound were manually optimised following direct infusion of the compounds using a syringe pump. Compound detection was carried out following ionisation using either electro-spray ionisation (ESI) as the preferred mode or, in a few instances, atmospheric pressure chemical ionisation (APCI).

The following MS detection modes were used to analyse the incubation samples for trapped reactive metabolite adducts:

i. Enhanced mass spectrum (EMS) scans in either or both positive and negative ionisation mode were the primary detection modes employed. The range of *m/z* values scanned was typically 150 – 900 and facilitated the scanning of full mass spectra on LC eluent samples using the increased sensitivity on the incorporated linear ion trap present in the mass spectrometer used.

ii. Information dependent acquisition enhanced product ion scans (IDA EPI) were used to automatically detect and obtain mass fragmentation data of the most intense peaks observed from the initial EMS scans. By directly coupling this detection mode to the EMS scans, the need to rerun samples to obtain mass spectral fragmentation data was eliminated.

iii. Constant neutral loss (CNL) scans were used to detect reactive metabolite adducts of trapping reagents known to undergo characteristic fragmentation by losing neutral fragments having specific *m/z* values.

iv. Precursor ion scans were used as an optional confirmatory detection mode to determine the presence of glutathione trapped reactive metabolites which are often observed to undergo collision-induced dissociation to yield fragment ions having *m/z* 272.09 in negative ion mode.

3.6.1 Trapping Reactive Metabolites Using Cyanide

Cyclic tertiary amines are principally metabolized by CYP450 or monoamine oxidase (MAO) enzymes via α-carbon oxidation that generates the corresponding endocyclic iminium ion. Alternatively, these compounds may also undergo oxidative *N*-dealkylation via oxidation to the exocyclic iminium ion intermediate that is subsequently hydrolysed to form the corresponding secondary amine and an aldehyde. Unlike the exocyclic iminium ion intermediate, hydrolysis of the endocyclic iminium ion to the corresponding aminoaldehyde is reversible, allowing possible further metabolic processing of the former. Whereas the iminium ion intermediates of aliphatic tertiary amines are in equilibrium with carbinolamines that dissociate to aldehyde and secondary amine (i.e. via the *N*-dealkylation metabolic pathway), carbinolamine dissociation remains reversible for cyclic tertiary amines, increasing the effective lifetime of the iminium ion species. Endocyclic iminium ion intermediates are often oxidized by hepatic aldehyde oxidase to the biologically less active lactams. If special structural features are present in the substrate molecule or if the cyclic iminium ion intermediate is generated in extrahepatic tissue lacking aldehyde oxidase, these reactive intermediates may undergo alternative chemical transformations that can produce toxic products (**Figure 3.7**).[70]

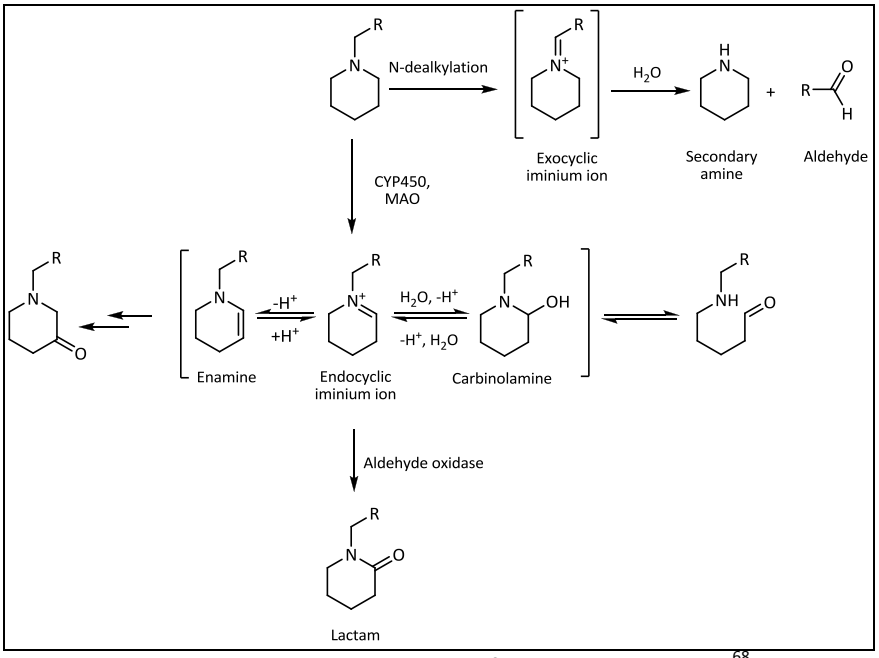

Figure 3.7: Metabolic pathways of cyclic tertiary amines[68]

Iminium ions are 'hard' electrophiles that cannot be effectively trapped using soft nucleophiles such as glutathione. Instead, *in vitro* trapping experiments make use of cyanide ions as the preferred trapping agent. In this reaction, it is hypothesized that the endocyclic iminium ions undergo reversible conversion to their corresponding cyclic α-carbocations which subsequently undergo nucleophilic attack by the cyanide anion to form stable cyano adducts (**Figure 3.8**). On LC-MS, successful cyanide trapping is evidenced by presence of substrate peaks having a net mass gain of +25 Da corresponding to initial loss of hydrogen to form the iminium and carbocation, followed by addition of the cyanide ion (i.e. -1 then +26 Da). Following collision-induced fragmentation of the cyanide adducts, the cyano group is relatively easily lost as hydrogen cyanide (*m/z* 27 Da). This characteristic can be used to confirm the presence of cyanide trapped intermediates by combining constant neutral loss scans in positive ion mode to detect the loss of the 27 Da and the EMS scans used to detect the intact cyano adduct.

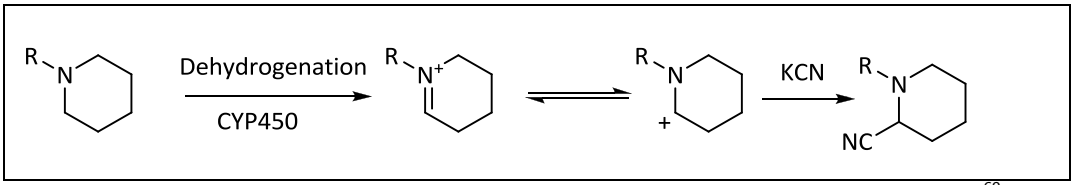

Figure 3.8: Bioactivation of tertiary cyclic amine to iminium ion and trapping using KCN[69]

The drug rimonabant was used as a positive control to confirm that reactive iminium intermediates could be trapped and detected using LC-MS as reported in the literature.[68] Rimonabant was incubated in both human (HLM) and rat liver microsomes (RLM) fortified with KCN to capture the iminium ion arising from suspected bioactivation of the tertiary N-atom in the piperidine ring (**Figure 3.9**).

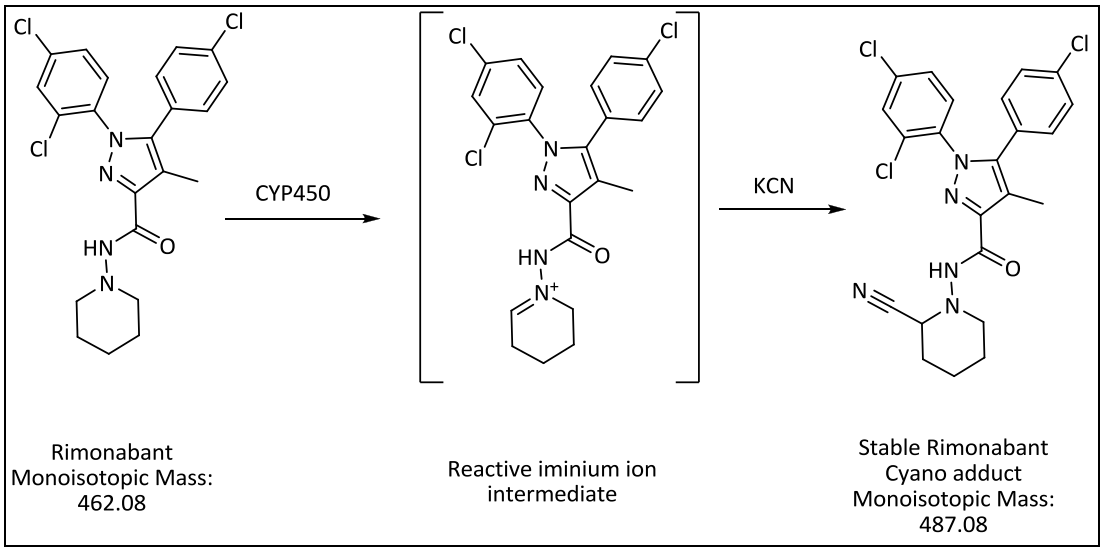

Figure 3.9: Hypothesized bioactivation of rimonabant and subsequent trapping of reactive intermediate using KCN

In the RLM test incubation (**Figure 3.10 and 3.11**), extracted ion chromatograms (XIC) from the LC-MS EMS data generated clearly showed the presence of two distinct adduct peaks corresponding to mass shifts of +25 and +41 greater than the *m/z* value of the parent rimonabant (MH^+ 463.1) and both eluting before the parent compound.

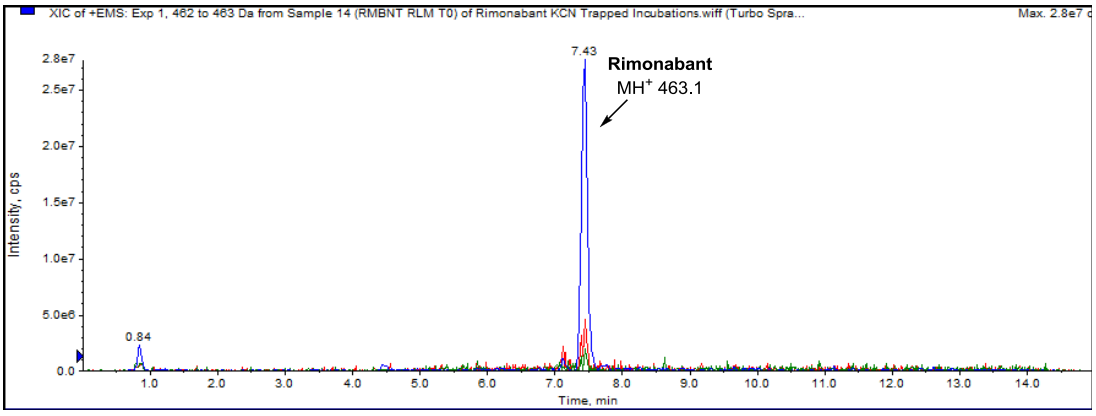

Figure 3.10: XIC of T0 rimonabant incubation in presence of RLM fortified with KCN. As expected, no obvious degradation or metabolite peaks are observed in this incubation which illustrates compounds present at the start of the trapping experiment.

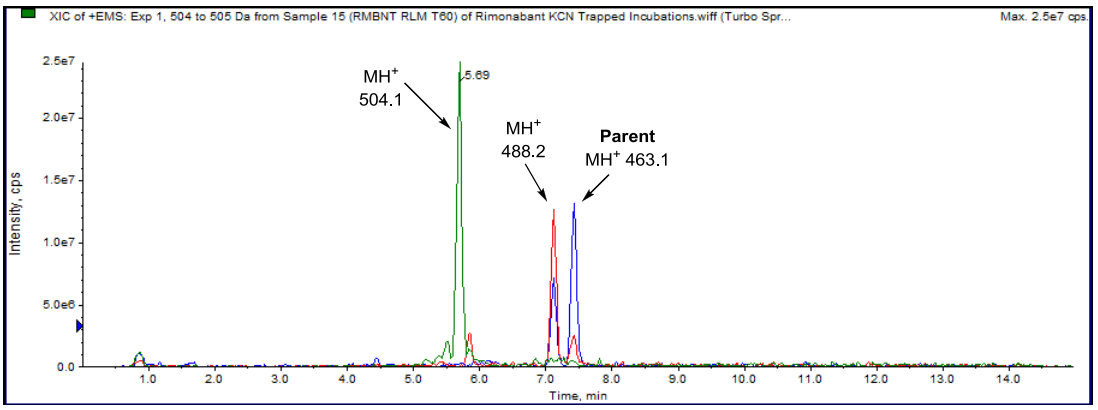

Figure 3.11: XIC of rimonabant incubation in presence of RLM fortified with KCN after 60 min (T60) indicating presence of two suspected cyanide adduct peaks

The peak having *m/z* 488.2 was suspected to be the direct cyanide adduct of the parent, especially since its fragmentation pattern was identical to that of rimonabant with the sole exception of a mass spectral signal corresponding to the protonated molecular ion at 488.2 not present in the parent. The peak with *m/z* 504.1 was suspected to be the cyanide adduct of the oxidized rimonabant resulting in the net mass gain of +41 (i.e. +16 then +25).

In the HLM incubations, only the adduct peak corresponding to *m/z* 488.2 was detected, with no sign of the (suspected) oxidized rimonabant cyanide peak (**Figure 3.12**). This variance was attributed to differences in the CYP450 composition of the HLM and RLM enzyme systems and suggested that perhaps rimonabant is preferably metabolized to reactive intermediates by an isoform of the CYPs that is more abundant/active in RLMs compared to HLMs.

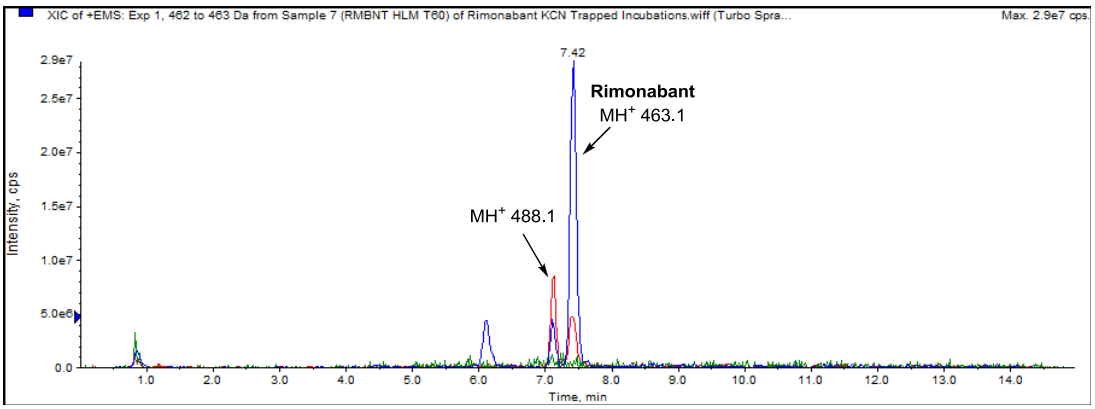

Figure 3.12: XIC of rimonabant incubation in HLM fortified with KCN after 60 min indicating presence of single suspected cyanide adduct peak (MH^+*m/z* 488.1)

Further proof that the peak with *m/z* 488.2 was a cyanide adduct was provided by the fact that fragmentation of the compound afforded a distinct loss of 27 Da as

revealed from its enhanced product ion (EPI) spectrum, consistent with collision induced loss of neutral hydrogen cyanide (**Figure 3.13**).

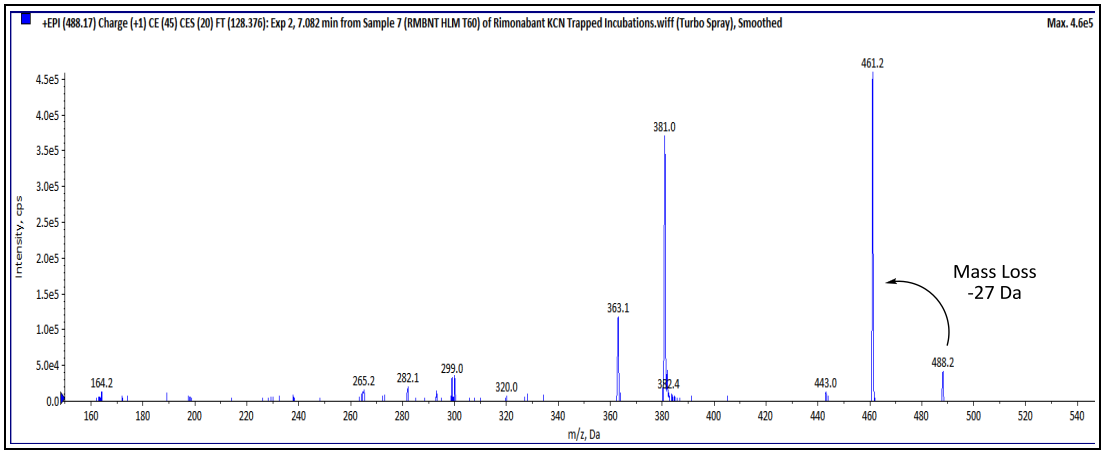

Figure 3.13: EPI spectrum of suspected cyanide-trapped reactive rimonabant metabolite showing fragmentation involving loss of 27 Da hydrogen cyanide molecule.

Metergoline was the only one of the test compounds that possessed a tertiary cyclic amine that could potentially undergo bioactivation to form a reactive iminium intermediate (**Figure 3.14**). The compound also contained a second structural alert in the form of a masked 3-methylindole moiety commonly implicated in the formation of reactive epoxide, iminium or quinone imine intermediates.[2] To trap potential reactive iminium metabolites, KCN fortified trapping incubations were carried out on metergoline as performed on rimonabant in both RLM and HLM.

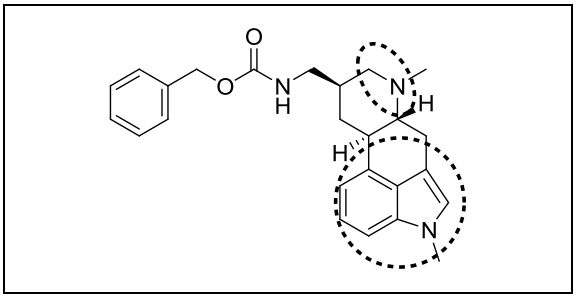

Figure 3.14: Metergoline with structural alerts circled

Contrary to the findings with rimonabant, incubation of metergoline in KCN fortified microsomes did not appear to result in the formation of cyanide trapped reactive metabolic intermediates. The 60 minute (T60) test incubation of metergoline in HLM+KCN revealed only the presence of the same compound/metabolite peaks as observed in the control incubation devoid of KCN (**Figure 3.15**).

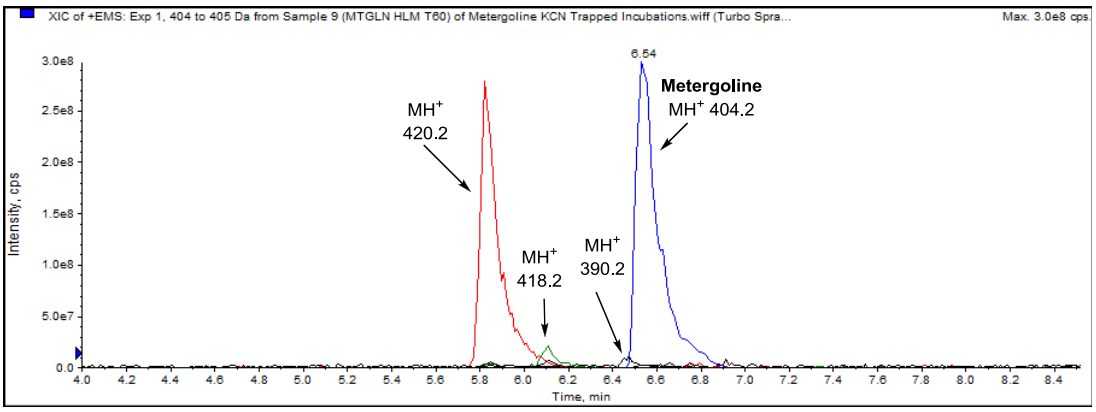

Figure 3.15: XIC of T60 incubation of metergoline in KCN fortified HLMs indicating presence of metabolite peaks but no obvious cyanide adducts.

The main peak observed at retention time 5.82 min had *m/z* 420.2 corresponding to a direct mono-oxidation of the parent (MH^+ 404.2) which eluted at 6.54 min. Two other peaks were observed and suspected to represent minor metabolites of metergoline at *m/z* 418.2 (Rt 6.11 min) corresponding to a direct mono-oxidation possibly resulting in formation of a keto-group, and *m/z* 390.2 (Rt 6.47 min) thought to represent an *N*-demethylated metabolite. No peak appeared to result from the parent metergoline or any of the observed metabolites gaining 25 Da.

3.6.2 Trapping Reactive Metabolites Using Glutathione

Reduced L-glutathione (GSH) is the most commonly used *in vitro* reactive metabolite trapping agent. Its utility is based on the fact that *in vivo* this endogenous tripeptide (γ-L-glutamyl-cysteinyl-glycine) serves as a potent scavenger of reactive electrophilic species and toxic free radicals and acts as a crucial substrate for detoxification reactions. In the body, glutathione exists in both its reduced and oxidized forms (**Figure 3.16**) with the former being predominant and present in virtually all tissues at fairly high concentrations especially in the liver (5 - 10 mM).[71]

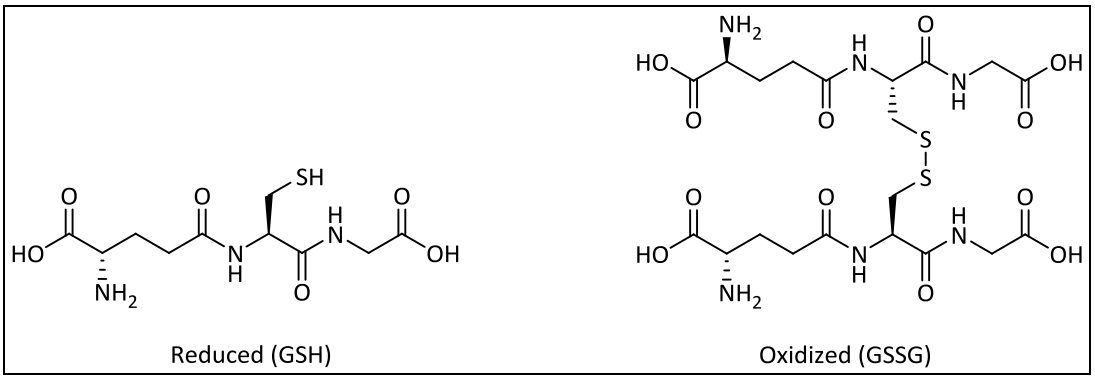

Figure 3.16: Reduced and oxidized forms of glutathione

Glutathione serves as a substrate for Phase II metabolic conjugations catalyzed by the enzyme glutathione-*S*-transferase. In addition, however, GSH readily forms conjugates with soft electrophilic species spontaneously even in the absence of the conjugating enzyme. In the body, such conjugates may be directly excreted into urine or bile, or undergo further biotransformation to recycle the amino acid residues glutamic acid and glycine before forming mercapturic acid metabolites of the original substrates which are then excreted (**Figure 3.17**).

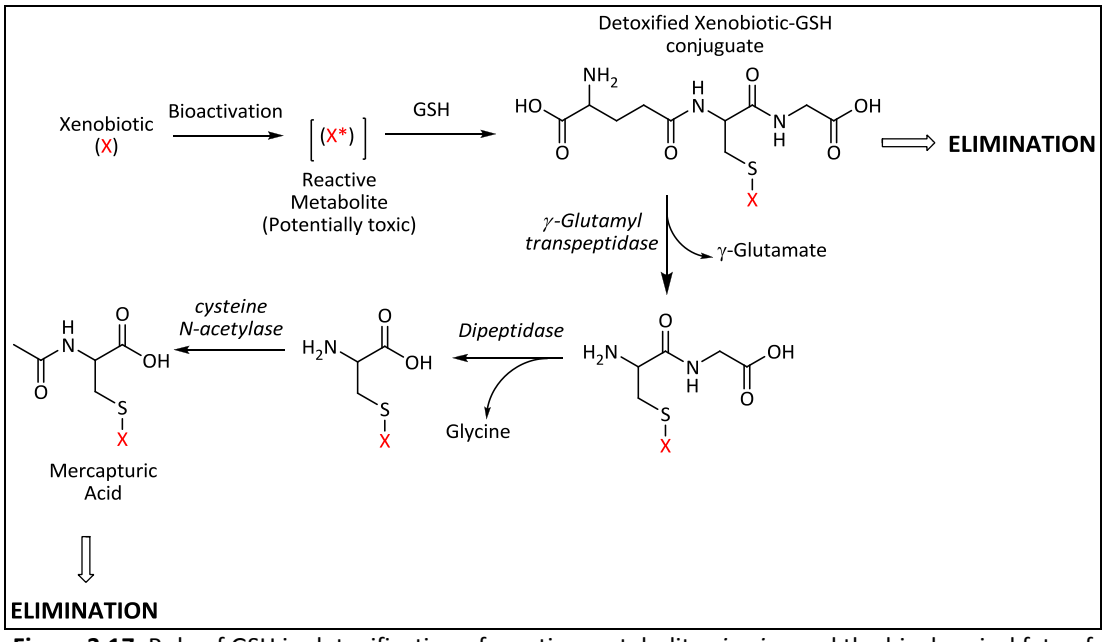

Figure 3.17: Role of GSH in detoxification of reactive metabolites *in vivo* and the biochemical fate of resultant GSH conjugates

GSH-fortified microsome *in vitro* trapping experiments were conducted on test compounds to determine if they might undergo bioactivation to 'soft' electrophilic reactive metabolites. As a positive control, the antimalarial drug amodiaquine was

used due to its reported bioactivation to a reactive quinone imine metabolite (**Figure 3.18**).[72]

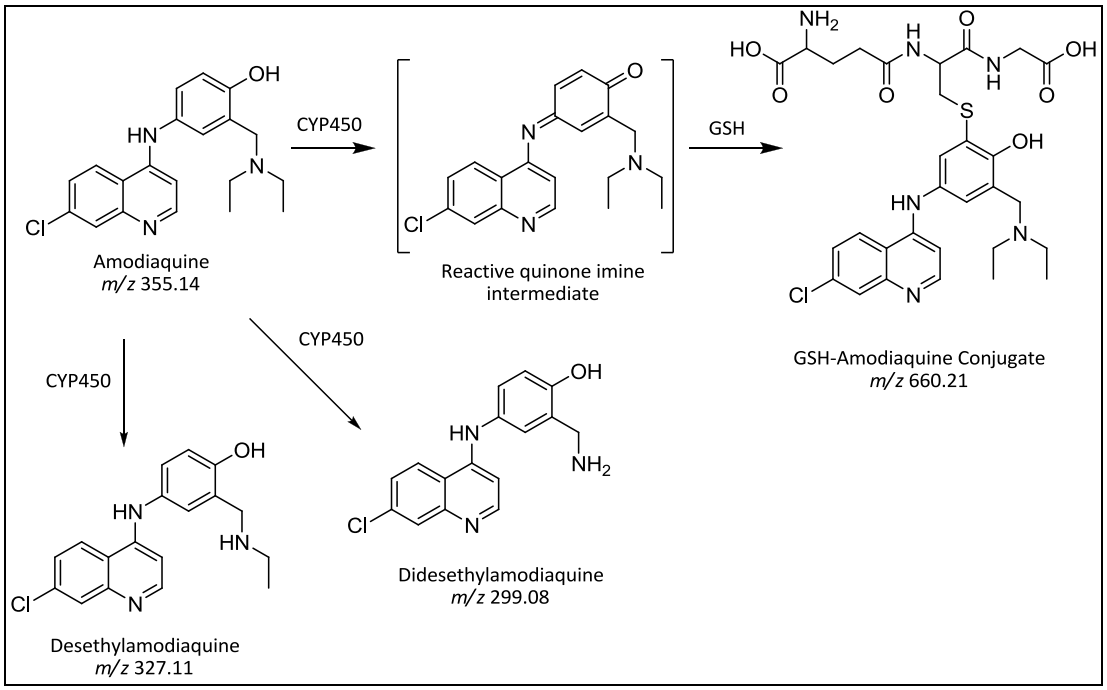

Figure 3.18: Major metabolites of amodiaquine and GSH trapping of reactive quinone imine intermediate

For LC-MS detection of GSH adducts, full survey EMS scans in either positive or negative modes were conducted as the primary detection mode and where necessary, followed by precursor ion scans for the parents of the m/z 272 Da fragment in –ve ion mode, for confirmation. In the EMS scans, direct GSH conjugates would be observed as substrate or metabolite peaks with a net mass gain of +305 Da (+/- H^+ depending on polarity). Loss of the 272 Da fragment - a characteristic of GSH adducts, would provide further confirmation of the presence of the conjugates.[73] Constant neutral loss scans for peaks that showed a loss of 129 Da in positive ion mode also provided alternative proof of the presence of glutathione adducts. The origin of these characteristic glutathione fragments is illustrated in **Figure 3.19**.

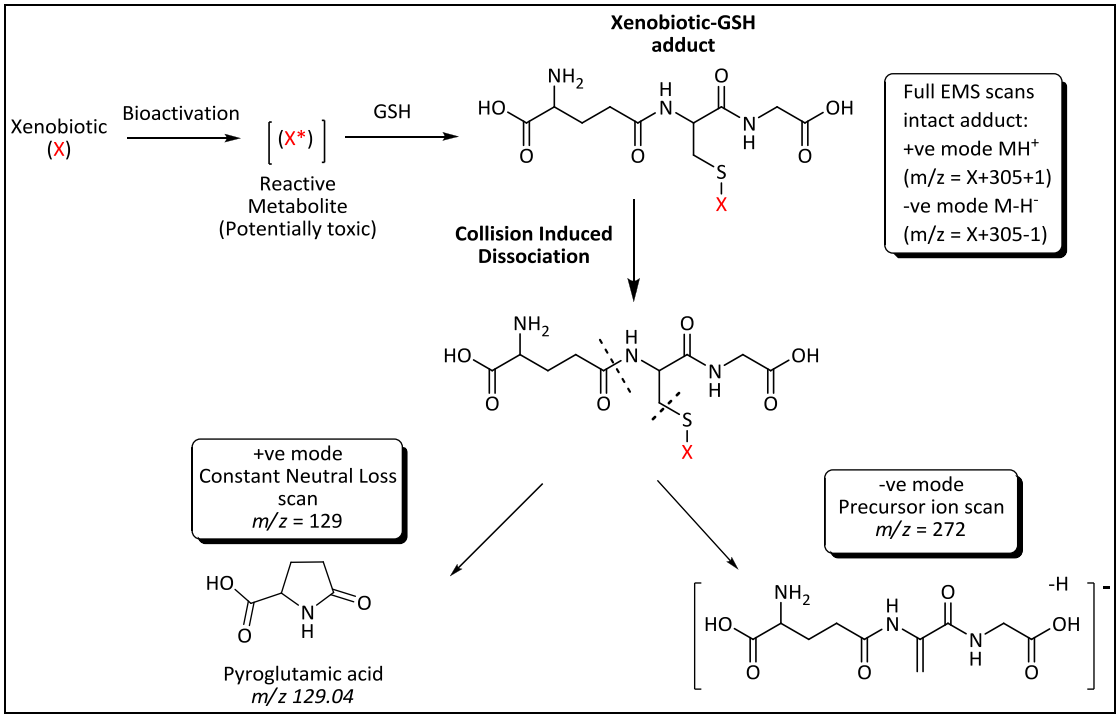

Figure 3.19: Detection of GSH adducts and characteristic fragments using different MS scanning modes

On the full survey EMS scans in both +ve and –ve ion mode, residual parent amodiaquine and its two main metabolites could be clearly observed as distinct peaks in the T60 incubation (**Figure 3.20**).

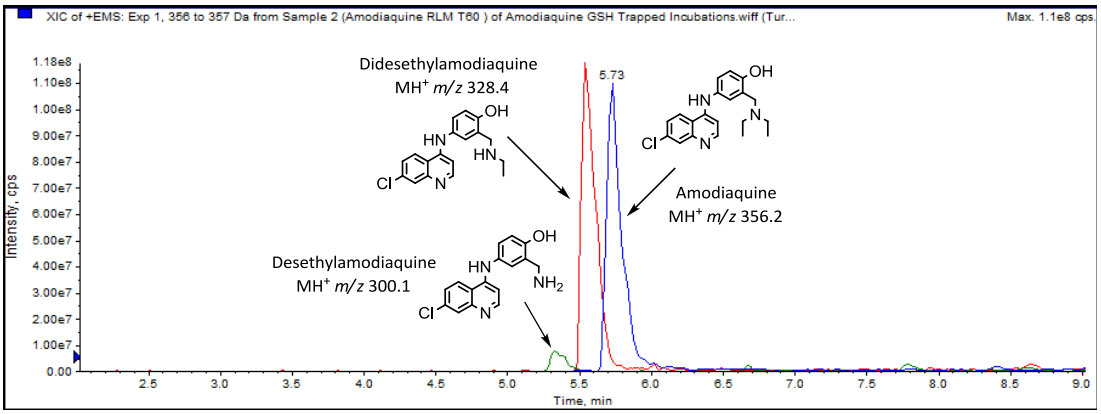

Figure 3.20: XIC +ve ion mode EMS of T60 aliquot of amodiaquine incubated with GSH fortified RLM

Whereas the expected amodiaquine-GSH conjugate was not observed in the +ve mode, it was distinctly visible in –ve ion mode at Rt 5.52 min albeit appearing to co-elute with the desethylamodiaquine peak (**Figure 3.21**).

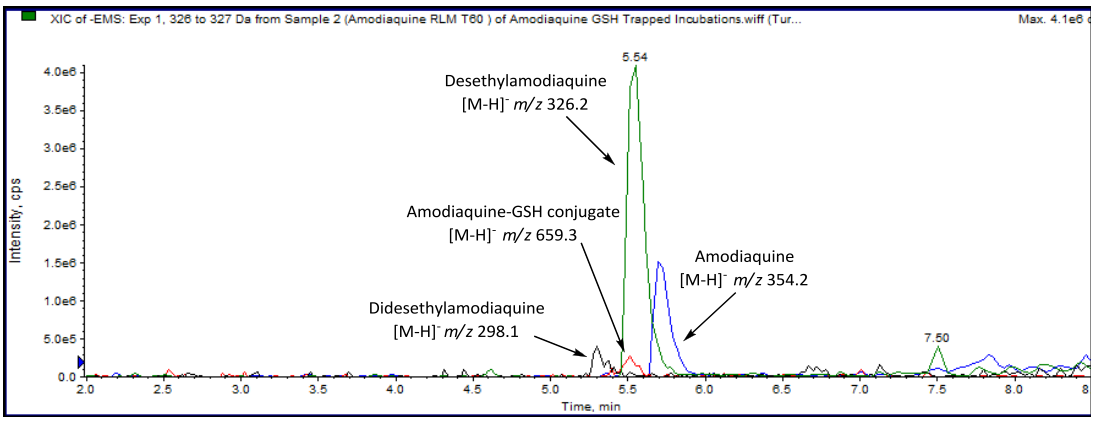

Figure 3.21: XIC of -ve mode EMS of T60 amodiaquine incubation in GSH fortified RLMs indicating presence of GSH-conjugate co-eluting with desethylamodiaquine

Further proof that the peak at Rt 5.52 min was most likely that of a GSH-trapped conjugate was provided by re-analyzing the sample and detecting using a precursor ion scan of the 272 Da fragment in –ve ion mode (**Figure 3.22**).

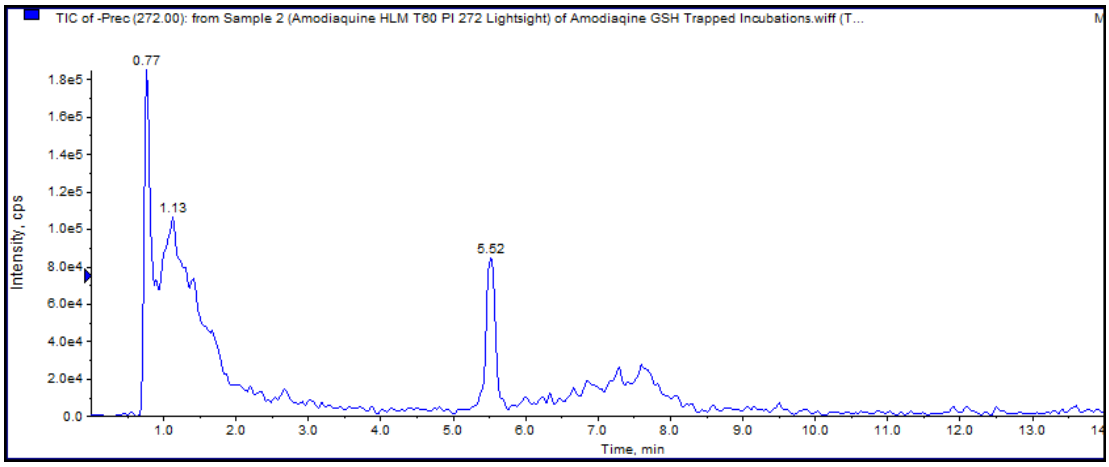

Figure 3.22: TIC of -ve ion mode precursor ion scan of *m/z* 272 Da fragment of T60 amodiaquine incubation in GSH fortified RLMs

Constant neutral loss scans to detect the loss of a neutral 129 Da pyroglutamic acid fragment characteristic of glutathione-conjugated substrates did not yield conclusive data. The LC-MS peaks generated in this scan mode had very low intensity and could not be well distinguished from the baseline. By contrast, the PI scans in -ve ion mode were noted to have less noisy baseline signals owing to the fact that few compounds would be expected to form negatively charged ions under the analysis conditions used. Based on the observations from amodiaquine incubations, LC-MS detection for the subsequent test compounds for reactive metabolite trapping using GSH was conducted using +ve and/or –ve mode EMS scans followed by –ve mode PI scans for the *m/z* 272 fragment or +ve mode CNL scans of *m/z* 129.

Eleven compounds were incubated in human liver microsomes (mixed gender, pooled from 50 individuals) to determine their bioactivation to reactive metabolites and subsequent trapping with glutathione. The general incubation and LC-MS detection strategy employed with amodiaquine was used to analyze the incubation samples. A summary of the main diagnostic peaks detected for each sample with their corresponding m/z values and the conclusion drawn from LC-MS data is outlined in **Table 3.2**.

Table 3.2: Main diagnostic LC-MS peaks observed to determine presence of GSH trapped reactive metabolites

	Monoisotopic mass	**Detection mode: Main Peaks (*m/z*)**	**Comment**
Gedunin	482.23	ESI+: 483.2	No GSH-adduct observed
Metergoline	403.23	ESI+: 404.2; 420.2; 418.2; 390.2	No GSH-adduct observed
DC3	352.22	ESI+: 353.3	No GSH-adduct observed
DC14	316.20	ESI+: 317.1	No GSH-adduct observed
Justicidin A	394.11	ESI+: 394.8	No GSH-adduct observed
Jamaicin	378.11	ESI+: 379.6	No GSH-adduct observed
SQTL	244.11	ESI+: 245.2	(See below)
CLPG	334.12	ESI+: 335.8	No GSH-adduct observed
Formononetin	268.07	ESI-: 266.8	No GSH-adduct observed
Fusidic acid	516.35	ESI-: 515.3; 513.1	No GSH-adduct observed
Cuc-B	558.32	ESI+: 499.4; 866.3	(See below)
Muzigadial	248.14	-	(See below)
Muzi-04	305.17	-	(See below)

Although the tested compounds all possessed structural alerts that were anticipated to undergo bioactivation to reactive species, none appeared to form intermediates that could be detected as GSH conjugates using the LC-MS detection modes established using amodiaquine which was used as the positive control in all assays.

The results from incubations of **SQTL** and **CUC-B** were particularly interesting, however. Analysis of **SQTL** samples at the beginning of the incubation (**Figure 3.23**) clearly indicated the presence of the unmetabolized parent before addition of

NADPH to initiate the metabolic reaction as a peak eluting at Rt 6.88 min (ESI + MH^+ *m/z* 245.2).

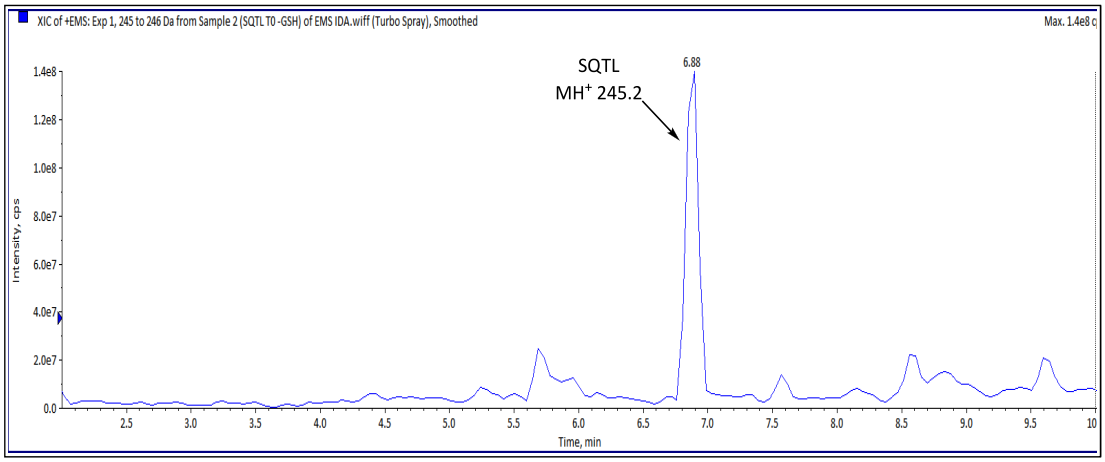

Figure 3.23: XIC of **SQTL** peak only observed in incubation preparations devoid of GSH but absent in all incubations in which GSH was present

The **SQTL** peak was, however, completely absent in all subsequent incubations to which GSH was present regardless of whether microsomes, NADPH or even acetonitrile had been added to quench the incubation beforehand. This phenomenon pointed towards the likelihood that **SQTL** was reactive enough even in its unmetabolized form to react with the trapping agent (GSH). The possibility that the **SQTL** peak disappeared owing to the compound being an unstable lactone that rapidly undergoes hydrolysis in aqueous medium was ruled out by the fact that scans to detect the hypothesized hydrolysis product were unsuccessful. Furthermore, when **SQTL** was incubated on its own in aqueous buffer devoid of microsomal proteins, NADPH or GSH for 90 minutes at 37 °C, the compound was easily detectable at virtually the same intensity as fresh solutions. However, although all the evidence pointed to a metabolism-independent reaction taking place between **SQTL** and GSH, the resultant product could not be detected on LC-MS.

In the case of **CUC-B**, all incubation preparations in which GSH was present appeared to form adducts corresponding to a direct reaction between the substrate and GSH. The reaction appeared to be independent of enzymatic involvement and took place even in the absence of microsomal proteins. Unlike the case with **SQTL**, the suspected GSH adduct peaks were easily detected on LC-MS EMS scans and fragmentation data from EPI scans confirmed the presence of fragments commonly associated with glutathione adducts.

Reactive metabolite trapping incubations of **MZG** and its derivative **Muzi-04** were not carried out owing to difficulties in optimising LC-MS detection parameters to attain the sensitivity required to detect trapped intermediates. Despite these compounds being readily separated and observed using HPLC-DAD detection, the mass spectral signal remained very weak, despite attempts to optimise compound ionisation by systematically altering ion source conditions (temperature, declustering potential, polarity etc.) and ionisation mode i.e. both ESI and APCI attempted.

3.6.3 Trapping Reactive Metabolites Using Methoxylamine

Furan and mono-substituted furan ring-containing xenobiotics are known to undergo bioactivation catalyzed by CYP450 enzymes resulting in opening up of the aromatic ring to form highly reactive aldehyde intermediates. Proposed mechanisms for this bioactivation hypothesize that ring opening is preceded by the formation of an epoxide intermediate. The final products of the bioactivation are dependent upon the substitutions on the parent furan ring. Substitutions at position 2 of the ring may result in formation of a γ-keto-α-β unsaturated aldehyde whereas unsubstituted and 3-subsituted furans may form the corresponding highly reactive enedial metabolite (**Figure 3.24**).

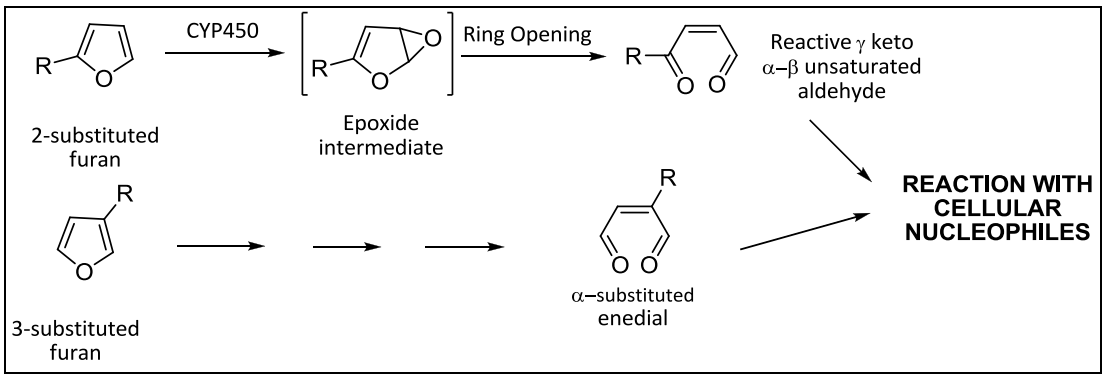

Figure 3.24: Proposed bioactivation of furan containing compounds to aldehyde intermediates

Aldehydes, like iminium ions, are 'hard' electrophiles that cannot be reliably trapped using glutathione. GSH, as a soft nucleophile may, however, be capable of trapping the α-β unsaturated groups by conjugating via substitution at the unsaturated β-carbon of the aldehyde or enedial. More reliable trapping agents for aldehyde reactive intermediates are available in the form of methoxylamine, as illustrated in **Figure 3.25**, and semicarbazide.[74]

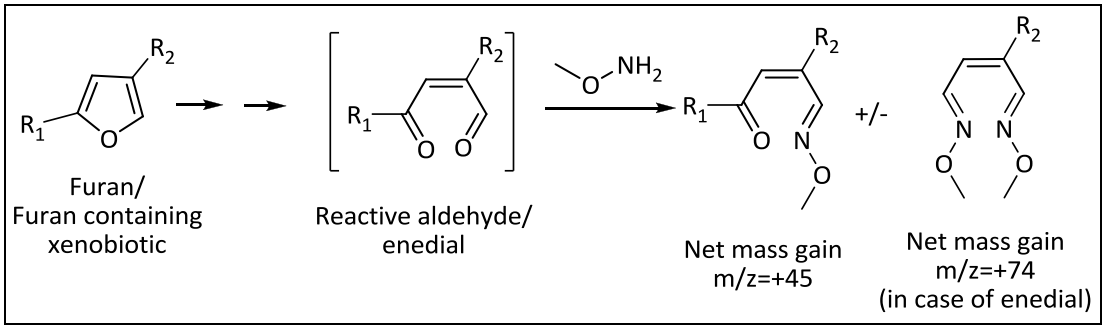

Figure 3.25: Trapping furan-derived aldehyde reactive intermediates using methoxylamine

Prazosin was used as the positive control to demonstrate bioactivation and detectable trapping of aldehyde intermediate thus formed using methoxylamine. The reported bioactivation of the furan ring in prazosin and its subsequent trapping is illustrated in **Figure 3.26**.

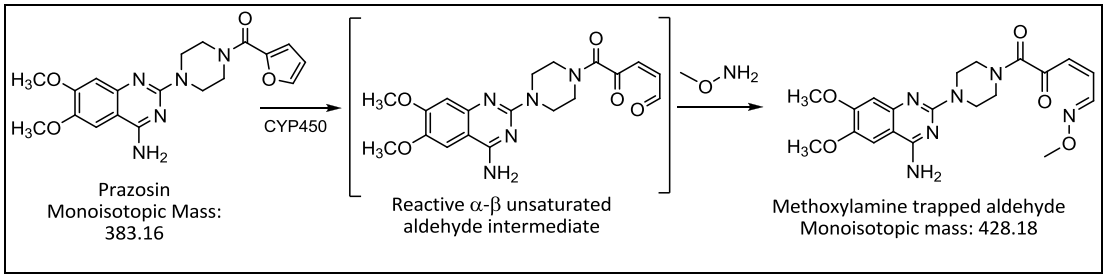

Figure 3.26: Bioactivation of furan ring in prazosin and trapping of aldehyde intermediate using methoxylamine

On LC-MS analysis of the incubation samples, successful trapping of the reactive aldehyde intermediates would be suspected from the presence of peaks corresponding to test substrates with a net mass gain of +45 or +74 on the EMS scans. These shifts in mass values were due to the initial oxidation of the furan ring to first form the short-lived epoxide and subsequently the ring opened aldehyde susceptible to methoxylamine addition that formed the *O*-methyl oxime species detected.

The test incubations of prazosin containing pooled, mixed gender human or male rat liver microsomes, cofactor and trapping agent (methoxylamine) indicated the presence of a peak with the +45 mass gain not present in any of the control incubations in which one of these components was absent. Additionally, +ve mode EMS XICs revealed the presence of known metabolites of prazosin as reported in literature in the test incubation as well as in control incubation in which only trapping agent was absent (**Figure 3.27** and **3.28**).[75]

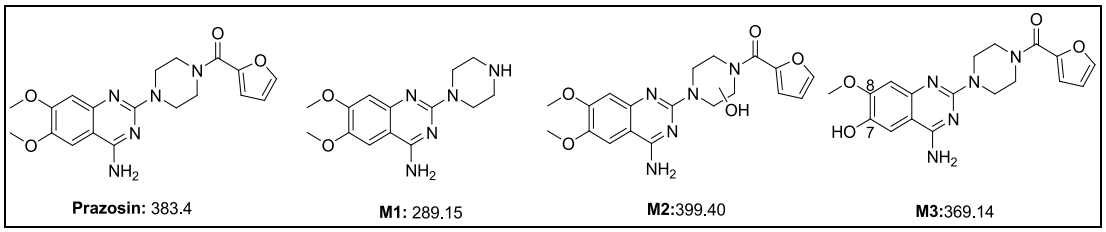

Figure 3.27: Prazosin and some of its known metabolites detected from trapping incubations

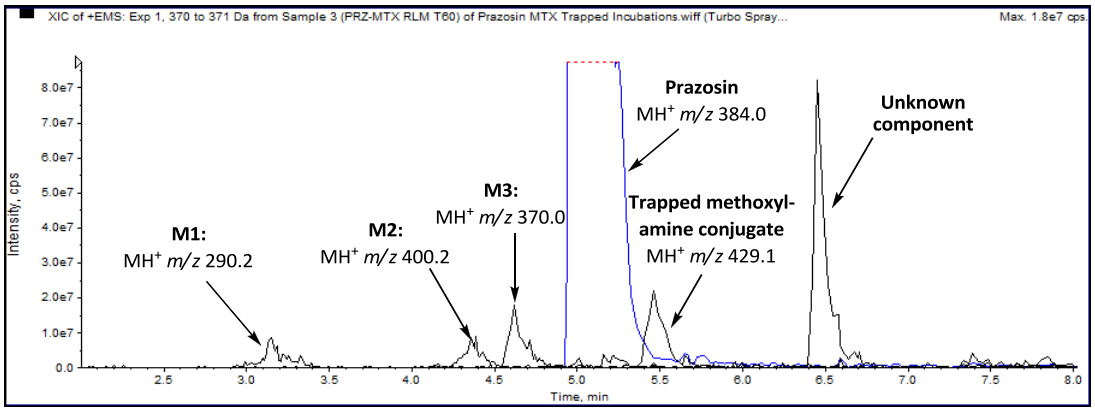

Figure 3.28: XIC of +ve ion mode EMS of T60 incubation of prazosin in methoxylamine fortified RLM. The peak labeled 'unknown component' was unrelated to prazosin and present in all the incubation preparations

Only the three compounds previously incubated with GSH containing furan rings in their structures (i.e. **GEDN**, **DC3** and **DC14**) were further tested for reactive aldehyde metabolic intermediate trapping using methoxylamine. Evidence of successful trapping of the aldehyde from furan ring bioactivation was provided by +ve mode EMS scans which showed peaks having the expected mass shifts of +45 or +74. Fragmentation of such components, if present, on subsequent EPI scans to lose 32 Da from the loss of neutral methanol molecule from the *O*-methyl oxime portion of the trapped adduct was considered further proof of successful trapping.

Chromatograms of T60 test incubations of **GEDN** indicated two peaks (Rt 7.36 min and 8.46 min) with a mass gain of +45 and one with a shift of +74 (Rt 9.00 min)from the parent (Rt 8.57 min) but absent in the control incubations. Of the two *m/z* +45 peaks, only the later eluting component at 8.46 min was intense enough to allow for controlled fragmentation and indicated the loss of a 32 Da fragment, strongly suggesting that it might represent a methoxylamine trapped aldehyde (**Figure 3.29** and **Figure 3.30**).

The peak suspected to represent a di-methoxylamine substituted adduct could not be confirmed to be such due to its low intensity and the fact that it appeared to co-elute with a much more intense component (*m/z* 577) present as an artefact in all the incubated samples.

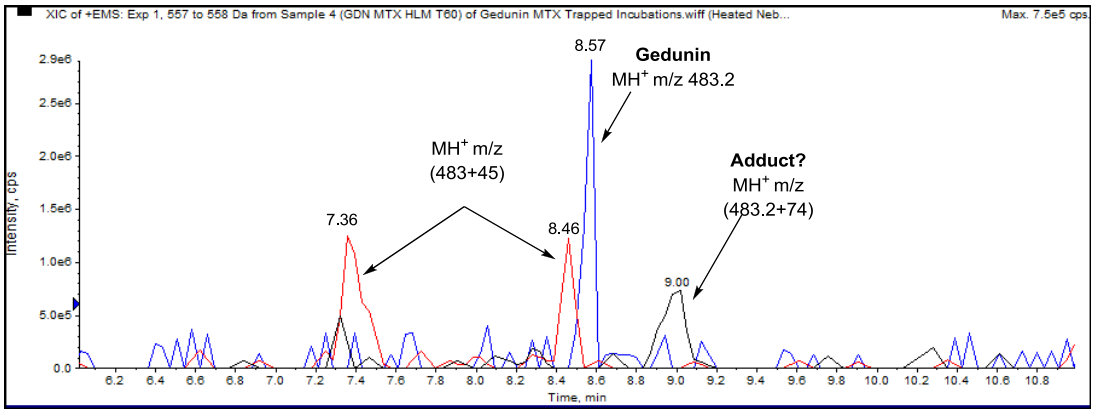

Figure 3.29: XICs of T60 **GEDN** incubation in methoxylamine fortified microsomes showing suspected trapped metabolites

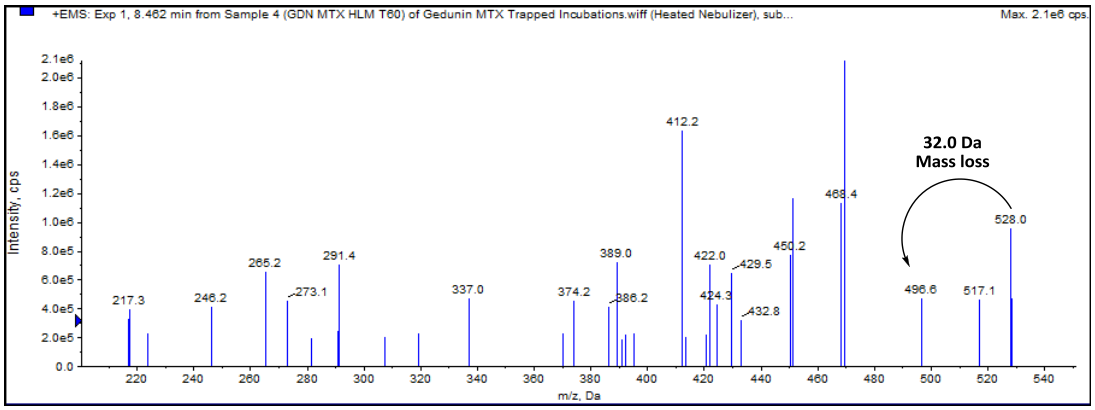

Figure 3.30: Enhanced mass spectrum of peak in T60 **GEDN** incubation eluting at 8.46 min showing loss of 32 Da fragment from suspected methoxylamine trapped metabolite (MH^+ *m/z* 528.0)

Compound **DC14** did not appear to form any reactive intermediates trapped using methoxylamine since no conjugate peaks on the EMS scans showed a *m/z* net gain of +45 or +74.

Compound **DC3** on the other hand appeared to be metabolized to a reactive intermediate trapped by methoxylamine and exhibited a very distinct *m/z* +45 adduct peak at Rt 5.34 min from the T60 incubation sample (**Figure 3.31**). Proof that this peak represented a distinct compound was the fact that apart from forming the H^+ adduct, it also formed both the Na^+ (*m/z* 420.2) and K^+ (*m/z* 436.2) adducts and was well resolved from the parent peak which eluted at Rt 6.74 min.

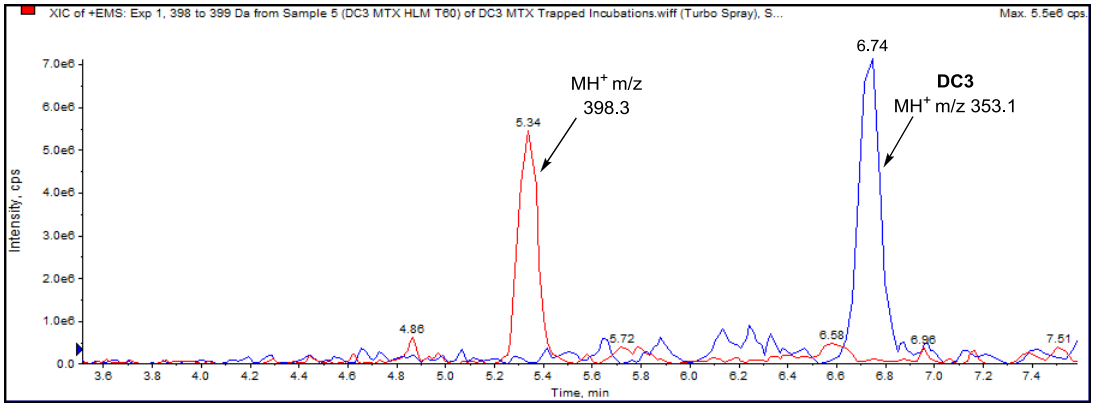

Figure 3.31: XIC of T60 **DC3** incubation in methoxylamine fortified microsomes indicating presence of suspected trapped metabolite at Rt 5.34 min

However, on enhanced product ion scans of the fragmented suspected adduct, no loss of the diagnostic 32 Da neutral fragment was observed, raising some doubt as to whether the component peak (*m/z* 398.3) actually represented a methoxylamine trapped aldehyde metabolite (**Figure 3.32**).

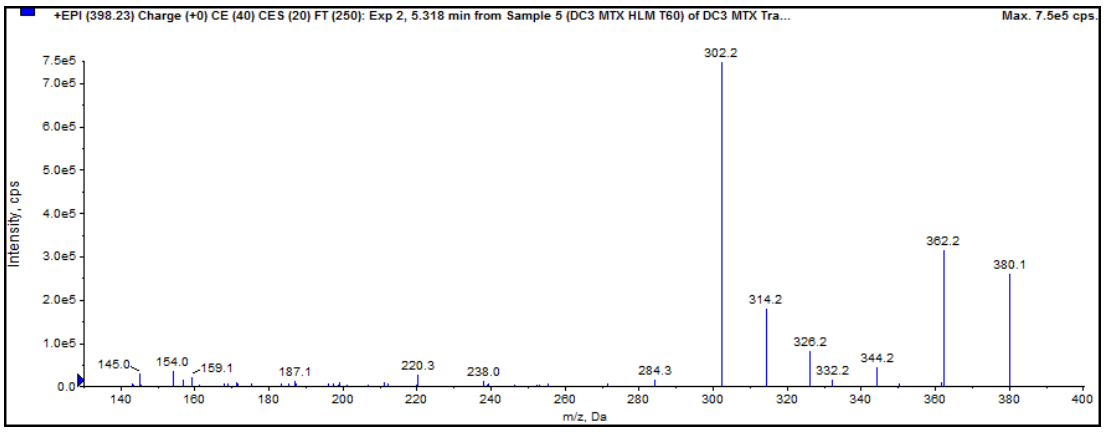

Figure 3.32: EPI of suspected methoxylamine trapped metabolite (peak Rt 5.34 min, *m/z* 398.2) from T60 microsomal incubation of **DC3**

3.7 Conclusion

A set of natural products and selected semi-synthetic compounds were evaluated for clinical drug-drug interaction risk and *in vitro* metabolic bioactivation using both CYP450 inhibition assays and reactive metabolite trapping experiments. Of the 4 main drug metabolizing enzymes tested, CYP3A4 was found to be the most susceptible to inhibition by a majority of the compounds. Time-dependent inhibition assays on the most potent inhibitor compounds of this isoform, however, suggested that none appeared to be a mechanism-based enzyme inhibitor.

Data from the reactive metabolite trapping experiments revealed that two of the eleven compounds tested (i.e. **DC3** and to a lesser extent **GEDN**) seemed to form detectable trapped metabolic intermediates using methoxylamine. On the other hand, no detectable enzymatically-mediated trapped intermediates from any of the compounds were observed when either reduced glutathione or potassium cyanide was employed as the trapping agent. **CUC-B** was observed to form detectable GSH adducts even in the absence of microsomal protein or co-factors, suggesting direct reactivity of this compound with GSH. It was postulated that the adduct might arise from a direct Michael-addition reaction involving the thiol group of GSH and the α,β-unsaturated ketone on the side chain of CUC-B in a reaction that did not require enzymatic catalysis.

REFERENCES:

(1) Park, K.; Williams, D. P.; Naisbitt, D. J.; Kitteringham, N. R.; Pirmohamed, M. Investigation of Toxic Metabolites during Drug Development. *Toxicology and Applied Pharmacology* **2005**, *207*, 425–434.

(2) Edwards, P. J.; Sturino, C. Managing the Liabilities Arising from Structural Alerts: A Safe Philosophy for Medicinal Chemists. *Current Medicinal Chemistry* **2011**, *18*, 3116–3135.

(3) Kalgutkar, A. S. Handling Reactive Metabolite Positives in Drug Discovery: What Has Retrospective Structure-Toxicity Analyses Taught Us? *Chemico-Biological Interactions* **2011**, *192*, 46–55.

(4) Stepan, A. F.; Walker, D. P.; Bauman, J. N.; Price, D. A.; Baillie, T. A.; Kalgutkar, A. S.; Aleo, M. D. Structural Alert/reactive Metabolite Concept as Applied in Medicinal Chemistry to Mitigate the Risk of Idiosyncratic Drug Toxicity: A Perspective Based on the Critical Examination of Trends in the Top 200 Drugs Marketed in the United States. *Chemical Research in Toxicology* **2011**, *24*, 1345–1410.

(5) Shu, Y.-Z.; Johnson, B. M.; Yang, T. J. Role of Biotransformation Studies in Minimizing Metabolism-Related Liabilities in Drug Discovery. *The AAPS Journal* **2008**, *10*, 178–192.

(6) Yan, Z.; Maher, N.; Torres, R.; Caldwell, G. W.; Huebert, N. Rapid Detection and Characterization of Minor Reactive Metabolites Using Stable-Isotope Trapping in Combination with Tandem Mass Spectrometry. *Rapid Communications in Mass Spectrometry* **2005**, *19*, 3322–3330.

(7) Ma, S.; Zhu, M. Recent Advances in Applications of Liquid Chromatography-Tandem Mass Spectrometry to the Analysis of Reactive Drug Metabolites. *Chemico-Biological Interactions* **2009**, *179*, 25–37.

(8) Tolonen, A.; Turpeinen, M.; Pelkonen, O. Liquid Chromatography-Mass Spectrometry in in Vitro Drug Metabolite Screening. *Drug Discovery Today* **2009**, *14*, 120–133.

(9) Tan, Q.; Luo, X. Meliaceous Limonoids: Chemistry and Biological Activities. *Chemical Reviews* **2011**, *111*, 7437–7522.

(10) MacKinnon, S.; Durst, T.; Arnason, J. T.; Angerhofer, C.; Pezzuto, J.; Sanchez-Vindas, P. E.; Poveda, L. J.; Gbeassor, M. Antimalarial Activity of Tropical Meliaceae Extracts and Gedunin Derivatives. *Journal of Natural Products* **1997**, *60*, 336–341.

(11) Khalid, S. A.; Duddeck, H.; Gonzalez-Sierra, M. Isolation and Characterization of an Antimalarial Agent of the Neem Tree Azadirachta Indica. *Journal of Natural Products* **1989**, *52*, 922–927.

(12) Chianese, G.; Yerbanga, S. R.; Lucantoni, L.; Habluetzel, A.; Basilico, N.; Taramelli, D.; Fattorusso, E.; Taglialatela-Scafati, O. Antiplasmodial Triterpenoids from the Fruits of Neem, Azadirachta Indica. *Journal of Natural Products* **2010**, *73*, 1448–1452.

(13) Uddin, S. J.; Nahar, L.; Shilpi, J. A.; Shoeb, M.; Borkowski, T.; Gibbons, S.; Middleton, M.; Byres, M.; Sarker, S. D. Gedunin, a Limonoid from Xylocarpus Granatum, Inhibits the Growth of CaCo-2 Colon Cancer Cell Line in Vitro. *Phytotherapy Research* **2007**, *21*, 757–761.

(14) Brandt, G. E. L.; Schmidt, M. D.; Prisinzano, T. E.; Blagg, B. S. J. Gedunin, a Novel hsp90 Inhibitor: Semisynthesis of Derivatives and Preliminary Structure-Activity Relationships. *Journal of Medicinal Chemistry* **2008**, *51*, 6495–6502.

(15) Lakshmi, V.; Singh, N.; Shrivastva, S.; Mishra, S. K.; Dharmani, P.; Mishra, V.; Palit, G. Gedunin and Photogedunin of Xylocarpus Granatum Show Significant Anti-Secretory Effects and Protect the Gastric Mucosa of Peptic Ulcer in Rats. *Phytomedicine* **2010**, *17*, 569–574.

(16) Fukamiya, N.; Lee, K.-H. Antitumor Agents, 81. Justicidin-A and Diphyllin, Two Cytotoxic Principles from Justicia Procumbens. *Journal of Natural Products* **1986**, *49*, 348–350.

(17) Chen, C.-C.; Hsin, W.-C.; Ko, F.-N.; Huang, Y.-L.; Ou, J.-C.; Teng, C.-M. Antiplatelet Arylnaphthalide Lignans from Justicia Procumbens. *Journal of Natural Products* **1996**, *59*, 1149–1150.

(18) Asano, J.; Chiba, K.; Tada, M.; Yoshii, T. Antiviral Activity of Lignans and Their Glycosides from Justicia Procumbens. *Phytochemistry* **1996**, *42*, 713–717.

(19) Day, S.-H.; Lin, Y.-C.; Tsai, M.-L.; Tsao, L.-T.; Ko, H.-H.; Chung, M.-I.; Lee, J.-C.; Wang, J.-P.; Won, S.-J.; Lin, C.-N. Potent Cytotoxic Lignans from Justicia P Rocumbens and Their Effects on Nitric Oxide and Tumor Necrosis Factor-A Production in Mouse Macrophages. *Journal of Natural Products* **2002**, *65*, 379–381.

(20) Lee, J.-C.; Lee, C.-H.; Su, C.-L.; Huang, C.-W.; Liu, H.-S.; Lin, C.-N.; Won, S.-J. Justicidin A Decreases the Level of Cytosolic Ku70 Leading to Apoptosis in Human Colorectal Cancer Cells. *Carcinogenesis* **2005**, *26*, 1716–1730.

(21) Su, C.-L.; Huang, L. L. H.; Huang, L.-M.; Lee, J.-C.; Lin, C.-N.; Won, S.-J. Caspase-8 Acts as a Key Upstream Executor of Mitochondria during Justicidin A-Induced Apoptosis in Human Hepatoma Cells. *FEBS Letters* **2006**, *580*, 3185–3191.

(22) Fouche, G.; Khorombi, E.; Maharaj, V. J. Treatment of Erectile Dysfunction and Libido Enhancement. US 8,609,151 B2, 2013.

(23) Bohlmann, F.; Zdero, C. Sesquiterpene Lactones from Brachylaena Species. *Phytochemistry* **1982**, *21*, 647–651.

(24) Higuchi, Y.; Shimoma, F.; Koyanagi, R.; Suda, K.; Mitsui, T.; Kataoka, T.; Nagai, K.; Ando, M. Synthetic Approach to Exo-Endo Cross-Conjugated Cyclohexadienones and Its Application to the Syntheses of Dehydrobrachylaenolide, Isodehydrochamaecynone, and Trans-Isodehydrochamaecynone. *Journal of Natural Products* **2003**, *66*, 588–594.

(25) Rademeyer, M.; van Heerden, F. R.; van der Merwe, M. M. Dehydro-Brachylaenolide: An Eudesmane-Type Sesquiterpene Lactone. *Acta Crystallographica* **2008**, *65*, o196.

(26) Shale, T. L.; Stirk, W. A.; Staden, J. Van. Screening of Medicinal Plants Used in Lesotho for Anti-Bacterial and Anti-Inflammatory Activity. *Journal of Ethnopharmacology* **1999**, *67*, 347–354.

(27) Steenkamp, V.; Mathivha, E.; Gouws, M. C.; van Rensburg, C. E. J. Studies on Antibacterial, Antioxidant and Fibroblast Growth Stimulation of Wound Healing Remedies from South Africa. *Journal of Ethnopharmacology* **2004**, *95*, 353–357.

(28) Semenya, S. S.; Maroyi, A. Medicinal Plants Used by the Bapedi Traditional Healers to Treat Diarrhoea in the Limpopo Province, South Africa. *Journal of Ethnopharmacology* **2012**, *144*, 395–401.

(29) Becker, J. V. W.; van der Merwe, M. M.; van Brummelen, A. C.; Pillay, P.; Crampton, B. G.; Mmutlane, E. M.; Parkinson, C.; van Heerden, F. R.; Crouch, N. R.; Smith, P. J.; Mancama, D. T.; Maharaj, V. J. In Vitro Anti-Plasmodial Activity of Dicoma Anomala Subsp. Gerrardii (Asteraceae): Identification of Its Main Active Constituent, Structure-Activity Relationship Studies and Gene Expression Profiling. *Malaria Journal* **2011**, *10*, 295.

(30) Lee, M. R. The History of Ergot of Rye (Claviceps Purpurea) II: 1900–1940. *The Journal of the Royal College of Physicians of Edinburgh* **2009**, *39*, 365–369.

(31) Beretta, C.; Ferrini, R.; Glasser, A. H. 1-Methyl-8 B-Carbobenzyloxy-Aminomethyl-10 A-Ergoline, a Potent and Long-Lasting 5-Hydroxytryptamine Antagonist. *Nature* **1965**, *207*, 421–422.

(32) Kang, K.; Wong, K.-S.; Fong, W.-P.; Tsang, P. W.-K. Metergoline-Induced Cell Death in Candida Krusei. *Fungal Biology* **2011**, *115*, 302–309.

(33) Ch'ng, J.-H.; Mok, S.; Bozdech, Z.; Lear, M. J.; Boudhar, A.; Russell, B.; Nosten, F.; Tan, K. S.-W. A Whole Cell Pathway Screen Reveals Seven Novel Chemosensitizers to Combat Chloroquine Resistant Malaria. *Scientific Reports* **2013**, *3*, 1734.

(34) Godtfredsen, W. O.; Roholt, K.; Tybring, L. FUCIDIN: A New Orally Active Antibiotic. *The Lancet* **1962**, *279*, 928–931.

(35) Turnidge, J. Fusidic Acid Pharmacology, Pharmacokinetics and Pharmacodynamics. *International Journal of Antimicrobial Agents* **1999**, *12*, S23–S34.

(36) Christiansen, K. Fusidic Acid Adverse Drug Reactions. *International Journal of Antimicrobial Agents* **1999**, *12 Suppl 2*, S3–9.

(37) Fernandes, P.; Pereira, D. Efforts to Support the Development of Fusidic Acid in the United States. *Clinical Infectious Diseases* **2011**, *52*, S542–6.

(38) Kubo, I.; Miura, I.; Pettei, M. J.; Lee, Y.-W.; Pilkiewicz, F.; Nakanishi, K. Muzigadial and Warburganal, Potent Antifungal Antiyeast, and African Army Worm Antifeedant Agents. *Tetrahedron Letters* **1977**, *18*, 4553–4556.

(39) Rabe, T.; van Staden, J. Isolation of an Antibacterial Sesquiterpenoid from Warburgia Salutaris. *Journal of Ethnopharmacology* **2000**, *73*, 171–174.

(40) Drewes, S. E.; Crouch, N. R.; Mashimbye, M. J.; de Leeuw, B. M.; Horn, M. M. A Phytochemical Basis for the Potential Use of Warburgia Salutaris (pepper-Bark Tree) Leaves in Place of Bark. *South African Journal of Science* **2001**, *97*, 383–386.

(41) Maroyi, A. Warburgia Salutaris (Bertol. F.) Chiov.: A Multi-Use Ethnomedicinal Plant Species. *Journal of Medicinal Plants Research* **2013**, *7*, 53–60.

(42) Jansen, B. J. M.; de Groot, A. The Occurrence and Biological Activity of Drimane Sesquiterpenoids. *Natural Product Reports* **1991**, *8*, 309–318.

(43) Jansen, B. J. M.; de Groot, A. Occurrence, Biological Activity and Synthesis of Drimane Sesquiterpenoids. *Natural Product Reports* **2004**, *21*, 449–477.

(44) Ying, B.-P.; Peiser, G.; Ji, Y.-Y.; Mathias, K.; Tutko, D.; Hwang, Y. Phytotoxic Sesquiterpenoids from Canella Winterana. *Phytochemistry* **1995**, *38*, 909–915.

(45) Grace, M. H.; Lategan, C.; Mbeunkui, F.; Graziose, R.; Smith, P. J.; Raskin, I.; Lila, M. A. Antiplasmodial and Cytotoxic Activities of Drimane Sesquiterpenes from Canella Winterana. *Natural Product Communications* **2010**, *5*, 1869–1872.

(46) Chen, J. C.; Chiu, M. H.; Nie, R. L.; Cordell, G. A.; Qiu, S. X. Cucurbitacins and Cucurbitane Glycosides: Structures and Biological Activities. *Natural Product Reports* **2005**, *22*, 386–399.

(47) Lee, D. H.; Iwanski, G. B.; Thoennissen, N. H. Cucurbitacin: Ancient Compound Shedding New Light on Cancer Treatment. *The Scientific World Journal* **2010**, *10*, 413–418.

(48) Liu, T.; Zhang, M.; Zhang, H.; Sun, C.; Deng, Y. Inhibitory Effects of Cucurbitacin B on Laryngeal Squamous Cell Carcinoma. *European Archives of Otorhinolaryngology* **2008**, *265*, 1225–1232.

(49) Chan, K. T.; Li, K.; Liu, S. L.; Chu, K. H.; Toh, M.; Xie, W. D. Cucurbitacin B Inhibits STAT3 and the Raf/MEK/ERK Pathway in Leukemia Cell Line K562. *Cancer Letters* **2010**, *289*, 46–52.

(50) Chan, K. T.; Meng, F. Y.; Li, Q.; Ho, C. Y.; Lam, T. S.; To, Y.; Lee, W. H.; Li, M.; Chu, K. H.; Toh, M. Cucurbitacin B Induces Apoptosis and S Phase Cell Cycle Arrest in BEL-7402 Human Hepatocellular Carcinoma Cells and Is Effective via Oral Administration. *Cancer Letters* **2010**, *294*, 118–124.

(51) Haritunians, T.; Gueller, S.; Zhang, L.; Badr, R.; Yin, D.; Xing, H.; Fung, M. C.; Koeffler, H. P. Cucurbitacin B Induces Differentiation, Cell Cycle Arrest, and Actin Cytoskeletal Alterations in Myeloid Leukemia Cells. *Leukemia Research* **2008**, *32*, 1366–1373.

(52) Yin, D.; Wakimoto, N.; Xing, H.; Lu, D.; Huynh, T.; Wang, X.; Black, K. L.; Koeffler, H. P. Cucurbitacin B Markedly Inhibits Growth and Rapidly Affects the Cytoskeleton in Glioblastoma Multiforme. *International Journal of Cancer* **2008**, *123*, 1364–1375.

(53) Eagle, G. A.; Rivett, D. E. A. Diterpenoids of Leonotis Species. Part IV. Dubiin, a Furanoid Labdane Derivative of L. Dubia E. Mey. *Journal of the Chemical Society, Perkin Transactions 1* **1973**, *16*, 1701–1704.

(54) Wu, H.; Li, J.; Fronczek, F. R.; Ferreira, D.; Burandt, C. L.; Setola, V.; Roth, B. L.; Zjawiony, J. K. Phytochemistry Labdane Diterpenoids from Leonotis Leonurus. *Phytochemistry* **2013**, *91*, 229–235.

(55) Moore, J. A.; Eng, S. Some New Constituents of Piscidia Erythrina L. *Journal of the American Chemical Society* **1956**, *78*, 395–398.

(56) Derese, S.; Barasa, L.; Akala, H. M.; Yusuf, A. O.; Kamau, E.; Heydenreich, M.; Yenesew, A. 4'-Prenyloxyderrone from the Stem Bark of Millettia Oblata Ssp. Teitensis and the Antiplasmodial Activities of Isoflavones from Some Millettia Species. *Phytochemistry Letters* **2014**, *8*, 69–72.

(57) Dong, T. T. X.; Zhao, K. J.; Gao, Q. T.; Ji, Z. N.; Zhu, T. T.; Li, J.; Duan, R.; Cheung, A. W. H.; Tsim, K. W. K. Chemical and Biological Assessment of a Chinese Herbal Decoction Containing Radix Astragali and Radix Angelicae Sinensis: Determination of Drug Ratio in Having Optimized Properties. *Journal of Agricultural and Food Chemistry* **2006**, *54*, 2767–2774.

(58) Khan, I. A.; Avery, M. A.; Burandt, C. L.; Goins, D. K.; Mikell, J. R.; Nash, T. E.; Azadegan, A.; Walker, L. A. Antigiardial Activity of Isoflavones from Dalbergia Frutescens Bark. *Journal of Natural Products* **2000**, *63*, 1414–1416.

(59) Huh, J.-E.; Kwon, N.-H.; Baek, Y.-H.; Lee, J.-D.; Choi, D.-Y.; Jingushi, S.; Kim, K.; Park, D.-S. Formononetin Promotes Early Fracture Healing through Stimulating Angiogenesis by up-Regulating VEGFR-2/Flk-1 in a Rat Fracture Model. *International Immunopharmacology* **2009**, *9*, 1357–1365.

(60) Huh, J.-E.; Nam, D.-W.; Baek, Y.-H.; Kang, J. W.; Park, D.-S.; Choi, D.-Y.; Lee, J.-D. Formononetin Accelerates Wound Repair by the Regulation of Early Growth Response Factor-1 Transcription Factor through the Phosphorylation of the ERK and p38 MAPK Pathways. *International Immunopharmacology* **2011**, *11*, 46–54.

(61) Wu, J.-H.; Li, Q.; Wu, M.-Y.; Guo, D.-J.; Chen, H.-L.; Chen, S.-L.; Seto, S.-W.; Au, A. L. S.; Poon, C. C. W.; Leung, G. P. H.; Lee, S. M. Y.; Kwan, Y.-W.; Chan, S.-W. Formononetin, an Isoflavone, Relaxes Rat Isolated Aorta through

Endothelium-Dependent and Endothelium-Independent Pathways. *The Journal of Nutritional Biochemistry* **2010**, *21*, 613–620.

(62) Li, Z.; Dong, X.; Zhang, J.; Zeng, G.; Zhao, H.; Liu, Y.; Qiu, R.; Mo, L.; Ye, Y. Formononetin Protects TBI Rats against Neurological Lesions and the Underlying Mechanism. *Journal of the Neurological Sciences* **2014**, *338*, 112–117.

(63) Crespi, C. L.; Miller, V. P.; Penman, B. W. Microtiter Plate Assays for Inhibition of Human, Drug-Metabolizing Cytochromes P450. *Analytical Biochemistry* **1997**, *248*, 188–190.

(64) Crespi, C. L.; Stresser, D. M. Fluorometric Screening for Metabolism-Based Drug-Drug Interactions. *Journal of Pharmacological and Toxicological Methods* **2001**, *44*, 325–331.

(65) Nakamura, K.; Hanna, I. H.; Cai, H.; Nishimura, Y.; Williams, K. M.; Guengerich, F. P. Coumarin Substrates for Cytochrome P450 2D6 Fluorescence Assays. *Analytical Biochemistry* **2001**, *292*, 280–286.

(66) Onderwater, R. C. A.; Venhorst, J.; Commandeur, J. N. M.; Vermeulen, N. P. Design, Synthesis, and Characterization of 7-Methoxy-4-(aminomethyl)coumarin as a Novel and Selective Cytochrome P450 2D6 Substrate Suitable for High-Throughput Screening. *Chemical Research in Toxicology* **1999**, *12*, 555–559.

(67) Thelingwani, R. S.; Zvada, S. P.; Dolgos, H.; Ungell, A.-L. B.; Masimirembwa, C. M. In Vitro and in Silico Identification and Characterization of Thiabendazole as a Mechanism-Based Inhibitor of CYP1A2 and Simulation of Possible Pharmacokinetic Drug-Drug Interactions. *Drug Metabolism and Disposition* **2009**, *37*, 1286–1294.

(68) Bergström, M. A.; Isin, E. M.; Castagnoli, N.; Milne, C. E. Bioactivation Pathways of the Cannabinoid Receptor 1 Antagonist Rimonabant. *Drug Metabolism and Disposition* **2011**, *39*, 1823–1832.

(69) Argoti, D.; Liang, L.; Conteh, A.; Chen, L.; Bershas, D.; Yu, C.-P.; Vouros, P.; Yang, E. Cyanide Trapping of Iminium Ion Reactive Intermediates Followed by Detection and Structure Identification Using Liquid Chromatography-Tandem Mass Spectrometry (LC-MS/MS). *Chemical Research in Toxicology* **2005**, *18*, 1537–1544.

(70) Mašič, L. P. Role of Cyclic Tertiary Amine Bioactivation to Reactive Iminium Species: Structure Toxicity Relationship. *Current Drug Metabolism* **2011**, *12*, 35–50.

(71) Lu, S. C. Regulation of Glutathione Synthesis. *Molecular Aspects of Medicine* **2009**, *30*, 42–59.

(72) Johansson, T.; Jurva, U.; Grönberg, G.; Weidolf, L.; Masimirembwa, C. Novel Metabolites of Amodiaquine Formed by CYP1A1 and CYP1B1: Structure Elucidation Using Electrochemistry, Mass Spectrometry, and NMR. *Drug Metabolism and Disposition* **2009**, *37*, 571–579.

(73) Ma, S.; Subramanian, R. Detecting and Characterizing Reactive Metabolites by Liquid Chromatography/tandem Mass Spectrometry. *Journal of Mass Spectrometry* **2006**, *41*, 1121–1139.

(74) Kalgutkar, A. S.; Gardner, I.; Obach, R. S.; Shaffer, C. L.; Callegari, E.; Henne, K. R.; Mutlib, A. E.; Dalvie, D. K.; Lee, J. S.; Nakai, Y.; O'Donnell, J. P.; Boer, J.; Harriman, S. P. A Comprehensive Listing of Bioactivation Pathways of Organic Functional Groups. *Current Drug Metabolism* **2005**, *6*, 161–225.

(75) Erve, J. C. L.; Vashishtha, S. C.; DeMaio, W.; Talaat, R. E. Metabolism of Prazosin in Rat, Dog, and Human Liver Microsomes and Cryopreserved Rat and Human Hepatocytes and Characterization of Metabolites by Liquid Chromatography/tandem Mass Spectrometry. *Drug Metabolism and Disposition* **2007**, *35*, 908–916.

CHAPTER FOUR:
INVESTIGATING THE CROSS-REACTIVITY OF CHEMICAL INHIBITORS USED IN HEPATIC MICROSOMAL CYP450 ENZYME PHENOTYPING

4.1 Summary

In this Chapter, an overview of the different approaches employed by the pharmaceutical industry in enzyme phenotyping is presented as a primer to highlight certain drawbacks intended to be addressed by the work presented here. Detailed *in vitro* assays carried out to determine the extent to which chemical inhibitors routinely used in hepatic microsomal CYP450 phenotyping assays in early drug discovery exhibit cross-inhibition are described. Quantitative analysis of the data obtained from these assays and their application in improving calculations for determining the contribution of different CYP450 enzymes in drug metabolism is presented.

The work described in this Chapter was carried out in the Drug Metabolism and Pharmacokinetics (DMPK) Department at the Novartis Institute of Biomedical Research (NIBR) in Basel, Switzerland.

4.2 General Introduction

In early DMPK studies, identification of the enzymes principally responsible for the biotransformation of lead compounds is crucial in understanding the metabolic fate and anticipating potential liabilities in the disposition of such *potential* drugs *in vivo*. The principle phase I oxidative enzymes involved in biotransformation of xenobiotics include the various CYP450 isoforms and the flavin-containing monoxygenases (FMOs) previously described in **Chapter 1**. The CYP450 enzymes are responsible for the biotransformation of more than 75% of drugs used clinically. Thus, investigating which of these enzymes are involved in biotransformation of potential new drugs, as would be expected, is often carried out early in the development process. 'CYP450 Reaction Phenotyping' refers to the process of identifying the specific CYP450 enzyme isoforms responsible for metabolism of xenobiotics and quantifying their individual contribution to overall metabolism.

CYP450 reaction phenotyping is important for several reasons:

1. It allows for early detection of potential metabolic liabilities, including:
    - Identifying whether a compound is predominantly a metabolic substrate of major CYP450 isoforms such as CYP2C9, CYP2C19 or CYP2D6, which are known to exhibit phenotypic polymorphism in different human populations.[1] Such a scenario may necessitate consideration of different dosing strategies of such a compound in different patient populations.
    - Prediction of the major site (organ or tissue) of metabolism e.g. hepatic/ extra-hepatic. This is possible if the main metabolizing enzyme(s) are predominantly localized in specific tissues or organs and may aid in anticipating potential targets for toxicity related to compound metabolism, for example, via reactive metabolite formation.
    - Identification of whether a compound is metabolized by multiple isoforms and hence subject to metabolic switching in the event of inhibition of any of its metabolic pathways. Drugs significantly metabolized by more than one isoform might be more prone to drug-drug interactions when co-administered with other xenobiotics. Additionally, depending on the individual isoform affinities for the substrate, this may also contribute to low metabolic stability for such compounds.
2. By establishing the contribution of individual CYP450 enzymes to metabolism of a compound, one can more readily estimate the potential or risk and magnitude of undesirable drug-drug interactions in patients under concomitant medication with several drugs that are metabolised by the same enzymes.

4.3 *In vitro* CYP450 Phenotyping Techniques

There are several common *in vitro* techniques used in conducting early CYP450 phenotyping studies: (1) phenotyping using pooled hepatic microsomes and specific chemical inhibitors or monoclonal antibodies; (2) CYP450 isoform mapping using purified recombinant human CYP450 enzymes (rhCYP450);[2] (3) a third, less common *in vitro* technique, involves correlation analysis based on statistical comparison of the rate of metabolism of test compounds to that of marker substrates in unpooled microsomes obtained from individual donors.[3]

4.3.1 Chemical Inhibition CYP450 Phenotyping

This phenotyping method involves incubating the test compound in microsomal proteins to which inhibitors of specific CYP450 isoforms are also included. As a reference, incubations with no inhibitor serve as controls for standardizing metabolism. The incubation(s) in which compound metabolism is found to be significantly reduced by the presence of the included inhibitor point to the fact that the CYP450 isoform(s) responsible for compound metabolism is/are the same one(s) inhibited by the chemical inhibitor (**Figure 4.1**). Thus, for example, if the compound's metabolism is impaired in the presence of ketoconazole, it can be concluded that CYP3A4/5 is responsible for metabolism since ketoconazole is a known inhibitor of the CYP3A enzymes. The percentage decline in metabolism in the presence of inhibitor is considered to represent the fraction of the drug metabolised by the isoform in question (i.e. *fm,*CYP). A variation of this *in vitro* technique involves the use of monoclonal antibodies in place of chemical inhibitors to effectively inhibit the activity of specific CYP450 isoforms.[4] Although this modified technique might give more accurate results, it is more expensive particularly for use in routine early phenotyping assays and therefore often only reserved for advanced phenotyping assays during later stages of compound development.

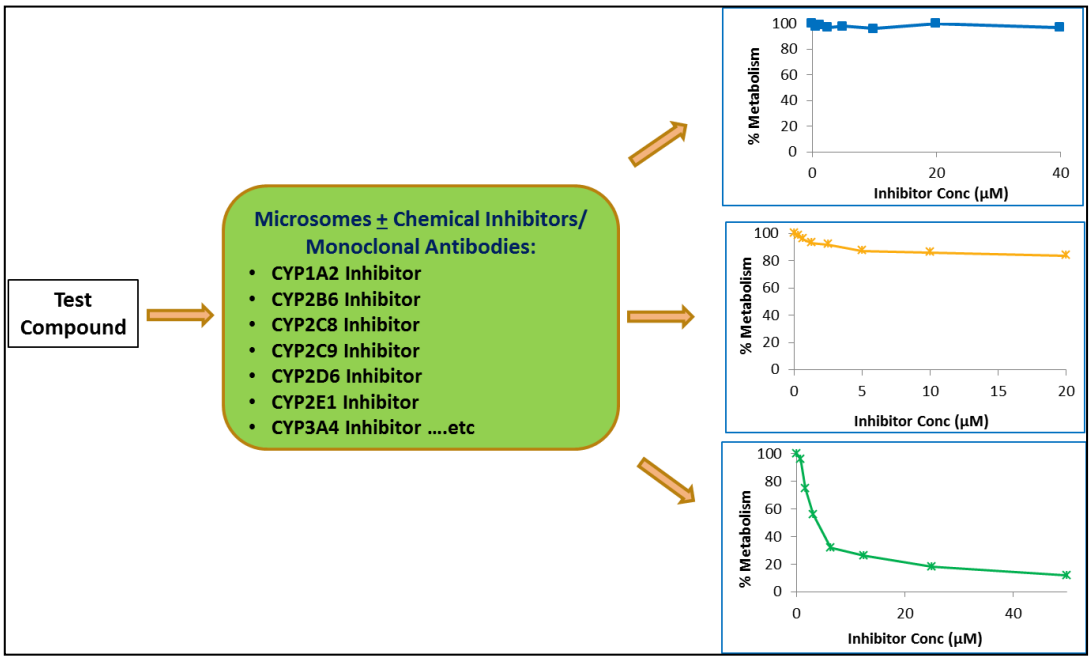

Figure 4.1: Schematic illustration of CYP450 phenotyping using chemical inhibitors or monoclonal antibodies. Decrease in metabolism with increasing inhibitor concentration reveals the relative contribution of the inhibited enzyme isoforms to compound metabolism.

4.3.2 CYP450 Isoform Mapping

This technique involves incubating the test compound individually in a panel of specific purified recombinant human CYP450 isoforms and monitoring metabolic turn-over in each case (**Figure 4.2**). From the incubations, it is possible to directly determine which enzyme is involved in the metabolism of the substrate by calculating the percentage of drug remaining at the end of the assay or alternatively, quantifying the metabolites formed - if known or possible.[5]

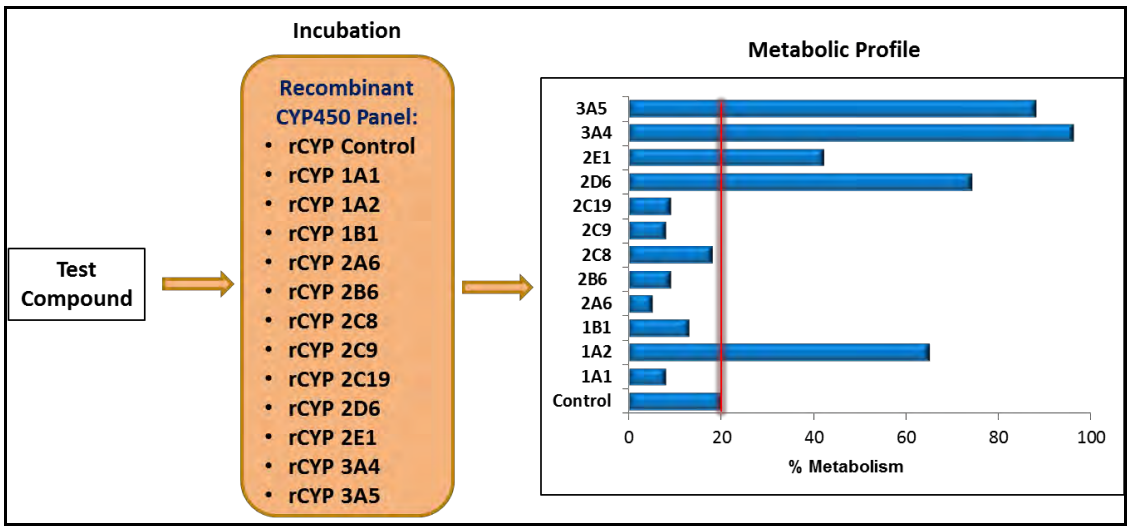

Figure 4.2: Schematic representation of CYP450 phenotyping data using recombinant enzymes. Only isoforms that show metabolism greater than control (i.e. red line in chart) are considered significant.

In these assays, a control incubation of the test compound in the system used to express the recombinant enzyme isoforms (e.g. yeast cells or *E. coli*) must be included to determine and eliminate any inherent contribution of the expression system to metabolism of the test compound in phenotyping calculations.[6]

CYP450 isoform mapping has the advantage of being simpler to perform and interpret data, since the incubation matrix is 'cleaner' and often has fewer confounding elements, such as reduced non-specific protein binding. It also allows for the contribution of CYP450 isoforms such as 1A1, 1B1, 2A3, 2B1, 2D4 and 4F that may not be present in hepatic microsomal fractions to be investigated unlike the case when using only liver microsomes or microsomes from other organs by including such in the panel of CYP450s to screen compounds with.[7]

4.3.3 Phenoyping Using CYP450 Correlation Analysis

Correlation of CYP450 phenotyping involves the use of statistical analysis to establish a correlation between the metabolic rates of the test compound and marker substrates of specific CYP450 isoforms. The procedure entails incubating the test drug individually in microsomes obtained from a small number of human donors (typically ±10 donors) and comparing its metabolic rate to that of the probe substrates in incubations from the same set of donor microsomes to establish correlation.[3] This method is prone to numerous sources of error and dependent on the precise control of numerous experimental procedures that render it unsuitable for routine use. Correlation analysis is therefore considered to be less accurate for CYP450 phenotyping but can serve as a useful tool in confirming the results obtained using recombinant CYP450s or chemical inhibitors.[8]

4.4 Drawbacks of Current CYP450 Phenotyping Methods

Although the phenotyping methods described above are used routinely in industry, there is often poor correlation between the data collected from them even when screening the same compound. In most cases, identification of the main metabolizing CYP450 isoforms can be unequivocally established, however, their individual relative contributions to overall metabolism (i.e. *fm*,CYP) as determined by each method may differ significantly.

Accurate CYP450 isoform mapping using recombinant enzymes is often undermined by the fact that the enzymes used are often expressed using heterologous systems (e.g. yeasts, bacullo-virus infected insect cells, *E. coli* etc.) much different from the *in vivo* human/mammalian environment. Consequently, their metabolic activity may not necessarily be identical or representative of the endogenous CYP450s.[9] Also, because test compounds are incubated in individual recombinant enzymes, possible enzyme competition that might be prominent *in vivo* may not be observed, leading to overestimation of the contribution of some isoforms to metabolism while at the same time underestimating that of others. In practice, data from CYP450 isoform mapping must be normalized, for example by applying intersystem extrapolation factors (ISEF), to take into consideration the different activities and abundances of specific isoforms, which might further complicate the use of this technique.[10,11]

On the other hand, the major shortcoming of CYP450 phenotyping using chemical inhibitors lies in the relative selectivity of the compounds used routinely as reference inhibitors for the different CYP450 isoforms.[12] In practice, though the compounds used are known to inhibit specific enzymes to a high degree, they often demonstrate some extent of cross-inhibition resulting in the under- or over-estimation of the metabolic contribution of the affected CYP450 isoforms. Due to this cross-reactivity, it is not uncommon for phenotyping data to yield cumulative *fm*,CYP values that total more than 100%. Substituting chemical inhibitors with the use of monoclonal antibodies that inactivate specific CYP450 isoforms more selectively can significantly improve accuracy, but requires greater capital outlay and experimental complexity. Alternatively, more selective synthetic inhibitors than those used routinely could be identified and used. This is, however, complicated by the fact that existing compounds possess the advantage of having been studied over a long period of time under different settings and by different researchers, and are mostly compounds used clinically as drugs or which were originally designed as such. Furthermore, most chemical inhibitors in current use can also be used for *in vivo* studies. Replacement inhibitors would need to have undergone a similarly thorough evaluation prior to their acceptance and adoption for routine application.

A more feasible approach in improving CYP450 phenotyping using chemical inhibitors lies in experimentally quantifying the actual extent to which such compounds exhibit cross-reactivity under particular assay settings. From such data, correction factors can be applied in CYP450 phenotyping calculations to more accurately determine *fm*,CYP.

Such an approach has previously been reported by Lu *et al.* in a study aimed at predicting *in vivo* drug-drug interaction based on *in vitro* CYP450-phenotyping data determined using chemical inhibitors corrected for cross-reactivity.[13]

The aim of the present study was to use a similar approach but in which the experimental protocols differed from the work carried out by Lu *et al.* by evaluating the cross-inhibitory effects of a greater number of chemical inhibitors in addition to maintaining *in vitro* incubation conditions aimed at ensuring linearity of enzymatic activity throughout.

4.5 Probe CYP450 Isoform Reactions and Chemical Inhibitors

Ideally, CYP450 reaction phenotyping using human liver microsomes and chemical inhibitors would make use of probe substrates that are entirely metabolised by a single enzyme isoform through a metabolic transformation that can be monitored using an inhibitor that is wholly specific to that isoform. In practice, this scenario does not exist, instead, the compounds used routinely in CYP450 phenotyping are a collection of marker substrates predominantly metabolised by a particular isoform and chemical inhibitors considered to be highly, but not entirely, selective to the main drug metabolising CYP450 isoforms.[14]

The eight (8) chemical inhibitors investigated for cross-reactivity in this work, specific CYP450 isoforms and the probe metabolic reactions monitored to quantify the extent of cross-inhibition are summarized in **Table 4.1** and **Figure 4.3** - **Figure 4.5**.

Table 4.1: CYP450 isoforms, their respective probe substrates, metabolites and chemical inhibitors evaluated in this work

CYP450 isoform	Inhibitor	Probe substrate	Marker metabolite
CYP1A2	Furafylline	Phenacetin	Acetaminophen
CYP2B6	Ticlopidine	Bupropion	Hydroxybupropion
CYP2C19		(*S*)-mephenytoin	4'-Hydroxymephenytoin
CYP2C9	Sulfaphenazole	Diclofenac	4'-Hydroxydiclofenac
CYP2C8	Montelukast	Paclitaxel	6α-Hydroxypaclitaxel
CYP2D6	Quinidine	Bufuralol	1'-Hydroxybufuralol
CYP2E1	Diethylthiocarbamate (DETC)	Chlorzoxazone	6-Hydroxychlorzoxazone
CYP3A	Azamulin	Midazolam	1'-Hydroxymidazolam
	Ketoconazole		

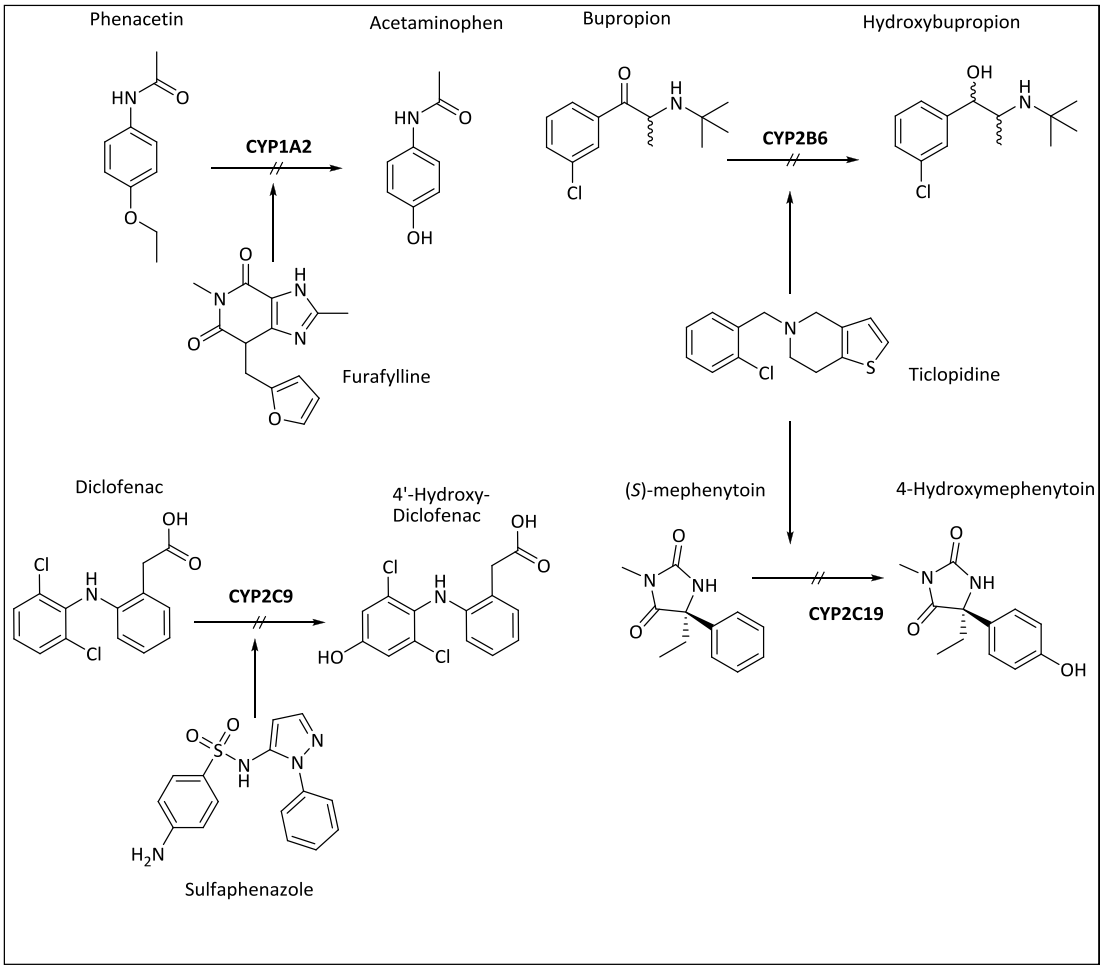

Figure 4.3: Probe metabolic reactions of CYP1A2, CYP2B6, CYP2C9 and CYP2C19 and their respective chemical inhibitors evaluated for cross-reactivity

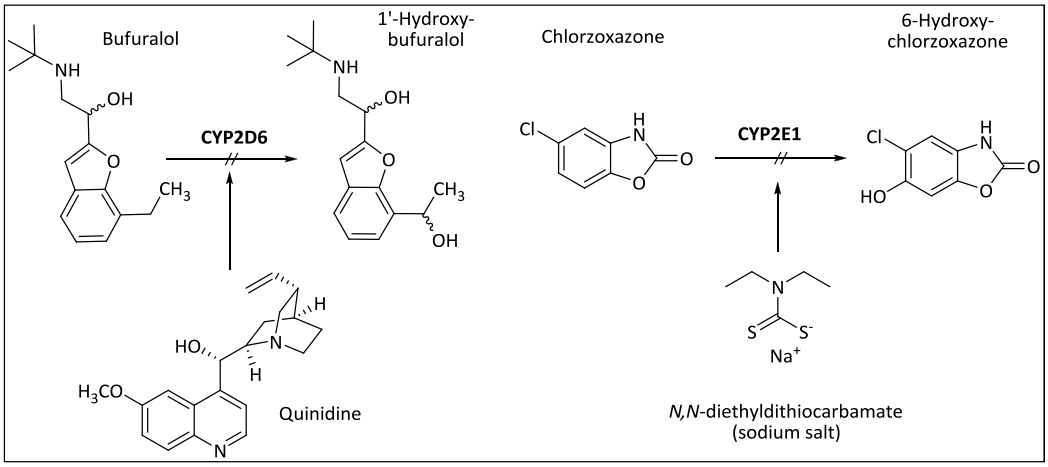

Figure 4.4: Probe metabolic reactions of CYP2D6 and CYP2E1 and their respective chemical inhibitors evaluated for cross-reactivity

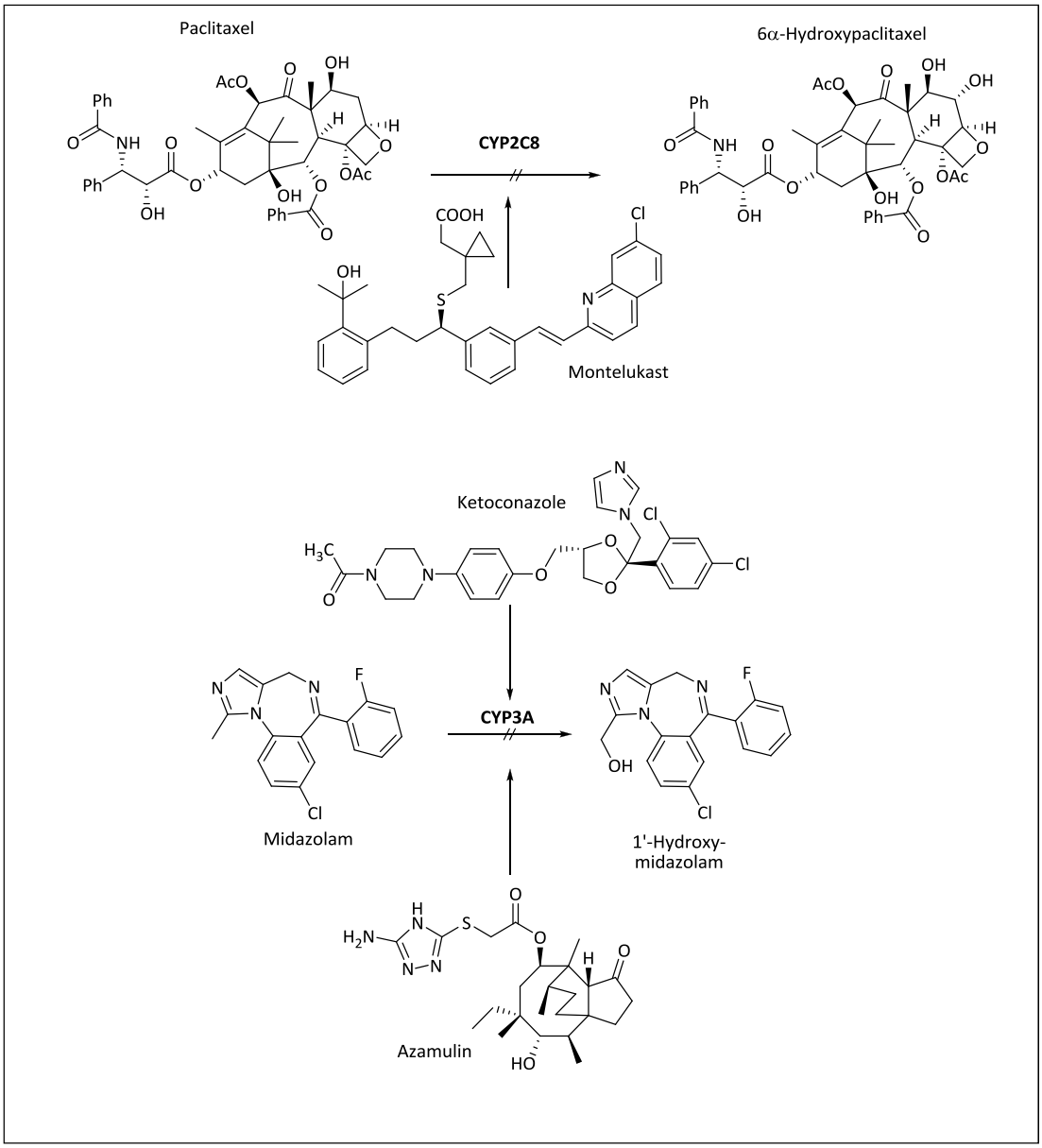

Figure 4.5: Probe metabolic reactions of CYP2C8 and CYP3A and their respective chemical inhibitors evaluated for cross-reactivity

4.6 Methodology

4.6.1 Incubation Conditions

Cross-inhibition of individual CYP450 isoforms was determined by incubating the specific marker substrates of each of the test CYP450s present in pooled, mixed gender human liver microsomes to which each of the inhibitors under test was included. The *in vitro* CYP450 inhibition assays were carried out in duplicate at 37 °C under optimized conditions with regard to microsomal protein concentration, probe substrate concentration and incubation duration (**Table 4.2**). Each inhibitor was incubated at a concentration 5 times greater than its reported K_i value to ensure maximal enzyme inhibition while probe substrate concentrations were at least 5 times less than their reported K_m values. Under these conditions, enzyme activity was expected to be linear and more reproducible. Incubation durations for each metabolic probe reaction were selected to ensure that not more than 20% of the probe substrate was metabolised, as recommended by Bjornsson *et al.*[9] The optimized incubation conditions used are summarized below and the experimental procedure described in greater detail in the **Experimental** Chapter.

Table 4.2: Summary of experimental probe substrate, chemical inhibitor and protein concentrations and experimental incubation duration

CYP450	Probe Substrate (µM)	Inhibitor (µM)	HLM Protein (mg/mL)	Incubation Duration (min)
CYP1A2	Phenacetin (2.0)	Furafylline (10.0)	0.20	20
CYP2B6	Bupropion (25.0)	Ticlopidine (10.0)	0.10	20
CYP2C8	Paclitaxel (1.0)	Montelukast (2.0)	0.20	20
CYP2C9	Diclofenac (1.0)	Sulfaphenazole (5.0)	0.05	8
CYP2C19	*S*-mephenytoin (10.0)	Ticlopidine (10.0)	0.50	20
CYP2D6	Bufuralol (5.0)	Quinidine (2.0)	0.20	20
CYP2E1	Chlorzoxazone (5.0)	Diethylthiocarbamate - DETC (100.0)	0.50	20
CYP3A	Midazolam (0.5)	Azamulin (5.0)	0.05	8
		Ketoconazole (1.0)		

4.6.2 Quantification of Probe Metabolites and Inhibition of Isoform Activity

Metabolic activity of each enzyme was determined in both the presence and absence of inhibitor by quantifying the amount of probe substrate metabolite formed at the end of each incubation. Detection and quantification of metabolites was achieved by LC-MS analysis of the incubation samples each spiked with a known concentration of the respective ^{13}C or ^{2}H radiolabelled metabolite to serve as internal standard. Metabolite concentrations were calculated from chromatographic peak areas determined using the MRM transitions of characteristic fragments of the analyte metabolite being intrapolated from peak area ratio vs concentration calibration curves from standard solutions of each metabolite. Each 7-concentration point metabolite standard solution (**Table 4.3**) was prepared fresh on the day of analysis and analysed before testing incubation samples on the same LC-MS system to ensure linearity of response. For all the probe metabolite calibration curves, a minimum concentration vs analyte/IS peak area ratio Pearson correlation coefficient (r^2) of 0.98 was deemed acceptable for quantitative analysis (**Figure 4.6**).

Metabolite concentration in the incubations devoid of any inhibitor was calculated to represent 100% enzyme activity. From this, the inhibition of enzyme activity was computed as a percentage fraction based on the metabolite content in the probe substrate incubations performed in the presence of the various inhibitors.

Table 4.3: Metabolites analysed and concentrations used for plotting calibration curves

CYP450 Isoform	Analyte Metabolite	Calibration Standard Concentrations [ng/mL]
CYP1A2	Acetaminophen	0; 1.0; 2.5; 5.0; 10; 25; 50; 100
CYP2B6	Hydroxybupropion	0; 10; 25; 50; 100; 250; 500; 1000
CYP2C19	4'-Hydroxymephenytoin	0; 0.4; 1.0; 2.0; 4.0; 10; 20; 40
CYP2C9	4'-Hydroxydiclofenac	0; 10; 25; 50; 100; 250; 500; 1000
CYP2C8	6α-Hydroxypaclitaxel	0; 1.0; 2.5; 5.0; 10; 25; 50; 100
CYP2D6	1'-Hydroxybufuralol	0; 2.0; 5.0; 10; 25; 50; 100; 200
CYP2E1	6-Hydroxychlorzoxazone	0; 0.4; 1.0; 2.0; 4.0; 10; 20; 40
CYP3A	1'-Hydroxymidazolam	0; 4.0; 10; 20; 40; 100; 200; 400

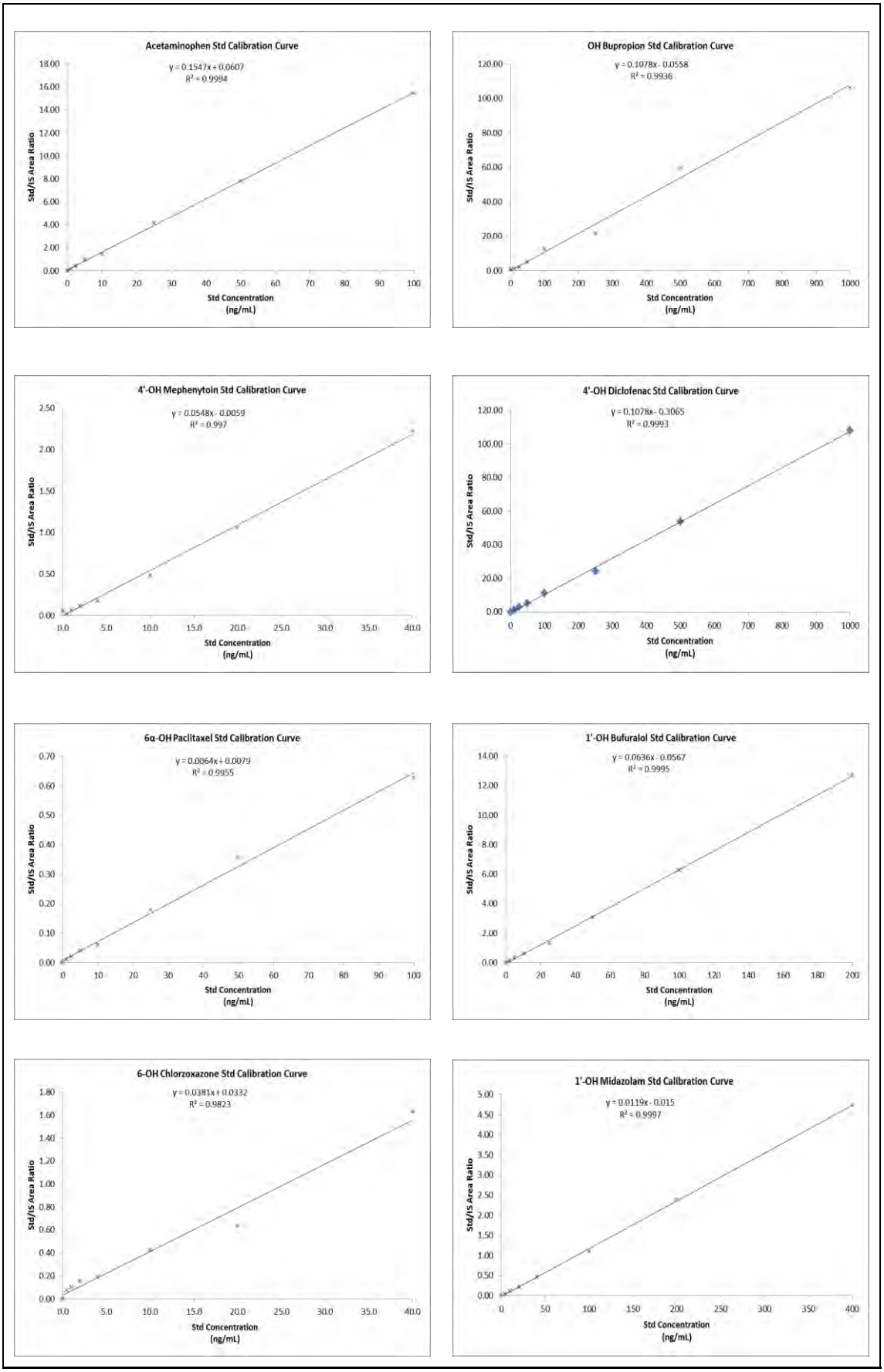

Figure 4.6: Representative concentration vs response calibration curves of metabolite standard solutions used for LC-MS quantification of enzyme inhibition

4.7 Cross-Inhibition Assays Results

4.7.1 Furafylline

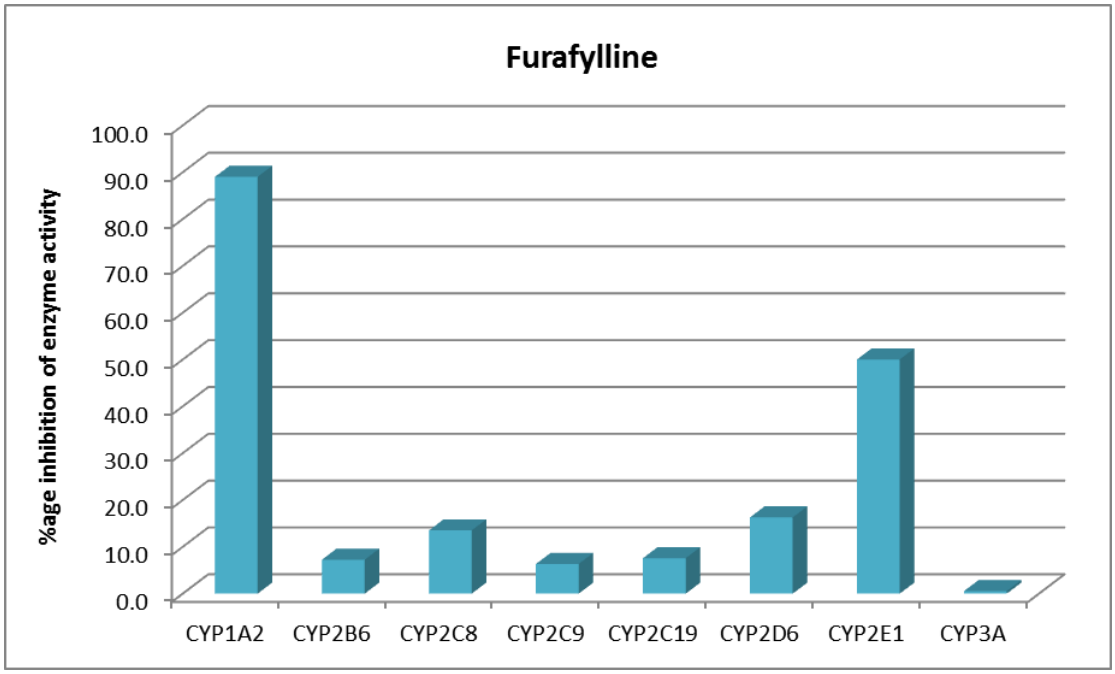

Figure 4.7: Inhibitory effect of furafylline on 8 different CYP450 isoform metabolic probe reactions

The inhibitory effects of furafylline, a methylxanthine developed in the 1980s as a long acting antiasthmatic agent, on CYP1A2-mediated phenacetin *O*-deethylation is the basis for routine use of this compound in phenotyping metabolism mediated by CYP1A2.[15] The inhibition is non-competitive and thought to involve mechanism-based inactivation of the enzyme.[16]

Cross-reactivity results from the assay using furafylline indicated that this compound exhibited very high inhibition of CYP1A2 as expected (89.0%), but also some significant suppression of CYP2E1-mediated chlorzoxazone 6-hydroxylation (approximately 50%). The remaining CYP450 isoforms appeared to be much less affected by furafylline with all six exhibiting less than 20% inhibition and in the case of CYP3A (0.5% inhibition), being virtually unaffected even by the relatively high concentration of inhibitor used.

The relatively high selectivity observed with furafylline is perhaps not unusual considering that even its inhibition of CYP1A2 activity has been shown to vary significantly between reactions metabolised by the human enzyme compared to the same isoform in rat liver microsomes.[17] Cross-inhibition of CYP2E1 by furafylline has been reported previously, albeit to a lesser degree than observed here.[18]

4.7.2 Ticlopidine

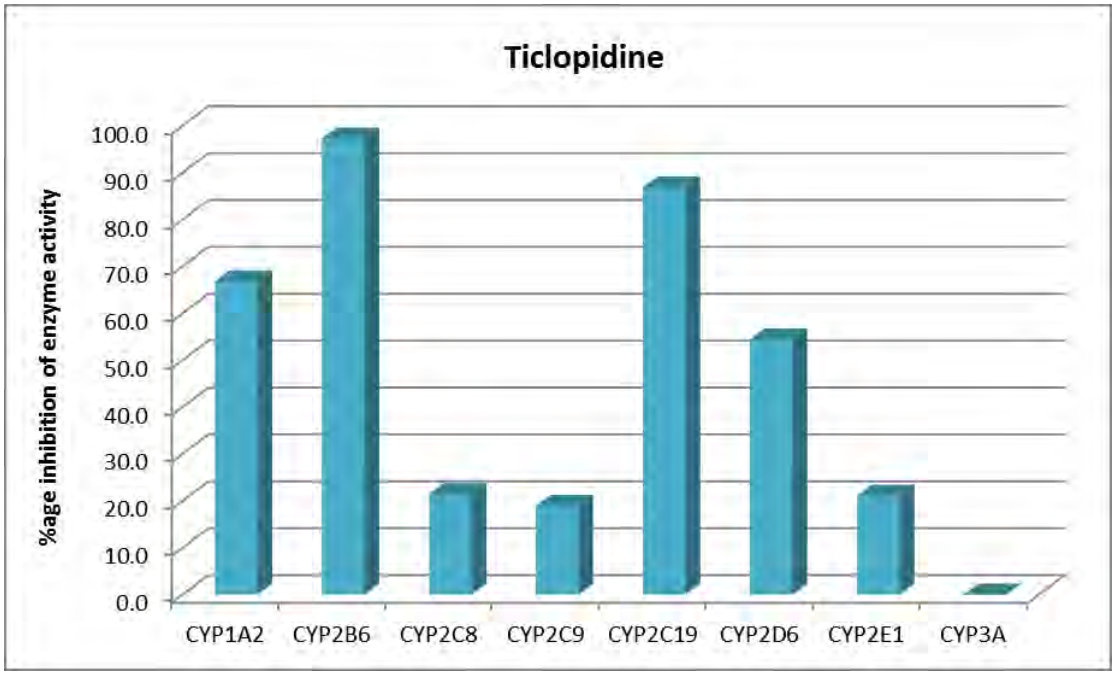

Figure 4.8: Inhibitory effect of ticlopidine on 8 different CYP450 isoform metabolic probe reactions

Ticlopidine is a thienopyridine anti-platelet aggregation drug that acts as an antagonist at adenosine diphosphate receptors and which is used clinically in the management of conditions such as thromboembolic strokes and to prevent thrombus formation secondary to cardiovascular surgical procedures.[19]

Ticlopidine has been reported to be a suicide inhibitor of CYP2C19, acting as a substrate of the enzyme,which undergoes biotransformation into a metabolite that then subsequently causes mechanism-based inhibition.[20] Ticlopidine and related thienopyridines such as clopidogrel have similarly been reported to inhibit the metabolism of fluorogenic probe subtrates by CYP2C19.[21] Ticlopidine is also a potent inhibitor of CYP2B6-mediated bupropion hydroxylation *in vivo.*[22] In addition to its potent inhibitory activity against these two isoforms, *in vitro* studies have also revealed low selectivity and potential inhibition of other CYP450s.[23] However, Walsky and Obach reported that ticlopidine was found to be markedly more selective to CYP2B6 when pre-incubated with hepatic microsomes prior to addition of probe substrates for other CYP450 isoforms.[24]

In our cross-inhibition assays, ticlopidine was unsurprisingly found to markedly inhibit the probe metabolic reactions of both CYP2B6 (97.2% inhibition) and CYP2C19 (86.8%) as anticipated. Ticlopidine was also found to inhibit both CYP1A2 and

CYP2D6 very strongly, reducing enzyme activity by more than fifty percent (66.7% and 54.4% inhibition, respectively). CYP 2C8, 2C9 and 2E1-mediated probe reactions appeared to be inhibited to an almost similar extent by ticlopidine (approximately 20%) with only the CYP3A-mediated biotransformation of midazolam appearing to be unaffected by this inhibitor.

4.7.3 Montelukast

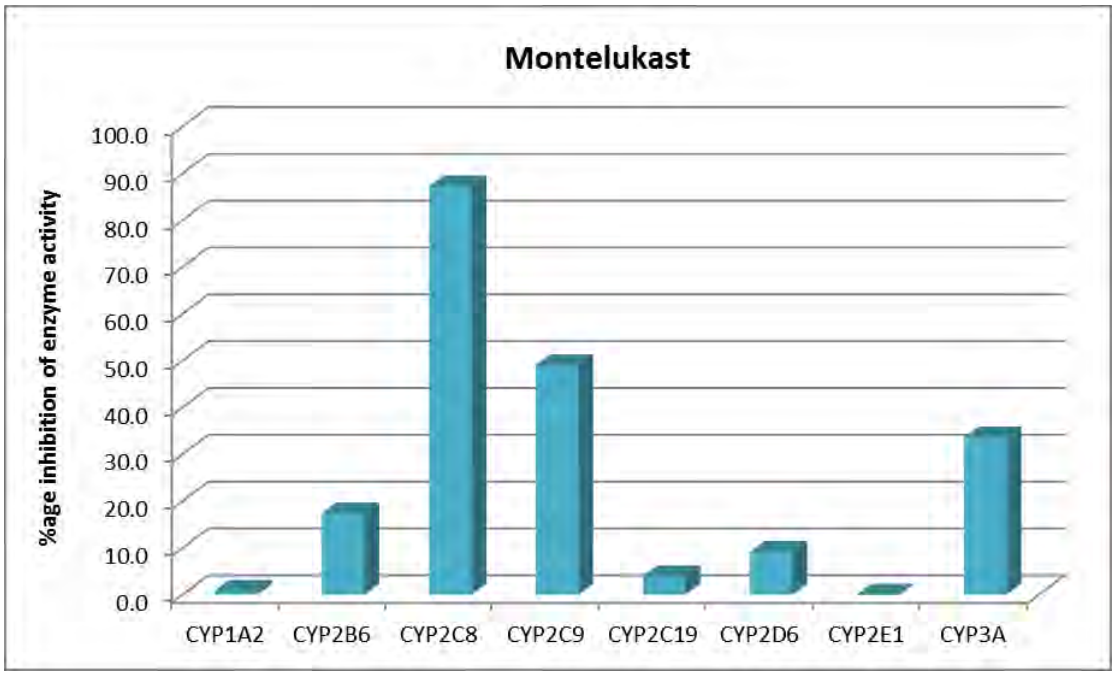

Figure 4.9: Inhibitory effect of montelukast on 8 different CYP450 isoform metabolic probe reactions

Results obtained from the cross-reactivity assay for montelukast were consistent with CYP450 inhibition data reported by Walsky *et al* in which the compound was found to be a potent reversible inhibitor of CYP2C8 and to a lesser extent, CYP2C9-mediated diclofenac-4'-hydroxylase activity and CYP3A-mediated midazolam 1'-hydroxylation.[25] Whereas the work by Walsky noted only marginal cross-inhibition with the other CYP450 isoforms, the cross reactivity of montelukast in our assays was quite significant with CYP2C9 activity being reduced to almost half (i.e. 49.0% inhibition) and CYP3A by one-third (33.6% inhibition).

With the exception of CYP2B6 (17.4% inhibition), however, the remaining CYP450 isoforms all exhibited low susceptibility to cross-inhibition by montelukast (less than 10%).

4.7.4 Quinidine

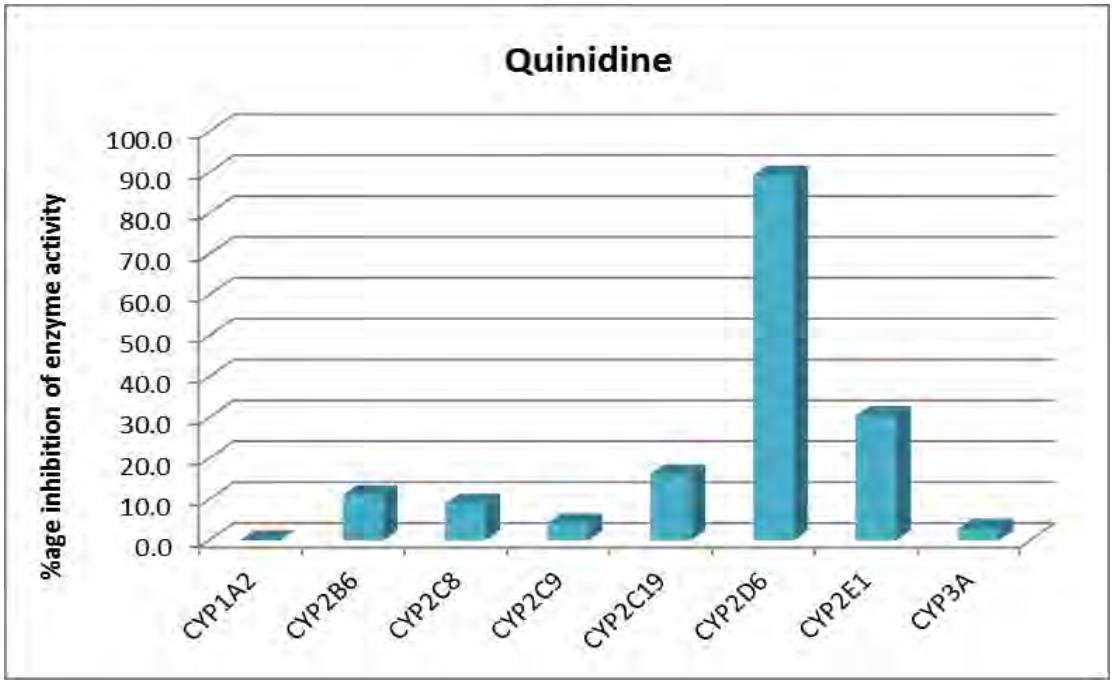

Figure 4.10: Inhibitory effect of quinidine on 8 different CYP450 isoform metabolic probe reactions

Quinidine is an isomer of the anti-malaria drug quinine used clinically as an anti-arrhythmic agent and is a well established inhibitor of CYP2D6 first reported to suppress the oxidative metabolism of another anti-arrhythmic agent, sparteine, in the 1980s by Otton *et al*.[26] Inhibition of recombinant CYP2D6 expressed from yeasts by quinidine and its related cinchona alkaloid dihydroquinidine has similarly been reported.[27] Based on these and other reports of its well studied metabolic enzyme inhibition profile, quinidine is commonly used in chemical inhibition CYP450 phenotyping to identify candidate substrates of CYP2D6.

Cross-reactivity results of the effect of quinidine on the metabolism of probe substrates of the other CYP450 enzymes revealed consistently low cross-inhibition, with values of less than 10% against CYP1A2, CYP2B6, CYP2C8, CYP2C9 and CYP3A. Even though the cross-inhibition of CYP2C19 by quinidine was higher than for these five isoforms, it was still not considered to be significant at only 16.2%.

On the other hand, in addition to its expected effect on CYP2D6-mediated metabolism (89.3% inhibition), quinidine was observed to strongly inhibit CYP2E1-mediated chlorzoxazone hydroxylation (30.4%).

4.7.5 Sulfaphenazole

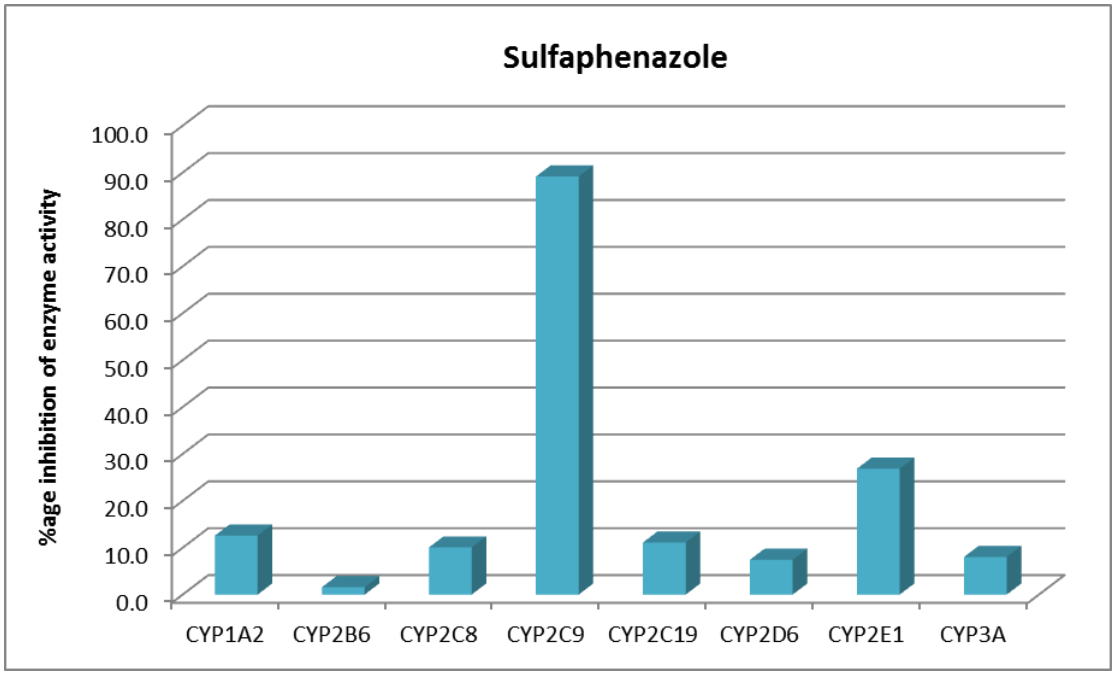

Figure 4.11: Inhibitory effect of sulfaphenazole on 8 different CYP450 isoform metabolic probe reactions

Sulfaphenazole is a long acting synthetic sulphonamide originally developed in the 1950s for the treatment of bacterial infections then subsequently discovered to be a potent inhibitor of CYP450 enzyme and now routinely used as a competitive and selective *in vitro* inhibitor of CYP2C9.[28,29]

Cross-reactivity assays using sulfaphenazole confirmed its potent inhibition of CYP2C9 activity (89.1% inhibition) as reported in the literature. Inhibition of other CYP450 isoforms was low and ranged over 1.5% - 12.5% for CYPs 1A2, 2B6, 2C8, 2C19, 2D6 and 3A. The only exception to this trend was CYP2E1 in which case sulfaphenazole reduced activity by 26.8%, which was considered low but nevertheless significant.

4.7.6 Diethylthiocarbamate

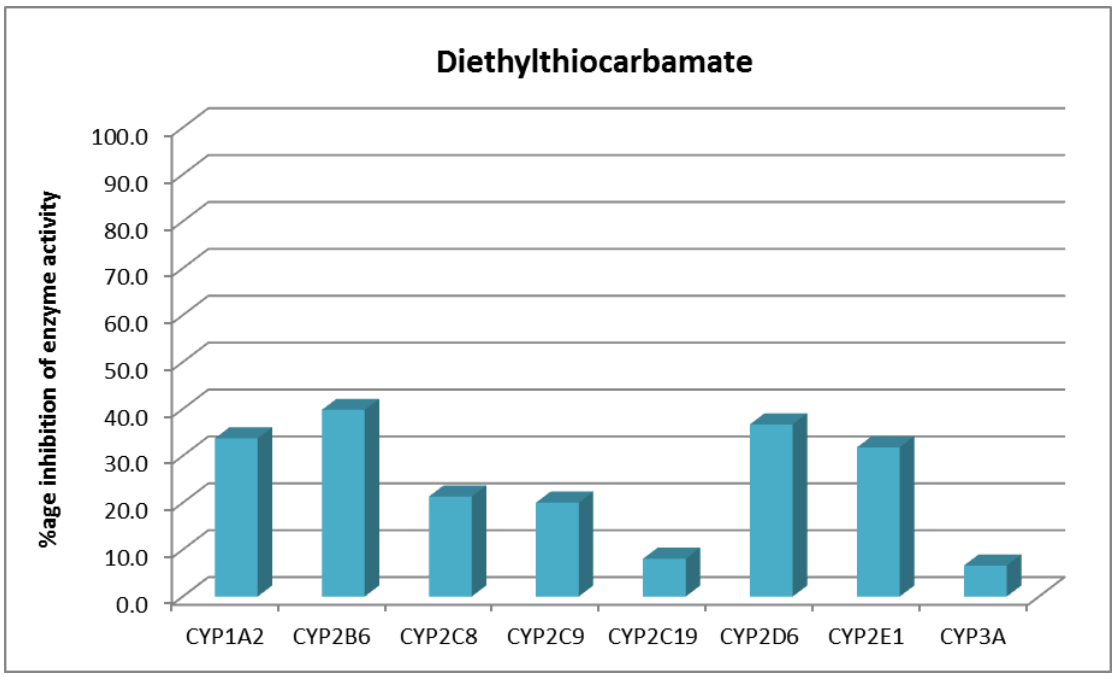

Figure 4.12: Inhibitory effect of diethylthiocarbamate on 8 different CYP450 isoform metabolic probe reactions

Diethyldithiocarbamate was evaluated as the routine inhibitor used to establish the metabolic contribution of CYP2E1 and found to be the least potent of the compounds tested and by far the least selective.

Despite significant loss of CYP2E1 activity (31.8% inhibition) in the presence of DETC, this value was considerably lower than inhibitions achieved with the other inhibitors on their respective probe reactions, all of which were typically in excess of 85%. Furthermore, DETC actually appeared to inhibit the activity of other isoforms to a slightly greater degree than observed with CYP2E1 i.e. CYP1A2 (33.7% inhibition), CYP2B6 (39.8%) and CYP2D6 (36.7% inhibition). The activities of both CYP2C8 and CYP2C9 were also significantly reduced by approximately 20% in either case and only CYP2C19 and CYP3A showed less than 10% inhibition.

These somewhat idiosyncratic results for DETC inhibition potency and cross-reactivity have previously been reported using recombinant cDNA-expressed human CYP450 enzymes by Chang *et al*., but contrasted with previous work by Guengerich *et al.* on the selectivity of DETC for CYP2E1 in microsomal preparations.[30,31]

4.7.7 Ketoconazole

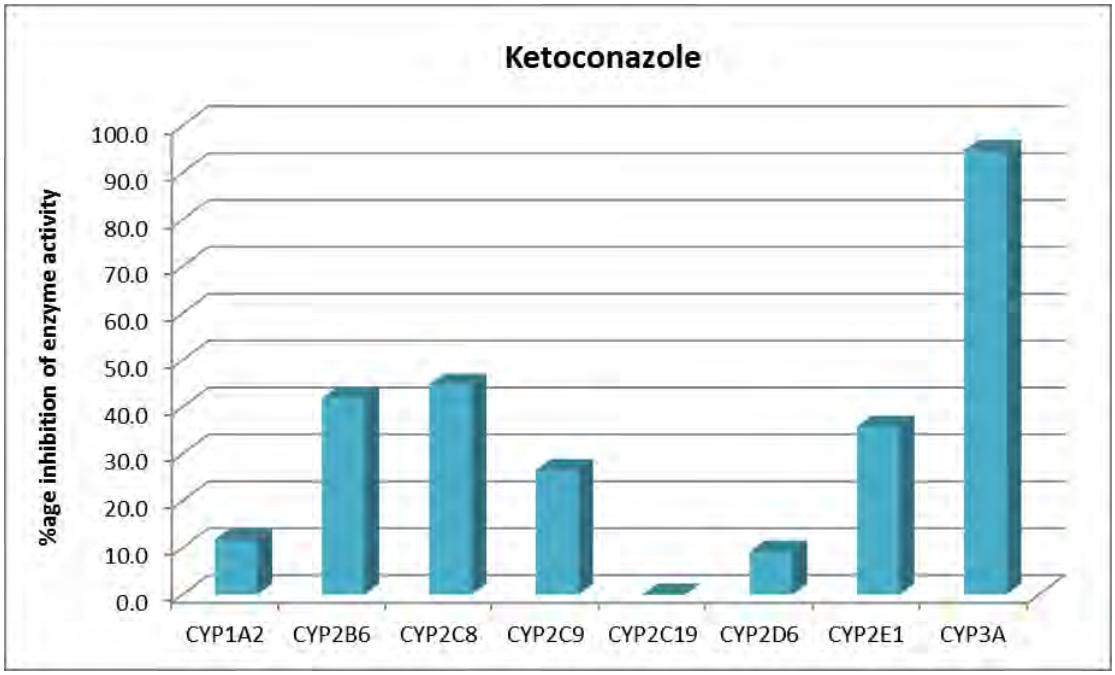

Figure 4.13: Inhibitory effect of ketoconazole on 8 different CYP450 isoform metabolic probe reactions

Ketoconazole was found to exhibit significant cross-inhibition of CYP2B6, CYP2C8, CYP2C9 and CYP2E1 in addition to its established mixed competitive and non-competitive inhibition of CYP3A-mediated 1'-hydroxylation of midazolam.[32]

The activities of CYP1A2 and CYP2D6 were both only reduced by about 10% while CYP2C19 activity appeared to be entirely unaffected following co-incubation with ketoconazole. In the case of both CYP2B6 and CYP2C8, ketoconazole accounted for approximately 40% loss in enzymatic activity, while CYP2E1 was comparatively only slightly less affected (35.8% inhibition) with CYP2C9 activity being reduced by 26.5%.

The cross-inhibition findings with ketoconazole were not unexpected, particularly based on the large volume of information published regarding this and other azole antifungal drugs' clinically significant drug-drug interactions with numerous other medications.[33] It was, however, observed that the absolute rank order of *in vitro* cross-inhibition by ketoconazole (CYP3A > CYP2C8 ≈ CYP2B6 > CYP2E1> CYP2C9) differed from that reported by Obach *et al* (CYP3A > CYP2C9 ≈ CYP2C19 > CYP1A2 ≈ CYP2D6) particularly regarding CYP2C19, which was observed to be virtually uninhibited in our study.[34] A possible explanation for these differences might be variance in experimental conditions e.g. protein and substrate concentrations.

4.7.8 Azamulin

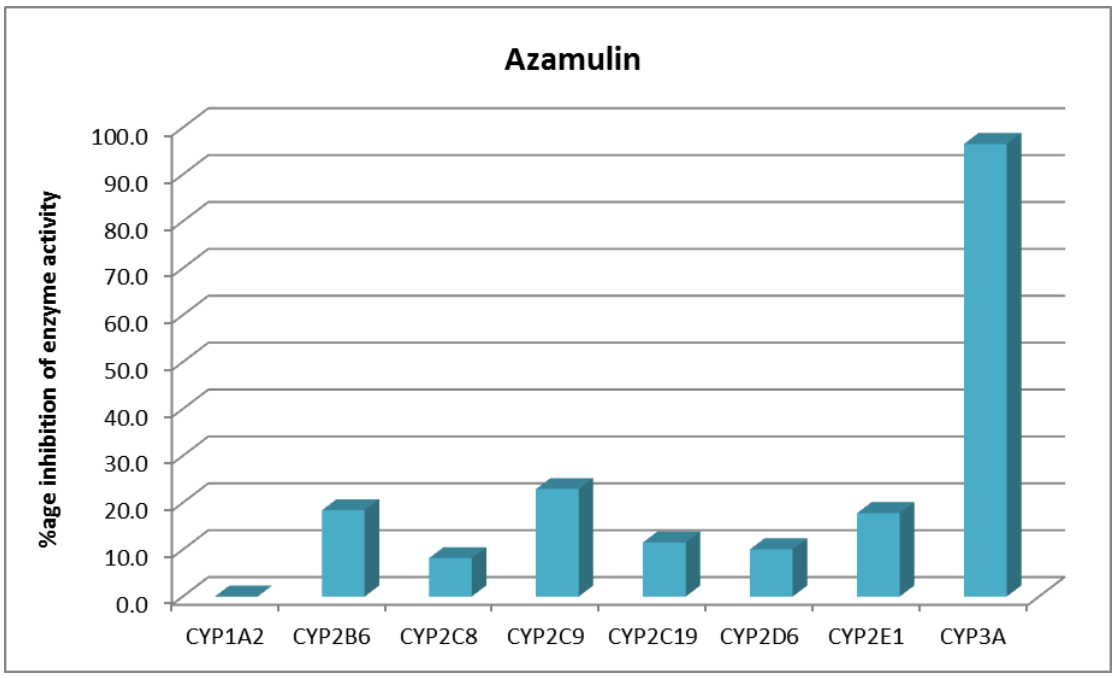

Figure 4.14: Inhibitory effect of azamulin on 8 different CYP450 isoform metabolic probe reactions

Azamulin is a synthetic azole derivative of pleuromutilin, a diterpene antibiotic first isolated from the fungus *Pleurotusmutilis*. This compound has been reported to be as potent an inhibitor of CYP3A isoforms as ketoconazole but more selective than the latter.[35]

Results from the cross inhibition assay for azamulin were consistent with data from the literature. Compared to ketoconazole, azamulin was observed to be a significantly more selective inhibitor, reducing CYP3A-mediated metabolism of midazolam by more than 95% while generally reducing the activity of the other CYP450 isoforms by less than 20%. A notable exception to the selectivity of azamulin appeared to be its relatively high cross-inhibition of CYP2C9 (22.9% inhibition) which was comparable to the effect observed with ketoconazole (26.5% inhibition). Considering that the concentration of all inhibitors used in these experiments were deliberately higher than their K_i values, the data obtained for azamulin cross-inhibition might suggest that in routine CYP450phenotyping assays, this compound might not significantly distort phenotyping data.

4.8 Compensating for Inhibitor Cross-Reactivity in CYP450 Phenotyping Data

The same mathematical approach reported by Lu *et al.* was applied to recalculate CYP450 phenotyping data by taking into consideration the determined maximal cross-inhibition effects of the 8 inhibitors tested.[13]

For this, a summary cross-inhibition matrix was generated as shown in **Table 4.4**:

Table 4.4: Percentage inhibition of CYP450 isoform activity by different chemical inhibitors

Inhibitor	CYP1A2	CYP2B6	CYP2C8	CYP2C9	CYP2C19	CYP2D6	CYP2E1	CYP3A
Furafylline	89.01	7.24	13.50	6.33	7.57	16.28	50.01	0.55
Montelukast	0.82	17.37	87.17	49.00	3.93	9.09	-1.02	33.56
Sulfaphenazole	12.57	1.56	10.04	89.14	11.10	7.42	26.84	8.02
Ticlopidine	66.76	97.23	21.37	18.89	86.81	54.38	21.04	-13.55
Quinidine	-0.21	11.06	8.99	4.14	16.19	89.33	30.43	2.87
DETC	33.74	39.81	21.33	20.02	8.05	36.72	31.81	6.62
Ketoconazole	11.68	41.90	44.74	26.52	-2.64	9.16	35.79	94.64
Azamulin	-2.64	18.40	8.17	22.90	11.52	10.06	17.77	96.52

Using the percentage cross-inhibition values determined for each inhibitor against the different CYP450 isoforms, it was possible to formulate simultaneous equations from data previously generated using conventional CYP450 phenotyping to more accurately represent the corrected contribution of different isoforms to compound metabolism.

An example of how this was done is illustrated. In this case, assuming a test compound determined to undergo metabolism mediated by more than one CYP450 isoform as follows:

Table 4.5: Hypothetical CYP450 phenotyping data uncorrected for inhibitor cross-reactivity

	CYP1A2	CYP2C8	CYP2C9	CYP2C19	CYP3A
Test Drug	17%	13%	19%	35%	70%

Incorporation of the corresponding cross-inhibition matrix data for the CYP450 isoforms involved in metabolism of such a compound would generate the following table and could be expressed in the form of an algebraic simultaneous equation as shown:

		% inhibition by chemical Inhibitor					
		CYP1A2	**CYP2C8**	**CYP2C9**	**CYP2C19**	**CYP3A**	***fm*,CYP(%)**
Furafylline	1A2	89.01	13.50	6.33	7.57	0.55	**17**
Montelukast	2C8	0.82	87.17	49.00	3.93	33.56	**13**
Sulfaphenazole	2C9	12.57	10.04	89.14	11.10	8.02	**19**
Ticlopidine	2C19	66.76	21.37	18.89	86.81	-13.55	**35**
Ketoconazole	3A	11.68	44.74	26.52	-2.64	94.64	**70**

$$
\begin{aligned}
0.8901q + 0.135r + 0.0633x + 0.0757y + 0.0055z &= 0.17\\
0.0082q + 0.8717r + 0.490x + 0.0393y + 0.3356z &= 0.13\\
0.1257q + 0.1004r + 0.8914x + 0.111y + 0.0802z &= 0.19\\
0.6676q + 0.2137r + 0.1889x + 0.8681y + 0.000z &= 0.35\\
0.1168q + 0.4474r + 0.2652x + 0.000y + 0.9464z &= 0.70
\end{aligned}
$$

Where the variables ***q, r, x, y,*** and***z*** represent the corrected *fm*,CYP values for CYP1A2, CYP2C8, CYP2C9, CYP2C19 and CYP3A, respectively.

Solving the equation can then be achieved using matrix calculations involving initial computation of an inverse matrix of all coefficients, as shown:

$$
\begin{pmatrix}
0.8901 & 0.1350 & 0.0633 & 0.0757 & 0.0055\\
0.0082 & 0.8717 & 0.4900 & 0.0393 & 0.3356\\
0.1257 & 0.1004 & 0.8914 & 0.1110 & 0.0802\\
0.6676 & 0.2137 & 0.1889 & 0.8681 & 0.0000\\
0.1168 & 0.4474 & 0.2652 & 0.0000 & 0.9464
\end{pmatrix}
\rightarrow
\begin{pmatrix}
1.1874 & -0.1933 & 0.0250 & -0.0979 & 0.0595\\
0.1337 & 1.4333 & -0.6645 & 0.0084 & -0.4527\\
-0.0483 & -0.0527 & 1.2105 & -0.1482 & -0.0836\\
-0.9355 & -0.1927 & -0.1190 & 1.2575 & 0.0839\\
-0.1962 & -0.06390 & -0.0282 & 0.0496 & 1.2867
\end{pmatrix}
$$

And then multiplying the inverse inhibition matrix with the original *fm,*CYP values thus:

$$
\begin{pmatrix}
1.1874 & -0.1933 & 0.0250 & -0.0979 & 0.0595\\
0.1337 & 1.4333 & -0.6645 & 0.0084 & -0.4527\\
-0.0483 & -0.0527 & 1.2105 & -0.1482 & -0.0836\\
-0.9355 & -0.1927 & -0.1190 & 1.2575 & 0.0839\\
-0.1962 & -0.06390 & -0.0282 & 0.0496 & 1.2867
\end{pmatrix}
\times
\begin{pmatrix}
17\\13\\19\\35\\70
\end{pmatrix}
=
\begin{pmatrix}
q, 18.88\\
r, -23.11\\
x, 10.45\\
y, 29.21\\
z, 79.63
\end{pmatrix}
$$

The final step in calculating corrected *fm*,CYP is the determination of metabolic contributions of each isoform as a percentage of the sum total of all the solved variables whose magnitude is greater than 0. Solved variables with negative values are interpreted to represent nil metabolic contribution by the isoform in question.

Thus, based on the foregoing correction calculation strategy, the corrected *fm,*CYP data for the hypothetical test drug is as tabulated below.

Table 4.6: Unmodified and corrected *fm*,CYP data based on consideration of inhibitor cross-reactivity for a hypothetical drug

	CYP1A2	**CYP2C8**	**CYP2C9**	**CYP2C19**	**CYP3A**
Unmodified *fm,CYP*	17%	13%	19%	35%	70%
Corrected *fm,CYP*	13.7%	0	7.6%	21.1%	57.6%

4.9 Application of Cross-Reactivity Correction to *fm*,CYP450 Data

The calculation strategy described in the previous section was applied in determining the corrected *fm,*CYP values for 15 Novartis in-house development compounds (**Table 4.7**) previously phenotyped using both conventional recombinant CYP450 mapping (**Table 4.8**) and pooled human liver microsomes with chemical inhibition. The uncorrected and modified chemical inhibition CYP450 phenotyping data for these compounds are summarised in **Table 4.9**.

Table 4.7: Physico-chemical properties of 15 test compounds phenotyped for CYP450 metabolism using conventional *in vitro* methods

Compound	Physico-Chemical Properties			
	Mwt	pKa	Log P	Solubility (g/L)
1	288.73	4.1/5.7	4.8	0.23
2	560.49	8.2/3.5	4.6	0.02
3	446.90	5.4/7.2	4.85	0.08
4	403.40	7.1/10.6	1.6	0.02
5	306.40	3.89/10.9	2.81	300
6	453.54	5.2	3.2	0.2
7	659.28	3.6/5.7	4.8	0.02
8	453.60	3.4	2.0	0.20
9	441.48	3.6/9.5	3.1	0.02
10	443.54	8.52/5.63	1.954	9.5
11	377.42	6.7/10.6	1.6	0.2
12	444.00	7.9	5.1	0.34
13	313.40	-	4.7	0.025
14	516.60	3.3/8.6	1.8	0.868
15	609.80	9.18	1.01	3.50

CYP450 isoform mapping using recombinant enzymes was performed by incubating the radiolabelled test compounds in a panel of 14 different recombinant human CYP450 (rhCYP450) enzymes expressed using bacullo-virus infected insect cells and quantifying the formation of metabolites by means of post-column radio-fluorescence detection following HPLC analysis of incubation samples.

Table 4.8: CYP450 phenotyping data from incubation of 15 Novartis test compounds in recombinant CYP450 isoforms

Compound	*fm*, CYP (%) using rhCYP450					
	CYP1A2	**CYP2C8**	**CYP2C9**	**CYP2C19**	**CYP2D6**	**CYP3A**
1	35.0	0	0	2.5	0.8	59.9
2	0	0	0	0	0.1	97.5
3	0.3	0	0	0	0.1	99.6
4	0	0	0	8.2	0	91.6
5	4.2	1.4	18.5	0.6	0.1	75.1
6	0.7	0	0	0	0.4	98.9
7	0	0	0	0	0	94.8
8	0.6	0	1.7	0.1	0.1	96.3
9	0.7	2.6	0	0.2	0	92.0
10	1.1	0	0	0	0	98.2
11	0	ND	0	ND	0	100
12	0	0.4	0	0.6	88.6	10.5
13	0	0.8	6.6	3.7	0.2	88.8
14	0	1.7	79.2	0.1	0	18.5
15	0	ND	0	0	0.4	99.6

Note: "ND" indicates that values were Not Determined for this compound. Only the contribution of the main hepatic CYP450 enzymes is tabulated.

All 15 test compounds were found to be substrates of rhCYP3A, which was the main enzyme contributing to the majority of metabolism in all except two cases (i.e. *fm*,CYP3A > 50%).

In the majority of cases, the contribution to metabolism of the other rhCYP450 isoforms appeared to be marginal at typically less than 5%. Notable exceptions to this trend were compounds **1** (where *fm,*CYP1A2 = 35.0%), **4**, (*fm,*CYP2C19 = 8.2%), **5** (*fm,*CYP2C9 = 18.5%), **12** (*fm,*CYP2D6 = 88.6%), **13** (*fm,*CYP2C8 = 6.6%) and compound **14** (*fm,*CYP2C9 = 79.2%).

Compound **5** was the only substrate found to be metabolised by 6 different isoforms to a quantifiable extent with most of the remaining compounds being metabolised by 2 to 4 different isoforms, with the exception of compound **7** which was only metabolised by CYP3A4 (*fm,*CYP = 94.8%) and extra-hepatic rhCYP450 enzymes (data not presented).

Table 4.9: Original unmodified and modified chemical inhibition CYP450 phenotyping data for 15 Novartis test compounds after correction for inhibitor cross-reactivity

Cmpd	CYP1A2		CYP2C8		CYP2C9		CYP2C19		CYP2D6		CYP3A*	
	Orig	Mod	Orig	Mod	Orig	Mod	Orig	Mod	Orig	Mod	Orig	Mod
1	56	71	-	-	-	-	23	0	-	-	33	29
2	16	16	4	0	3	0	-	-	12	11	77	74
3	-	-	-	-	-	-	-	-	-	-	80	100
4	-	-	-	-	-	-	23	25	-	-	75	75
5	17	14	13	0	19	8	35	21	-	-	70	58
6	-	-	-	-	-	-	-	-	19	15	100	85
7	-	-	-	-	10	3	-	-	-	-	88	97
8	-	-	-	-	-	-	-	-	-	-	99	100
9	-	-	-	-	-	-	-	-	-	-	100	100
10	-	-	-	-	-	-	-	-	-	-	75	100
11	13	8	-	-	21	9	-	-	13	8	100	75
12	-	-	65	45	-	-	37	0	49	36	55	19
13	-	-	19	0	32	26	-	-	12	10	71	64
14	-	-	31	0	77	73	29	13	10	5	25	9
15	-	-	-	-	-	-	-	-	1	0	96	100

***Note:** *fm,*CYP3A values reported here were determined using ketoconazole as chemical inhibitor.
'Orig' refers to the original *fm*,CYP450 values uncorrected for inhibitor cross-reactivity, '*Mod'* denotes recalculated *fm*,CYP450 after correction for inhibitor cross-reactivity

Since metabolism by CYP3A4 appeared to be universally significant for all 15 test compounds regardless of which phenotyping method was used, data from this enzyme was plotted to determine if correlation between CYP450 isoform mapping and chemical inhibition phenotyping was improved by correcting for inhibitor cross-reactivity (**Figure 4.15** and **Figure 4.16**).

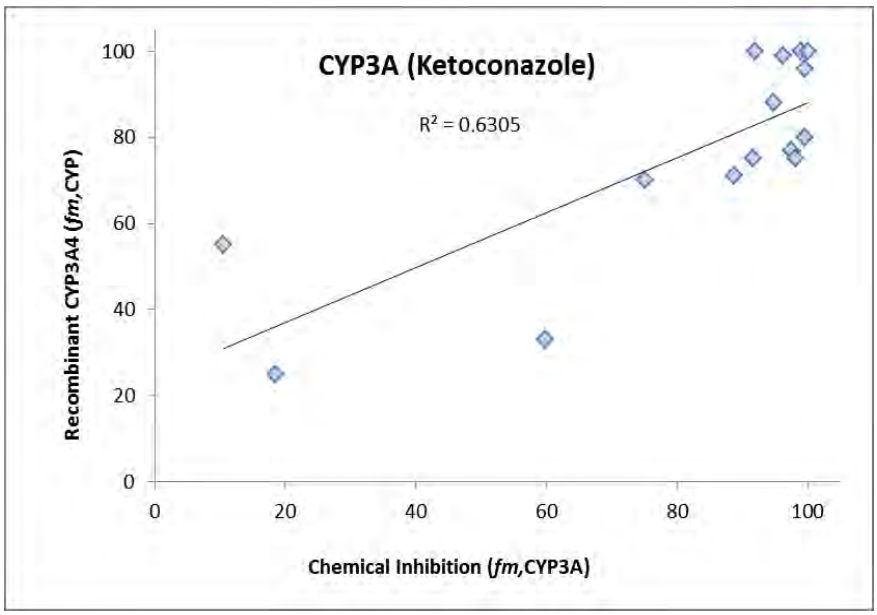

Figure 4.15: Correlation plot of *fm*,CYP3A using rhCYP3A4 and HLM + ketoconazole before correction for inhibitor cross-reactivity

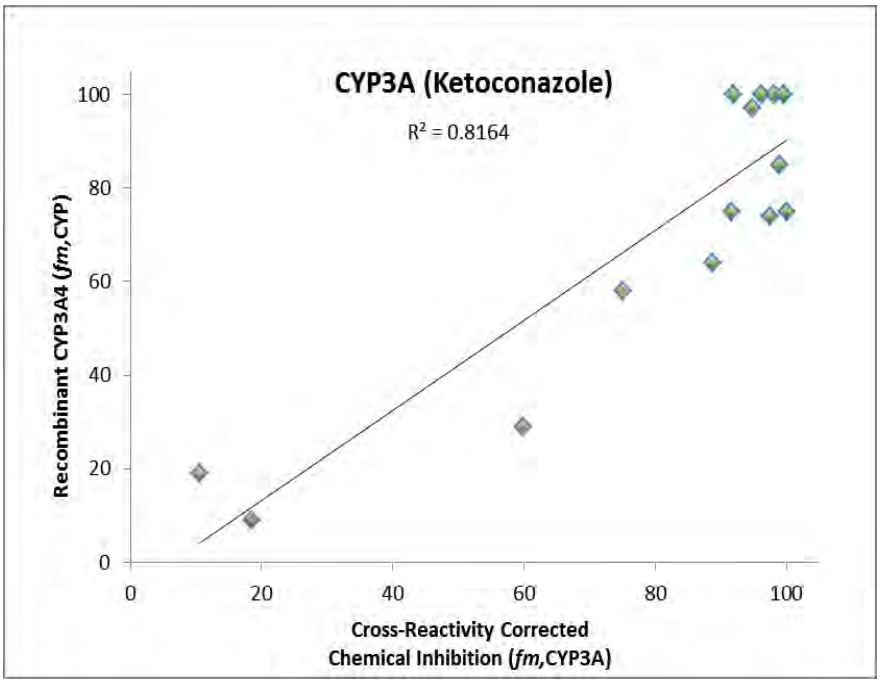

Figure 4.16: Correlation plot of *fm*,CYP3A data using rhCYP3A4 and HLM + ketoconazole after correction for inhibitor cross-reactivity

The square of the Pearson correlation coefficient (r^2) for *fm*,CYP3A data for the 15 test compounds from phenotyping using recombinant enzymes and chemical inhibition with ketoconazole increased from 0.6305 to 0.8164 when corrected for cross-inhibition.

Similar evaluation of the impact of cross-reactivity correction was carried out using data obtained when azamulin had been used as the chemical inhibitor to determine CYP3A contribution to metabolism. In this case, however, only 11 of the 15 test compounds had been phenotyped using azamulin, and therefore fewer data points were available for comparison against rCYP3A data.

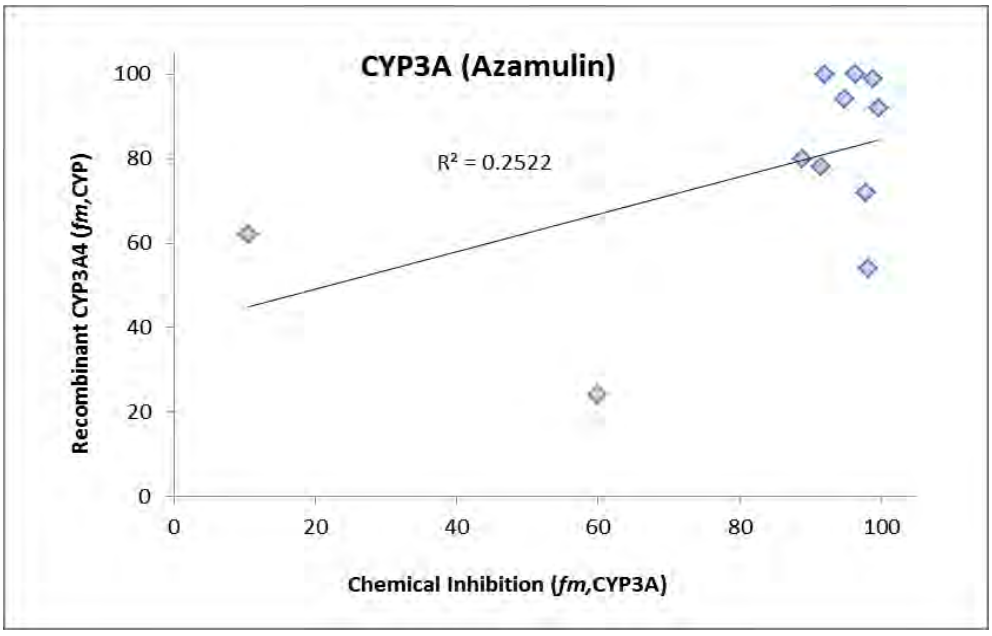

Figure 4.17: Correlation plot of *fm*,CYP3A using rCYP3A4 and HLM + azamulin before correction for inhibitor cross-reactivity

As observed with ketoconazole, cross-reactivity correction with azamulin also appeared to improve the correlation between rCYP3A and chemical inhibition phenotyping data, with the r^2 value increasing from 0.2522 (**Figure 4.17**) to 0.6100 (**Figure 4.18**).

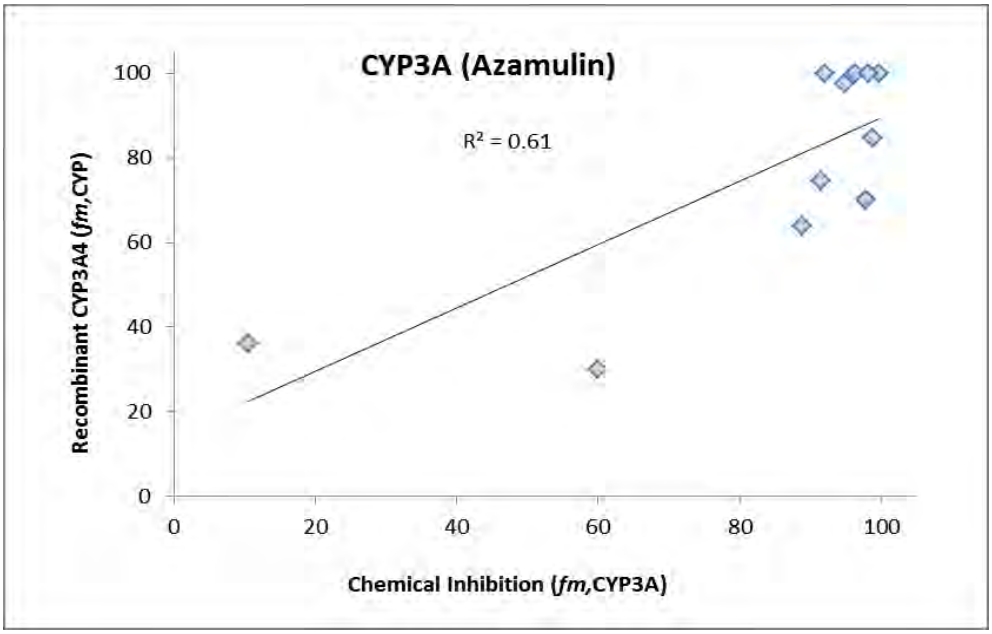

Figure 4.18: Correlation plot of *fm*,CYP3A using rCYP3A4 and HLM + azamulin after correction for inhibitor cross-reactivity

A final comparison of the effect of correcting for inhibitor cross-reactivity involved testing the improvement in correlation of *fm*,CYP3A among the same compounds from the test set for which metabolic contribution of CYP3A isoform had been determined using both azamulin and ketoconazole.

Table 4.10: Uncorrected *fm*,CYP3A values for compounds phenotyped using both azamulin and ketoconazole

	***fm*,CYP3A (%)**										
Compound	**1**	**2**	**3**	**4**	**6**	**7**	**8**	**9**	**10**	**12**	**13**
Azamulin	24	72	92	78	99	94	100	100	54	62	80
Ketoconazole	33	77	80	75	100	88	99	100	75	55	71
						r^2 = 0.8509					

Table 4.11: Modified *fm*,CYP3A values for compounds phenotyped using both azamulin and ketoconazole after correction for inhibitor cross-reactivity

	Corrected *fm*,CYP3A (%)										
Compound	**1**	**2**	**3**	**4**	**6**	**7**	**8**	**9**	**10**	**12**	**13**
Azamulin	29.9	70.1	100	74.5	84.8	97.5	100	100	100	36.2	63.9
Ketoconazole	29.3	73.6	100	74.9	85.3	96.9	100	100	100	18.8	64.4
						r^2 = 0.9734					

The uncorrected CYP3A chemical inhibition values for the 11 compounds showed a high degree of similarity even before the effects of inhibitor cross-reactivity were taken into consideration. The two sets of data had a correlation coefficient (r^2) of 0.8509 for *fm,*CYP3A. However, correction of the phenotyping data by factoring in the cross-reactivity of both ketoconazole and azamulin markedly improved the observed correlation to r^2 = 0.9734, further illustrating the ability of the correction calculation to minimise differences in the data sets.

4.10 Conclusions

The cross-reactivity experiments described in this Chapter confirmed the CYP450 enzyme inhibition activity of 7 out of the 8 chemical inhibitors routinely used in early CYP450 metabolic phenotyping assays. All the compounds tested exhibited varying degrees of cross-reactivity against different CYP450-mediated metabolic reactions both in terms of the absolute number of reactions (or enzyme isoforms) affected, as well as the degree to which the individual reactions were inhibited. Of the inhibitors evaluated, only diethyldithiocarbamate exhibited poor potency against its established marker metabolic probe reaction (i.e. conversion of chlorzoxazone to 6-hydroxychlorzoxazone by CYP2E1). In contrast, all the other chemical inhibitors were found to reduce the activity of each of their respective marker probe reactions by between 86.8% and 97.2%. In addition, DETC was found to exhibit the highest relative cross-inhibitory effect against the other CYP450 isoforms, inhibiting CYP1A2, CYP2B6 and CYP2D6 to an even greater extent than its observed inhibition of CYP2E1.

On the basis of absolute magnitude and number of cross-inhibitions observed from the compounds evaluated, furafylline and sulfaphenazole appeared to be the most selective of the CYP450 inhibitors tested. These two compounds were each found to inhibit only one other metabolic reaction by more than 20%, in addition to inhibiting their respective probe substrate biotransformations by almost 90%.

Evaluation of the effect of correcting for inhibitor cross-reactivity on CYP450 reaction phenotyping data determined using different *in vitro* techniques for a set of 15 in-house compounds was performed by calculating statistical correlation. Correction of ketoconazole and azamulin cross-reactivity appeared to improve the correlation in

CYP3A phenotyping data separately determined using rCYP450 and HLM with chemical inhibition. Additionally, it was also observed to improve the correlation of *fm*,CYP3A data from microsomal chemical inhibition individually determined using both ketoconazole or azamulin on the same set of test compounds.

REFERENCES:

(1) Wijnen, P. A. H. M.; Op den Buijsch, R. A. M.; Drent, M.; Kuijpers, P. M. J. C.; Neef, C.; Bast, A.; Bekers, O.; Koek, G. H. The Prevalence and Clinical Relevance of Cytochrome P450 Polymorphisms. *Alimentary Pharmacology & Therapeutics* **2007**, *26 Suppl 2*, 211–219.

(2) Zhang, H.; Davis, C. D.; Sinz, M. W.; Rodrigues, A. D. Cytochrome P450 Reaction-Phenotyping: An Industrial Perspective. *Expert Opinion on Drug Metabolism & Toxicology* **2007**, *3*, 667–687.

(3) Lu, A. Y. H.; Wang, R. W.; Lin, J. H. Cytochrome P450 In Vitro Reaction Phenotyping: A Re-Evaluation of Approaches Used for P450 Isoform Identification. *Drug Metabolism and Disposition* **2003**, *31*, 345–350.

(4) Krausz, K. W.; Goldfarb, I.; Buters, J. T. M.; Yang, T. J.; Gonzalez, F. J.; Gelboin, H. V. Monoclonal Antibodies Specific and Inhibitory to Human Cytochromes P450 2C8, 2C9, and 2C19. *Drug Metabolism and Disposition* **2001**, *29*, 1410–1423.

(5) Harper, T. W.; Brassil, P. J. Reaction Phenotyping: Current Industry Efforts to Identify Enzymes Responsible for Metabolizing Drug Candidates. *The AAPS Journal* **2008**, *10*, 200–207.

(6) Crespi, C. L.; Miller, V. P. The Use of Heterologously Expressed Drug Metabolizing Enzymes-State of the Art and Prospects for the Future. *Pharmacology & Therapeutics* **1999**, *84*, 121–131.

(7) Madan, A.; Usuki, E.; Burton, L. A.; Ogilvie, B. W.; Parkinson, A. In Vitro Approaches for Studying the Inhibition of Drug-Metabolizing Enzymes and Identifying the Drug-Metabolizing Enzymes Responsible for the Metabolism of Drugs. In *Drug-Drug Interactions*; Rodrigues, A. D., Ed.; Marcel Dekker, Inc: New York, NY, 2002; pp. 217–294.

(8) Tucker, G. T.; Houston, J. B.; Huang, S. M. Optimizing Drug Development: Strategies to Assess Drug Metabolism/transporter Interaction Potential-

toward a Consensus. *Clinical Pharmacology and Therapeutics* **2001**, *70*, 103–114.

(9) Bjornsson, T. D.; Callaghan, J. T.; Einolf, H. J.; Fischer, V.; Gan, L.; Grimm, S.; Kao, J.; King, S. P.; Miwa, G. T.; Ni, L.; Kumar, G.; McLeod, J.; Obach, R. S.; Roberts, S.; Roe, A.; Shah, A.; Snikeris, F.; Sullivan, J. T.; Tweedie, D.; Vega, J. M.; Walsh, J.; Wrighton, S. A. The Conduct of in Vitro and in Vivo Drug-Drug Interaction Studies: A Pharmaceutical Research and Manufacturers of America (PhRMA) Perspective. *Drug Metabolism and Disposition* **2003**, *31*, 815–832.

(10) Rodrigues, A. D. Integrated Cytochrome P450 Reaction Phenotyping. *Biochemical Pharmacology* **1999**, *57*, 465–480.

(11) Proctor, N. J.; Tucker, G. T.; Rostami-Hodjegan, A. Predicting Drug Clearance from Recombinantly Expressed CYPs: Intersystem Extrapolation Factors. *Xenobiotica* **2004**, *34*, 151–178.

(12) Khojasteh, S. C.; Prabhu, S.; Kenny, J. R.; Halladay, J. S.; Lu, A. Y. H. Chemical Inhibitors of Cytochrome P450 Isoforms in Human Liver Microsomes: A Re-Evaluation of P450 Isoform Selectivity. *European Journal of Drug Metabolism and Pharmacokinetics* **2011**, *36*, 1–16.

(13) Lu, C.; Miwa, G. T.; Prakash, S. R.; Gan, L.; Balani, S. K. A Novel Model for the Prediction of Drug-Drug Interactions in Humans Based on in Vitro Cytochrome p450 Phenotypic Data. *Drug Metabolism and Disposition* **2007**, *35*, 79–85.

(14) Yuan, R.; Madani, S.; Wei, X.-X.; Reynolds, K.; Huang, S.-M. Evaluation of Cytochrome P450 Probe Substrates Commonly Used by the Pharmaceutical Industry to Study in Vitro Drug Interactions. *Drug Metabolism and Disposition* **2002**, *30*, 1311–1319.

(15) Sesardic, D.; Boobis, A. R.; Murray, B. P.; Murray, S.; Segura, J.; de la Torre, R.; Davies, D. S. Furafylline Is a Potent and Selective Inhibitor of Cytochrome P450IA2 in Man. *British Journal of Clinical Pharmacology* **1990**, *29*, 651–663.

(16) Kunze, K. L.; Trager, W. F. Isoform-Selective Mechanism-Based Inhibition of Human Cytochrome P450 1A2 by Furafylline. *Chemical Research in Toxicology* **1993**, *6*, 649–656.

(17) Eagling, V. A.; Tjia, J. F.; Back, D. J. Differential Selectivity of Cytochrome P450 Inhibitors against Probe Substrates in Human and Rat Liver Microsomes. *British Journal of Clinical Pharmacology* **1998**, *45*, 107–114.

(18) Newton, D. J.; Wang, R. W.; Lu, A. Y. H. Evaluation of Specificities in the the in Vitro Metabolism of Therapeutic Agents by Human Liver Microsomes. *Drug Metabolism and Disposition* **1995**, *23*, 154–158.

(19) Maffrand, J.-P. The Story of Clopidogrel and Its Predecessor, Ticlopidine: Could These Major Antiplatelet and Antithrombotic Drugs Be Discovered and Developed Today? *Comptes Rendus Chimie* **2012**, *15*, 737–743.

(20) Ha-Duong, N.-T.; Dijols, S.; Macherey, A.-C.; Goldstein, J. A.; Dansette, P. M.; Mansuy, D. Ticlopidine as a Selective Mechanism-Based Inhibitor of Human Cytochrome P450 2C19 †. *Biochemistry* **2001**, *40*, 12112–12122.

(21) Hagihara, K.; Nishiya, Y.; Kurihara, A.; Kazui, M.; Farid, N. A.; Ikeda, T. Comparison of Human Cytochrome P450 Inhibition by the Thienopyridines Prasugrel, Clopidogrel, and Ticlopidine. *Drug Metabolism and Pharmacokinetics* **2008**, *23*, 412–420.

(22) Turpeinen, M.; Tolonen, A.; Uusitalo, J.; Jalonen, J.; Pelkonen, O.; Laine, K. Effect of Clopidogrel and Ticlopidine on Cytochrome P450 2B6 Activity as Measured by Bupropion Hydroxylation. *Clinical Pharmacology and Therapeutics* **2005**, *77*, 553–559.

(23) Turpeinen, M.; Nieminen, R.; Juntunen, T.; Taavitsainen, P.; Raunio, H.; Pelkonen, O. Selective Inhibition of CYP2B6-Catalyzed Bupropion Hydroxylation in Human Liver Microsomes in Vitro. *Drug Metabolism and Disposition* **2004**, *32*, 626–631.

(24) Walsky, R. L.; Obach, R. S. A Comparison of 2-Phenyl-2-(1-Piperidinyl)propane (ppp), 1,1',1''-Phosphinothioylidynetrisaziridine (thioTEPA), Clopidogrel, and

Ticlopidine as Selective Inactivators of Human Cytochrome P450 2B6. *Drug Metabolism and Disposition* **2007**, *35*, 2053–2059.

(25) Walsky, R. L.; Obach, R. S.; Gaman, E. A.; Gleeson, J.-P. R.; Proctor, W. R. Selective Inhibition of Human Cytochrome P4502C8 by Montelukast. *Drug Metabolism and Disposition* **2005**, *33*, 413–418.

(26) Otton, S. V.; Inaba, T.; Kalow, W. Competitive Inhibition of Sparteine Oxidation in Human Liver by B-Adrenoceptor Antagonists and Other Cardiovascular Drugs. *Life Sciences* **1984**, *34*, 73–80.

(27) Ching, M. S.; Blake, C. L.; Ghabrial, H.; Ellis, S. W.; Lennard, M. S.; Tucker, G. T.; Smallwood, R. A. Potent Inhibition of Yeast-Expressed CYP2D6 by Dihydroquinidine, Quinidine, and Its Metabolites. *Biochemical Pharmacology* **1995**, *50*, 833–837.

(28) Pelkonen, O.; Maenpaa, J.; Taavitsainen, P.; Rautio, A.; Raunio, H. Inhibition and Induction of Human Cytochrome P450 (CYP) Enzymes. *Xenobiotica* **1998**, *28*, 1203–1253.

(29) Pelkonen, O.; Turpeinen, M.; Hakkola, J.; Honkakoski, P.; Hukkanen, J.; Raunio, H. Inhibition and Induction of Human Cytochrome P450 Enzymes: Current Status. *Archives of Toxicology* **2008**, *82*, 667–715.

(30) Chang, T. K. H.; Gonzalez, F. J.; Waxman, D. J. Evaluation of Triacetyloleandomycin, A-Nasymphthoflavone and Diethyldithiocarbamate as Selective Chemical Probes for Inhibition of Human Cytochromes P450. *Archives of Biochemistry and Biophysics* **1994**, *311*, 437–442.

(31) Guengerich, F. P.; Kim, D. H.; Iwasaki, M. Role of Human Cytochrome P-450 IIE1 in the Oxidation of Many Low Molecular Weight Cancer Suspects. *Chemical Research in Toxicology* **1991**, *4*, 168–179.

(32) Greenblatt, D. J.; Zhao, Y.; Venkatakrishnan, K.; Duan, S. X.; Harmatz, J. S.; Parent, S. J.; Court, M. H.; von Moltke, L. L. Mechanism of Cytochrome P450-3A Inhibition by Ketoconazole. *The Journal of Pharmacy and Pharmacology* **2011**, *63*, 214–221.

(33) Venkatakrishnan, K.; von Moltke, L. L.; Greenblatt, D. J. Effects of the Antifungal Agents on Oxidative Drug Metabolism: Clinical Relevance. *Clinical Pharmacokinetics* **2000**, *38*, 111–180.

(34) Obach, R. S.; Walsky, R. L.; Venkatakrishnan, K.; Gaman, E. A.; Houston, J. B.; Tremaine, L. M. The Utility of in Vitro Cytochrome P450 Inhibition Data in the Prediction of Drug-Drug Interactions. *The Journal of Pharmacology and Experimental Therapeutics* **2006**, *316*, 336–348.

(35) Stresser, D. M.; Broudy, M. I.; Ho, T.; Cargill, C. E.; Blanchard, A. P.; Sharma, R.; Dandeneau, A. A.; Goodwin, J. J.; Turner, S. D.; Erve, J. C. L.; Patten, C. J.; Dehal, S. S.; Crespi, C. L. Highly Selective Inhibition of Human CYP3A in Vitro by Azamulin and Evidence That Inhibition Is Irreversible. *Drug Metabolism and Disposition* **2004**, *32*, 105–112.

CHAPTER FIVE:

SUMMARY, CONCLUSIONS AND RECOMMENDATIONS FOR FUTURE WORK

5.1 Summary and Conclusions

A virtual database of 335 natural products was designed, created and populated with compounds isolated from medicinal plants reported in the *African Herbal Pharmacopoeia.* The chemical space of these compounds was mapped by conducting statistical comparisons of their 'drug-like properties' against those for 608 conventional drug molecules selected from the *British Pharmacopoeia 2009.* The *in silico* profiling data showed that the chemical space of the natural products was significantly different from that of synthetic drugs with regard to molecular weight, rotatable bonds and H-bond donor distributions but not with regard to lipophilicity (cLogP) and H-bond acceptor distributions. In general, the natural products were found to exhibit a higher degree of deviation from Lipinski's 'Rule-of-Five'. The observations based on evaluation of the five physico-chemical parameters outlined above were further confirmed using 2D principle component analysis based on a more comprehensive *in silico* prediction of 196 properties for the natural product and BP 2009 compound datasets. Again using *in silico* tools to identify structural alerts in the different compound sets, the natural products appeared to possess a slightly greater number of structural alerts per molecule (1.18) compared to conventional drugs (0.99), suggesting that they might be more prone to metabolic bioactivation.

Although used principally as a repository for compound data from which predictions of physico-chemical properties of natural products could be made, the natural products database created in this work could conceivably serve as a starting point for a larger collection of compounds not restricted to monographs from the *African Herbal Pharmacopoeia*. Even in its current unexpanded format, the compounds in the database could be used in ligand or structure based virtual screening to identify potential hits against known pharmacological targets or in docking studies to predict binding to known protein drug targets.

Evaluation of a set of 15 natural product and natural product-derived compounds for *in vitro* bioactivation was conducted using a combination of CYP450 enzyme inactivation assays and reactive metabolite trapping experiments. Of the major recombinant CYP450 drug metabolizing isoforms screened, CYP3A4 was found to be most prone to inhibition by the test compounds. This phenomenon was presumably due to the fact that the active site of CYP3A4 is relatively large and capable of accommodating a broad array of substrates possessing diverse chemical scaffolds. Among the compounds screened for enzyme inhibition, **GEDN, JSTN and JMCN** were the most potent CYP3A4 inhibitors with **GEDN** in particular also exhibiting potent inhibition of CYP2C19. Although the observed inhibition of CYP3A4 by these three compounds was significant, assays to determine their normalized inhibition ratios indicated that the reactions were not time-dependent and therefore unlikely to be due to reactive metabolite-mediated mechanism-based inactivation of the enzyme. These results were further validated by the fact that inclusion of reduced glutathione in the assays had no effect on the observed inhibition of the enzyme. Inhibition of the other main drug metabolising CYP450 isoforms (i.e. CYP1A2, CYP2C9 and CYP2C19) was markedly less pronounced, with only one or two compounds reducing enzyme activity by up to 50% at the lower assay concentration in all cases.

Direct assessment of the formation of reactive metabolic intermediates was conducted by incubating 11 of the 15 compounds in microsomal preparations fortified with nucleophilic trapping agents. None of the test compounds appeared to form detectable reactive intermediates that could be trapped using reduced glutathione. On the other hand, however, using methoxylamine as the trapping agent, metabolic incubations of the monosubstituted furan ring-containing compounds **GEDN** and the tetraol **DC3** were found to contain components strongly suspected to be trapped reactive metabolites. Despite its structural similarity to **DC3**, the α,β-unsaturated cyclic ketone **DC14** did not appear to form reactive metabolic intermediates that could be trapped using methoxylamine. This observation was presumably partly due to the relatively lower ability of **DC14** to interact with enzyme amino acid residues via H-bonding owing to the presence of far fewer hydroxyl groups compared to **DC3**. Only **MTGN** possessed the structural features necessary to

undergo bioactivation resulting in formation of reactive iminium ion intermediates. However, absence of detectable trapped adducts in microsomal incubations fortified with potassium cyanide as the trapping agent suggested that metabolic bioactivation did not occur as hypothesized.

The results from *in vitro* bioactivation assays highlighted the difficulties of predicting reactive metabolite formation based only on the presence of structural alerts in substrate molecules. Despite most of the tested natural products bearing a potential structural liability that could easily be detected using *in silico* tools, their metabolic liability did not appear to be supported by *in vitro* results. In the case of **DC14** and **DC3**, for example, *in vitro* data seemed to contradict the expected greater risk of bioactivation of **DC14** compared to **DC3** based on the greater number of structural alerts present in the former (2) compared to the latter (1). The set of compounds studied cannot realistically be used as a basis for drawing concrete conclusions regarding the bioactivation potential of natural products in general, owing to its limited size. However, the results obtained seemed to suggest that bioactivation risks might be more accurately predicted on the basis of the type of structural alert present on the test compound, rather than by the absolute number of structural alerts present in the molecule.

Evaluation of the cross-reactivity of eight chemical inhibitors commonly used in early CYP450 phenotyping assays confirmed the relatively high selectively of furafylline and sulfaphenazole while conversely revealing the low selectivity of ticlopidine and diethyldithiocarbamate. These experiments also highlighted the particularly low potency of diethylthiocarbamate as the routinely preferred inhibitor for determining the contribution of hepatic CYP2E1 to xenobiotic metabolism. The data obtained provided good evidence for the need to identify and characterise a superior replacement inhibitor for CYP2E1 phenotyping.

The compound data set used to test the hypothesis that factoring-in inhibitor cross-reactivity in CYP450 phenotyping calculations could improve the correlation of data obtained from different phenotyping approaches was of limited size. Consequently, it was not possible to confirm the statistical significance of improvement in CYP450

phenotyping correlation for the majority of enzyme isoforms for which inhibitor cross-reactivity was evaluated. In the case of CYP3A4, however, there were sufficient, albeit few, data points to provide evidence that consideration of inhibitor cross-reactivity in *fm,*CYP3A4 calculations appeared to improve phenotyping data correlation. Improvement in the *fm,*CYP3A4 correlation was observed both between data values obtained using different CYP3A4 chemical inhibitors (i.e. ketoconazole and azamulin) as well as with hepatic microsome+chemical inhibitor-derived vs recombinant enzyme-determined *fm,*CYP3A4 values.

From a pharmaceutical industry DMPK perspective, the potential to improve CYP450 phenotyping by correcting for inhibitor cross-reactvity offers an opportunity of eliminating the need to use multiple phenotyping techniques as is currently the norm, when conducting routine CYP450 phenotyping. Having a single method that is validated to provide consistent and accurately correlated data would contribute in reducing the time, cost and effort needed to assess the metabolic fate of drug leads during development, without compromising on the accuracy of such assessments.

5.2 Recommendations for Future Work

Of the natural products tested for *in vitro* bioactivation in this work, **GEDN, CLPG, JMCN** and **JSTN** were each found to be potent inhibitors of at least one of the four CYP450 enzyme isoforms involved in drug metabolism (i.e. CYP1A2, CYP2C9, CYP2C19 and CYP3A4). However, since the enzyme inhibition assays carried out in this project were designed more for use in rapid screening of large compound sets to identify potential bioactivation liabilities early, comprehensive determination of IC_{50} values was not carried out. It might therefore be of interest to conduct further work aimed at determining the enzyme inhibition characteristics of these specific compounds and establish the mode in which they curtail enzyme activity i.e. is the observed inhibition competitive, non-competitive, uncompetitive or mixed.

Although the natural products mentioned above inhibited recombinant CYP450 enzymes *in vitro*, the actual impact of such inhibition *in vivo* is difficult to predict although the potential for herb-drug interaction exists. Based on data obtained in

this work, it might be of particular interest to investigate, possibly *in vivo* using an animal model, the effect of co-administration of these natural products on the metabolism of conventional drug substrates of the CYP450 isoforms affected. For example, the impact of inhibition of CYP2C19 and CYP3A4 by **Gedunin** in neem extract in patients also taking the prophylactic antimalarial proguanil, which is metabolised to its active form (cycloguanil) by these two isoforms, could be investigated both *in vitro* and *in vivo* using the pure natural product or the standardized crude plant extract.

The trapped reactive intermediates detected from microsomal incubations of **GEDN** and **DC3** with methoxylamine were hypothesized to arise from bioactivation of the furan-ring, based on cited literature. Isolation and actual characterisation of these intermediates using spectroscopic techniques such as NMR would provide structural data that could more conclusively shed light on the actual bioactivation mechanism involved and the molecular structure of the stable adducts detected using LC-MS. A key consideration in successful implementation of such an enterprise would involve the need to generate a sufficient amount of the trapped intermediate possibly through scaling-up of metabolic incubations to facilitate comprehensive structure elucidation.

Another area for possible exploration regarding the formation of reactive metabolites from **GEDN** and **DC3** would be to determine the specific enzyme isoform(s) responsible for the suspected bioactivation by conducting enzyme phenotyping assays modified to incorporate trapping agents.

The consideration of chemical inhibitor cross-reactivity in routine *in vitro* CYP450 phenotyping calculations offers potential advantages from a drug development perspective, not least in significantly reducing the time and effort taken to obtain reliable CYP450 phenotyping data without compromising accuracy and integrity. Inasmuch as the data obtained from this work showed promise in application, several other considerations require further investigation to develop this approach as a robust cross-reactivity compensation strategy. For example, testing the cross-reactivity of the different inhibitors evaluated under a range of concentrations below and above their established K_i or IC_{50} values would provide greater insights on the actual impact of cross-reactivity. Furthermore, in order to gauge the true impact of

compensating for chemical inhibitor cross-reactivity, the correlation of a much larger data set of compounds tested using traditional CYP450 isoform mapping and uncorrected chemical inhibition would need to be compiled and computed, and preferably include as many of the main drug metabolising CYP450 isoforms as possible.

The cross-reactivity data obtained in this work highlighted the particularly poor potency and low selectivity of diethyldithiocarbamate (DETC), underscoring the need to identify and characterise the enzyme inhibition properties of superior substitute CYP2E1 chemical inhibitors. Based on the potent enzyme inhibition activities observed from the few natural products studied in this work, it might be worthwhile to consider the search for new selective inhibitors for CYP2E1 phenotyping from among existing natural product libraries.

CHAPTER SIX:

EXPERIMENTAL

6.1 Reagents and Solvents

All commercially available analytical grade chemicals and reagents were purchased from Sigma Aldrich. HPLC grade acetonitrile and methanol for mobile phase preparation were purchased from Romil Ltd (Cambridge, UK). Analytical grade solvents including hexane, dichloromethane, ethyl acetate, acetone, methanol and ethanol were purchased from Kimix Chemicals (Eppindust, South Africa) and used without further purification. Ultra purified water for *in vitro* assays was prepared in-house using a Millipore Direct-Q®3 laboratory water purification system (Millipore SAS, Molsheim, France).

6.2 Turbidimetric Solubility[1]

Solubility of the test compounds was determined using the turbidimetric method described by Bevan and Lloyd.[2] Stock solutions of test and control compounds were prepared by dissolving an accurately weighed amount of each in HPLC-grade DMSO to a 10 mM concentration.

Predilutions of the stock solutions, also in DMSO, were then prepared in clear, v-shaped bottom 96-well polystyrene microtitre plates**.** For this, each stock solution was diluted serially in triplicate by first pipetting 20 µL DMSO into wells in row G on the plate and 50 µL DMSO to the wells in the rows above (i.e. rows F, E, D…A). 80 µL of the 10 mM stock solutions was then pipetted to the wells in row G and mixed to give a starting concentration of 8 mM (100 µL). Serial dilution of this solution was achieved by subsequently transferring 50 µL to the well in the row above (row F), mixing and then repeating this sequence to wells from row F through to B. The final predilution concentrations obtained ranged from 0.25 mM (Row B) to 8.0 mM (Row G). All wells in row A contained only DMSO with no compound present, while those in row H contained the undiluted 10 mM stock solution as illustrated in **Figure 6.1**.

Conc (mM)		Compound 1 (in triplicate)			Compound 2 (in triplicate)…		
		1	2	3	4	5	6
0.00	A						
0.25	B						
0.50	C						
1.00	D						
2.00	E						
4.00	F						
8.00	G						
10.00 (stock)	H						

Figure 6.1: Turbidimetric solubility assay pre-dilution plate set-up

From each pre-dilution solution, secondary dilutions of the compounds in both DMSO and 0.01M pH 7.4 phosphate buffered saline (PBS) were prepared in a second 96-well plate, also in triplicate (**Figure 6.2**). Wells in columns 1-6 contained the test compound dissolved in DMSO while those in columns 7-12 contained samples in PBS at similar nominal concentrations. Because compounds were tested in triplicate, only two (2) could be accommodated on each plate.

Conc (µM)		DMSO						0.01M pH 7.4 PBS					
		Cmpd 1 (tripl)			Cmpd 2 (tripl)			Cmpd 1 (tripl)			Cmpd 2 (tripl)		
		1	2	3	4	5	6	7	8	9	10	11	12
0.0	A												
5.0	B												
10.0	C												
20.0	D												
40.0	E												
80.0	F												
160.0	G												
200.0	H												

Figure 6.2: Turbidimetric assay plate lay-out

The final volume of solution in the assay plate wells was 200 µL, prepared by pipetting 4 µL each of solution from the pre-dilution plate to the corresponding well into both DMSO and PBS (both 196 µL). The final concentration of DMSO in the PBS aqueous buffer preparations was therefore 2% v/v.

The concentrations of test compounds in DMSO served as controls for determining potential false turbidimetric absorbance readings arising from the compounds in solution absorbing radiation at the analysis wavelength.

The plates were covered and left to equilibrate for 2 hours at ambient room temperature. After incubation, UV-VIS absorbance readings were measured at 620 nm using a SpectraMax 340PC[384] microplate reader (Molecular Devices, Sunnydale, CA). Absorbance from the wells containing only DMSO and 2%v/v DMSO in PBS (i.e. denoted as 0.0 μM in plate layout, Row A) served as controls and blanks.

Obstruction of incident radiation by particles of the test compounds that crashed out of solution at concentrations in excess of the limit of solubility, denoted by an increase in the apparent absorbance measurement, was used as the basis for determining approximate compound solubility.

6.3 Physical and Spectroscopic Characterization

Melting points were determined using a Reichert-Jung Thermovar hot stage microscope based on methods described by Kofler and Kofler and are reported as uncorrected values.[3,4]

^{1}H NMR spectral data was recorded on a Varian Mercury (300MHz), a Varian Unity (400 MHz) or a Bruker Ultrashield-Plus (400MHz) spectrometer. All NMR samples were dissolved in deuterated chloroform ($CDCl_3$) or dimethylsulfoxide (DMSO-d_6) with tetramethylsilane (TMS) as the internal standard. ^{13}C NMR spectral data were recorded on the same instruments at 100 MHz. Chemical shifts (δ) are reported in parts per million (ppm) downfield with reference to the internal standard tetramethylsilane. Coupling constants (*J*) are reported in Hertz (Hz). The abbreviations used in assigning ^{1}H-NMR signals are: d (doublet), dd (doublet of doublets), m (multiplet), q (quartet), s (singlet) or t (triplet).

6.4 Chromatography

6.4.1 Thin Layer Chromatography

Preliminary natural product compound purity checks and reactions in the synthesis of CYP450 fluorogenic probe substrates were monitored on aluminium-backed, pre-coated thin layer chromatography (TLC) plates and visualized under ultraviolet light at 254 nm and 366 nm or by spraying with a detection solution of ninhydrin in acidified ethanol.

6.4.2 Flash Column Chromatography

Compound purification was achieved using automated low pressure flash column chromatography carried out on a Biotage Isolera™ Prime Flash Chromatography system (Biotage AB, Uppsala, Sweden). Compound separation and elution were monitored on the in-built dual wavelength UV-detector. Separations were achieved on 25 g Biotage SNAP™ cartridges packed with 40-65 µm diameter KP-Sil normal silica particles as stationary phase.

6.4.3 High Performance Liquid Chromatography

6.4.3.1 System 1 and 2 - Compound purity and molecular mass checks

The purities of the synthesized fluorogenic enzyme probe substrates and natural products were determined using HPLC using either of two chromatographic systems. **System 1** was a SpectraSERIES™ HPLC (Thermo Separations Products, Waltham, MA, USA) consisting of a SpectraSERIES P200 mobile phase pump, SpectraSERIES AS100 autosampler equipped with a 20 µL sample loop and a SpectraSERIES UV100 variable wavelength UV detector. Data processing on this system was performed on an interfaced desktop PC running Delta Chromatography Data System software (version 5.0, DataworX Pty Ltd., Kangaroo Point, QLD, Australia).

HPLC **system 2** was used for both purity checks and low resolution molecular weight determination. This system consisted of an Agilent 1260 Infinity HPLC with a UV-photodiode array detector and coupled to an Agilent 6120 single quadrupole multi-mode ion source mass spectrometer (Agilent Technologies, Santa Clara, CA, USA). Instrument control and data processing on this system was achieved using an interfaced desktop PC running OpenLAB CDS Chemstation Edition software (rev. c.01.05, Agilent Technologies, Santa Clara, CA, USA).

For purity determinations using either system, approximately 1 mg of test compound was dissolved in 1 mL HPLC grade MeOH, filtered through a 0.22 µm nylon syringe filter and the filtrate injected into the chromatograph for analysis.

6.4.3.2 System 3 - Reactive metabolite trapping experiments

Analysis of reactive metabolite trapping experiment incubation samples was carried out using LC-MS on **system 3** comprising an Agilent 1200 Rapid Resolution HPLC system coupled to an API4000Q Triple Quadrupole Linear Ion Trap mass spectrometer equipped with a Turbo V® ion source with an installed electrospray interface (AB Sciex, Framingham, MA, USA). The liquid chromatography system consisted of a binary gradient pump equipped with a solvent degassing unit, an autosampler with a chilled sample tray maintained at 4 °C, column compartment set at 40 °C and UV-photodiode array detector programmed to scan UV wavelengths over 200 - 400 nm. Instrument control and data processing was achieved by means of an integrated desktop PC running AB Sciex Analyst™ software (ver. 1.5).

6.4.3.3 System 4 - CYP450 phenotyping chemical inhibitor cross-reactivity assays

Analysis of microsomal incubations to determine the cross-reactivity of CYP450 isoform inhibitors was carried out using LC-MS on **system 4** composed of a Rheos 2200 microflow HPLC pump equipped with an online degasser (Flux Instruments GmbH & Co KG, Basel, Switzerland) coupled to a Triple Quadrupole Micromass Quattro Ultima Pt Mass Spectrometer detector (Waters Corporation, Milford, MA, USA). Automated sample injection was achieved by means of a PAL HTS autosampler equipped with a 20 µL sample loop (CTC Analytics AG, Swingen, Switzerland) with the sample tray maintained at 14 °C. The chromatographic column was maintained at 30 °C by means of a heated column oven (Jones Chromatography Ltd, Mid Glamorgan, UK) Programmable control of the gradient pump was achieved using an interfaced desktop computer running Janeiro II software while control of the mass spectrometer was performed using MassLynx software (v.4.1, Waters Corp., Milford, MA, USA).

6.4.3.4 HPLC and LC-MS chromatographic conditions

The chromatographic conditions and methods used to analyse samples using each of the systems described above are summarized in **Table 6.1**.

Table 6.1: Chromatographic method conditions used for HPLC and LC-MS sample analysis

System	Mobile Phase		Gradient			Flow Rate/ Column
	A	B	Time (min)	% A	%B	
1	5% AcN: 95% H_20	5% H_20: 95% AcN	0.0 7.0 10.0 12.0 15.0	100 0 0 100 100	0 100 100 0 0	700 µL/min Luna® C18, 150 x 4.6 mm, 3 µm, 100Å (Phenomenex, Torrance, CA, USA)
2	10 mM NH_4OAc pH 3.7 in H_2O	10 mM NH_4OAc pH 3.7 in 90% MeOH	0.0 0.5 2.5 6.0 6.1 8.0	90 90 10 10 90 90	10 10 90 90 10 10	1.0 mL/min Zorbax Poroshell 120, C18 2.7 µm 3.0 x 50 mm (Agilent Technologies, Santa Clara, CA, USA)
3	5 mM $HCOONH_4$ pH 3.0 in 5% AcN	5 mM $HCOONH_4$ pH 3.0 in 95% AcN	0.0 9.0 12.0 12.1 15.0	100 0 0 100 100	0 100 100 0 0	400 µL/min Kinetex C18, 150 x 2.1 mm, 2.6 µm, 100 Å (Phenomenex, Torrance, CA, USA)
4A	0.1% HCOOH in H_20	0.1% HCOOH in AcN	Isocratic	70	30	100 µL/min Micro-bore Luna® Phenyl-Hexyl, 50 x 1.0 mm, 3 µm (Phenomenex, Torrance, CA, USA)
4B			0.0 0.5 2.0 4.0 4.2 8.0	85 85 5 5 85 85	15 15 95 95 15 15	

6.5 rCYP450 Enzyme Inhibition Assays

6.5.1 Direct CYP450 Inhibition Assay

CYP450 fluorometric inhibition assays were conducted according to the method of Crespi *et al*.[5] Purified isoforms of recombinant human CYP450 and CYP450-reductase enzymes co-expressed in *Escherichia coli* were obtained from Cypex Limited (Dundee, Scotland, UK). rCYP450 enzyme control inhibitors were purchased from Sigma Aldrich (St. Louis, MO, USA). The fluorogenic probe substrates for monitoring enzyme activity were synthesized as described in this work (see Appendices). Fluorescence readings were measured either using a Wallac Victor2™ Multilabel Counter (Wallac AB, Oxfordhuset, Upplands Vasby, Sweden) or Varian Cary Eclipse Fluorescence Spectrophotometer (Varian GmbH, Darmstadt, Germany). Both instruments were equipped with 96-well microplate readers. Test preparations were incubated at 37 °C in a Memmert INE 500 natural convection incubator (Memmert GmbH + Co. KG, Schwabach, Germany).

Incubations were carried out in black 96-well Corning® Costar® microtiter plates for readings measured using the Wallac Victor2™ and in white 96-well Nunc™ microtitre plates for readings using the Cary Eclipse spectrophotometer.

The following general procedure was used: An incubation master mix was prepared by adding ice cold ultra-pure water, 0.2 M pH 7.4 mixed potassium phosphate buffer, flourogenic probe substrate and recombinant enzyme, in that order, to a clean mixing tube. Solutions of 1000 µM and 150 µM test compound were prepared by appropriately diluting in 25% acetonitrile from 10 mM stock solutions of each prepared in DMSO.

Aliquots of 186 µL master mix were transferred to all the 96 wells and 4 µL of either diluted positive control inhibitor, test compound solution or 25% acetonitrile solvent as blank was added to appropriate wells of the incubation plate. The plate was pre-incubated for 15 min at 37 °C before adding 10 µL of 20 mM NADPH to all wells except the blanks to initiate the metabolic reaction. The final incubation concentrations for the test compounds were 3 µM and 20 µM in a volume of 200 µL per well. The plate was incubated for a further 30 min at 37 °C after addition of NADPH and the reaction terminated by adding 75 µL of an ice-cold solution of 1 mM

Tris in 80% AcN. 10 µL of 20 mM NADPH was added to the wells containing blanks. Fluorescence was measured at appropriate excitation and emission wavelengths.

The final incubation plate setup was as illustrated in **Figure 6.3**. Detailed incubation preparations for the various CYP450 enzymes tested for inhibition are summarized in **Table 6.2 - Table 6.5**.

Figure 6.3: Incubation plate set-up for rCYP450 inhibition assays

	1	2	3	4	5	6
A	Blank	Control	Inhibitor Low	Inhibitor High	Cmpd 1 3 µM	Cmpd 1 20 µM
B	Blank	Control	Inhibitor Low	Inhibitor High	Cmpd 1 3 µM	Cmpd 1 20 µM
C						
D						
E						
F						
G						
H						

Note: *Incubations were performed in duplicate on adjacent rows. Only solvent containing no compound (25% AcN) was added to the master mix in wells marked blank and control. Different control inhibitors were used for different enzymes and incubated at a concentration greater than and lower than established* IC_{50} *value.*

Results of enzyme inhibition by the positive control were used as the basis for determining assay validity. The criteria used were as follows: at low positive control concentration, enzyme inhibition must not be > 25%, while at high concentration, inhibition was expected to be > 75%.

CYP3A4 inhibition assays in the presence of reduced glutathione were set-up exactly as described above with the only difference being that 5 µL of 40 mM GSH was substituted for the same volume of distilled water in each well.

Table 6.2: Summary incubation setup for CYP1A2 inhibition assay

	All volumes refer to µL/well								
	Distilled H_2O	**pH 7.4 $-PO_4^{3-}$ BUFFER**	**CEC (in 40% AcN)**	**rCYP1A2**	**Control Inhibitor Lo**	**Control Inhibitor Hi**	**Test Cmpd Lo**	**Test Cmpd Hi**	**NADPH**
	Prepared as Master Mix				**α-naphthaflavone (in 25% AcN)**		**Diluted in 25% AcN**		
Stock Concentration	-	**0.2 M**	**120 µM**	**13.3 pmol/µL**	**0.05 µM**	**0.5 µM**	**150 µM**	**1000 µM**	**20 mM**
Incubation Concentration	-	**0.1 M**	**3 µM**	**0.5 pmol/well**	**0.001 µM**	**0.01 µM**	**3 µM**	**20 µM**	**1 mM**
Blank Incubation	80.96	100.00	5.00	0.04	-	-	4 (25% AcN)		10.00
Control Incubation	80.96	100.00	5.00	0.04	-	-	4 (25% AcN)		10.00
Inhibitor Low	80.96	100.00	5.00	0.04	4.00	-	-	-	10.00
Inhibitor High	80.96	100.00	5.00	0.04	-	4.00	-	-	10.00
Test Compound Low	80.96	100.00	5.00	0.04	-	-	4.00	-	10.00
Test Compound High	80.96	100.00	5.00	0.04	-	-	-	4.00	10.00
Fluorimeter Settings	Excitation/Emission λ (nm) 405/460								

Table 6.3: Summary incubation setup for rCYP2C9 inhibition assay

	All volumes refer to µL/well								
	Distilled H_2O	**pH 7.4 $-PO_4^{3-}$ BUFFER**	**MFC (in 40% AcN)**	**rCYP2C9**	**Control Inhibitor Lo**	**Control Inhibitor Hi**	**Test Cmpd Lo**	**Test Cmpd Hi**	**NADPH**
	Prepared as Master Mix				**Sulphafenazole (25% AcN)**		**Diluted in 25% AcN**		
Stock Concentration	-	**0.2 M**	**3.4 mM**	**2.1 pmol/µL**	**5 µM**	**50 µM**	**150 µM**	**1000 µM**	**20 mM**
Incubation Concentration	-	**0.1 M**	**0.085 mM**	**5 pmol/well**	**0.1 µM**	**1 µM**	**3 µM**	**20 µM**	**1 mM**
Blank Incubation	80.96	100.00	5.00	2.38	-	-	4 (25% AcN)		10.00
Control Incubation	80.96	100.00	5.00	2.38	-	-	4 (25% AcN)		10.00
Inhibitor Low	80.96	100.00	5.00	2.38	4.00	-	-	-	10.00
Inhibitor High	80.96	100.00	5.00	2.38	-	4.00	-	-	10.00
Test Compound Low	80.96	100.00	5.00	2.38	-	-	4.00	-	10.00
Test Compound High	80.96	100.00	5.00	2.38	-	-	-	4.00	10.00
Fluorimeter Settings	Excitation/Emission λ (nm) 405/535								

Table 6.4: Summary incubation setup for rCYP2C19 inhibition assay

	All volumes refer to µL/well								
	Distilled H_2O	**pH 7.4 -PO_4^{3-} BUFFER**	**MFC (in 40% AcN)**	**rCYP2C19**	**Control Inhibitor Lo**	**Control Inhibitor Hi**	**Test Cmpd Lo**	**Test Cmpd Hi**	**NADPH**
	Prepared as Master Mix				**Ticlopidine (in 25% AcN)**		**Diluted in 25% AcN**		
Stock Concentration	-	**0.2 M**	**1400 µM**	**5.5 pmol/µL**	**50 µM**	**500 µM**	**150 µM**	**1000 µM**	**20 mM**
Incubation Concentration	-	**0.1 M**	**35 µM**	**2 pmol/well**	**1 µM**	**10 µM**	**3 µM**	**20 µM**	**1 mM**
Blank Incubation	80.96	100.00	5.00	0.36	-	-	4 (25% AcN)		10.00
Control Incubation	80.96	100.00	5.00	0.36	-	-	4 (25% AcN)		10.00
Inhibitor Low	80.96	100.00	5.00	0.36	4.00	-	-	-	10.00
Inhibitor High	80.96	100.00	5.00	0.36	-	4.00	-	-	10.00
Test Compound Low	80.96	100.00	5.00	0.36	-	-	4.00	-	10.00
Test Compound High	80.96	100.00	5.00	0.36	-	-	-	4.00	10.00
Fluorimeter Settings	Excitation/Emission λ (nm) 405/535								

Table 6.5: Summary incubation setup for rCYP3A4 inhibition assay

	All volumes refer to µL/well								
	Distilled H_2O	**pH 7.4 -PO_4^{3-} BUFFER**	**BFC (in 40% AcN)**	**rCYP3A4**	**Control Inhibitor Lo**	**Control Inhibitor Hi**	**Test Cmpd Lo**	**Test Cmpd Hi**	**NADPH**
	Prepared as Master Mix				**Ketoconazole (in 25% AcN)**		**Diluted in 25% AcN**		
Stock Concentration	-	**0.2 M**	**400 µM**	**3.9 pmol/ µL**	**0.5 µM**	**5.0 µM**	**150 µM**	**1000 µM**	**20 mM**
Incubation Concentration	-	**0.1 M**	**10 µM**	**2 pmol/well**	**0.01 µM**	**0.1 µM**	**3 µM**	**20 µM**	**1 mM**
Blank Incubation	80.96	100.00	5.00	0.51	-	-	4 (25% AcN)		10.00
Control Incubation	80.96	100.00	5.00	0.51	-	-	4 (25% AcN)		10.00
Inhibitor Low	80.96	100.00	5.00	0.51	4.00	-	-	-	10.00
Inhibitor High	80.96	100.00	5.00	0.51	-	4.00	-	-	10.00
Test Compound Low	80.96	100.00	5.00	0.51	-	-	4.00	-	10.00
Test Compound High	80.96	100.00	5.00	0.51	-	-	-	4.00	10.00
Fluorimeter Settings	Excitation/Emission λ (nm) 405/535								

6.5.2 Time-Dependent CYP3A4 Inhibition Assay

The assay to determine time-dependent inhibition of rCYP3A4 involved two incubations as described here.

6.5.2.1 Inactivation assay

A volume of 85 µL master mix comprising 0.1 M mixed phosphate buffer and rCYP3A4 was added to wells in a 96-well microtitre plate. A 5 µL solution of either test or control compound was added to wells in columns 1 - 4 and 7 - 8 of the plate in duplicate while plain solvent (25% AcN) was added to wells in columns 5, 6, 11 and 12. The plate was pre-incubated at 37 °C for 10 minutes before adding 10 µL of distilled water to all wells in columns 1 - 6 and 10 µL of 10 mM NADPH in wells in columns 7 - 12.The plate was then further incubated for 15 min at 37 °C. Test and control compounds were incubated at final concentrations of 1 µM and 5 µM in wells containing 5 pmol of enzyme each (**Figure 6.4**).

Figure 6.4: Inactivation assay plate lay-out for rCYP3A4 TDI assay

	NO NADPH						+ NADPH					
	1 µM		5 µM		-	-	1 µM		5 µM		-	-
	1	2	3	4	5	6	7	8	9	10	11	12
A	Cpd 1	Cpd 1	Cpd 1	Cpd 1	Cntrl	Blank	Cpd 1	Cpd 1	Cpd 1	Cpd 1	Cntrl	Blank
B	Cpd 2	Cpd 2	Cpd 2	Cpd 2	Cntrl	Blank	Cpd 2	Cpd 2	Cpd 2	Cpd 2	Cntrl	Blank
C	…etc	…etc	…etc	…etc	…etc	…etc	…etc	…etc	…etc	…etc	…etc	…etc
D												

6.5.2.2 Activity assay

To a second 96-well microtitre plate, 170 µL of a master mix comprising 520 µM fluorogenic enzyme substrate BFC in 0.1 M mixed phosphate buffer pH 7.4 was added to all wells and warmed for 5 min at 37 °C. A 20 µL aliquot was transferred from each well in the inactivation assay plate, described in **Section 6.5.2.1** above, to the corresponding well in the activity plate containing the fluorogenic substrate. A further 10 µL aliquot of 20 mM NADPH solution was added to all wells except those marked as blanks and the plate incubated for 15 min at 37 °C. The incubation was terminated by adding 75 µL ice-cold stop solution to all wells and adding 10 µL NADPH to the wells containing blanks. Fluorescence measurements were taken at the specific wavelengths highlighted before and the results analysed as described previously to calculate the Normalized Inhibition Ratios.[6]

6.6 Reactive Metabolite Trapping Experiments

Incubations to trap reactive metabolic intermediates were performed in 1.5 mL microcentrifuge Eppendorf® tubes using a generic procedure adopted from methods described previously in the literature.[7–9] Human liver microsomes (20 mg protein/mL, mixed gender, pooled from 50 individuals) and rat liver microsomes (20 mg protein/mL, male, pooled from 400 individuals) were sourced from Xenotech LLC (Kansas, USA). Positive control substrates rimonabant hydrochloride and prazosin hydrochloride were obtained from Proactive Molecular Research (Alachua, FL) while amodiaquine hydrochloride dihydrate, potassium cyanide, reduced glutathione and methoxylamine hydrochloride were all purchased from Sigma-Aldrich Chemie GmBH (Schnelldorf, Germany).

6.6.1 Microsomal Incubation Conditions

Test compounds were dissolved in DMSO to prepare 10 mM stock solutions and incubated separately at a concentration of 10 µM in 0.1M mixed phosphate buffer pH 7.4 containing 5 mM $MgCl_2$, 1 mM nucleophilic trapping agent (KCN, GSH or methoxylamine) and 1 mg/mL human (or rat) liver microsomes. The metabolic incubations were initiated, following 5 min pre-incubation at 37 °C, by addition of 20 mM NADPH to a final concentration of 1 mM. Total incubation volume per sample was 200 µL. Incubations in which individual components were omitted from the preparation i.e. test compound, trapping agent, HLM or NADPH were included to serve as controls. The incubation tubes were maintained at 37 °C in a shaking water bath set at 50 rpm with the preparations exposed to atmospheric oxygen throughout. Metabolic reactions were terminated after 60 min by addition of 200 µL ice-cold acetonitrile to precipitate microsomal proteins. The incubation tubes were then placed on ice for 10 min and subsequently centrifuged at 14,000 rpm in a chilled centrifuge at 4 °C for 15 min. The recovered supernatants was filtered through 0.22 um PTFE syringe filters and analysed on LC-MS.

6.6.2 LC-MS Analysis of Trapped Reactive Metabolite Samples

Filtered supernatant solutions of the incubation preparations were analysed using LC-MS using the system and chromatographic conditions described in **Section 6.4.3.4** above. Detection of trapped reactive metabolites was carried out using different mass

spectral scanning modes including enhanced mass spectral (EMS) scans over a range of *m/z* values in either positive or negative ion mode, neutral loss and enhanced product ion scans for detection of glutathione adducts in particular. The ionisation source conditions were optimised by direct infusion of test compounds dissolved in 5 mM ammonium formate pH 3.0 in 50% AcN to a concentration of 0.5 µg/mL at a flow rate of 10 µL/min injected into the ion source using a HA11 syringe pump (Harvard Apparatus, Holliston, MA, USA).

Optimised ion source conditions for the detection of test compounds are summarised in **Table 6.6**.

Table 6.6: Optimized ion source conditions for LC-MS analysis of reactive metabolite trapping incubations

	Ionisation Mode	Polarity	Temp. (°C)	Ion Spray Voltage (V)	Declustering Potential (V)
Gedunin	APCI	+	500	-	111
Metergoline	ESI	+	400	5500	111
DC3	ESI	+	400	5000	66
DC14	ESI	+	400	5000	86
Justicidin A	ESI	+	550	5200	91
Jamaicin	ESI	+	500	5000	116
SQTL	ESI	+	500	5000	71
CLPG	ESI	+	500	5000	91
Formononetin	ESI	+	300	4000	66
Fusidic acid	ESI	-	100	-3500	-105
CUC-B	ESI	+	500	5000	51

6.7 CYP450 Phenotyping Chemical Inhibitor Cross-Reactivity Assays

Microsomal incubations to determine the cross-reactivity of CYP450 phenotyping chemical inhibitors were performed in 1.5 mL polypropylene Eppendorf™ microcentrifuge tubes. Predilutions of probe substrates of each of the eight CYP450 reactions monitored were prepared from stock solutions of different concentrations stored at -20 °C by diluting in water to working concentrations 40× higher than final incubation concentrations. For each incubation, 0.5 M pH 7.4 mixed phosphate buffer (BD Gentest, Oxford, UK) and 50 mM $MgCl_2$ were both diluted to a working concentration of 0.1 M and 5 mM respectively by adding an appropriate volume of HPLC grade water. Human liver microsomes (mixed gender, pooled from 150 individuals) were added to the buffer mixture to varying protein concentrations depending on the probe reaction and the pre-diluted (40×) probe substrate pipetted into the master mix. For test incubations, the chemical inhibitor under evaluation for cross reactivity was then added to the mixture while only the dilution solvent was added to the control incubations. The mixtures were pre-incubated at 37 °C for 10 min and the metabolic reactions initiated by addition of NADPH. All reactions were performed in duplicate and the tubes maintained at 37 °C while exposed to atmospheric oxygen by means of an Eppendorf ThermoMixer™ F1.5 benchtop incubator shaking at 300 rpm. The durations of the microsomal incubations were optimised for each probe substrate and selected to ensure that metabolism did not exceed 20%.

Incubations were terminated by addition of 50% formic acid solution (10 µL per 100 µL incubation volume). A precise amount of ^{13}C or ^{2}H radiolabelled metabolite was added to the preparations to serve as internal standard and the samples subsequently purified using solid phase extraction. The purified eluents from SPE were loaded into a 2 mL deep-well plate, evaporated to dryness under a stream of nitrogen at 40 °C and then dissolved in a mixture of 10% AcN in HPLC-grade water containing 0.1% formic acid. The resultant solutions were analyzed using LC-MS System 4 (**Section 6.4.3.3**) to quantify the probe metabolites. The mass spectrometer was operated in multiple reaction monitoring mode (MRM) at a source temperature of 120 °C and desolvation temperature of 300 °C. Analysis parameters for the different analytes are summarized in **Table 6.7**.

Table 6.7: LC-MS Parameter settings for detection and quantification of chemical inhibitor cross reactivity

	Probe substrate metabolites	Ionisation Mode	MRM Transitions Q1/Q3 (*m/z*)	Internal Standards	IS MRM Transitions Q1/Q3 (*m/z*)	Cone Voltage (V)	Collision Energy (eV)	LC Method Conditions[‡]
CYP1A2	Acetaminophen	ESI +	152.1/110.1	[$^{2}H_4$] Acetaminophen	156.0/114.0	34	16	4A
CYP2B6	Hydroxybupropion	ESI +	256.0/139.0	[$^{2}H_6$] Hydroxybupropion	262.0/139.0	24	18	4B
CYP2C8	6α-Hydroxypaclitaxel	ESI +	870.1/286.1	Warfarin	309.2/163.05	25 (20)[*]	16 (14)[†]	4B
CYP2C9	4'-Hydroxydiclofenac	ESI +	312.1/230.0	[$^{13}C_6$] 4'-Hydroxydiclofenac	319.0/237.0	20	32	4B
CYP2C19	4'-Hydroxymephenytoin	ESI -	233.05/190.05	[$^{2}H_3$] 4'-OH-mephenytoin	236.15/193.05	58 (56)[*]	15	4A
CYP2D6	1'-Hydroxybufuralol	ESI +	278.2/186.05	[$^{2}H_9$] 1'-Hydroxybufuralol	287.2/186.0	20	18	4B
CYP2E1	6-Hydroxychlorzoxazone	ESI -	183.9/119.95	[$^{2}H_3$] 4'-OH-mephenytoin	236.15/193.05	58 (56)[*]	20 (15)[†]	4A
CYP3A	1'-Hydroxymidazolam	ESI +	342.1/203.5	[$^{2}H_4$] 1'-Hydroxymidazolam	346.1/203.05	40	24	4A

Note: *[*] and [†] denote different cone voltage and collision energy values used to detect each metabolite and internal standard, respectively. Values in parentheses are the settings used to detect the internal standard. In all other instances, the single values indicated were optimal for detection of both metabolites and internal standard.*

[‡] *Denotes LC-MS chromatographic conditions as described in* ***Table 6.1***

REFERENCES:

(1) Lipinski, C. A.; Lombardo, F.; Dominy, B. W.; Feeney, P. J. Experimental and Computational Approaches to Estimate Solubility and Permeability in Drug Discovery and Development Settings. *Advanced Drug Delivery Reviews* **2001**, *46*, 3–26.

(2) Bevan, C. D.; Lloyd, R. S. A High-Throughput Screening Method for the Determination of Aqueous Drug Solubility Using Laser Nephelometry in Microtiter Plates. *Analytical Chemistry* **2000**, *72*, 1781–1787.

(3) McCrone, W. C. Application of Fusion Methods in Chemical Microscopy. *Analytical Chemistry* **1949**, *21*, 436–441.

(4) Vitez, I. M.; Newman, A. W.; Davidovich, M.; Kiesnowski, C. The Evolution of Hot-Stage Microscopy to Aid Solid-State Characterizations of Pharmaceutical Solids. *Thermochimica Acta* **1998**, *324*, 187–196.

(5) Crespi, C. L.; Miller, V. P.; Penman, B. W. Microtiter Plate Assays for Inhibition of Human, Drug-Metabolizing Cytochromes P450. *Analytical Biochemistry* **1997**, *248*, 188–190.

(6) Thelingwani, R. S.; Zvada, S. P.; Dolgos, H.; Ungell, A.-L. B.; Masimirembwa, C. M. In Vitro and in Silico Identification and Characterization of Thiabendazole as a Mechanism-Based Inhibitor of CYP1A2 and Simulation of Possible Pharmacokinetic Drug-Drug Interactions. *Drug Metabolism and Disposition* **2009**, *37*, 1286–1294.

(7) Argoti, D.; Liang, L.; Conteh, A.; Chen, L.; Bershas, D.; Yu, C.-P.; Vouros, P.; Yang, E. Cyanide Trapping of Iminium Ion Reactive Intermediates Followed by Detection and Structure Identification Using Liquid Chromatography-Tandem Mass Spectrometry (LC-MS/MS). *Chemical Research in Toxicology* **2005**, *18*, 1537–1544.

(8) Bergström, M. A.; Isin, E. M.; Castagnoli, N.; Milne, C. E. Bioactivation Pathways of the Cannabinoid Receptor 1 Antagonist Rimonabant. *Drug Metabolism and Disposition* **2011**, *39*, 1823–1832.

(9) Erve, J. C. L.; Vashishtha, S. C.; DeMaio, W.; Talaat, R. E. Metabolism of Prazosin in Rat, Dog, and Human Liver Microsomes and Cryopreserved Rat and Human Hepatocytes and Characterization of Metabolites by Liquid Chromatography/tandem Mass Spectrometry. *Drug Metabolism and Disposition* **2007**, *35*, 908–916.

APPENDIX 1:

EXPERIMENTALLY DETERMINED PHYSICO-CHEMICAL PROPERTIES OF TEST COMPOUNDS

	Mwt	LC-MS-DAD		†Melting Point (°C)	Solubility (µM)
		(*m/z*)*	Peak Purity		
Gedunin	482.57	483.2; 505.1	96.9%	192 - 196	20 - 40
Justicidin A	394.37	395.0; 417.0	99.5%	248 - 252	10 - 20
Dehydrobrachylaenolide	244.29	267.1; 245.0	98.6%	225 - 228	> 200
Metergoline	403.52	404.1; 426.1	97.9%	143 - 145	80 - 160
Fusidic acid	516.71	539.2	97.3%	178 - 180	> 200
Muzigadial	248.32	271.1	99.1%	125 - 128	> 200
Muzi-04	305.37	306.1; 328.1	99.5%	249 - 252	20 - 40
Cucurbitacin A	574.70	597.2; 613.1	96.5%	195 - 197	> 200
Cucurbitacin B	558.70	581.2; 597.2	98.4%	172 - 175	> 200
Cucurbitacin C	560.72	583.2	95.7%	198 - 201	> 200
DC3	352.47	353.1	98.4%	218 - 220	> 200
DC14	316.43	317.2; 339.1	97.9%	112 - 115	> 200
Jamaicin	378.37	379.0; 401.0	96.2%	156 - 158	ND‡
Calopogonium isoflavone	334.37	335.1; 357.0	96.3%	136 - 139	ND‡
Formononetin	268.26	269.0; 291.0	98.9%	250 - 254	20 - 40

Note: **Compound peak signals in low resolution LC-MS mass spectra were detected as adducts of H^+ and/or Na^+ (i.e. $[MH]^+$ = M+1 and $[M+Na^+]$ = M+23) and in a few cases, as $[M+K^+]$ i.e. M+39;*
†Melting point values are uncorrected and reported as determined;
‡Not determined. Quantities of jamaicin and calopogonium isoflavone were insufficient for determination of solubility

APPENDIX 2:

DESIGN AND SYNTHESIS OF FLUOROGENIC CYP450 PROBE SUBSTRATES

Four fluorogenic probe substrates were synthesized, purified and characterised for use in testing inhibition of CYP450 enzymes by the natural products described in **Chapter 3.**

7-Methoxy-4-(trifluoromethyl)coumarin (MFC) and 7-Benzyloxy-4-(trifluoromethyl) coumarin (BFC)

The respective fluorogenic probe substrates for assessing inhibition of the recombinant CYP2C9 and CYP2C19 (MFC), and CYP3A4 (BFC) were each synthesized from commercially sourced 7-hydroxy-4-(trifluoromethyl)coumarin (HFC) via a single step Williamson ether synthesis as summarized in **Scheme A.1.**

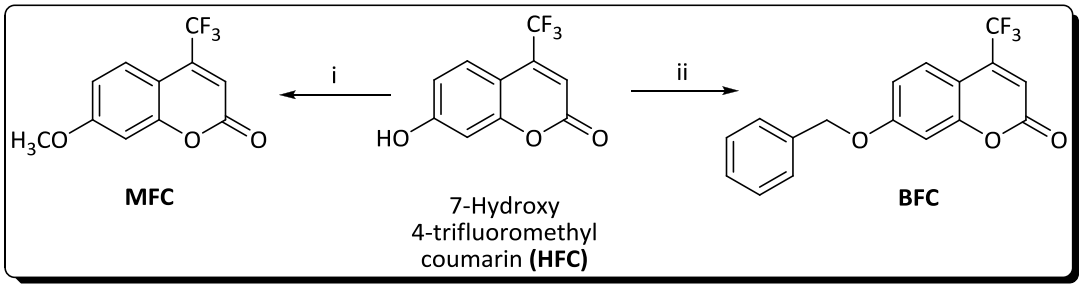

Scheme A.1: *Reagents and conditions for the synthesis of MFC and BFC* (i) Iodomethane, K_2CO_3, DMF, 25 °C, 8h (ii) Benzylbromide, K_2CO_3, THF, reflux, 12h

7-methoxy-4-(trifluoromethyl) coumarin (MFC)

Commercially sourced 7-hydroxy-4-(trifluoromethyl) coumarin (100 mg, 0.43 mmol) was dissolved in 3 mL anhydrous *N,N*-dimethylformamide and K_2CO_3 (125 mg, 0.90 mmol) added. To the stirred mixture, iodomethane (55 µL, 127 mg, 0.89 mmol) was introduced using a micropipette and the solution stirred at room temperature for 8 h. Progress of the reaction was monitored by TLC. The reaction was quenched by adding 15 mL distilled water and extracted with 3 x 25 mL portions of ethyl acetate. The combined extracts were dried over anhydrous $MgSO_4$, concentrated *in vacuo* and purified in a silica gel cartridge using automated flash chromatography to obtain the target compound.

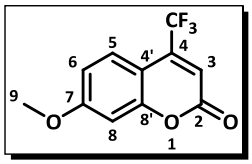

Pale yellow coloured crystalline powder (85.2 mg, 80.3%); m.p. 98 - 101 °C; R_f (EtOAc:Hex, 1:1), 0.74; ^{1}H NMR (400 MHz, $CDCl_3$) δ: 7.63 (d, *J* = 7.1 Hz, 1H, H-5), 6.92 (dd, *J* = 9.0 and 2.5 Hz, 1H, H-6), 6.88 (d, *J* = 2.5 Hz, 1H, H-8), 6.62 (s, 1H, H-3), 3.90 (s, 3H, -OCH_3). HPLC purity 95.2% (System 2; Rt = 3.54 min)

7-benzyloxy-4-(trifluoromethyl) coumarin (BFC)

Commercially sourced 7-hydroxy-4-(trifluoromethyl) coumarin (100 mg, 0.43 mmol) was dissolved in 10 mL anhydrous tetrahydrofuran and K_2CO_3 (123 mg, 0.90 mmol) added. To the stirred mixture, benzyl bromide (0.2 mL, 287 mg, 1.68 mmol) was introduced dropwise using a micropipette and the solution stirred under reflux for 12 h. Progress of the reaction was monitored on TLC. The mixture was left to cool, then filtered under vacuum using a Buchner funnel and the filtrate washed with 3 x 15 mL portions of distilled water. The organic layer was dried over anhydrous $MgSO_4$, concentrated and adsorbed onto silica gel *in vacuo* then purified using automated flash chromatography to obtain the target compound.

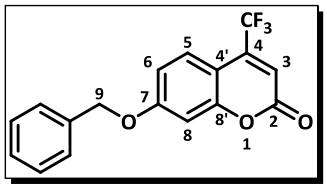

Off-white coloured crystalline powder (104.0 mg, 74.7%); m.p. 103 - 105 °C; R_f (EtOAc:Hex, 1:1), 0.83; ^{1}H NMR (400 MHz, $CDCl_3$) δ: 7.56 (d, *J* = 9.0 Hz, 1H, H-5), 7.37 – 7.28 (m, 4H, Ar-H), 7.18 (d, *J* = 1.3 Hz, 1H, *para* Ar-H), 6.92 (dd, *J* = 9.0 and 2.5 Hz, 1H, H-6), 6.87 (d, *J* = 2.2 Hz, 1H, H-8), 6.54 (s, 1H, H-3), 5.09 (s, 2H, -CH_2-, H-9). ^{13}C NMR (100 MHz, DMSO-d_6) δ: 162.6, 159.3, 156.3, 141.4, 135.4, 128.8, 128.5, 127.5, 126.4, 123.0, 120.2, 114.0, 112.3, 112.4, 107.3, 102.5, 70.7. Low resolution LC-ESI-MS (-ve ion mode): *m/z* 319.1 $[M-H]^-$; HPLC purity 99.3% (System 2; Rt = 3.96 min).

3-Cyano-7-ethoxycoumarin (CEC)

CEC was synthesized as the probe substrate for monitoring the inhibition of CYP1A2. Preparation of this compound involved the initial synthesis, via a 'green' Knoevenagel condensation of malononitrile with 2,4-dihydroxybenzaldehyde in aqueous medium followed by Williamson etherification of the resultant 3-cyano-7-hydroxycoumarin intermediate. The steps in this reaction are illustrated in **Scheme A.2.**

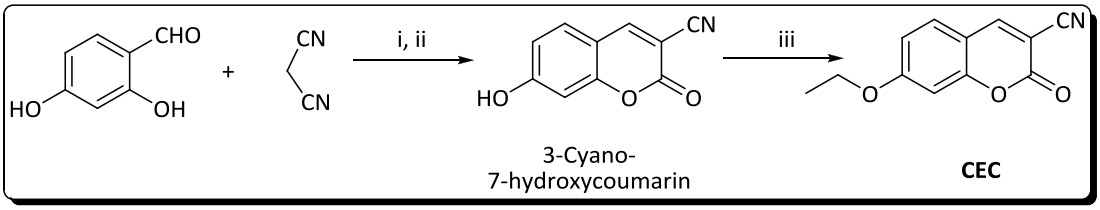

Scheme A.2: *Reagents and conditions for the synthesis of CEC* (i) 0.05M aq. $NaHCO_3$, 25 °C, 1.5h (ii) Conc. HCl, 90 °C, 1h (iii) Bromoethane, K_2CO_3, DMF, 25 °C, 12h

3-Cyano-7-hydroxycoumarin

To a 25 mL aqueous solution of 0.05M $NaHCO_3$, 2,4-dihydroxybenzaldehyde (680 mg, 4.92 mmol) and malononitrile (400 mg, 6.05 mmol) were added and stirred vigorously at room temperature for 1.5 h. 0.6 mL concentrated HCl was then added to the reaction and the heterogenous mixture heated at 90 °C for 1 h. The mixture was cooled and the desired compound recovered by filtration under vacuum using a Buchner funnel before drying at 50 °C to afford the target compound.

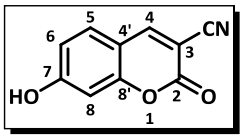

Brown/red powder (842.4 mg, 91.4%); m.p. 269 - 272°C; R_f (EtOAc:Hex, 1:1), 0.18; ^{1}H NMR (400 MHz, DMSO-d_6) δ 11.29 (s, broad, 1H, -OH), 8.75 (s, 1H, H-4), 7.63 (d, *J* = 8.6 Hz, 1H, H-5), 6.88 (dd, 1H, *J* = 8.6 and 2.3 Hz, H-6), 6.77 (d, *J* = 2.2 Hz, 1H, H-8). ^{13}C NMR (100 MHz, DMSO-d_6) δ: 165.3 (C-7), 158.0 (C-2), 157.1 (C-8'), 153.8 (C-4), 131.8 (C-5), 115.7 (-CN), 115.1 (C-6), 110.8 (C-4'), 103.0 (C-8), 96.5 (C-3). Low resolution LC-ESI-MS (-ve ion mode): *m/z* 186.1 $[M-H]^-$; HPLC purity 98.3% (System 2; Rt = 2.55 min).

3-cyano-7-ethoxycoumarin (CEC)

3-cyano-7-hydroxycoumarin (200 mg, 1.07 mmol) was dissolved in 3 mL anhydrous *N,N*-dimethylformamide to which K_2CO_3 (300 mg, 2.17 mmol) was added. To the stirred mixture, bromoethane (0.2 mL, 292 mg, 2.68 mmol) was introduced using a syringe and the solution stirred at room temperature for 12 h. Progress of the reaction was monitored by TLC. The mixture was quenched by adding 15 mL distilled water and extracted with 3 x 25 mL portions of ethyl acetate. The combined extracts were dried over anhydrous $MgSO_4$, concentrated *in vacuo* and purified in a silica gel cartridge using automated flash chromatography to obtain the target compound.

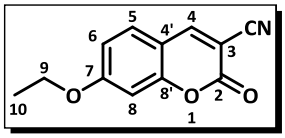

Pale yellow coloured crystalline powder (122 mg, 53.2%); m.p. 201 - 204°C; R_f (EtOAc:Hex, 1:1), 0.41; ^{1}H NMR (400 MHz, DMSO-d_6) δ: 8.81 (s, 1H, H-4), 7.71 (d, *J* = 8.6 Hz, 1H, H-5), 7.07 (d, *J* = 2.3 Hz, 1H, H-8), 7.03 (dd, *J* = 8.4 and 2.1 Hz, 1H, H-6), 4.19 (q, *J* = 7.0 Hz, 2H, -CH_2-), 1.35 (t, *J* = 7.0 Hz, 3H, -CH_3). ^{13}C NMR (100 MHz, DMSO-d_6) δ: 165.2 (C-7), 157.9 (C-2), 157.1 (C-8'), 153.7 (C-4), 131.8 (C-5), 115.5 (-CN), 114.6 (C-6), 111.7 (C-4'), 101.9 (C-8), 97.8 (C-3), 65.2 (C-9), 14.7 (C-10). Low resolution LC-ESI-MS (+ve ion mode): *m/z* 216.1 $[M+H]^+$; 233.1 $[M+NH_4]^+$; 238.0 $[M+Na]^+$ HPLC purity 97.4% (System 2; Rt = 3.14 min).

4-Methylamino-7-methoxycoumarin (MAMC)

The synthesis of MAMC, the fluorogenic probe substrate for investigating the inhibition of rCYP2D6, was accomplished via a three step procedure (**Scheme A.3**) that involved initial Pechmann condensation of 3-methoxyphenol and ethyl-4-chloro-3-oxobutanoate to form 4-chloromethyl-7-methoxycoumarin (**a**) which was subsequently converted to the corresponding azide (**b**) through a substitution reaction using sodium azide. The 4-azidomethyl-7-methoxycoumarin was then converted to the target primary amine via a Staudinger reduction.

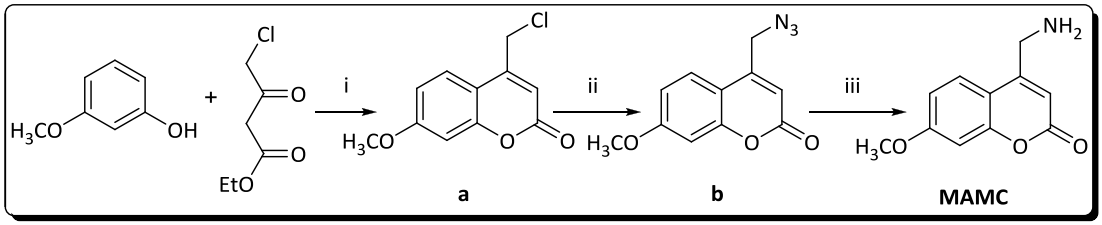

Scheme A.3: *Reagents and conditions for the synthesis of MAMC* (i) Amberlyst®-15, toluene, reflux, 12h (ii) NaN_3, DMF, 25 °C, 1h (iii) Triphenylphosphine, H_2O, THF, reflux, 2h

4-chloromethyl-7-methoxy coumarin

3-methoxy-phenol (500 mg, 4.02 mmol) and ethyl-4-chloroacetoacetate (695 mg, 4.22 mmol) were added to 10 mL anhydrous THF and Amberlyst®-15 pellets (1 g) then added. The mixture was stirred under reflux for 12 h and progress of the reaction monitored on TLC. The mixture was allowed to cool and a minimum volume of DCM sufficient to dissolve the solid product formed added. This was then filtered to remove the Amberlyst® pellets and solvent evaporated from the filtrate *in vacuo.* The pure target product was obtained from the solid residue by crystallization using ethanol.

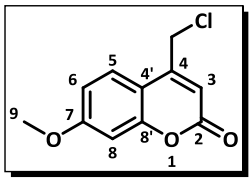

Off-white coloured crystalline powder (843 mg, 93.6%); m.p. 193 – 195 °C; R_f (EtOAc:Hex, 1:1), 0.58; ^{1}H NMR (400 MHz, $CDCl_3$) δ 7.49 (d, *J* = 8.8 Hz, 1H, H-5), 6.83 (dd, *J* = 8.8 and 2.5 Hz, 1H, H-6), 6.78 (d, *J* = 2.5 Hz, 1H, H-8), 6.33 (s, 1H, H-3), 4.55 (s, 2H, -CH_2-), 3.81 (s, 3H, -OCH_3, H-9). ^{13}C NMR (100 MHz, $CDCl_3$) δ: 163.0, 160.7, 155.8, 149.6, 125.1, 112.7, 110.8, 101.4, 101.3, 55.8. 41.3. Low resolution LC-ESI-MS (+ve ion mode): *m/z* 225.0 $[M+H]^+$; HPLC purity 98.1% (System 2; Rt = 3.26 min).

4-azidomethyl-7-methoxy coumarin

4-chloromethyl-7-methoxy coumarin (275 mg, 1.2 mmol) was dissolved in 2 mL anhydrous DMF and sodium azide (90 mg, 1.4 mmol) added portion wise. The mixture was stirred at room temperature for 1 h and monitored by TLC. The reaction was quenched by adding 15 mL distilled water and the resultant solution extracted using 3 x 15 mL portions of ethyl acetate. The combined organic extracts were dried over anhydrous $MgSO_4$ and the solvent evaporated under vacuum to afford the target compound.

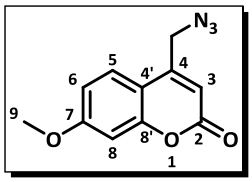

Reddish-brown powder (256 mg, 90.4%); m.p. 124 - 126 °C; R_f (EtOAc:Hex, 1:1), 0.52; ^{1}H NMR (400 MHz, $CDCl_3$) δ: 7.36 (d, *J* = 8.7 Hz, 1H, H-5), 6.82 - 6.78 (m, 2H, H-6, H-8), 6.28 (t, *J* = 1.2 Hz, 1H, H-3), 4.43 (d, *J* = 1.2 Hz, 2H, -CH_2-), 3.81 (s, 3H, -OCH_3, H-9). ^{13}C NMR (100 MHz, $CDCl_3$) δ: 163.0, 160.6, 155.8, 148.6, 124.8, 112.7, 111.6, 110.8, 101.3, 55.8, 50.9. Low resolution LC-ESI-MS (+ve ion mode): *m/z* 232.0 $[M+H]^+$; HPLC purity 96.4% (System 2; Rt = 3.27 min).

4-methylamino-7-methoxycoumarin (MAMC)

4-azidomethyl-7-methoxy coumarin (200 mg, 0.86 mmol) was dissolved in 5 mL THF to which triphenyl phosphine (450 mg, 1.72 mmol) and 0.5 mL H_2O were added. The mixture was stirred under reflux for 2 h and monitored by TLC using both UV and ninhydrin detection. The solution was cooled then concentrated by evaporating the solvent under vacuum and the product purified by flash silica column chromatography to afford the target compound.

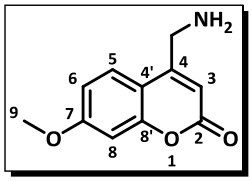

Pale yellow coloured crystalline solid. (76 mg, 42%); m.p. 121 - 124 °C; R_f (DCM:MeOH, 9:1), 0.51; ^{1}H NMR (400 MHz, DMSO-d_6) δ: 7.67 (d, *J* = 8.8 Hz, 1H, H-5), 6.97 (d, *J* = 2.4 Hz, 1H, H-8), 6.92 (dd, *J* = 8.8 and 2.4 Hz, 1H, H-6), 6.38 (s, 1H, H-3), 3.91 (s, 2H, -CH_2-), 3.84 (s, 3H, -OCH_3), 1.98 (broad, s, 2H, -NH_2). ^{13}C NMR (100 MHz, DMSO-d_6) δ: 162.6, 161.2, 158.6, 155.2, 125.9, 112.5, 112.1, 108.7, 101.3, 56.3, 42.1. Low resolution LC-ESI-MS (+ve ion mode): *m/z* 206.1 $[M+H]^+$; HPLC purity 96.7% (System 2; Rt = 1.45 min)